# EXACT SOLUTIONS FOR BUCKLING OF STRUCTURAL MEMBERS

CRC Series in
# COMPUTATIONAL MECHANICS and APPLIED ANALYSIS

Series Editor: J.N. Reddy
Texas A&M University

———————

Published Titles

**APPLIED FUNCTIONAL ANALYSIS**
J. Tinsley Oden and Leszek F. Demkowicz

**THE FINITE ELEMENT METHOD IN HEAT TRANSFER AND FLUID DYNAMICS, Second Edition**
J.N. Reddy and D.K. Gartling

**MECHANICS OF LAMINATED COMPOSITE PLATES AND SHELLS: THEORY AND ANALYSIS, Second Edition**
J.N. Reddy

**PRACTICAL ANALYSIS OF COMPOSITE LAMINATES**
J.N. Reddy and Antonio Miravete

**SOLVING ORDINARY and PARTIAL BOUNDARY VALUE PROBLEMS in SCIENCE and ENGINEERING**
Karel Rektorys

**ADVANCED THERMODYNAMICS ENGINEERING**
Kalyan Annamalai and Ishwar K. Puri

# EXACT SOLUTIONS FOR BUCKLING OF STRUCTURAL MEMBERS

C. M. Wang

C. Y. Wang

J. N. Reddy

### Visit the CRC Press Web site at www.crcpress.com

# Dedication

Our wives

*Sherene Wang*

*Dora Wang*

*Aruna Reddy*

# About the Authors

**C. M. Wang** is a Professor of Civil Engineering at the National University of Singapore (NUS). He obtained his B.Eng., M.Eng.Sc., and Ph.D. from Monash University, Australia. He has published over 280 scientific publications in structural stability, vibration and optimization. He is an Editor-in-Chief of the *International Journal of Structural Stability and Dynamics* and an editorial board member of the *Journal of Computational Structural Engineering.* He has co-authored two books *Vibration of Mindlin Plates* (with K. M. Liew et al.) and *Shear Deformable Beams and Plates: Relationships with Classical Solutions* (with J.N. Reddy and K.H. Lee), both published by Elsevier. Dr. Wang is the recipient of the NUS Innovative Teaching Awards 1997/1998 and the University Teaching Excellence Awards 1998/1999.

**C. Y. Wang** is Professor of Mathematics, with joint appointments in the Departments of Physiology and Mechanical Engineering, at Michigan State University, East Lansing, Michigan. He obtained B.S. from Taiwan University and Ph.D. from Massachusetts Institute of Technology. Dr. Wang has published over 320 papers in fluid mechanics (unsteady viscous flow, exact solutions, Stokes flow), solid mechanics (elastica, torsion, stability, vibrations) and heat transfer and biomechanics. Dr. Wang published a monograph on *Perturbation Methods* (printed by Taiwan University). He is currently serving as a Technical Editor for *Applied Mechanics Reviews.*

**J. N. Reddy** is a Distinguished Professor and the holder of the Oscar S. Wyatt Endowed Chair in the Department of Mechanical Engineering at Texas A&M University, College Station, Texas. He is the author of over 300 journal papers and 13 other books, including *An Introduction to the Finite Element Method* (3rd ed.), McGraw-Hill; *Mechanics of Laminated Composite Plates and Shells: Theory and Analysis* (2nd ed.), CRC Press; *Theory and Analysis of Elastic Plates,* Taylor & Francis; *Energy Principles and Variational Methods in Applied Mechanics* (2nd ed.), John Wiley & Sons; and *An Introduction to Nonlinear Finite Element Analysis,* Oxford University Press. Professor Reddy is the main editor of the journal *Mechanics of Advanced Materials and Structures*, an Editor-in-Chief of *International Journal of Computational Methods in Engineering Science and Mechanics* and *International Journal of Structural Stability and Dynamics*, and serves on the editorial boards of over two dozen other journals.

# Preface

In his book "Structural Design via Optimality Criteria", George Rozvany articulates William Prager's personal preferences in research on structural mechanics which may be summarized as:

- Research should reveal some fundamental and unexpected features of the structural problem studied.
- Closed form analytical solutions are preferable to numerical ones because the latter often obscure intrinsic features of the solution.
- Proofs should be based, whenever possible, on principles of mechanics rather than advanced mathematical concepts in order to make them comprehensible to the majority of engineers.
- The most challenging and intellectually stimulating problems should be selected in preference to routine exercises.

A large number of papers published in the high impact factored journals bear testimony to the fact that many researchers do subscribe to Professor Prager's research values. The authors, in particular, found it challenging to obtain closed form analytical solutions which elucidate the intrinsic, fundamental and unexpected features of the solution. It is this interest for analytical solutions that drove the authors to collate the closed form buckling solutions of columns, beams, arches, rings, plates and shells that are dispersed in the vast literature into a single volume. Here, we define a closed form solution as one that can be expressed in terms of a finite number of terms and it may contain elementary or common functions such as harmonic or Bessel functions (special functions such as hypergeometric functions will be excluded). In elastic buckling, the solution (critical buckling load) may indeed sometimes be of closed form, but these solutions are few. We have therefore expanded the contents of this book to include closed form characteristic equations that furnish the critical buckling load. We admit that these characteristic equations could be transcendental and do not yield a closed form buckling solution. However, nowadays a simple root search (such as the bisection technique) would yield the buckling load to any desired accuracy. What is not included in this book are buckling loads that require solution of partial or ordinary differential equations by numerical methods.

Chapter 1 gives the introduction to buckling and the importance of the critical buckling load in design. Chapter 2 presents the flexural buckling solutions for columns under various loading, restraints and boundary conditions. The effect of transverse shear deformation on the buckling load of columns, a brief discussion on the flexural–torsional buckling of columns for thin-walled members with open-profile, and inelastic buckling of columns are presented in Chapter 2. Chapter 3 contains the exact flexural–torsional buckling solutions of beams and the buckling solutions of circular arches and rings. Chapter 4 deals with the buckling of thin and thick plates under inplane loads for various shapes and boundary conditions. Results for inelastic buckling of circular, rectangular and polygonal plates are also presented. Finally, Chapter 5 presents buckling solutions for cylindrical shells, spherical shells and truncated conical shells.

It is hoped that this book will be a useful reference source for benchmark solutions that is so needed in checking the validity, accuracy and convergence of numerical results.

This book contains so many mathematical equations and numbers that it is impossible not to have typographical and other kinds of errors. We wish to thank in advance those readers who are willing to draw attention to typos and errors, using the e-mail addresses: *cvewcm@nus.edu.sg*, *cywang@math.msu.edu*, or *jnreddy@tamu.edu*.

*C. M. Wang*
Singapore

*C. Y. Wang*
East Lansing, Michigan

*J. N. Reddy*
College Station, Texas

# Contents

CHAPTER 1

# INTRODUCTION

## 1.1 What Is Buckling?

When a slender structure is loaded in compression, for small loads it deforms with hardly any noticeable change in geometry and load-carrying ability. On reaching a critical load value, the structure suddenly experiences a large deformation and it may lose its ability to carry the load. At this stage, the structure is considered to have buckled. For example, when a rod is subjected to an axial compressive force, it first shortens slightly but at a critical load the rod bows out, and we say that the rod has buckled. In the case of a thin circular ring under radial pressure, the ring decreases in size slightly before buckling into a number of circumferential waves. For a cruciform column under axial compression, it shortens and then buckles in torsion.

Buckling, also known as structural instability, may be classified into two categories [Galambos (1988) and Chen and Lui (1987)]: (1) *bifurcation buckling* and (2) *limit load buckling.* In bifurcation buckling, the deflection under compressive load changes from one direction to a different direction (e.g., from axial shortening to lateral deflection). The load at which the bifurcation occurs in the load-deflection space is called the *critical buckling load* or simply *critical load.* The deflection path that exists prior to bifurcation is known as the *primary path*, and the deflection path after bifurcation is called the *secondary* or *postbuckling path.* Depending on the structure and loading, the secondary path may be symmetric or asymmetric, and it may rise or fall below the critical buckling load (see Fig. 1.1). In limit load buckling, the structure attains a maximum load without any previous bifurcation, i.e., with only a single mode of deflection (see Fig. 1.2). The snap-through (observed in shallow arches and spherical caps) and finite-disturbance buckling (only unique to shells) are examples of limit load buckling. Other classifications of buckling are made according to the displacement magnitude (i.e., small or large), or static versus dynamic buckling, or material behavior such as elastic buckling or inelastic buckling (see El Naschie, 1990).
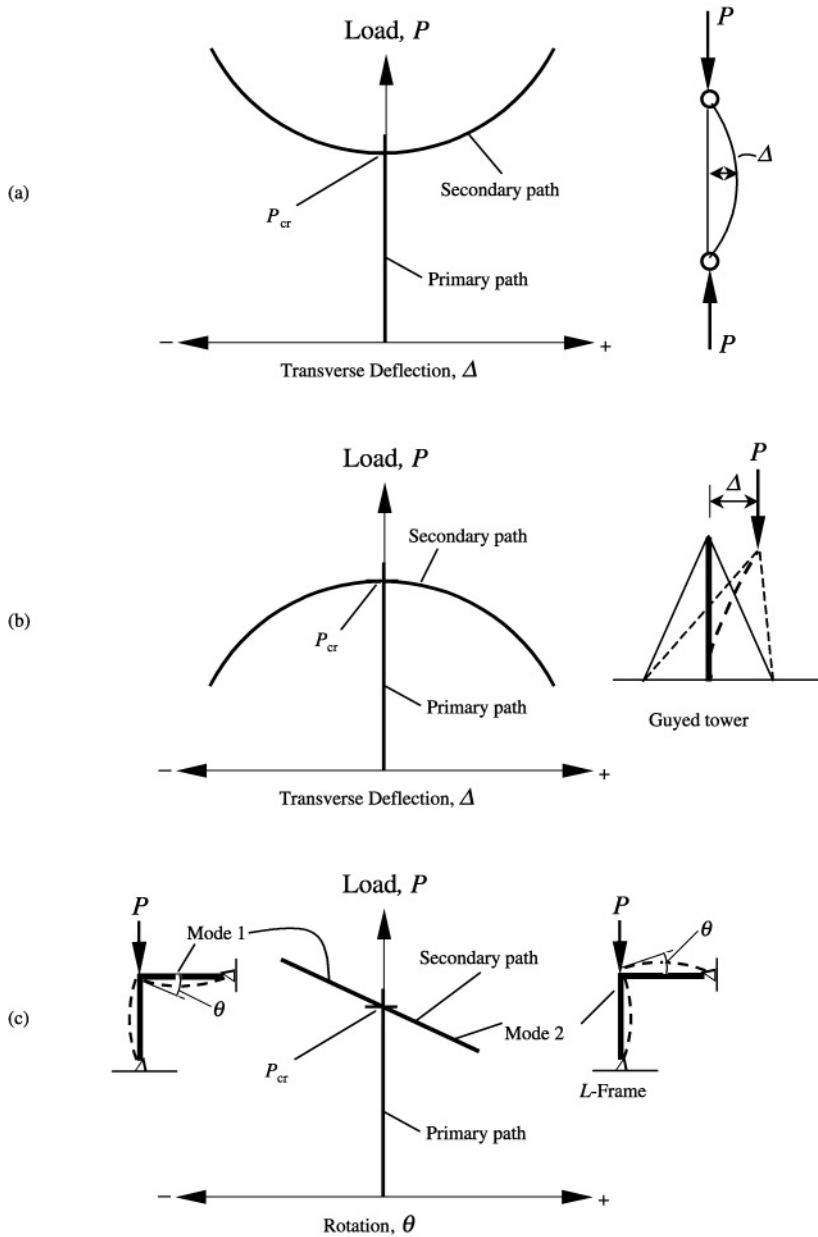
**Figure 1.1:** Bifurcation buckling: (a) symmetric bifurcation and stable postbuckling curve; (b) symmetric bifurcation and unstable postbuckling curve; (c) asymmetric bifurcation.
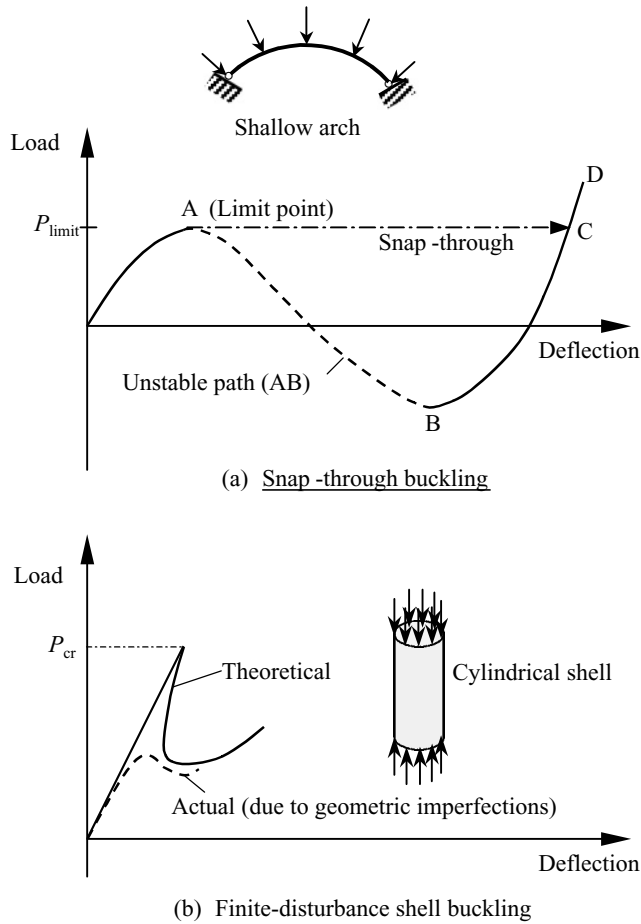
**Figure 1.2:** Limit load buckling: (a) snap-through buckling; and (b) finite-disturbance buckling.

## 1.2 Importance of Buckling Load

Design of structures is often based on strength and stiffness considerations. *Strength* is defined to be the ability of the structure to withstand the applied load, while *stiffness* is the resistance to deformation (i.e., the structure is sufficiently stiff not to deform beyond permissible limits). However, a structure may become unstable (in the sense described above) long before the strength and stiffness criteria

are violated. For example, one can show that a spherical shell made of concrete and with a thickness-to-radius ratio of $h/R = 1/500$ and modulus of $E = 20$ GPa buckles at a critical stress $[\sigma_{\mathrm{cr}} = k(Eh/R)$ and $k \approx 0.25]$ of 10MPa. However, the ultimate strength of the concrete is 21MPa. Thus, buckling load governs the design before the strength criterion does. Therefore, buckling is an important consideration in structural design, especially when the structure is slender and lightweight.

Linear elastic bifurcation buckling of structural members is the most elementary form of buckling, and its study is an essential step towards understanding the buckling behavior of complex structures, including structures incorporating inelastic behavior, initial imperfections, residual stresses, etc. [see Bažant (2000) and Bažant and Cedolin (1991)]. The load at which linear elastic buckling occurs is important, because it provides the basis for commonly used buckling formulas used in design codes. For example, the American Institute of Steel Construction (AISC) Load and Resistance Factor Design (LRFD, 1994) specification applies a moment-gradient factor, $C_b$, to the exact lateral buckling solution of beams under uniform moment in order to account for the variable moment along an unbraced steel girder length.

In the open literature and standard text books, buckling loads for different kinds of structures under various loading and boundary conditions are often expressed using approximate simple formulae and design charts to aid designers in estimating the buckling strength of structural members. It is still necessary, however, for designers to perform the buckling analysis if more accurate results are required or if there are no standard solutions available. Apart from a few problems (such as the elastic buckling of perfect and prismatic struts under an axial force or the lateral buckling of simply supported beams under uniform moment and axial force), it is generally rather laborious and in some cases impossible to obtain exact analytical solutions. Thus, it becomes necessary to resort to numerical techniques. In determining the elastic buckling load, there are many techniques. These techniques may be grouped under two general approaches: (a) the vector approach and (b) the energy approach (Reddy, 2002). In the vector approach, Newton's second law is used to obtain the governing equations, whereas in the energy approach the total energy (which is the sum of internal energy and potential energy due to the loads) is minimized to obtain the governing equations. They correspond to the different strategies used in satisfying the state of equilibrium for the deformed member. The governing equations are in the form of an eigenvalue problem in

which the eigenvalue represents the buckling load and eigenvector the buckling mode. The smallest buckling load is termed the *critical buckling load*. Note that the critical buckling load is associated with the state of neutral equilibrium, i.e., characterized by the stationarity condition of the load with respect to the displacement. In order to ascertain whether the equilibrium position is stable or unstable, we use the perturbation technique for the vector approach or by examining the second derivative of the total potential energy.

## 1.3 Historical Review

The first study on elastic stability is attributed to Leonhard Euler [1707–1783], who used the theory of calculus of variations to obtain the equilibrium equation and buckling load of a compressed elastic column. This work was published in the appendix "De curvis elasticis" of his book titled *Methodus inveniendi lineas curvas maximi minimive proprietate gaudentes*, Lausanne and Geneva, 1744. Joseph-Louis Lagrange [1736–1813] developed the energy approach that is more general than Newton's vector approach for the study of mechanics problems. This led naturally to the fundamental energy theorem of minimum total potential energy being sufficient for stability.

Jules Henry Poincaré [1854–1912] is known as the founder of bifurcation theory and the classification of the singularities. On the other hand, Aleksandr Mikhailovich Liapunov [1857–1918] gave the basic definitions of stability and introduced the generalized energy functions that bear his name, Liapunov functions. Furthermore, Lev Semenovich Pontryagin [1908–1988] introduced, with A. A. Andronov, the important topological concept of structural stability. This work has led to the well known classification theory presented in a treatise, *Stabilite structurelle et morphogenese: Essai d'une theorie generale des modeles (Structural Stability and Morphogenesis: An Outline of General Theory of Models)* by R. Thom.

Theodore von Kármán [1881–1963] began his work on inelastic buckling of columns. He devised a model to explain hysteresis loops and conducted research on plastic deformation of beams. Warner Tjardus Koiter [1914–1997] initiated the classical nonlinear bifurcation theory in his dissertation, "Over de Stabiliteit van het Elastisch Evenwicht", at Delft. Budiansky and his colleagues (1946, 1948) gave a modern account of the nonlinear branching of continuous elastic structures under conservative loads. Furthermore, Hutchinson (1973a, b) made an important contribution to the nonlinear branching theory of structures loaded in the plastic range.

Pioneering research by a number of other individuals is also significant and some of them are: F. Engesser and S. P. Timoshenko on buckling of shear–flexural buckling of columns; A. Considere, F. Engesser and F. R. Shanley on inelastic buckling of columns; G. R. Kirchhoff on buckling of elastica; J. A. Haringx on buckling of springs; V. Vlasov on torsional buckling; L. Prandtl, A. G. M. Michell, S. P. Timoshenko, H. Wagner and N. S. Trahair on flexural–torsional buckling of beams (see Trahair and Bradford, 1991); B. W. James, R. K. Livesly and D. B. Chandler, R. von Mises and J. Ratzersdorfer, and E. Chwalla on buckling of frames; H. Lamb, J. Boussinesq, C. B. Biezeno and J. J. Koch on buckling of rings and arches; E. Hurlbrink, E. Chwalla, E. L. Nicolai, I. J. Steuermann, A. N. Dinnik and K. Federhofer on arches; G. H. Bryan, S. P. Timoshenko, T. von Karman, E. Trefftz, A. Kromm, K. Marguerre and G. Herrmann on buckling (and postbuckling) of plates; G. H. Handelmann, W. Prager, E. I. Stowell, S. B. Batdorf, F. Bleich and P. P. Bijlaard on plastic buckling of plates; R. Lorentz, R. von Mises, S. P. Timoshenko, R. V. Southwell, T. von Kármán and H. S. Tsien on cylindrical shells under combined axial and lateral pressure; L. H. Donnell, K. M. Marguerre and K. M. Mushtari on the postbuckling of shells; A. Pflüger on buckling of conical shells; and R. Zoelly and E. Schwerin on buckling of spherical shells. Additional references can be found in the book by Timoshenko and Gere (1961) and the survey article by Bažant (2000).

## 1.4 Scope of the Book

In this book, we focus our attention on buckling characterized by bifurcation and static buckling. There is a fundamental difference between the formulations of static and buckling equilibrium problems of linear elasticity. In formulating the static equilibrium (differential) equations, the undeformed geometry is used to sum the forces and moments. In contrast, in deriving the buckling equilibrium equations one must use forces and moments acting on the deformed configuration under applied loads. The latter leads to eigenvalue problems in which the buckling load is the eigenvalue and buckling mode is the eigenvector.

Analytical solution of the eigenvalue problem is not possible for complicated geometries, boundary conditions and loads. In such cases, numerical methods are required. However, for some cases of structural geometries, loads and boundary conditions, it is possible to solve the differential equations exactly in closed form. In this book the authors present as many exact buckling solutions as possible in one single volume for ready use by engineers, academicians and researchers.

# REFERENCES

*Load and Resistance Factor Design,* 2nd ed. (1994), American Institute of Steel Construction, Chicago, Illinois, USA.

Bažant, Z. P. (2000), "Stability of elastic, anelastic, and disintegrating structures: a conspectus of main results," *ZAMM*, **80**(11–12), 709–732.

Bažant, Z. P. and Cedolin, L. (1991), *Stability Structures. Elastic, Inelastic Fracture and Damage Theories,* Oxford University Press, New York.

Budiansky, B. and Hu, P. C. (1946), "The Lagrangian multiplier method for finding upper and lower limits to critical stresses of clamped plates," NACA Report No. 848, Washington, DC.

Budiansky, B., Hu, P. C. and Connor, R. W. (1948), "Notes on the Lagrangian multiplier method in elastic-stability analysis," NACA Technical Note No. 1558, Washington, DC.

Chen, W. F. and Lui, E. M. (1987), *Structural Stability. Theory and Implementation,* PTR, Prentice-Hall, Englewood Cliffs, NJ.

El Naschie, M. S. (1990), *Stress, Stability, and Chaos in Structural Engineering: An Energy Approach,* McGraw-Hill, London, UK.

Galambos, T. V. (ed.) (1988), *Guide to Stability Design Criteria for Metal Structures,* 4th ed., John Wiley, New York.

Hutchinson, J. W. (1973a), "Postbifurcation behavior in the plastic range," *Journal of Mechanics and Physics of Solids,* **21**, 163–190.

Hutchinson, J. W. (1973b), "Imperfection–sensitivity in the plastic range," *Journal of Mechanics and Physics of Solids,* **21**, 191–204.

Reddy, J. N. (2002), *Energy Principles and Variational Methods in Applied Mechanics,* 2nd ed., John Wiley, New York.

Trahair, N. S. and Bradford, M. A. (1991), *The Behavior and Design of Steel Structures,* Revised 2nd ed., Chapman & Hall, London, UK.

Timoshenko, S. P. and Gere, J. M. (1961), *Theory of Elastic Stability,* McGraw-Hill, New York.

# CHAPTER 2
# BUCKLING OF COLUMNS

## 2.1 Euler Columns under End Axial Load

### 2.1.1 Governing Equations and Boundary Conditions

Consider a perfectly straight, uniform, homogeneous column of flexural rigidity $EI$, length $L$ which is subjected to an end axial compressive load $P$. The moment-displacement relation according to the Euler–Bernoulli beam theory is given by

$$M = -EI\frac{d^2\bar{w}}{d\bar{x}^2} \qquad (2.1.1)$$

in which $\bar{x}$ is the longitudinal coordinate measured from the column base, $\bar{w}$ the transverse displacement and $M$ the bending moment. The Euler–Bernoulli beam theory is based on the assumption that plane normal cross-sections of the beam remain plane and normal to the deflected centroidal axis of the beam, and the transverse normal stresses are negligible (Reddy, 2002).

It can be readily shown that the equilibrium equations are (Bažant and Cedolin, 1991)

$$\frac{dM}{d\bar{x}} = Q \qquad (2.1.2)$$

$$\frac{dQ}{d\bar{x}} = P\frac{d^2\bar{w}}{d\bar{x}^2} \qquad (2.1.3)$$

where $Q$ is the shear force normal to the deflected column axis. The substitution of Eqs. (2.1.1) and (2.1.2) into Eq. (2.1.3) yields the following governing Euler column buckling equation

$$\frac{d^4w}{dx^4} + \alpha\frac{d^2w}{dx^2} = 0, \quad \alpha = \frac{PL^2}{EI} \qquad (2.1.4)$$

where $w = \bar{w}/L$ and $x = \bar{x}/L$.

The general solution of (2.1.4) is

$$w = C_1 \sin \sqrt{\alpha}x + C_2 \cos \sqrt{\alpha}x + C_3 x + C_4 \qquad (2.1.5)$$

The four constants $C_i$ $(i = 1, 2, 3, 4)$ can be evaluated by the two boundary conditions at each end of the column, which may be written in the following general forms

$$\bar{s}_1 w + \bar{s}_2 \frac{dw}{dx} + \bar{s}_3 \frac{d^2 w}{dx^2} + \bar{s}_4 \frac{d^3 w}{dx^3} = 0 \qquad (2.1.6)$$

and

$$\hat{s}_1 w + \hat{s}_2 \frac{dw}{dx} + \hat{s}_3 \frac{d^2 w}{dx^2} + \hat{s}_4 \frac{d^3 w}{dx^3} = 0 \qquad (2.1.7)$$

where $\bar{s}_i$ and $\hat{s}_i$ are parameters whose values will be apparent in the sequel.

By substituting Eq. (2.1.5) into the boundary conditions given by Eqs. (2.1.6) and (2.1.7) at $x = 0$ and $x = 1$, we obtain four homogeneous equations which may be expressed as

$$
\begin{bmatrix}
\sqrt{\alpha}(\bar{s}_2^0 - \bar{s}_4^0 \alpha) & \bar{s}_1^0 - \bar{s}_3^0 \alpha & \bar{s}_2^0 & \bar{s}_1^0 \\[4pt]
\sqrt{\alpha}(\hat{s}_2^0 - \hat{s}_4^0 \alpha) & \hat{s}_1^0 - \hat{s}_3^0 \alpha & \hat{s}_2^0 & \hat{s}_1^0 \\[4pt]
\begin{array}{l} \bar{s}_1^1 \sin\sqrt{\alpha} + \bar{s}_2^1 \sqrt{\alpha}\cos\sqrt{\alpha} \\ -\bar{s}_3^1 \alpha \sin\sqrt{\alpha} - \bar{s}_4^1 \alpha\sqrt{\alpha}\cos\sqrt{\alpha} \end{array} & \begin{array}{l} \bar{s}_1^1 \cos\sqrt{\alpha} - \bar{s}_2^1 \sqrt{\alpha}\sin\sqrt{\alpha} \\ -\bar{s}_3^1 \alpha\cos\sqrt{\alpha} + \bar{s}_4^1 \alpha\sqrt{\alpha}\sin\sqrt{\alpha} \end{array} & \bar{s}_1^1 + \bar{s}_2^1 & \bar{s}_1^1 \\[12pt]
\begin{array}{l} \hat{s}_1^1 \sin\sqrt{\alpha} + \hat{s}_2^1 \sqrt{\alpha}\cos\sqrt{\alpha} \\ -\hat{s}_3^1 \alpha \sin\sqrt{\alpha} - \hat{s}_4^1 \alpha\sqrt{\alpha}\cos\sqrt{\alpha} \end{array} & \begin{array}{l} \hat{s}_1^1 \cos\sqrt{\alpha} - \hat{s}_2^1 \sqrt{\alpha}\sin\sqrt{\alpha} \\ -\hat{s}_3^1 \alpha\cos\sqrt{\alpha} + \hat{s}_4^1 \alpha\sqrt{\alpha}\sin\sqrt{\alpha} \end{array} & \hat{s}_1^1 + \hat{s}_2^1 & \hat{s}_1^1
\end{bmatrix}
$$

$$
\times
\begin{Bmatrix} C_1 \\ C_2 \\ C_3 \\ C_4 \end{Bmatrix}
=
\begin{Bmatrix} 0 \\ 0 \\ 0 \\ 0 \end{Bmatrix}
\qquad (2.1.8)
$$

where the superscript '0' ('1') of $s$ identifies the value of $s$ at $x = 0$ $(x = 1)$. For example, the boundary conditions for a clamped end at $x = 0$ would be defined by $\bar{s}_1^0 = \hat{s}_2^0 = 1$, $\bar{s}_2^0 = \bar{s}_3^0 = \bar{s}_4^0 = \hat{s}_1^0 = \hat{s}_3^0 = \hat{s}_4^0 = 0$.

The stability criterion is furnished by the vanishing of the determinant of the above matrix. This general stability criterion applies to all kinds of boundary conditions which are embedded in the general boundary conditions given in Eqs. (2.1.6) and (2.1.7). Below we present the stability criteria and critical loads for columns with various forms of boundary equations.

## 2.1.2 Columns with Classical Boundary Conditions
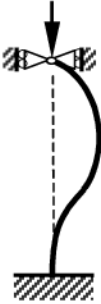
The classical boundary conditions are given below.

- Fixed end: $w = 0$ and $\frac{dw}{dx} = 0$

- Pinned end: $w = 0$ and $\frac{d^2w}{dx^2} = 0$

- Free end: $\frac{d^2w}{dx^2} = 0$ and $\frac{d^3w}{dx^3} + \alpha\frac{dw}{dx} = 0$

- Sliding restraint: $\frac{dw}{dx} = 0$ and $\frac{d^3w}{dx^3} + \alpha\frac{dw}{dx} = 0$

where $\alpha$ denotes the stability parameter defined in Eq. (2.1.4).

The stability criteria and the critical buckling load (smallest eigenvalue) for columns with classical end restraints are summarized in Table 2.1.

**Table 2.1:** Classical Euler column restraints and critical loads.

| Classical Cases | C–F Column | P–P Column | C–P Column | C–C Column | C–S Column |
|---|---|---|---|---|---|
| Nonzero values of $\bar{s}$ and $\hat{s}$ | $\bar{s}_1^0 = \hat{s}_2^0 = 1$ $\bar{s}_3^1 = \hat{s}_4^1 = 1$ $\hat{s}_2^1 = \alpha$ | $\bar{s}_1^0 = \hat{s}_3^0 = 1$ $\bar{s}_1^1 = \hat{s}_3^1 = 1$ | $\bar{s}_1^0 = \hat{s}_2^0 = 1$ $\bar{s}_1^1 = \hat{s}_3^1 = 1$ | $\bar{s}_1^0 = \hat{s}_2^0 = 1$ $\bar{s}_1^1 = \hat{s}_2^1 = 1$ | $\bar{s}_1^0 = \hat{s}_2^0 = 1$ $\bar{s}_2^1 = \hat{s}_4^1 = 1$ $\hat{s}_1^2 = \alpha$ |
| Buckled shape |  |  |  |  |  |
| Stability Criterion | $\cos\sqrt{\alpha} = 0$ | $\sin\sqrt{\alpha} = 0$ | $\sqrt{\alpha} = \tan\sqrt{\alpha}$ | $\sin\frac{\sqrt{\alpha}}{2} = 0$ | $\cos\frac{\sqrt{\alpha}}{2} = 0$ |
| Critical Buckling Load | $\alpha = \frac{\pi^2}{4}$ | $\alpha = \pi^2$ | $\alpha = 2.0457\pi^2$ | $\alpha = 4\pi^2$ | $\alpha = \pi^2$ |

C = clamped (fixed); F = free; P = pinned; S = sliding restraint.

### 2.1.3 Columns with Elastic End Restraints

In the general case of a column with elastic restraints as shown in Fig. 2.1, one of the boundary conditions has the form

$$w(0) = 0 \qquad (2.1.9)$$

whereas the other three conditions can be written in the form

$$\xi_0 \left[ \frac{dw}{dx} \right]_{x=0} - \left[ \frac{d^2w}{dx^2} \right]_{x=0} = 0 \qquad (2.1.10)$$

$$\xi_1 \left[ \frac{dw}{dx} \right]_{x=1} + \left[ \frac{d^2w}{dx^2} \right]_{x=1} = 0 \qquad (2.1.11)$$

$$\zeta w(1) + \left[ \frac{d^3w}{dx^3} + \alpha \frac{dw}{dx} \right]_{x=1} = 0 \qquad (2.1.12)$$

Here, $\xi_0$ and $\xi_1$ represent the rotational spring constants. Zero values of $\xi_0$ and $\xi_1$ imply free rotation of the column end and infinite values imply no rotation at the column end; $\zeta$ denotes the translational spring constant against sidesway, with a zero value implying free lateral translation and an infinite value implying no lateral translation at that column end. The foregoing boundary conditions imply the nonzero values of $\bar{s}$ and $\hat{s}$ listed in Eq. (2.1.13) on the next page.
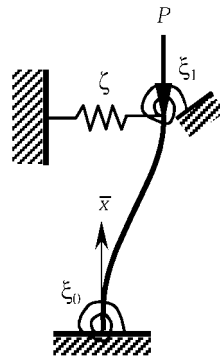


**Figure 2.1:** Buckling of column with elastic end restraints.

$$\bar{s}_1^0 = 1, \quad \hat{s}_2^0 = \xi_0, \quad \hat{s}_3^0 = -1, \quad \bar{s}_2^1 = \xi_1,$$
$$\bar{s}_3^1 = 1, \quad \hat{s}_1^1 = \zeta, \quad \hat{s}_2^1 = \alpha, \quad \hat{s}_4^1 = 1 \tag{2.1.13}$$

Thus, the general stability criterion reduces to

$$\begin{vmatrix} 0 & 1 & 0 & 1 \\ \sqrt{\alpha}\xi_0 & \alpha & \xi_0 & 0 \\ \sqrt{\alpha}\xi_1 \cos\sqrt{\alpha} - \alpha\sin\sqrt{\alpha} & -\sqrt{\alpha}\xi_1\sin\sqrt{\alpha} - \alpha\cos\sqrt{\alpha} & \xi_1 & 0 \\ \zeta\sin\sqrt{\alpha} & \zeta\cos\sqrt{\alpha} & \zeta+\alpha & \zeta \end{vmatrix} = 0 \tag{2.1.14}$$

or in the form of a transcendental equation given by

$$2 + \left[ -1 + \left( \frac{1}{\xi_0} + \frac{1}{\xi_1} \right) + \alpha \left( \frac{1}{\xi_0\xi_1} - \frac{1}{\zeta} + \frac{\alpha}{\xi_0\xi_1\zeta} \right) \right] \sqrt{\alpha}\sin\sqrt{\alpha}$$
$$- \left[ 2 + \alpha \left( \frac{1}{\xi_0} + \frac{1}{\xi_1} \right) \left( 1 + \frac{\alpha}{\zeta} \right) \right] \cos\sqrt{\alpha} = 0 \tag{2.1.15}$$

The above problem may be specialized to the various end conditions given next.

• If the top end is elastically laterally supported with spring constant $\zeta$ (and $\xi_1 = 0$) while the lower end is fixed $\xi_0 = \infty$, Eq. (2.1.15) reduces to

$$\sqrt{\alpha}\left( 1 + \frac{\alpha}{\zeta} \right) - \tan\sqrt{\alpha} = 0 \tag{2.1.16}$$

• If the top end is elastically laterally supported with spring constant $\zeta$ (and $\xi_1 = 0$) while the lower end is elastically rotationally supported with spring constant $\xi_0$, Eq. (2.1.15) reduces to

$$\left[ 1 + \frac{\alpha}{\xi_0}\left( 1 + \frac{\alpha}{\zeta} \right) \right] \sqrt{\alpha}\tan\sqrt{\alpha} - \left[ 1 + \alpha\left( 1 + \frac{\alpha}{\zeta} \right) \right] = 0 \tag{2.1.17}$$

• If the top end is prevented from lateral movement, $\zeta = \infty$, Eq. (2.1.15) reduces to

$$[2\xi_0\xi_1 + \alpha(\xi_0 + \xi_1)]\cos\sqrt{\alpha} - \sqrt{\alpha}(\alpha + \xi_0 + \xi_1 - \xi_0\xi_1)\sin\sqrt{\alpha} - 2\xi_0\xi_1 = 0 \tag{2.1.18}$$

The results for some special cases are shown in the first part of Table 2.2. Owing to symmetry, the normalized spring constants $\xi_0$ and $\xi_1$ can be interchanged. When the spring constants are both zero, the critical load is $\pi^2$, which is the same as that for a column with both ends pinned.

When the spring constants are both infinite, the critical load is $4\pi^2$, the same as that for the column with both ends fixed. The value of 20.191, of course, is $2.0457\pi^2$ of the fixed–pinned column.

• If there is no lateral constraint, or the top end can freely slide laterally, $\zeta = 0$, Eq. (2.1.15) reduces to

$$\sqrt{\alpha}(\xi_0 + \xi_1) + (\xi_0\xi_1 - \alpha)\tan\sqrt{\alpha} = 0 \qquad (2.1.19)$$

Sample critical load parameters are given in the second part of Table 2.2. In this case, the critical load is zero when the spring constants are zero, since the column can have a rigid rotation. The critical value of $\pi^2$ corresponds to the classical fixed–sliding restraint column in section 2.1.2 and the value of $\pi^2/4$ corresponds to the classical fixed–free column.

**Table 2.2:** Critical load parameters $\alpha$ for columns with various elastic end conditions.

| $\xi_1$ | $\xi_0$ | | | | | | | |
|---|---|---|---|---|---|---|---|---|
| | 0 | 0.5 | 1 | 2 | 4 | 10 | 20 | $\infty$ |
| Columns with only end rotational restraints | | | | | | | | |
| $\xi_0$ | $\pi^2$ | 11.772 | 13.492 | 16.463 | 20.957 | 28.168 | 30.355 | $4\pi^2$ |
| 0 | $\pi^2$ | 10.798 | 11.598 | 12.894 | 14.660 | 17.076 | 18.417 | 20.191 |
| $\infty$ | 20.191 | 21.659 | 22.969 | 25.182 | 28.397 | 33.153 | 35.902 | $4\pi^2$ |
| Columns with the top end free to slide laterally | | | | | | | | |
| $\xi_0$ | 0 | 0.9220 | 1.7071 | 2.9607 | 4.6386 | 6.9047 | 8.1667 | $\pi^2$ |
| 0 | 0 | 0.4268 | 0.7402 | 1.1597 | 1.5992 | 2.0517 | 2.2384 | $\pi^2/4$ |
| $\infty$ | $\pi^2/4$ | 3.3731 | 4.1159 | 5.2392 | 6.6071 | 8.1955 | 8.9583 | $\pi^2$ |

## 2.2 Euler Columns under End Load Dependent on Direction

Consider a fixed–free, uniform homogeneous column of flexural rigidity $EI$, length $L$ which is subjected to a load $P$ that is dependent on the deflection and slope of the free end of the buckled column as shown by the various column problems in Fig. 2.2 (Zyczkowski, 1991).

For such columns, the governing buckling equation and the general solutions are given by Eq. (2.1.4) and Eq. (2.1.5), respectively. The boundary conditions may be canonically written as
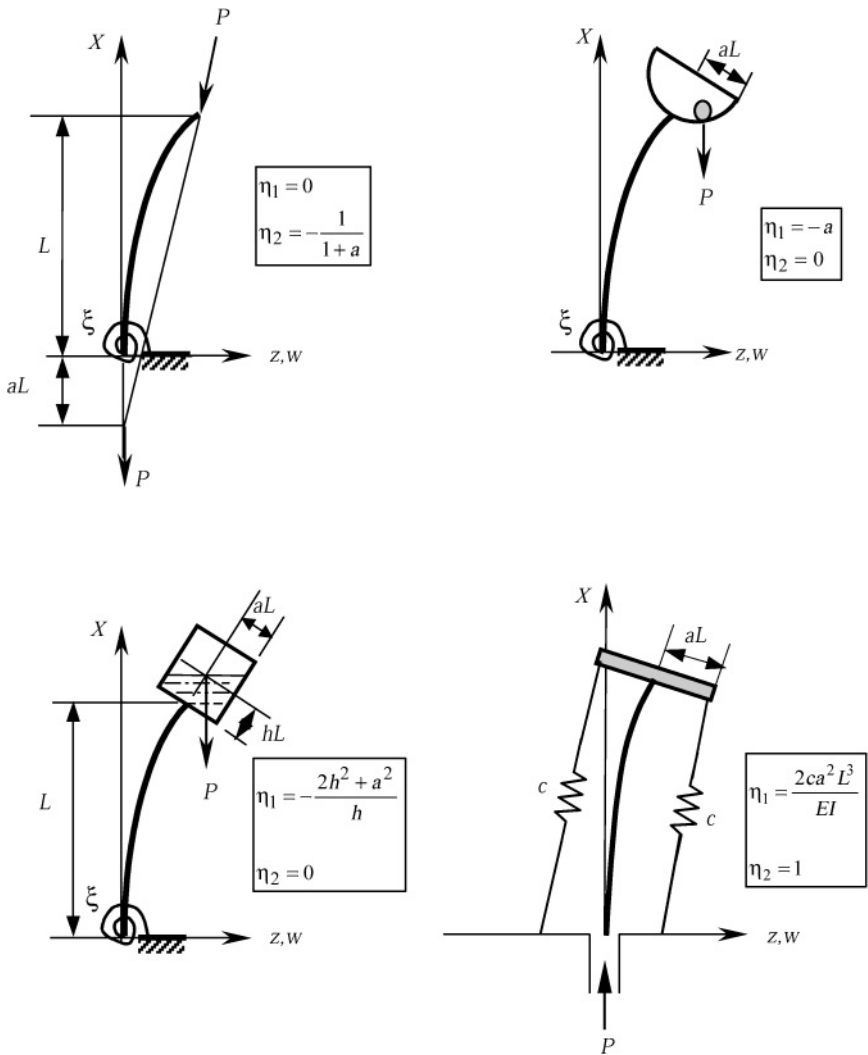
**Figure 2.2:** Buckling of various types of columns.

$$w(0) = 0 \tag{2.2.1}$$

$$\left[ \xi \frac{dw}{dx} - \frac{d^2w}{dx^2} \right]_{x=0} = 0 \tag{2.2.2}$$

$$\left[ \frac{d^2w}{dx^2} + \alpha\eta_1 \frac{dw}{dx} \right]_{x=1} = 0 \tag{2.2.3}$$

$$\left[ \frac{d^3w}{dx^3} + \alpha \frac{dw}{dx} \right]_{x=1} + \alpha\eta_2 w(1) = 0 \tag{2.2.4}$$

where $\eta_1$ and $\eta_2$ are nondimensional parameters defined in Fig. 2.2 and $\alpha = PL^2/(EI)$.

In view of the general solution given by Eq. (2.1.5) and the aforementioned boundary conditions, the stability criteria take the following transcendental form

$$
\begin{aligned}
2 + &\left[ -1 + \left( \frac{1}{\xi} + \frac{1}{\alpha\eta_1} \right) + \left( \frac{1}{\xi\eta_1} - \frac{1}{\eta_2} + \frac{1}{\xi\eta_1\eta_2} \right) \right] \sqrt{\alpha} \sin\sqrt{\alpha} \\
&- \left[ 2 + \alpha \left( \frac{1}{\xi} + \frac{1}{\alpha\eta_1} \right) \left( 1 + \frac{1}{\eta_2} \right) \right] \cos\sqrt{\alpha} = 0
\end{aligned}
\tag{2.2.5}
$$

As an example, the stability criterion for the fixed–free column problem with load through the fixed point a vertical distance $aL$ below the fixed end is given by Eq. (1.20) with $\xi = \infty$, $\eta_1 = 0$ and $\eta_2 = -[1/(1+a)]$:

$$a\sqrt{\alpha} + \tan\sqrt{\alpha} = 0 \tag{2.2.6}$$

Table 2.3 presents some sample critical load parameters furnished by the above stability criterion.

**Table 2.3:** Critical load parameters $\sqrt{\alpha}$ for fixed–free column with load through a fixed point.

| $a$ | 0.1 | 0.2 | 0.3 | 0.5 | 0.7 | 0.9 | 1.0 |
|---|---|---|---|---|---|---|---|
| $\sqrt{\alpha}$ | 2.86277 | 2.65366 | 2.49840 | 2.28893 | 2.15598 | 2.06453 | 2.02876 |

## 2.3 Euler Columns with an Intermediate Axial Load

This section presents exact stability criteria for the elastic buckling of columns with intermediate and end concentrated axial loads (Wang,

Wang and Nazmul, 2003). An obvious practical example for the application of the criteria is the determination of the buckling capabilities of columns in structural buildings that have to support intermediate floors.

Consider a uniform homogeneous column of flexural rigidity $EI$ and length $L$. It is subjected to a concentrated axial force $P_2$ at its top end and a concentrated axial force $P_1$ at a distance of $\bar{x} = aL$ from the bottom end as shown in Fig. 2.3.
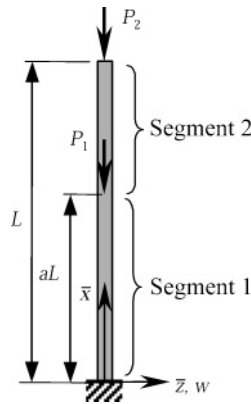


**Figure 2.3:** Column with intermediate and end axial loads.

To solve this column buckling problem, we divide the column into two segments, *viz.* segment 1 $(0 \leq \bar{x} < aL)$ and segment 2 $(aL \leq \bar{x} \leq L)$. Also, we can identify a number of cases, depending on the nature (compressive or tensile) or magnitude of the two applied forces. Noting the positive direction of $P$ as shown in Fig. 2.3, the nontrivial cases are:

- Case 1: $P_2 > 0$ and $(P_1 + P_2) > 0$, implying that both segments 1 and 2 are in compression.

- Case 2a: $P_2 > 0$ and $(P_1 + P_2) < 0$, implying that segment 2 is in compression while segment 1 is in tension.

- Case 2b: $P_2 < 0$ and $(P_1 + P_2) > 0$, implying that segment 2 is in tension while segment 2 is in compression.

- Case 3a: $P_2 = 0$ and $P_1 > 0$, implying that segment 2 is subjected to zero axial load while segment 1 is in compression.

- Case 3b: $P_2 > 0$ and $P_1 + P_2 = 0$, implying that segment 2 is in compression while segment 1 has zero axial load.

It is clear that one can obtain Case 2b from Case 2a through suitable parametric changes; the same applies for Case 3a and Case 3b. Therefore, we shall also focus our attention on Cases 1, 2a and 3a to avoid routine repetitive derivations. Table 2.4 summarizes the governing equations and the general solutions for the two segments for Cases 1, 2a and 3a.

**Table 2.4:** Governing equations and general solutions for Cases 1, 2a and 3a.

| Cases | (1) $P_2 > 0, P_1 + P_2 > 0$ | (2a) $P_2 > 0, P_1 + P_2 < 0$ | (3a) $P_2 = 0, P_1 > 0$ |
|---|---|---|---|
| | $\frac{d^4 w_2}{dx^4} + \alpha_2 \frac{d^2 w_2}{dx^2} = 0$ | $\frac{d^4 w_2}{dx^4} + \alpha_2 \frac{d^2 w_2}{dx^2} = 0$ | $\frac{d^4 w_2}{dx^4} = 0$ |
| | $\alpha_2 = \frac{P_2 L^2}{EI}$ | $\alpha_2 = \frac{P_2 L^2}{EI}$ | $\alpha_2 = 0$ |
| | $\frac{d^4 w_1}{dx^4} + \alpha_1 \frac{d^2 w_1}{dx^2} = 0$ | $\frac{d^4 w_1}{dx^4} + \alpha_1 \frac{d^2 w_1}{dx^2} = 0$ | $\frac{d^4 w_1}{dx^4} + \alpha_1 \frac{d^2 w_1}{dx^2} = 0$ |
| | $\alpha_1 = \frac{(P_1 + P_2) L^2}{EI}$ | $\alpha_1 = \frac{|P_1 + P_2| L^2}{EI}$ | $\alpha_1 = \frac{P_1 L^2}{EI}$ |
| | $w_2 = C_1 \sin \sqrt{\alpha_2} x$ $+ C_2 \cos \sqrt{\alpha_2} x$ $+ C_3 x + C_4$ | $w_2 = C_1 \sin \sqrt{\alpha_2} x$ $+ C_2 \cos \sqrt{\alpha_2} x$ $+ C_3 x + C_4$ | $w_2 = C_1 x^3 + C_2 x^2$ $+ C_3 x + C_4$ |
| | $w_1 = B_1 \sin \sqrt{\alpha_1} x$ $+ B_2 \cos \sqrt{\alpha_1} x$ $+ B_3 x + B_4$ | $w_1 = B_1 \sinh \sqrt{\alpha_1} x$ $+ B_2 \cosh \sqrt{\alpha_1} x$ $+ B_3 x + B_4$ | $w_1 = B_1 \sin \sqrt{\alpha_1} x$ $+ B_2 \cos \sqrt{\alpha_1} x$ $+ B_3 x + B_4$ |

The solutions contain eight constants, *viz.* $B_i$ and $C_i$ $(i = 1, 2, 3, 4)$, as shown in Table 2.4. However, these constants are related to each other through the following four continuity relations at $x = a$:

$$w_1 = w_2 \tag{2.3.1}$$

$$\frac{dw_1}{dx} = \frac{dw_2}{dx} \tag{2.3.2}$$

$$\frac{d^2 w_1}{dx^2} = \frac{d^2 w_2}{dx^2} \tag{2.3.3}$$

and

$$\frac{d^3 w_1}{dx^3} + \alpha_1 \frac{dw_1}{dx} = \frac{d^3 w_2}{dx^3} + \alpha_2 \frac{dw_2}{dx} \quad \text{for Case 1} \tag{2.3.4a}$$

$$\frac{d^3 w_1}{dx^3} - \alpha_1 \frac{dw_1}{dx} = \frac{d^3 w_2}{dx^3} + \alpha_2 \frac{dw_2}{dx} \quad \text{for Case 2a} \tag{2.3.4b}$$

$$\frac{d^3 w_1}{dx^3} + \alpha_1 \frac{dw_1}{dx} = \frac{d^3 w_2}{dx^3} \quad \text{for Case 3a} \tag{2.3.4c}$$

where $\alpha_1$ and $\alpha_2$ are defined in .

**Case 1:** The relationships between the constants are given by

$$B_1 = C_1 \frac{\sqrt{\alpha_2}}{\alpha_1} \left[ \sqrt{\alpha_1} \cos\left(a\sqrt{\alpha_1}\right) \cos\left(a\sqrt{\alpha_2}\right) + \sqrt{\alpha_2} \sin\left(a\sqrt{\alpha_1}\right) \sin\left(a\sqrt{\alpha_2}\right) \right]$$
$$- C_2 \frac{\sqrt{\alpha_2}}{\alpha_1} \left[ \sqrt{\alpha_1} \cos\left(a\sqrt{\alpha_1}\right) \sin\left(a\sqrt{\alpha_2}\right) - \sqrt{\alpha_2} \sin\left(a\sqrt{\alpha_1}\right) \cos\left(a\sqrt{\alpha_2}\right) \right]$$
$$- C_3 \frac{\beta}{\sqrt{\alpha_1}} \cos\left(a\sqrt{\alpha_1}\right) \tag{2.3.5a}$$

$$B_2 = C_1 \frac{\sqrt{\alpha_2}}{\alpha_1} \left[ -\sqrt{\alpha_1} \sin\left(a\sqrt{\alpha_1}\right) \cos\left(a\sqrt{\alpha_2}\right) + \sqrt{\alpha_2} \cos\left(a\sqrt{\alpha_1}\right) \sin\left(a\sqrt{\alpha_2}\right) \right]$$
$$+ C_2 \frac{\sqrt{\alpha_2}}{\alpha_1} \left[ \sqrt{\alpha_1} \sin\left(a\sqrt{\alpha_1}\right) \sin\left(a\sqrt{\alpha_2}\right) + \sqrt{\alpha_2} \cos\left(a\sqrt{\alpha_1}\right) \cos\left(a\sqrt{\alpha_2}\right) \right]$$
$$+ C_3 \frac{\beta}{\sqrt{\alpha_1}} \sin\left(a\sqrt{\alpha_1}\right) \tag{2.3.5b}$$

$$B_3 = C_3 \frac{\alpha_2}{\alpha_1} \tag{2.3.5c}$$

$$B_4 = -\beta \left[ C_1 \sin\left(a\sqrt{\alpha_2}\right) + C_2 \cos\left(a\sqrt{\alpha_2}\right) + C_3 a \right] + C_4 \tag{2.3.5d}$$

where

$$\beta = \frac{\alpha_2}{\alpha_1} - 1 \tag{2.3.5e}$$

**Case 2a:** For this case, we find that

$$B_1 = C_1 \frac{\sqrt{\alpha_2}}{\alpha_1} \left[ \sqrt{\alpha_1} \cosh\left(a\sqrt{\alpha_1}\right) \cos\left(a\sqrt{\alpha_2}\right) + \sqrt{\alpha_2} \sinh\left(a\sqrt{\alpha_1}\right) \sin\left(a\sqrt{\alpha_2}\right) \right]$$
$$+ C_2 \frac{\sqrt{\alpha_2}}{\alpha_1} \left[ -\sqrt{\alpha_1} \cosh\left(a\sqrt{\alpha_1}\right) \sin\left(a\sqrt{\alpha_2}\right) + \sqrt{\alpha_2} \sinh\left(a\sqrt{\alpha_1}\right) \cos\left(a\sqrt{\alpha_2}\right) \right]$$
$$+ C_3 \frac{\gamma}{\sqrt{\alpha_1}} \cosh\left(a\sqrt{\alpha_1}\right) \tag{2.3.6a}$$

$$B_2 = -C_1 \frac{\sqrt{\alpha_2}}{\alpha_1} \left[ \sqrt{\alpha_1} \sinh\left(a\sqrt{\alpha_1}\right) \cos\left(a\sqrt{\alpha_2}\right) + \sqrt{\alpha_2} \cosh\left(a\sqrt{\alpha_1}\right) \sin\left(a\sqrt{\alpha_2}\right) \right]$$
$$- C_2 \frac{\sqrt{\alpha_2}}{\alpha_1} \left[ -\sqrt{\alpha_1} \sinh\left(a\sqrt{\alpha_1}\right) \sin\left(a\sqrt{\alpha_2}\right) + \sqrt{\alpha_2} \cosh\left(a\sqrt{\alpha_1}\right) \cos\left(a\sqrt{\alpha_2}\right) \right]$$
$$- C_3 \frac{\gamma}{\sqrt{\alpha_1}} \sinh\left(a\sqrt{\alpha_1}\right) \tag{2.3.6b}$$

$$B_3 = -C_3 \frac{\alpha_2}{\alpha_1} \tag{2.3.6c}$$

$$B_4 = \gamma \left[ C_1 \sin\left(a\sqrt{\alpha_2}\right) + C_2 \cos\left(a\sqrt{\alpha_2}\right) + C_3 a \right] + C_4 \tag{2.3.6d}$$

where

$$\gamma = \frac{\alpha_2}{\alpha_1} + 1 \tag{2.3.6e}$$

**Case 3a:** For this case, we find that

$$B_1 = C_1 \frac{3}{\alpha\sqrt{\alpha}} \left[a^2\alpha\cos\left(a\sqrt{\alpha}\right) - 2a\sqrt{\alpha}\sin\left(a\sqrt{\alpha}\right) - 2\cos\left(a\sqrt{\alpha}\right)\right]$$

$$+ C_2 \frac{2}{\alpha} \left[a\sqrt{\alpha}\cos\left(a\sqrt{\alpha}\right) - \sin\left(a\sqrt{\alpha}\right)\right] + C_3 \frac{1}{\sqrt{\alpha}}\cos\left(a\sqrt{\alpha}\right) \qquad (2.3.7a)$$

$$B_2 = -C_1 \frac{3}{\alpha\sqrt{\alpha}} \left[a^2\alpha\sin\left(a\sqrt{\alpha}\right) + 2a\sqrt{\alpha}\cos\left(a\sqrt{\alpha}\right) - 2\sin\left(a\sqrt{\alpha}\right)\right]$$

$$- C_2 \frac{2}{\alpha} \left[a\sqrt{\alpha}\sin\left(a\sqrt{\alpha}\right) + \cos\left(a\sqrt{\alpha}\right)\right] - C_3 \frac{1}{\sqrt{\alpha}}\sin\left(a\sqrt{\alpha}\right) \qquad (2.3.7b)$$

$$B_3 = C_1 \frac{6}{\alpha}, \quad B_4 = C_1 a^3 + C_2 \frac{a^2\alpha + 2}{\alpha} + C_3 a + C_4 \qquad (2.3.7c)$$

where $\alpha = P_1 L^2/(EI)$.

The buckling problem thus involves only four constants $C_i$ ($i = 1$, 2, 3, 4) with the expressions of constants $B_i$ ($i = 1,2,3,4$) in terms of the former constants. Using the two boundary conditions at each end, we can develop an eigenvalue equation of the form

$$[A]\{c\} = \begin{bmatrix} a_{11} & a_{12} & a_{13} & a_{14} \\ a_{21} & a_{22} & a_{23} & a_{24} \\ a_{31} & a_{32} & a_{33} & a_{34} \\ a_{41} & a_{42} & a_{43} & a_{44} \end{bmatrix} \begin{Bmatrix} C_1 \\ C_2 \\ C_3 \\ C_4 \end{Bmatrix} = \begin{Bmatrix} 0 \\ 0 \\ 0 \\ 0 \end{Bmatrix} \qquad (2.3.8)$$

The vanishing of the determinant of matrix $[A]$ yields the stability criterion.

For example, consider a column that is pinned at both ends and loaded at an intermediate distance $x = a$ from the base. This problem corresponds to the above Case 3a. The boundary conditions are

$$w(0) = 0, \quad \left[\frac{d^2w}{dx^2}\right]_{x=0} = 0, \quad w(1) = 0, \quad \left[\frac{d^2w}{dx^2}\right]_{x=1} = 0 \qquad (2.3.9)$$

By substituting the general solutions given in Table 2.4 into Eq. (2.3.9) and noting the expressions of constants $B$ given by Eq. (2.3.7), we find that

$$a_{11} = 1, \quad a_{12} = 1, \quad a_{13} = 1, \quad a_{14} = 1, \quad a_{21} = 6, \quad a_{22} = 2, \quad a_{23} = 0$$

$$a_{24} = 0, \quad a_{31} = -\frac{3}{\alpha\sqrt{\alpha}} \left[\left(a^2\alpha - 2\right)\sin\left(a\sqrt{\alpha}\right) + 2a\sqrt{\alpha}\cos\left(a\sqrt{\alpha}\right)\right]$$

$$a_{32} = \frac{2}{\alpha} \left[a\sqrt{\alpha}\sin\left(a\sqrt{\alpha}\right) + \cos\left(a\sqrt{\alpha}\right)\right], \quad a_{33} = -\frac{1}{\sqrt{\alpha}}\sin\left(a\sqrt{\alpha}\right)$$

$$a_{34} = 0, \quad a_{41} = a^3, \quad a_{42} = \frac{a^3\alpha + 2}{\alpha}, \quad a_{43} = a, \quad a_{44} = 1 \qquad (2.3.10)$$

and thus the stability criterion is given by

$$3(1-a)^2 \sqrt{\alpha} \cos\left(a\sqrt{\alpha}\right) + \left[3\left(2-a\right) - \left(1-a\right)^3 \alpha\right] \sin\left(a\sqrt{\alpha}\right) = 0 \quad (2.3.11)$$

where $\alpha = P_1 L^2/(EI)$.

The stability criterion for other three cases, Case 1, Case 2a and Case 3a, and various combinations of classical boundary conditions are derived in the manner described above and are presented in Tables 2.5, 2.6 and 2.7.

## 2.4 Euler Columns with an Intermediate Restraint

Frame buildings are usually braced to resist lateral loads. In a loaded cross-bracing system, one bracing member will be under compression while the other under tension. In the design of the compression member, the restraint provided by the tension member may be exploited. The tension brace may be modeled as a discrete lateral elastic spring attached to the compression member (see, for example, papers by Mutton and Trahair, 1973; Kitipornchai and Finch, 1986); Stoman, 1988; and Mau, 1989). Therefore, the prediction of the elastic buckling loads of columns with an intermediate elastic restraint is of practical interest.

There are stability criteria for some special cases dispersed in the literature. For example, in the *Handbook of Structural Stability* and papers such as Rozvany and Mröz (1977) and Wang and Liew (1991), we find exact stability criteria for columns with an internal support which is a special case of the elastic restraint with infinite stiffness. But most papers on the subject offer numerical methods for determining the buckling loads. For example, Wang and Ang (1988) and Olhoff and Akesson (1991) used the Timoshenko energy approach for determining the buckling loads of braced columns under distributed load and end concentrated load while Thevendran and Wang (1993) used a variant of the Ritz method to compute the buckling capacity of the compression member in a nonsymmetric cross-bracing system.

This section presents a comprehensive set of exact stability criteria for Euler columns with an intermediate elastic restraint. The special case of the elastic restraint where its stiffness is infinite (or reaches a critical value in special locations which will be discussed later), so as to make the restraint behave like a rigid support, is treated as a byproduct of the more general problem at hand. The exact stability criteria presented herein can be readily used to calculate the buckling capacity of the compression member in a cross-bracing system.

**Table 2.5:** Stability criteria and critical load parameters $\sqrt{\alpha_1}$ for columns with compressive intermediate and end axial loads.

| B.C. | Stability criteria | | Sample critical load parameters $\sqrt{\alpha_1} = \sqrt{(P_1 + P_2)L^2/EI}$ | | | | |
|---|---|---|---|---|---|---|---|
| | | $a$ | 0.1 | 0.3 | 0.5 | 0.7 | 0.9 |
| C–F* | $1 - \sqrt{\lambda}\tan\left(a\sqrt{\alpha_1}\right)\tan\left[(1-a)\sqrt{\alpha_1}\sqrt{\lambda}\right] = 0$ | $\lambda = 0.25$ | 3.13371 | 2.93360 | 2.4619 | 2.02223 | 1.69808 |
| | where $\lambda = \frac{\alpha_2}{\alpha_1}$, $\quad \alpha_2 = \frac{P_2 L^2}{EI}$ | $\lambda = 0.50$ | 2.21961 | 2.17345 | 2.03334 | 1.83963 | 1.65327 |
| | | $\lambda = 0.75$ | 1.81330 | 1.80088 | 1.76005 | 1.69161 | 1.61087 |
| P–P* | $\left\{\sqrt{\alpha_2}[a(1-\lambda)-1] + (1-\lambda)^2\tan\left[(1-a)\sqrt{\alpha_2}\right]\right\} \times$ | $\lambda = 0.25$ | 4.84596 | 4.00896 | 3.93202 | 3.78990 | 3.37633 |
| | $\tan\left(a\sqrt{\alpha_1}\right) + \sqrt{\alpha_2}[a(1-\lambda)-1]\tan\left[(1-a)\sqrt{\alpha_2}\right] = 0$ | $\lambda = 0.50$ | 4.04138 | 3.66322 | 3.61553 | 3.54775 | 3.29703 |
| | | $\lambda = 0.75$ | 3.51290 | 3.37792 | 3.35643 | 3.33141 | 3.21855 |
| C–P* | $\left\{\sqrt{\alpha_2}[1 - a(1-\lambda)] + [2\lambda(1-\lambda)-1]\tan\left[\sqrt{\alpha_2}(1-a)\right]\right\}$ | $\lambda = 0.25$ | 8.79815 | 6.75004 | 6.02299 | 5.88884 | 5.01596 |
| | $-\left\{\lambda^{3/2} + \sqrt{\alpha_1}\lambda[1 - a(1-\lambda)]\tan\left[\sqrt{\alpha_2}(1-a)\right]\right\}\tan\left(a\sqrt{\alpha_1}\right)$ | $\lambda = 0.50$ | 6.31460 | 5.74370 | 5.37750 | 5.32344 | 4.83825 |
| | $-2\lambda(1-\lambda)\tan[\sqrt{\alpha_2}(1-a)]\sec\left(a\sqrt{\alpha_1}\right) = 0$ | $\lambda = 0.75$ | 5.17801 | 5.01892 | 4.88261 | 4.86368 | 4.66277 |
| P–C* | $\left\{\sqrt{\alpha_2}[1 - a(1-\lambda)]\tan\left[\sqrt{\alpha_2}(1-a)\right]\right.$ | $\lambda = 0.25$ | 6.30114 | 5.33088 | 5.25365 | 4.81143 | 4.51283 |
| | $+ [\lambda(\lambda-2)+2] - 2(1-\lambda)\sec\left[\sqrt{\alpha_2}(1-a)\right]\left.\right\}\tan\left(a\sqrt{\alpha_1}\right)$ | $\lambda = 0.50$ | 5.53038 | 5.01442 | 4.97371 | 4.70922 | 4.50652 |
| | $-\sqrt{\alpha_1}\lambda[1 - a(1-\lambda)] + \sqrt{\lambda}\tan\left[\sqrt{\alpha_2}(1-a)\right] = 0$ | $\lambda = 0.75$ | 4.94355 | 4.73715 | 4.72028 | 4.60266 | 4.50005 |
| C–C* | $\left\{\sqrt{\lambda}(1+\lambda)\tan\left[\sqrt{\alpha_2}(1-a)\right] - \sqrt{\alpha_2}[1 - a(1-\lambda)]\right\} \times$ | | | | | | |
| | $\tan\left(a\sqrt{\alpha_1}\right) - \sqrt{\alpha_2}[1 - a(1-\lambda)]\tan\left[\sqrt{\alpha_2}(1-a)\right]$ | $\lambda = 0.25$ | 11.95146 | 8.33161 | 7.86204 | 7.08305 | 6.33641 |
| | $+ 2[\lambda(1-\lambda)-1] - 2\lambda(1-\lambda)\sec\left(a\sqrt{\alpha_1}\right)$ | $\lambda = 0.50$ | 8.76636 | 7.53174 | 7.23087 | 6.83035 | 6.31954 |
| | $- 2[(1-\lambda) + \lambda\sec\left(a\sqrt{\alpha_1}\right)]\sec\left[\sqrt{\alpha_2}(1-a)\right] = 0$ | $\lambda = 0.75$ | 7.22480 | 6.84940 | 6.71286 | 6.55846 | 6.30182 |

*C–F: Clamped–Free;  P–P: Pinned–Pinned;  C–P: Clamped–Pinned;  P–C: Pinned–Clamped;  C–C: Clamped–Clamped.

**Table 2.6:** Stability criteria and critical load parameters $\sqrt{\alpha_1}$ for columns with tensile intermediate and compressive end loads.

| B.C. | Stability criteria | Sample critical load parameters $\sqrt{\alpha_1} = \sqrt{(P_1 + P_2)L^2/EI}$ | | | | | |
|---|---|---|---|---|---|---|---|
| | | $a$ | 0.1 | 0.3 | 0.5 | 0.7 | 0.9 |
| C–F* | $1 - \sqrt{\lambda}\tanh\left(a\sqrt{\alpha_1}\right)\tan\left\{(1-a)\sqrt{\alpha_2}\right\} = 0$ | $\lambda = 0.5$ | 2.22678 | 2.35305 | 2.85282 | 4.51143 | 13.51022 |
| | where $\lambda = \frac{\alpha_2}{\alpha_1}$, $\alpha_1 = \frac{[P_1+P_2]L^2}{EI}$, $\alpha_2 = \frac{P_2L^2}{EI}$ | $\lambda = 1.0$ | 1.57333 | 1.63457 | 1.87510 | 2.69463 | 7.85400 |
| | | $\lambda = 2.0$ | 1.11207 | 1.14497 | 1.27166 | 1.67127 | 4.35473 |
| P–P* | $\left\{\sqrt{\alpha_2}[a(1+\lambda)-1] + (1+\lambda)^2\tan\left[(1-a)\sqrt{\alpha_2}\right]\right\} \times$ | $\lambda = 0.5$ | 5.65149 | 7.54131 | 10.22487 | 13.64288 | 19.02687 |
| | $\tanh\left(a\sqrt{\alpha_1}\right) - \sqrt{\alpha_2}\lambda[a(1+\lambda)-1]\tan\left[(1-a)\sqrt{\alpha_2}\right] = 0$ | $\lambda = 1.0$ | 3.75533 | 4.92863 | 6.28319 | 6.73827 | 10.78470 |
| | | $\lambda = 2.0$ | 2.55315 | 3.22010 | 3.75903 | 3.86610 | 6.26468 |
| C–P* | $\left\{\sqrt{\alpha_2}[1-a(1+\lambda)] + [2\lambda(1+\lambda)+1]\tan\left[\sqrt{\alpha_2}(1-a)\right]\right\}$ | $\lambda = 0.5$ | 6.45307 | 7.68541 | 10.36932 | 14.46242 | 19.40444 |
| | $+\lambda\left\{\sqrt{\lambda} - \sqrt{\alpha_1}[1-a(1+\lambda)]\tan\left[\sqrt{\alpha_2}(1-a)\right]\right\}\tanh\left(a\sqrt{\alpha_1}\right)$ | $\lambda = 1.0$ | 4.54209 | 5.22325 | 6.69977 | 7.69329 | 11.12279 |
| | $+2\lambda(1+\lambda)\tan\left[\sqrt{\alpha_2}(1-a)\right]\text{sech}\left(a\sqrt{\alpha_1}\right) = 0$ | $\lambda = 2.0$ | 3.20378 | 3.59219 | 4.36614 | 4.64982 | 6.63457 |
| P–C* | $\left\{-\sqrt{\alpha_2}[1-a(1+\lambda)]\tan\left[\sqrt{\alpha_2}(1-a)\right]\right.$ | $\lambda = 0.5$ | 8.62768 | 11.43014 | 15.99410 | 27.82300 | 42.88891 |
| | $\left. - [\lambda(\lambda+2)+2] + 2(1+\lambda)\sec\left[\sqrt{\alpha_2}(1-a)\right]\right\}\tanh\left(a\sqrt{\alpha_1}\right)$ | $\lambda = 1.0$ | 5.76803 | 7.79621 | 10.83363 | 12.78612 | 26.56463 |
| | $-\sqrt{\alpha_1}\lambda[1-a(1+\lambda)] + \sqrt{\lambda}\tan\left[\sqrt{\alpha_2}(1-a)\right] = 0$ | $\lambda = 2.0$ | 3.89664 | 5.26079 | 6.62288 | 7.36685 | 16.90332 |
| C–C* | $\left\{-\sqrt{\lambda}(1-\lambda)\tan\left[\sqrt{\alpha_2}(1-a)\right] + \sqrt{\alpha_1}\lambda[1-a(1+\lambda)]\right\} \times$ | | | | | | |
| | $\tanh\left(a\sqrt{\alpha_1}\right) + \sqrt{\alpha_2}[1-a(1+\lambda)]\tan\left[\sqrt{\alpha_2}(1-a)\right]$ | $\lambda = 0.5$ | 9.13062 | 11.43872 | 15.99721 | 26.31437 | 43.10975 |
| | $+2[\lambda(\lambda+1)+1] - 2\lambda(\lambda+1)\,\text{sech}\left(a\sqrt{\alpha_1}\right)$ | $\lambda = 1.0$ | 6.40934 | 7.84573 | 10.88683 | 13.56540 | 26.70697 |
| | $-2\left[(1+\lambda) - \lambda\,\text{sech}\left(a\sqrt{\alpha_1}\right)\right]\sec\left[\sqrt{\alpha_2}(1-a)\right] = 0$ | $\lambda = 2.0$ | 4.51296 | 5.39739 | 7.22622 | 7.94580 | 17.01189 |

*C–F: Clamped–Free; P–P: Pinned–Pinned; C–P: Clamped–Pinned; P–C: Pinned–Clamped; C–C: Clamped–Clamped.

**Table 2.7:** Stability criteria and critical load parameters $\sqrt{\alpha}$ for columns subjected to intermediate axial load.

| B.C. | Stability criteria | Sample critical load parameters $\sqrt{\alpha} = \sqrt{PL^2/(EI)}$ | | | | |
|---|---|---|---|---|---|---|
| | | $a = 0.1$ | $0.3$ | $0.5$ | $0.7$ | $0.9$ |
| C–F* | $\cos\left(a\sqrt{\alpha}\right) = 0$ <br> where $\alpha = \frac{PL^2}{EI}$ | $5\pi$ | $5\pi/3$ | $\pi$ | $5\pi/7$ | $5\pi/9$ |
| P–P* | $3\sqrt{\alpha}(1-a)^2\cos\left(\sqrt{\alpha}a\right)$ <br> $+\left[3(2-a) - \alpha(1-a)^3\right]\sin(\sqrt{\alpha}a) = 0$ | 6.07805 | 4.42466 | 4.32040 | 4.05031 | 3.45564 |
| C–P* | $24\sqrt{\alpha}(1-a) + 12[1 + \alpha(1-a)^2]\sin\left(\sqrt{\alpha}a\right)$ <br> $+4\sqrt{\alpha}[\alpha(1-a)^3 - 3(2-a)]\cos\left(\sqrt{\alpha}a\right) = 0$ | 17.84181 | 7.99675 | 6.88014 | 6.52453 | 5.19080 |
| P–C* | $4\sqrt{\alpha}[3a - \alpha(1-a)^3]\cos\left(\sqrt{\alpha}a\right)$ <br> $+[\alpha^2(1-a)^4 - 12\alpha(1-a) - 12]\sin\left(\sqrt{\alpha}a\right) = 0$ | 7.26971 | 5.69265 | 5.55565 | 4.90790 | 4.51898 |
| C–C* | $12[2 + \alpha(1-a)^2]$ <br> $+4\sqrt{\alpha}[3(1-2a) + \alpha(1-a)^3]\sin\left(\sqrt{\alpha}a\right)$ <br> $\left\{\alpha^2(1-a)^4 - 12[2 + \alpha(1-a)]\right\}\cos\left(\sqrt{\alpha}a\right) = 0$ | 18.62395 | 9.22950 | 8.62568 | 7.30338 | 6.35247 |

*C–F: Clamped–Free;  P–P: Pinned–Pinned;  C–P: Clamped–Pinned;  P–C: Pinned–Clamped;  C–C: Clamped–Clamped.

Consider a column of flexural rigidity $EI$, length $L$ and intermediately restrained at $x = aL$ by either an internal elastic restraint that is modeled by a lateral spring of stiffness $c$ [see Fig. 2.4(a)] or an internal roller support [see Fig. 2.4(b)]. The ends of the columns may have any combination of classical boundary conditions. The column is loaded at the free end by a concentrated compressive force $P$, as shown in Figs. 2.4(a) and 2.4(b).

To solve this column buckling problem, we divide the column into two segments, *viz.* segment 1 ($0 \leq \bar{x} < aL$) and segment 2 ($aL \leq \bar{x} \leq L$). The governing buckling equation for both segments may be expressed as

$$\frac{d^4 w_i}{dx^4} + \alpha \frac{d^2 w_i}{dx^2} = 0, \quad i = 1, 2 \tag{2.4.1}$$

where $x = \bar{x}/L$, $w = \bar{w}/L$ and $\alpha = PL^2/(EI)$ and the subscripts 1 and 2 denote the quantities belonging to segment 1 and segment 2, respectively. The general solution is given by

$$w_1 = B_1 \sin \sqrt{\alpha} x + B_2 \cos \sqrt{\alpha} x + B_3 x + B_4 \quad \text{for} \quad 0 \leq x < a \tag{2.4.2}$$

$$w_2 = C_1 \sin \sqrt{\alpha} x + C_2 \cos \sqrt{\alpha} x + C_3 x + C_4 \quad \text{for} \quad a \leq x \leq 1 \tag{2.4.3}$$
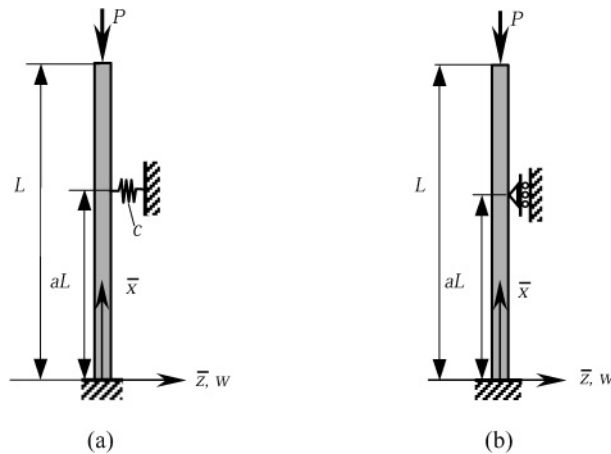


**Figure 2.4:** Column with (a) intermediate elastic restraint, and (b) an intermediate rigid support.

The continuity conditions (of deflection, slope, bending moment and shear force) at $x = a$ are:

$$w_1(a) - w_2(a) = 0 \tag{2.4.4}$$

$$\left[\frac{dw_1}{dx}\right]_{x=a} - \left[\frac{dw_2}{dx}\right]_{x=a} = 0 \tag{2.4.5}$$

$$\left[\frac{d^2w_1}{dx^2}\right]_{x=a} - \left[\frac{d^2w_2}{dx^2}\right]_{x=a} = 0 \tag{2.4.6}$$

$$\left[\frac{d^3w_1}{dx^3} + \alpha\frac{dw_1}{dx}\right]_{x=a} - \left[\frac{d^3w_2}{dx^3} + \alpha\frac{dw_2}{dx}\right]_{x=a} + \xi w_1(a) = 0 \tag{2.4.7}$$

where $\xi = cL^3/(EI)$. If the spring stiffness is infinite (i.e., the elastic restraint corresponds to an internal rigid support), Eq. (2.4.7) is to be replaced by

$$w_1(a) = 0 \tag{2.4.8}$$

By substituting Eqs. (2.4.2) and (2.4.3) into Eqs. (2.4.4) to (2.4.7), we obtain a set of homogeneous equations which may be expressed in the form of $B_i$ in terms of $C_i$

$$B_1 = -\frac{\xi}{\alpha\sqrt{\alpha}}\cos\left(a\sqrt{\alpha}\right)\left[C_1\sin\left(a\sqrt{\alpha}\right) + C_2\cos\left(a\sqrt{\alpha}\right) + C_3 a + C_4\right] \tag{2.4.9}$$

$$B_2 = \frac{\xi}{\alpha\sqrt{\alpha}}\sin\left(a\sqrt{\alpha}\right)\left[C_1\sin\left(a\sqrt{\alpha}\right) + C_2\cos\left(a\sqrt{\alpha}\right) + C_3 a + C_4\right] \tag{2.4.10}$$

$$B_3 = \frac{\xi}{\alpha}\left[C_1\sin\left(a\sqrt{\alpha}\right) + C_2\cos\left(a\sqrt{\alpha}\right) + C_3\left(a + \frac{\alpha}{\xi}\right) + C_4\right] \tag{2.4.11}$$

$$B_4 = -\frac{a\xi}{\alpha}\left[C_1\sin\left(a\sqrt{\alpha}\right) + C_2\cos\left(a\sqrt{\alpha}\right) + C_3 a + C_4\left(1 - \frac{\alpha}{a\xi}\right)\right] \tag{2.4.12}$$

The buckling problem thus involves only four constants $C_i$ ($i = 1, 2, 3, 4$) with the expressions of constants $B_i$ ($i = 1, 2, 3, 4$) in terms of the former constants. Using the two boundary conditions at each end, we can develop an eigenvalue equation of the form given in Eq. (2.3.9). The vanishing of the determinant of matrix $[A]$ yields the stability criterion.

Considering the various combinations of classical boundary conditions for column ends, the stability criteria are derived and presented in Table 2.8. In the special case of infinite spring support, the stability criteria simplify to those given in Table 2.9 by simply setting $\xi = \infty$.

**Table 2.8:** Stability criteria and critical load parameters $\sqrt{\alpha} = \sqrt{PL^2/(EI)}$ for columns with an intermediate elastic restraint of stiffness $\xi = cL^3/(EI)$.

| B.C. | Stability criteria | | Sample critical load parameters $\sqrt{\alpha}$ | | | | | | | | |
|------|-------------------|---|--------|--------|--------|--------|--------|--------|--------|--------|--------|
| | | $a$ | 0.1 | 0.2 | 0.3 | 0.4 | 0.5 | 0.6 | 0.7 | 0.8 | 0.9 |
| C–F* | $[2 - \cos(a\sqrt{\alpha})]\sin[(1-a)\sqrt{\alpha}] + \left(a - \frac{\alpha}{\xi}\right)\sqrt{\alpha}\cos\sqrt{\alpha}$ $- \sin\sqrt{\alpha} = 0$ | $\xi = 10$ | 1.5712 | 1.5768 | 1.5996 | 1.6538 | 1.7520 | 1.9033 | 2.1151 | 2.3947 | 2.7461 |
| | | $\xi = 40$ | 1.5723 | 1.5935 | 1.6680 | 1.8154 | 2.0373 | 2.3335 | 2.7134 | 3.1922 | 3.7616 |
| | | $\xi = 100$ | 1.5746 | 1.6214 | 1.7557 | 1.9691 | 2.2437 | 2.5805 | 2.9925 | 3.4870 | 4.0182 |
| P–P* | $\cos(a\sqrt{\alpha})\cos[(1-a)\sqrt{\alpha}] - \cos\sqrt{\alpha}$ $- \left[a(1-a) - \frac{\alpha}{\xi}\right]\sqrt{\alpha}\sin\sqrt{\alpha} = 0$ | $\xi = 10$ | 3.1720 | 3.2491 | 3.3427 | 3.4187 | 3.4481 | 3.4187 | 3.3427 | 3.2491 | 3.1720 |
| | | $\xi = 40$ | 3.2582 | 3.5300 | 3.8455 | 4.1136 | 4.2258 | 4.1136 | 3.8455 | 3.5300 | 3.2582 |
| | | $\xi = 100$ | 3.4111 | 3.9478 | 4.5231 | 5.0781 | 5.4126 | 5.0781 | 4.5231 | 3.9478 | 3.4111 |
| C–P* | $\sqrt{\alpha}[2(1-a) - \cos(a\sqrt{\alpha})]\sin[(1-a)\sqrt{\alpha}]$ $+ \cos(a\sqrt{\alpha})\cos[(1-a)\sqrt{\alpha}] - \left\{1 - a\alpha(1-a) + \frac{\alpha^2}{\xi}\right\}\cos\sqrt{\alpha}$ $- \left[(1-a) - \frac{\alpha}{\xi}\right]\sqrt{\alpha}\sin\sqrt{\alpha} = 0$ | $\xi = 10$ | 4.4944 | 4.5068 | 4.5452 | 4.6087 | 4.6735 | 4.7034 | 4.6752 | 4.6018 | 4.5258 |
| | | $\xi = 40$ | 4.4974 | 4.5448 | 4.6835 | 4.9075 | 5.1490 | 5.2774 | 5.1765 | 4.9030 | 4.6196 |
| | | $\xi = 100$ | 4.5033 | 4.6117 | 4.8980 | 5.3375 | 5.8544 | 6.2352 | 6.0225 | 5.4105 | 4.7924 |
| P–C* | $\sqrt{\alpha}[2(1-a) - \cos(a\sqrt{\alpha})]\cos[(1-a)\sqrt{\alpha}] - 2\sin[(1-a)\sqrt{\alpha}]$ $-2[a\sqrt{\alpha}\cos(a\sqrt{\alpha}) - \sin(a\sqrt{\alpha})] - \left[a - \frac{2\alpha}{\xi}\right]\sqrt{\alpha}\cos\sqrt{\alpha}$ $+ \left\{[2 - a\alpha(1-a)] - \frac{\alpha^2}{\xi}\right\}\sin\sqrt{\alpha} - \frac{2\alpha\sqrt{\alpha}}{\xi} = 0$ | $\xi = 10$ | 6.2846 | 6.3022 | 6.3508 | 6.4128 | 6.4423 | 6.4128 | 6.3508 | 6.3022 | 6.2846 |
| | | $\xi = 40$ | 6.2890 | 6.3562 | 6.5371 | 6.7746 | 6.8961 | 6.7746 | 6.5371 | 6.3562 | 6.2890 |
| | | $\xi = 100$ | 6.2975 | 6.4523 | 6.8423 | 7.3788 | 7.7178 | 7.3788 | 6.8423 | 6.4523 | 6.2975 |
| C–C* | $\sin(a\sqrt{\alpha})\sin[(1-a)\sqrt{\alpha}] - \left(a - \frac{\alpha}{\xi}\right)\sqrt{\alpha}\sin\sqrt{\alpha} = 0$ | $\xi = 10$ | 0.3120 | 0.6063 | 0.8813 | 1.1449 | 1.4086 | 1.6853 | 1.9893 | 2.3341 | 2.7281 |
| | | $\xi = 40$ | 0.6000 | 1.0765 | 1.4409 | 1.7452 | 2.0312 | 2.3233 | 2.6256 | 2.9055 | 3.0889 |
| | | $\xi = 100$ | 0.8812 | 1.4016 | 1.7172 | 1.9690 | 2.2127 | 2.4669 | 2.7261 | 2.9549 | 3.0994 |

*C–F: Clamped–Free; P–P: Pinned–Pinned; C–P: Clamped–Pinned; P–C: Pinned–Clamped; C–C: Clamped–Clamped.

**Table 2.9:** Stability criteria and critical load parameters for columns with an intermediate roller support.

| B.C. | Stability criteria | Sample critical load parameters $\sqrt{\alpha} = \sqrt{PL^2/EI}$ | | | | | | | | |
|------|-------------------|-----------|--------|--------|--------|--------|--------|--------|--------|--------|
| | | $a = 0.1$ 0.2 | 0.3 | 0.4 | 0.5 | 0.6 | 0.7 | 0.8 | 0.9 | |
| C–F* | $[2 - \cos(a\sqrt{\alpha})]\sin[(1-a)\sqrt{\alpha}] + a\sqrt{\alpha}\cos\sqrt{\alpha} - \sin\sqrt{\alpha} = 0$ | 1.6981  1.8478 | 2.0259 | 2.2407 | 2.5031 | 2.8266 | 3.2231 | 3.6862 | 4.1515 | |
| P–P* | $\cos(a\sqrt{\alpha})\cos[(1-a)\sqrt{\alpha}] - \cos\sqrt{\alpha}$ $-a\sqrt{\alpha}(1-a)\sin\sqrt{\alpha} = 0$ | 4.8192  5.2013 | 5.6352 | 6.0663 | 6.2832 | 6.0663 | 5.6352 | 5.2013 | 4.8192 | |
| C–P* | $\sqrt{\alpha}[2(1-a) - \cos(a\sqrt{\alpha})]\sin[(1-a)\sqrt{\alpha}]$ $+ \cos(a\sqrt{\alpha})\cos[(1-a)\sqrt{\alpha}]$ $- [1 - a\alpha(1-a)]\cos\sqrt{\alpha} - \sqrt{\alpha}(1-a)\sin\sqrt{\alpha} = 0$ | 4.8608  5.2997 | 5.8273 | 6.4558 | 7.1497 | 7.6704 | 7.6262 | 7.2087 | 6.7286 | |
| P–C* | $\sqrt{\alpha}[2(1-a) - \cos(a\sqrt{\alpha})]\cos[(1-a)\sqrt{\alpha}] - 2\sin[(1-a)\sqrt{\alpha}]$ $+2[a\sqrt{\alpha}\cos(a\sqrt{\alpha}) - \sin(a\sqrt{\alpha})] - \sqrt{\alpha}\cos\sqrt{\alpha}$ $+[2 - a\alpha(1-a)]\sin\sqrt{\alpha} = 0$ | 6.7915  7.3787 | 8.0348 | 8.6732 | 8.9868 | 8.6732 | 8.0348 | 7.3787 | 6.7915 | |
| C–C* | $\sin(a\sqrt{\alpha})\sin[(1-a)\sqrt{\alpha}] - a\sqrt{\alpha}\sin\sqrt{\alpha} = 0$ | 1.6829  1.8119 | 1.9609 | 2.1333 | 2.3311 | 2.5516 | 2.7796 | 2.9789 | 3.1043 | |

*C–F: Clamped –Free;  P –P: Pinned –Pinned;  C –P: Clamped –Pinned;  P –C: Pinned –Clamped;  C –C: Clamped –Clamped.

An interesting feature of this column buckling problem at hand is that there exists a critical elastic restraint stiffness when the restraint is positioned exactly at a node of a higher buckled mode of an equivalent column without any intermediate restraint. At this special restraint location, if one provides adequate intermediate restraint stiffness, the buckled mode switches to the higher buckling mode of the column without any intermediate restraint (see Timoshenko and Gere, 1961; Olhoff and Akesson, 1991; Kitipornchai and Finch, 1986). For example, the nodal point of the second buckled mode for a fixed–pinned column is at $a = 0.6405207$ from the fixed end. When the elastic restraint is placed at this location, the critical elastic restraint stiffness is $\xi_c = 216.6$ as given by the stability criterion in Table 2.10 by setting $a = 0.6405207$ and $\sqrt{\alpha} = 7.72525$. There is no critical elastic restraint stiffness apart from the critical location for the intermediate restraint.

The critical stiffness values and the corresponding locations of the elastic restraints are presented in Table 2.10. The critical load associated with the critical elastic stiffness and the corresponding restraint location is the highest possible critical load value that one may obtain for a column with an elastic intermediate restraint.

**Table 2.10:** Critical elastic restraint stiffnesses and the associated conditions.

| Boundary conditions | Buckling mode without intermediate restraint | Critical buckling load $\sqrt{\alpha}$ | Location of node of higher buckled mode or the intermediate support $(a)$ | Critical elastic restraint stiffness $\xi_{cr}*$ |
|---|---|---|---|---|
| Fixed–Free | Mode 3 | 7.8540 | 0.8 | 77.106 |
| Pinned–Pinned | Mode 2 | 6.2832 | 0.5 | 157.914 |
| Fixed–Pinned | Mode 2 | 7.7252 | 0.6405 | 216.630 |
| Fixed–Fixed | Mode 2 | 8.9868 | 0.5 | 207.75 |
| Pinned–Free | Mode 3 | 6.2832 | 0.5 | 78.957 |

*$\xi_{cr} = cL^3/(EI)$

## 2.5 Euler Columns with an Internal Hinge

### 2.5.1 Columns with an Internal Hinge

Consider a column of flexural rigidity $EI$, length $L$, and fixed at the base ($\bar{x} = 0$) and either fixed or pinned at the top end $\bar{x} = L$ (note that $\bar{x}$ is the distance from the bottom end of the column). The column has an internal frictionless free hinge at $\bar{x} = aL$ and is loaded at the top end by a concentrated compressive force $P$ as shown in Fig. 2.5.

The boundary conditions and continuity conditions are:

$$w_1(0) = 0 \tag{2.5.1}$$

$$\left[\frac{dw_1}{dx}\right]_{x=0} = 0 \tag{2.5.2}$$

$$w_2(1) = 0 \tag{2.5.3}$$

If the top end is *pinned*: $\left[\dfrac{d^2 w_2}{dx^2}\right]_{x=1} = 0$ or *fixed*: $\left[\dfrac{dw_2}{dx}\right]_{x=1} = 0$

$$\tag{2.5.4}$$

$$w_1(a) = w_2(a) \tag{2.5.5}$$

$$\left[\frac{d^2 w_1}{dx^2}\right]_{x=a} = \left[\frac{d^2 w_2}{dx^2}\right]_{x=a} = 0 \tag{2.5.6}$$

$$\left[\frac{d^3 w_1}{dx^3}\right]_{x=a} + \alpha \left[\frac{dw_1}{dx}\right]_{x=a} = \left[\frac{d^3 w_2}{dx^3}\right]_{x=a} + \alpha \left[\frac{dw_2}{dx}\right]_{x=a} \tag{2.5.7}$$
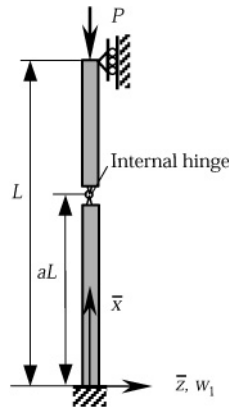


**Figure 2.5:** Column with an internal hinge.

where $x = \bar{x}/L$. The substitution of Eqs. (2.4.2) and (2.4.3) into Eqs. (2.5.1) to (2.5.7) yields an eigenvalue equation. For nontrivial solutions, this equation yields the following stability criteria (Wang, 1987a):

*The fixed–fixed column with an internal hinge:*

$$\tan\left(a\sqrt{\alpha}\right) + \tan\left\{(1-a)\sqrt{\alpha}\right\} - \sqrt{\alpha} = 0 \qquad (2.5.8)$$

*The fixed–pinned column with an internal hinge:*

$$\tan\left(a\sqrt{\alpha}\right) - \tan\sqrt{\alpha} = 0, \text{ for } 0 \le a \le 0.30084 \qquad (2.5.9\text{a})$$

$$\sqrt{\alpha} - \tan(a\sqrt{\alpha}) = 0, \quad \text{for } 0.30084 < a \le 1 \qquad (2.5.9\text{b})$$

The first stability criterion given by Eq. (2.5.9a) corresponds to a buckled mode in which the bottom segment of the column is straight (i.e., remains vertical). The second stability criterion given by Eq. (2.5.9b) corresponds to a buckled mode in which the top segment of the column undergoes a rigid body rotation. The variation of the critical load parameter with respect to the hinge location is shown in Figure 2.6.
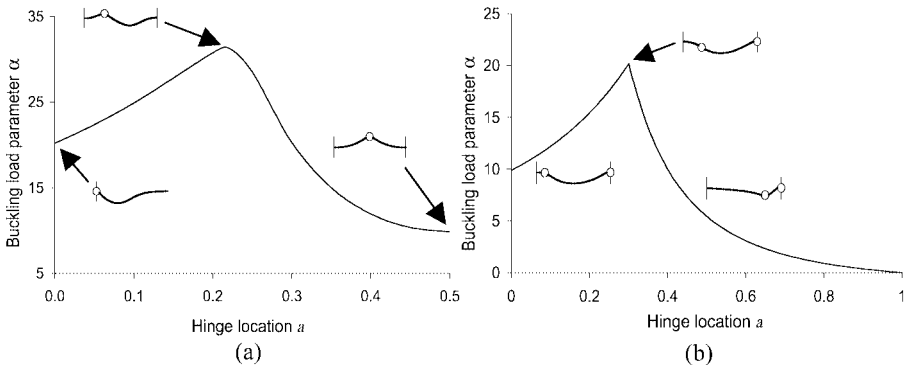


**Figure 2.6:** Variation of critical load parameter with respect to hinge location. (a) Fixed–fixed column. (b) Fixed–pinned column.

## 2.5.2 Columns with a Rotational Restrained Junction

Columns weakened at an interior location, due to the presence of a notch or a crack, may be modeled by columns with a rotational restraint (or spring) at the weakened junction (see, for example, Krawczuk and Ostachowitz, 1995). Such a junction also describes a stiffened human limb joint or a robotic arm joint. The junction effectively separates the column into two segments. At the junction, we require continuity of displacement and shear. The restraining moment of the spring is to be proportional to the difference of the junction slopes of the two segments. Thus, when the spring constant is infinite, the column is completely continuous. When the spring constant is zero, the two sections are connected by a frictionless free hinge as treated in Section 2.5.1.

Let $\xi$ be the internal torsional spring constant normalized by $EI/L$ and $a$ be the fractional distance of the hinge from the bottom. The conditions to be satisfied at the hinge are

$$w_1(a) = w_2(a) \tag{2.5.10}$$

$$\left[\frac{d^2 w_1}{dx^2}\right]_{x=a} = \left[\frac{d^2 w_2}{dx^2}\right]_{x=a} \tag{2.5.11}$$

$$\left[\frac{d^3 w_1}{dx^3} + \alpha \frac{dw_1}{dx}\right]_{x=a} = \left[\frac{d^3 w_2}{dx^3} + \alpha \frac{dw_2}{dx}\right]_{x=a} \tag{2.5.12}$$

$$\left[\frac{d^2 w_1}{dx^2}\right]_{x=a} = \xi \left[\frac{dw_2}{dx} - \frac{dw_1}{dx}\right]_{x=a} \tag{2.5.13}$$

Here the last equation signifies that (at the hinge) the moment is proportional to the angle difference between the two segments. If the column is pinned at both ends, the characteristic equation, after some work, is found to be

$$\tan\left[\sqrt{\alpha}\,(a-1)\right]\left[\sqrt{\alpha}\tan\left(\sqrt{\alpha}a\right) - \xi\right] + \xi \tan\left(\sqrt{\alpha}a\right) = 0 \tag{2.5.14}$$

Some values for the critical load are shown in Table 2.11. Owing to symmetry, only the range $0 \leq a \leq 0.5$ needs to be considered. Notice $\pi^2$ is the buckling load for the pinned–pinned column. When $\xi = 0$ and $a \neq 0$ the hinge has no torsional resistance, and the column can rotate freely with zero load. When $\xi = 0$ and $a = 0$, this rotation is absent, and the buckling load jumps to $\pi^2$.

The characteristic equation for the column with top end free and bottom end fixed is

$$\tan\left[\sqrt{\alpha}\,(a-1)\right]\left[\sqrt{\alpha}+\xi\tan\left(\sqrt{\alpha}a\right)\right]+\xi=0 \qquad (2.5.15)$$

Some values are given in Table 2.11. The value of $\pi^2/4$ is the buckling load of the fixed–free column. Similar to the previous case, there is a sudden jump of buckling load as $a \to 1$.

The governing equation for the buckling of an internally weakened column with the bottom end fixed and the top end free to slide transversely is

$$\sqrt{\alpha}+\xi\tan\left(\sqrt{\alpha}a\right)-\xi\tan\left[\sqrt{\alpha}\,(a-1)\right]=0 \qquad (2.5.16)$$

Table 2.11 shows some critical load values. When the torsional spring constant is infinity, the critical load is $\pi^2$, the same as the classical hingeless free sliding case given in Section 2.1.2. It is also $\pi^2$ when $a = 0.5$, regardless of the spring constant, or when the hinge is at the inflection point at the midpoint.

The characteristic equation for the column with one end fixed and one end pinned is

$$\xi\left[\sqrt{\alpha}-\tan\left(\sqrt{\alpha}a\right)\right]+\tan\left[\sqrt{\alpha}(a-1)\right]\left[\alpha+\xi+\sqrt{\alpha}\,(\xi-1)\tan\left(\sqrt{\alpha}a\right)\right]=0 \qquad (2.5.17)$$

When $\xi = \infty$, the critical load parameter $\alpha = 20.191$, which is the first root of the transcendental $\tan(\sqrt{\alpha}) = \sqrt{\alpha}$. This value corresponds to that of the classical fixed–pinned Euler column. When $\xi = 0$, the results reduce to those of an internal frictionless hinge. As $a$ approaches unity, the critical load $\alpha = 0$ for the case where $\xi = 0$ due to the swivel motion of two closely spaced hinges. But if $\xi > 0$, the critical load $\alpha$ rises to the maximum value as $a \to 1$. The optimum location of $a$ can be obtained by substituting $\alpha = 20.1908$ [or $\tan(\sqrt{\alpha}) = \sqrt{\alpha}$] into Eq. (2.5.17), wherein the stability criterion becomes independent of $\xi$ and the optimum location $a = 0.3008$, which also corresponds to the inflection point of a fixed–pinned Euler column without any weakness. At this optimum location, the junction (with any value of $\xi$) does not diminish the critical load.

Lastly, we present the fixed–fixed column with an internal resisting hinge. The characteristic equation is found to be

$$4\xi-(\alpha+4\xi)\cos\left(\sqrt{\alpha}\right)-\alpha\cos\left[\sqrt{\alpha}\,(1-2a)\right]+2\,(1-\xi)\,\sqrt{\alpha}\sin\left(\sqrt{\alpha}\right)=0 \qquad (2.5.18)$$

**Table 2.11:** Critical load parameters $\alpha$ for columns with various end conditions.

| $a$ | $\xi = 0$ | 0.1 | 0.5 | 1 | 2 | 4 | 10 | $\infty$ |
|---|---|---|---|---|---|---|---|---|
| Pinned–ended columns with an internal hinge and elastic rotational restraint | | | | | | | | |
| 0 | $\pi^2$ | $\pi^2$ | $\pi^2$ | $\pi^2$ | $\pi^2$ | $\pi^2$ | $\pi^2$ | $\pi^2$ |
| 0.1 | 0 | 1.0733 | 4.5392 | 6.9928 | 8.6259 | 9.3239 | 9.6696 | $\pi^2$ |
| 0.3 | 0 | 0.4607 | 2.0250 | 3.4829 | 5.3433 | 7.1102 | 8.6417 | $\pi^2$ |
| 0.5 | 0 | 0.3870 | 1.7071 | 2.9607 | 4.6386 | 6.3968 | 8.1667 | $\pi^2$ |
| Fixed–free columns with an internal hinge and elastic rotational restraint | | | | | | | | |
| 0 | 0 | 0.0968 | 0.4268 | 0.7402 | 1.1597 | 1.5992 | 2.0417 | $\pi^2/4$ |
| 0.1 | 0 | 0.1068 | 0.4614 | 0.7859 | 1.2052 | 1.6320 | 2.0563 | $\pi^2/4$ |
| 0.3 | 0 | 0.1356 | 0.5618 | 0.9221 | 1.3514 | 1.7534 | 2.1257 | $\pi^2/4$ |
| 0.5 | 0 | 0.1874 | 0.7402 | 1.1597 | 1.5592 | 1.9539 | 2.2384 | $\pi^2/4$ |
| 0.7 | 0 | 0.3076 | 1.1240 | 1.6100 | 1.9897 | 2.2190 | 2.3664 | $\pi^2/4$ |
| 0.9 | 0 | 0.8899 | 2.1418 | 2.3261 | 2.4021 | 2.4360 | 2.4551 | $\pi^2/4$ |
| 1 | $\pi^2/4$ | $\pi^2/4$ | $\pi^2/4$ | $\pi^2/4$ | $\pi^2/4$ | $\pi^2/4$ | $\pi^2/4$ | $\pi^2/4$ |
| Fixed–sliding restrained columns with an internal hinge and elastic rotational restraint | | | | | | | | |
| 0 | $\pi^2/4$ | 2.6634 | 3.3731 | 4.1159 | 5.2392 | 6.6071 | 8.1955 | $\pi^2$ |
| 0.1 | 3.0462 | 3.2623 | 4.0174 | 4.7662 | 5.8314 | 7.0486 | 8.4086 | $\pi^2$ |
| 0.3 | 5.0355 | 5.3076 | 6.1713 | 6.9046 | 7.7696 | 8.5578 | 9.2582 | $\pi^2$ |
| 0.5 | $\pi^2$ | $\pi^2$ | $\pi^2$ | $\pi^2$ | $\pi^2$ | $\pi^2$ | $\pi^2$ | $\pi^2$ |
| Fixed–pinned columns with an internal hinge and elastic rotational restraint | | | | | | | | |
| 0 | 9.870 | 10.067 | 10.798 | 11.598 | 12.894 | 14.660 | 17.076 | 20.191 |
| 0.1 | 12.185 | 12.401 | 13.170 | 13.951 | 15.104 | 16.497 | 18.180 | 20.191 |
| 0.3 | 20.142 | 20.185 | 20.190 | 20.190 | 20.190 | 20.191 | 20.191 | 20.191 |
| 0.5 | 5.434 | 5.998 | 7.960 | 9.870 | 12.474 | 15.201 | 17.844 | 20.191 |
| 0.7 | 1.730 | 2.315 | 4.391 | 6.491 | 9.518 | 12.961 | 16.637 | 20.191 |
| 0.9 | 0.363 | 1.539 | 5.712 | 9.743 | 14.472 | 17.636 | 19.300 | 20.191 |
| 1 | 20.191 | 20.191 | 20.191 | 20.191 | 20.191 | 20.191 | 20.191 | 20.191 |
| Fixed–ended columns with an internal hinge and elastic rotational restraint | | | | | | | | |
| 0 | 20.191 | 20.498 | 21.659 | 22.969 | 25.182 | 28.397 | 33.153 | $4\pi^2$ |
| 0.1 | 24.901 | 25.257 | 26.537 | 27.865 | 29.878 | 32.395 | 35.558 | $4\pi^2$ |
| 0.3 | 20.305 | 21.320 | 24.967 | 28.627 | 33.331 | 36.817 | 38.603 | $4\pi^2$ |
| 0.5 | 9.870 | 10.654 | 13.492 | 16.463 | 20.957 | 26.428 | 32.782 | $4\pi^2$ |

The critical loads are shown in Table 2.11. For constant $a$, the critical load increases with the spring constant $\xi$, reaching the value of $4\pi^2$ for fixed–fixed columns. For a given spring constant, the location of the hinge for maximum critical load is at $a = 0.25$ (the inflection point) if $\xi \geq 1$, but is less than 0.25 if $\xi < 1$. Variations of the critical load parameter with respect to the junction location for various values of spring parameter $\xi$ and column end conditions are shown in Figs. 2.7–2.11.



**Figure 2.7:** Critical load parameter $\alpha$ for *pinned–pinned* column versus weakened junction location $a$ with various constant junction stiffness $\xi$.

## 2.6 Euler Columns with a Continuous Elastic Restraint

Consider a uniform homogeneous column of flexural rigidity $EI$, length $L$, and continuously restrained along its length. The restraint consists of lateral springs of stiffness $c$ per unit length. It may model an elastic foundation or a wall cladding restraint. The column is loaded at the top end by a concentrated compressive force $P$ as shown in Fig. 2.12.
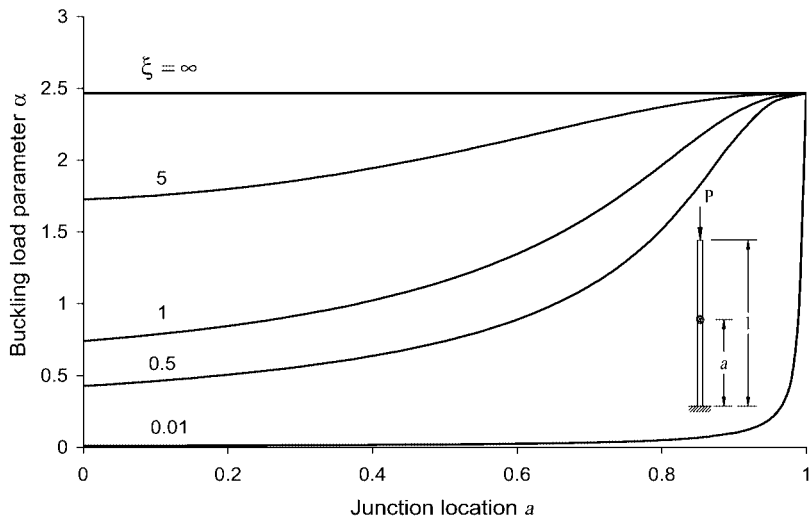
**Figure 2.8:** Critical load parameter $\alpha$ for *fixed–free* column versus weakened junction location $a$ with various constant junction stiffness $\xi$.
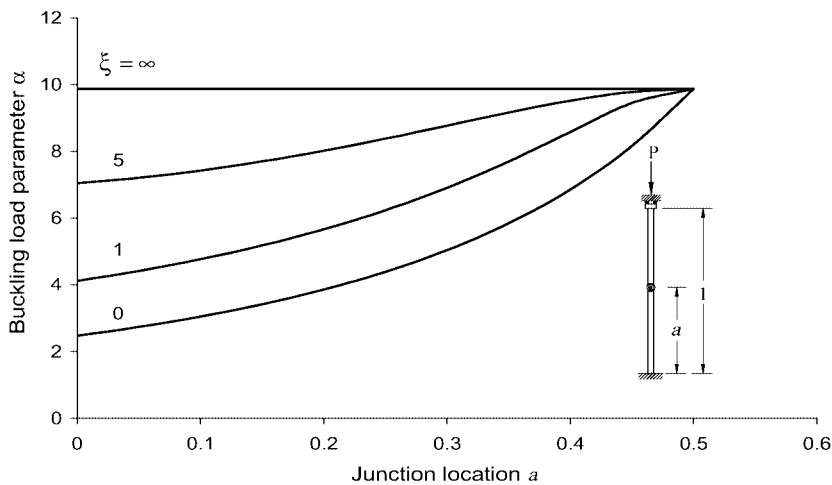


**Figure 2.9:** Critical load parameter $\alpha$ for *fixed–sliding restrained* column versus weakened junction location $a$ with various constant junction stiffness $\xi$.
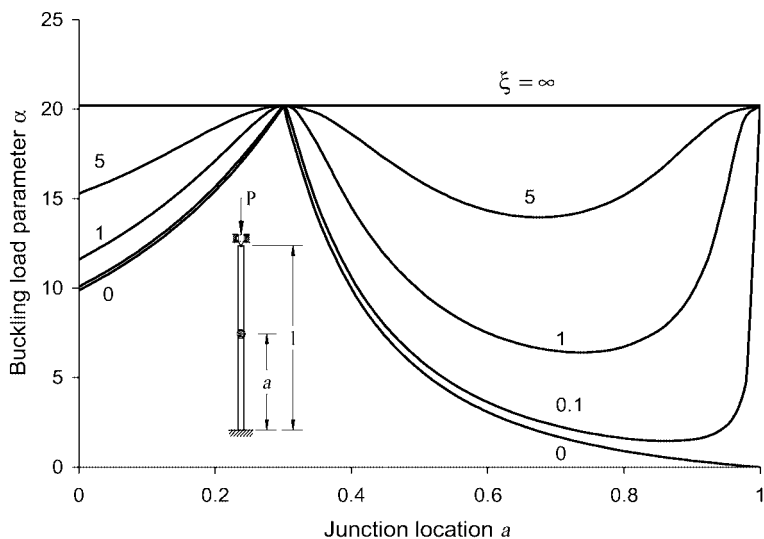
**Figure 2.10:** Critical load parameter $\alpha$ for *fixed–pinned* column versus weakened junction location $a$ with various constant junction stiffness $\xi$.



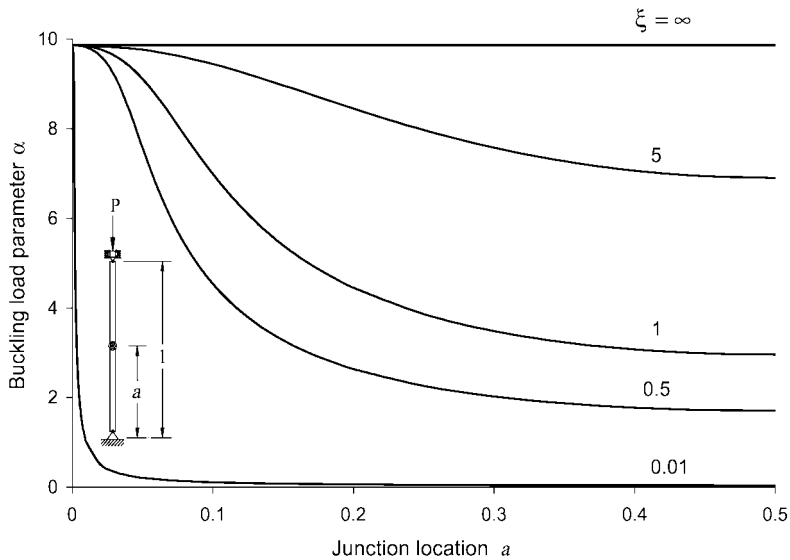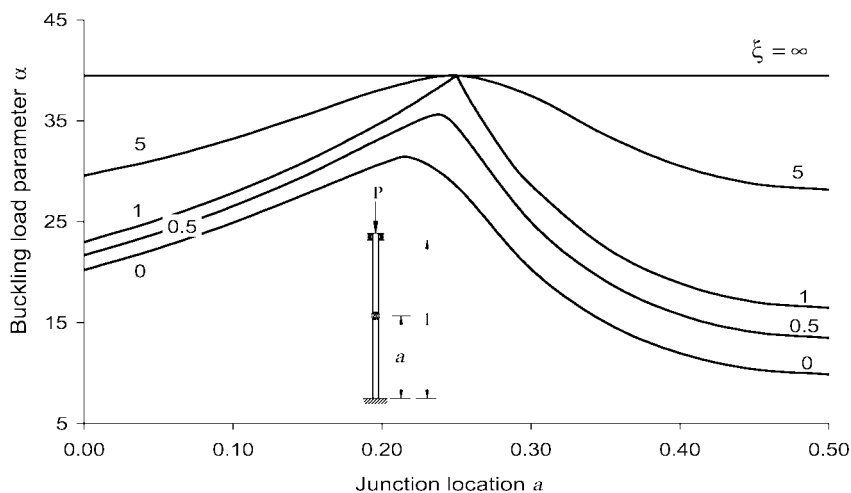**Figure 2.11:** Critical load parameter $\alpha$ for *fixed–fixed* column versus weakened junction location $a$ with various constant junction stiffness $\xi$.
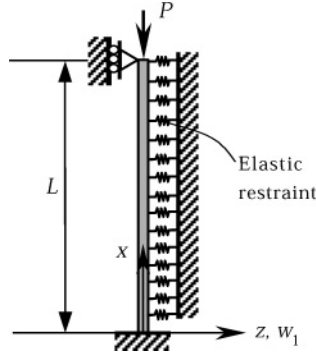
**Figure 2.12:** Column with elastic restraint.

The governing buckling equation is given by

$$\frac{d^4 w}{dx^4} + \alpha \frac{d^2 w}{dx^2} + \xi w = 0 \tag{2.6.1}$$

where $x = \bar{x}/L$, $w = \bar{w}/L$, $\alpha = PL^2/(EI)$ and $\xi = cL^4/(EI)$. The general solution to (2.6.1) is

$$w = C_1 \cos(Sx) + C_2 \sin(Sx) + C_3 \cos(Tx) + C_4 \sin(Tx) \tag{2.6.2}$$

where

$$S = \sqrt{\frac{\alpha}{2} - \sqrt{\left(\frac{\alpha}{2}\right)^2 - \xi}}, \quad T = \sqrt{\frac{\alpha}{2} + \sqrt{\left(\frac{\alpha}{2}\right)^2 - \xi}} \tag{2.6.3}$$

It is worth noting from Eq. (2.6.3) that the smallest critical load for a periodic solution is $(P_{cr})_{min} = 2\sqrt{cEI}$.

For the usual combinations of boundary conditions, the stability criteria are given below:

*Fixed–free column:*

$$\left[\alpha\left(S^2 + T^2\right) - 2S^2 T^2\right] \cos T \cos S - \alpha\left(S^2 + T^2\right) + \left(S^4 + T^4\right)$$

$$+ ST\left[2\alpha - \left(S^2 + T^2\right)\right] \sin T \sin S = 0 \tag{2.6.4}$$

*Pinned–pinned column:*

$$\sin T = 0 \tag{2.6.5}$$

*Fixed–pinned column:*

$$T \cos T \sin S - S \sin T \cos S = 0 \tag{2.6.6}$$

*Fixed–fixed column:*

$$2ST \left[\cos T \cos S - 1\right] + \left(T^2 + S^2\right) \sin T \sin S = 0 \tag{2.6.7}$$

*Pinned–fixed column with top sway:*

$$\cos T = 0 \tag{2.6.8}$$

*Fixed–fixed column with top sway:*

$$T \sin T \cos S - S \cos T \sin S = 0 \tag{2.6.9}$$

*Free–free column:*

$$2ST(S^2 - \alpha)(T^2 - \alpha) \cos S \, \cos T - 2S^3 T^3$$
$$+ \, \alpha(\alpha^2 - 2S^2 T^2) \sin S \, \sin T = 0 \tag{2.6.10}$$

The free–free case is of interest to foundation engineers/researchers (Hetenyi 1948).

The critical load is obtained by solving the transcendental stability criteria for the smallest value of $\alpha$. Table 2.12 contains critical loads for a pinned–pinned column and a fixed–pinned column. Note that buckled mode shape is dependent on the spring constant $c$. The number of half-waves for the critical buckling mode increases with increasing values of $c$ as it uses lesser energy than a buckled mode shape characterized by a single half wave. It is worth noting that the buckling problem of a column with continuous elastic restraint along its length is analogous to (a) the buckling problem of an end loaded column rotating with a constant angular velocity and (b) the free vibration problem of an axially loaded column (see paper by Wang et al., 1991).

**Table 2.12:** Critical load of continuously–restrained columns.

| Restraint stiffness parameter | Critical load parameter, $\alpha = PL^2/EI$ | |
|:---:|:---:|:---:|
| | Pinned–pinned column | Fixed–pinned column |
| 0 | 9.8696 | 20.1903 |
| 50 | 14.9357 | 24.2852 |
| 100 | 20.0017 | 28.3066 |

## 2.7 Euler Columns with Distributed Load

Axially distributed loads acting on columns include selfweight of the column, gravitational forces in an highly accelerated environment and weight of wet concrete during the construction of steel-tube–filled concrete columns.

### 2.7.1 Infinite Hanging Heavy Column with Bottom Load

Figure 2.13(a) shows a long column with density $\rho$ (weight per unit length), flexural rigidity $EI$, and subjected to a bottom compressive load of $F$.

A moment balance [Fig. 2.13(b)] yields the linearized equation

$$dM + (F - \rho x)\, \theta dx = 0 \qquad (2.7.1)$$

where $M$ is the local moment, related to the inclination angle $\theta$ by the Euler–Bernoulli relation

$$M = EI\frac{d\theta}{dx} \qquad (2.7.2)$$

By letting

$$r = \frac{\rho x - F}{(EI)^{1/3}\rho^{2/3}} \qquad (2.7.3)$$

Eq. (2.7.1) becomes the Airy equation

$$\frac{d^2\theta}{dr^2} - r\theta = 0 \qquad (2.7.4)$$

with the general solution

$$\theta = C_1 Ai(r) + C_2 Bi(r) \qquad (2.7.5)$$

where $Ai$ and $Bi$ are Airy functions (Abramowitz and Stegun, 1965). The boundary conditions are zero slope at infinity and zero moment at the bottom end at $x = 0$. Thus $C_2 = 0$ and

$$Ai' \left[ -F(EI)^{-1/3} \rho^{-2/3} \right] = 0 \tag{2.7.6}$$

The critical load (Wang, 1983) is the lowest root of Eq. (2.7.6) or

$$\frac{F}{(EI)^{1/3} \rho^{2/3}} = 1.018793 \tag{2.7.7}$$

In the case where the bottom end is constrained to be vertical, but can slide freely horizontally, the condition is

$$Ai \left[ -F(EI)^{-1/3} \rho^{-2/3} \right] = 0 \tag{2.7.8}$$

Then the critical load is

$$\frac{F}{(EI)^{1/3} \rho^{2/3}} = 2.338107 \tag{2.7.9}$$
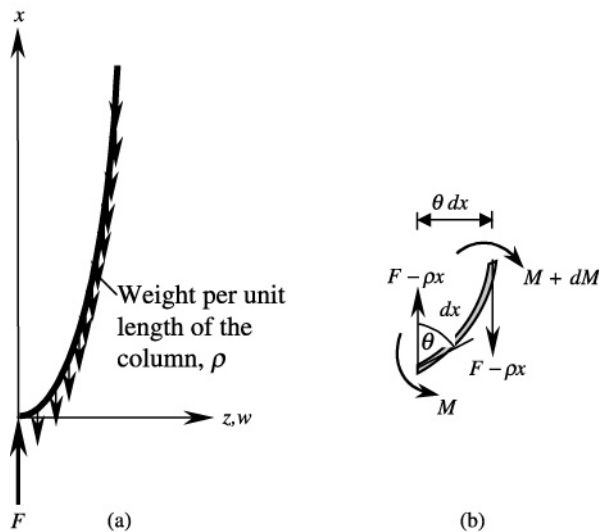


**Figure 2.13:** Infinite hanging column under its own weight.

### 2.7.2 Heavy Column with Top Load

Figure 2.14(a) shows a column of length $L$ and density $\rho$ subjected to a top load $P$. Both $\rho$ and $P$ are positive in the directions shown; $\rho$ can be negative if the column is hanging down from the base or when buoyancy is larger than the material weight.

A moment balance [Fig. 2.14(b)] yields the linearized equation

$$dM + [\rho(L - x) + P]\,\theta dx = 0 \tag{2.7.10}$$

This gives, in view of Eq. (2.7.2), the governing equation

$$EI\frac{d^2\theta}{dx^2} + [\rho(L - x) + P]\,\theta = 0 \tag{2.7.11}$$

The displacement $w$ is related to the slope $\theta$ by

$$\theta = \frac{dw}{dx} \tag{2.7.12}$$

Let

$$\alpha = \frac{PL^2}{EI}, \quad \beta = \frac{\rho L^3}{EI}, \quad s = \frac{x}{L} \tag{2.7.13}$$
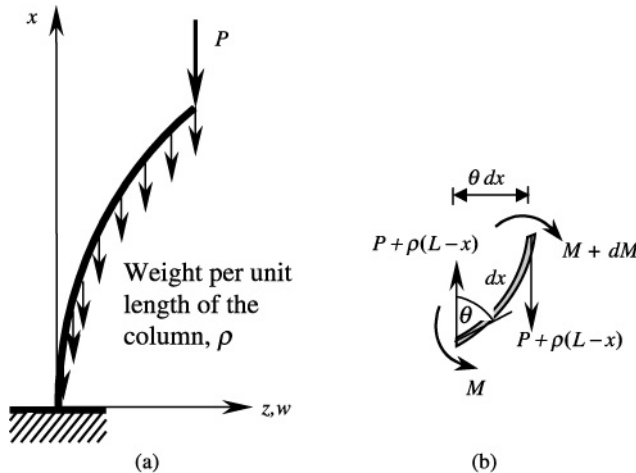


**Figure 2.14:** Heavy column with top load.

Then Eq. (2.7.11) becomes

$$\frac{d^2\theta}{ds^2} + [\alpha + \beta(1-s)]\theta = 0 \tag{2.7.14}$$

where $s$ is in $[0,1]$. If we define (Wang and Drachman, 1981)

$$r = \left(1 - s + \frac{\alpha}{\beta}\right)|\beta|^{1/3} \tag{2.7.15}$$

Eq. (2.7.15) then further simplifies to

$$\frac{d^2\theta}{dr^2} + \text{sgn}(\beta) r\theta = 0 \tag{2.7.16}$$

The general solution is

$$\theta = C_1 Ai\left[-\text{sgn}(\beta) r\right] + C_2 Bi\left[-\text{sgn}(\beta) r\right] \tag{2.7.17}$$

The Airy functions $Ai$ and $Bi$ are related to the Bessel functions by the following relations. If $z$ and $\zeta$ are positive, and

$$\zeta = \frac{2}{3} z^{3/2} \tag{2.7.18}$$

then

$$Ai(z) = \frac{1}{3}\sqrt{z}\left[I_{-1/3}(\zeta) - I_{1/3}(\zeta)\right], \quad Ai'(z) = \frac{z}{3}\left[I_{2/3}(\zeta) - I_{-2/3}(\zeta)\right]$$

$$Ai(-z) = \frac{1}{3}\sqrt{z}\left[J_{1/3}(\zeta) + J_{-1/3}(\zeta)\right], \quad Ai'(-z) = \frac{z}{3}\left[J_{2/3}(\zeta) - J_{-2/3}(\zeta)\right]$$

$$Bi(z) = \sqrt{\frac{z}{3}}\left[I_{-1/3}(\zeta) + I_{1/3}(\zeta)\right], \quad Bi'(z) = \frac{z}{\sqrt{3}}\left[I_{-2/3}(\zeta) + I_{2/3}(\zeta)\right]$$

$$Bi(-z) = \sqrt{\frac{z}{3}}\left[J_{-1/3}(\zeta) - J_{1/3}(\zeta)\right], \quad Bi'(-z) = \frac{z}{\sqrt{3}}\left[J_{-2/3}(\zeta) + J_{2/3}(\zeta)\right]$$

$$\tag{2.7.19}$$

Since $w$ cannot be integrated exactly from Eq. (2.7.12), only two types of boundary conditions are admissible for exact solutions. One is the fixed end or sliding restraint

$$\theta = 0 \tag{2.7.20}$$

The other is the pinned end or free end constraint

$$\frac{d\theta}{dr} = 0 \tag{2.7.21}$$

Upon a close examination of the problem, there are only six independent cases which yield an exact characteristic equation. Let

$$r_1 = \left(1 + \frac{\alpha}{\beta}\right)|\beta|^{1/3}, \quad r_2 = \frac{\alpha}{\beta}|\beta|^{1/3} \qquad (2.7.22)$$

$$\zeta_1 = \frac{2}{3}|1 + \frac{\alpha}{\beta}|^{3/2}|\beta|^{1/2} > 0, \quad \zeta_2 = \frac{2}{3}|\alpha|^{3/2}|\beta|^{-1} > 0 \qquad (2.7.23)$$

The stability criteria are shown in Table 2.13.

The buckling of a uniform free-standing column due to its own weight has been solved by Greenhill (1881). Greenhill's solution can be obtained by setting $\alpha = 0$ and $\beta > 0$ in Eq. (2.7.14) (i.e., Case 1 in Table 2.13); the solutions are Bessel functions of the first kind. Applying the boundary conditions at the top and bottom ends, one obtains the buckling condition

$$J_{-1/3}\left(\frac{2}{3}\beta^{1/2}\right) = 0 \qquad (2.7.24)$$

The lowest root is

$$\beta = \frac{\rho L^3}{EI} = 7.83735 \qquad (2.7.25)$$

### 2.7.3 Two-Segment Heavy Column – General Formulation

Figure 2.15 shows a column composed of two segments of different properties. The total length of the column is $L$ and the top load is $P$. Let the subscript 1 denote the bottom segment which is of length $aL$ and the subscript 2 denote the top segment which is of length $(1-a)L$. A moment balance similar to that of the previous section yields, for the top segment,

$$\frac{d^2\theta_2}{ds^2} + [\alpha_2 + \beta_2(1-s)]\theta_2 = 0, \quad a \leq s \leq 1 \qquad (2.7.26)$$

where $\theta$ is the angle of inclination, $s$ is the vertical coordinate normalized by the total length $L$ and

$$\alpha_2 = \frac{PL^2}{(EI)_2}, \quad \beta_2 = \frac{\rho_2 L^3}{(EI)_2} \qquad (2.7.27)$$

**Table 2.13:** Stability criteria for heavy columns with various end conditions.

| | | | |
|---|---|---|---|
| 1 | | $\alpha > 0, \beta > 0$ <br> $r_1 > 0, r_2 > 0$ | $J_{-1/3}(\zeta_1)J_{-2/3}(\zeta_2) + J_{1/3}(\zeta_1)J_{2/3}(\zeta_2) = 0$ <br> Wang and Drachman (1981) |
| 2 | | $-\alpha > \beta > 0$ <br> $r_1 > 0, r_2 < 0$ | $J_{-1/3}(\zeta_1)I_{-2/3}(\zeta_2) + J_{1/3}(\zeta_1)I_{2/3}(\zeta_2) = 0$ <br> Wang (1987b) |
| 3 | | $\alpha > 0, \beta > 0$ <br> $r_1 > 0, r_2 > 0$ | $J_{1/3}(\zeta_1)J_{-1/3}(\zeta_2) - J_{-1/3}(\zeta_1)J_{1/3}(\zeta_2) = 0$ <br> Wang (1987c) |
| 4 | | $\beta > -\alpha > 0$ <br> $r_1 > 0, r_2 < 0$ | $J_{1/3}(\zeta_1)I_{-1/3}(\zeta_2) + J_{-1/3}(\zeta_1)I_{1/3}(\zeta_2) = 0$ |
| 5 | | $-\beta > \alpha > 0$ <br> $r_1 > 0, r_2 < 0$ | $I_{-1/3}(\zeta_1)J_{-2/3}(\zeta_2) - I_{1/3}(\zeta_1)J_{2/3}(\zeta_2) = 0$ <br> Wang and Drachman (1981) |
| | | $\alpha > -\beta > 0$ <br> $r_1 < 0, r_2 < 0$ | $J_{-1/3}(\zeta_1)J_{-2/3}(\zeta_2) + J_{1/3}(\zeta_1)J_{2/3}(\zeta_2) = 0$ |
| 6 | | $-\beta > \alpha > 0$ <br> $r_1 > 0, r_2 < 0$ | $I_{2/3}(\zeta_1)J_{-2/3}(\zeta_2) - I_{-2/3}(\zeta_1)J_{2/3}(\zeta_2) = 0$ |
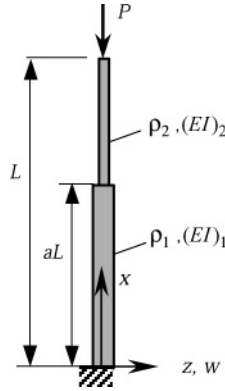
**Figure 2.15:** A heavy composite column.

Notice that both the load $P$ and/or the density $\rho$ may be negative. The general solution is

$$\theta_2 = C_1 Ai\left[- \text{sgn } (\beta_2) q\right] + C_2 Bi\left[- \text{sgn } (\beta_2) q\right] \tag{2.7.28}$$

where

$$q = \left(1 - s + \frac{\alpha_2}{\beta_2}\right) |\beta_2|^{1/3} \tag{2.7.29}$$

Depending on the sign of the arguments, the Airy functions in (2.7.19) would then transform the solution to the proper Bessel functions. Similarly for the bottom segment, we have

$$\frac{d^2\theta_1}{ds^2} + [\alpha_1 + \beta_1 (1 - s)] \theta_1 = 0, \quad 0 \leq s \leq a \tag{2.7.30}$$

where

$$\alpha_1 = \frac{P_1 L^2}{(EI)_1}, \quad \beta_1 = \frac{\rho_1 L^3}{(EI)_1} \tag{2.7.31}$$

$$P_1 = P + L (1 - a) (\rho_2 - \rho_1) \tag{2.7.32}$$

The general solution is

$$\theta_1 = C_3 Ai\left[- \text{sgn } (\beta_1) r\right] + C_4 Bi\left[- \text{sgn } (\beta_1) r\right] \tag{2.7.33}$$

where

$$r = \left(1 - s + \frac{\alpha_1}{\beta_1}\right) |\beta_1|^{1/3} \tag{2.7.34}$$

The solution of the top segment satisfies the boundary condition at $s = 1$, either zero inclination or zero moment, and that of the bottom satisfies the boundary condition at $s = 0$. The matching conditions at the joint at $s = a$ are given by the equality in the inclinations

$$\theta_1(a) = \theta_2(a) \qquad (2.7.35)$$

and the equality of bending moments

$$\left[ (EI)_1 \frac{d\theta_1}{ds} \right]_{s=a} = \left[ (EI)_2 \frac{d\theta_2}{ds} \right]_{s=a} \qquad (2.7.36)$$

Particular attention must be paid in choosing the right branch for the Airy functions, especially when the argument changes sign at an interior point of the column. In what follows, we shall give the details for some interesting special cases.

### 2.7.4 Heavy Column Partially Submerged in Liquid

For a uniform column that is partially submerged, the wetted portion has a lower effective density due to buoyancy. The flexural rigidity remains the same for the whole column [i.e., $(EI)_1 = (EI)_2 = EI$]. Let $\rho_c$ be the density of the column, $\rho_f$ be the density of the fluid, and $\lambda_\rho = \rho_f/\rho_c$. For a column with load $P$ at the top (see Fig. 2.14), we find

$$\alpha_2 = \frac{PL^2}{EI}, \quad \beta_2 = \frac{\rho_c L^3}{EI} > 0 \qquad (2.7.37)$$

$$\alpha_1 = \alpha_2 + (1-a)\,\lambda\beta_2, \quad \beta_1 = (1-\lambda)\,\beta_2 \qquad (2.7.38)$$

The solutions are

$$\theta_2 = C_1 Ai\,(-q) + C_2 Bi\,(-q)\,, \quad q = \left( 1 - s + \frac{\alpha_2}{\beta_2} \right) \beta_2^{1/3} \qquad (2.7.39)$$

$$\theta_1 = C_3 Ai(-gr) + C_4 Bi(-gr), \quad g = \text{sgn}\,(\beta_1), \quad r = \left( 1 - s + \frac{\alpha_1}{\beta_1} \right) |\beta_1|^{1/3} \qquad (2.7.40)$$

Let

$$q_2 = \alpha_2 \beta_2^{-2/3}, \quad q_a = \left( 1 - a + \frac{\alpha_2}{\beta_2} \right) \beta_2^{1/3} \qquad (2.7.41)$$

and

$$r_1 = \left(1 + \frac{\alpha_1}{\beta_1}\right)|\beta_1|^{1/3}, \quad r_a = \left(1 - a + \frac{\alpha_1}{\beta_1}\right)|\beta_1|^{1/3} \qquad (2.7.42)$$

The matching conditions at $s = a$ are

$$C_1 Ai\left(-q_a\right) + C_2 Bi\left(-q_a\right) - C_3 Ai\left(-gr_a\right) - C_4 Bi\left(-gr_a\right) = 0 \quad (2.7.43)$$

$$C_1 Ai'\left(-q_a\right) + C_2 Bi'\left(-q_a\right) - C_3 Ai'\left(-gr_a\right) - C_4 Bi'\left(-gr_a\right) = 0 \quad (2.7.44)$$

If the top is free,

$$C_1 Ai'\left(-q_2\right) + C_2 Bi'\left(-q_2\right) = 0 \qquad (2.7.45)$$

If the top has a sliding constraint,

$$C_1 Ai\left(-q_2\right) + C_2 Bi\left(-q_2\right) = 0 \qquad (2.7.46)$$

If the bottom is fixed,

$$C_3 Ai\left(-gr_1\right) + C_4 Bi\left(-gr_1\right) = 0 \qquad (2.7.47)$$

If the bottom is pinned,

$$C_3 Ai'\left(-gr_1\right) + C_4 Bi'\left(-gr_1\right) = 0 \qquad (2.7.48)$$

Table 2.14 shows the characteristic equations of a heavy column with a free top end and no external load. The functions used are defined by

$$\mu\left(s\right) = \frac{2}{3}\sqrt{\beta_2}\left[\text{ sgn }\left(\lambda_\rho - 1\right)|\lambda_\rho - 1|^{1/3}\left(\frac{1 - a\lambda_\rho}{\lambda_\rho - 1} + s\right)\right]^{3/2} \qquad (2.7.49)$$

$$\mu_0 = \mu(0), \quad \mu_1 = \mu(1) \qquad (2.7.50)$$

$$v_1 = \frac{2}{3}\sqrt{\beta_2}(1-a)^{3/2}, \quad \phi_1 = \frac{2}{3\mu_1}J_{1/3}\left(\mu_1\right) - J_{4/3}\left(\mu_1\right) \qquad (2.7.51)$$

$$\xi_0 = \beta_2^{1/3}\left(a\lambda_\rho - 1\right)\left(\lambda_\rho - 1\right)^{-2/3} \qquad (2.7.52)$$

**Table 2.14:** Stability criteria for columns partially submerged in liquid.

| | | |
|---|---|---|

$a\lambda_\rho < 1$    $J_{2/3}(v_1)\left[J_{-1/3}(\mu_1)J_{1/3}(\mu_0) + J_{1/3}(\mu_1)J_{-1/3}(\mu_0)\right]$
$+\text{sgn}\,(\lambda_\rho - 1)J_{-1/3}(v_1)\left[J_{2/3}(\mu_1)J_{1/3}(\mu_0)\right.$
$\left.+J_{-1/3}(\mu_0)\phi_1\right] = 0$

$a\lambda_\rho > 1$    $\left[Bi(\xi_0) - \sqrt{3}Ai(\xi_0)\right]\left[J_{2/3}(v_1)J_{-1/3}(\mu_1)+\right.$
$\left.J_{-1/3}(v_1)J_{2/3}(\mu_1)\right] + \left[Bi(\xi_0) + \sqrt{3}Ai(\xi_0)\right]$
$\times\left[J_{2/3}(v_1)J_{1/3}(\mu_1) - J_{-1/3}(v_1)\phi_1\right] = 0$

Wang (1987d)

---

$a^2\lambda_\rho > 1$    $v_1^{1/3}J_{2/3}(v_1)\left\{\left[Bi'(\xi_0) + \sqrt{3}Ai'(\xi_0)\right]J_{1/3}(\mu_1) +\right.$
$\left.\left[Bi'(\xi_0) - \sqrt{3}Ai'(\xi_0)\right]J_{-1/3}(\mu_1)\right\} - (\lambda_\rho - 1)^{1/3}$
$\times\mu_1^{1/3}J_{-1/3}(v_1)\left\{\left[Bi'(\xi_0) + \sqrt{3}Ai'(\xi_0)\right]J_{-2/3}(\mu_1)-\right.$
$\left.\left[Bi'(\xi_0) - \sqrt{3}Ai'(\xi_0)\right]J_{2/3}(\mu_1)\right\} = 0$

Wang (1991)

---

### 2.7.5 Standing Two-Segment Heavy Column

Here, we treat the two-segment column shown in Fig. 2.16. Assume there is no top load $P$, each section is uniform, of similar cross section, and made of the same material. If the cross section is similar, whether circular or square, the flexural rigidity and the density have the following relation

$$\frac{EI_2}{EI_1} = \left(\frac{\rho_2}{\rho_1}\right)^2 = \lambda_\rho^2 \tag{2.7.53}$$

Thus,

$$\beta_2 = \frac{\rho_2 L^3}{EI_2} > 0, \quad \beta_1 = \lambda_\rho\beta_2 > 0 \tag{2.7.54}$$

For the top section, the solution to Eq. (2.7.16) satisfying the zero moment condition at the top is

$$\theta_2 = C_1\zeta^{1/3}J_{-1/3}\left(\zeta\right) \tag{2.7.55}$$
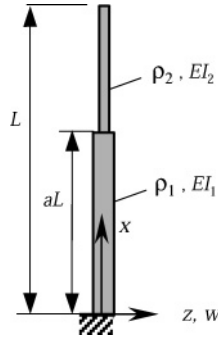
**Figure 2.16:** A heavy composite column under its own weight.

where

$$\zeta = \frac{2}{3}q^{3/2}, \quad q = (1-s)\beta_2^{1/3} \tag{2.7.56}$$

For the bottom section, the solution satisfying zero slope at the bottom is

$$\theta_1 = C_2\eta^{1/3}\left[J_{-1/3}(\eta_1)J_{1/3}(\eta) - J_{1/3}(\eta_1)J_{-1/3}(\eta)\right] \tag{2.7.57}$$

where

$$\eta(a) = \frac{2}{3}r^{3/2}, \quad r = [\lambda_\rho(1-a) + a - s]\beta_1^{1/3} \tag{2.7.58}$$

and

$$\eta_1 = \eta(0) \tag{2.7.59}$$

In view of the matching conditions (2.7.35) and (2.7.36), the stability condition is found to be

$$\lambda_\rho^3\left[J_{1/3}(\eta_a)J_{-1/3}(\eta_1) - J_{1/3}(\eta_1)J_{-1/3}(\eta_a)\right]\left\{2J_{-1/3}(\zeta_a)\right.$$

$$+ 3\xi_a\left[J_{-4/3}(\zeta_a) - J_{2/3}(\zeta_a)\right]\Big\}$$

$$= J_{-1/3}(\zeta_a)\left\{\left[2J_{1/3}(\eta_a) + 3\eta_a\left\langle J_{-2/3}(\eta_a) - J_{4/3}(\eta_a)\right\rangle\right]J_{-1/3}(\eta_1)\right.$$

$$\left. - J_{1/3}(\eta_1)\left[2J_{-1/3}(\eta_a) + 3\eta_a\left\langle J_{-4/3}(\eta_a) - J_{2/3}(\eta_a)\right\rangle\right]\right\} \tag{2.7.60}$$

where the subscript $a$ denotes the variable evaluated at the joint at $s = a$. Table 2.15 shows some typical results.

The value of $\lambda_\rho$ also represents the ratio of the area of the top segment to the area of the bottom segment. For the uniform column $\lambda_\rho = 1$, the buckling value $\beta_2$ is 7.83735, the same as Eq. (2.7.29), and similarly for $a = 0$. When $a = 1$ the size of the column is uniformly that of the bottom segment, and the buckling value is $7.83735/\lambda_\rho$. For $\lambda_\rho > 1$ the column is top-heavy and thus has a lower critical value.

**Table 2.15:** Critical values of $\beta_2$.

| $\lambda_\rho$ | $a = 0.10$ | 0.25 | 0.50 | 0.75 | 1.00 |
|---|---|---|---|---|---|
| 0.50 | 9.8980 | 14.430 | 24.428 | 22.184 | 15.675 |
| 0.75 | 8.9520 | 10.830 | 12.934 | 12.258 | 10.450 |
| 1.50 | 5.6620 | 4.281 | 3.720 | 4.026 | 5.225 |
| 2.00 | 4.0117 | 2.601 | 2.156 | 2.454 | 3.919 |

## 2.8 Euler Columns with Variable Cross Section

### 2.8.1 Introduction

In this section, we consider columns where their cross-sections vary along the length but still maintain the same principal bending axis. The most common type would be columns with similar cross sections, while the area of the cross section varies. In what follows, we present two cases. In the first case, the column has no distributed axial load and buckles by end compressive forces only. It can be shown that the lateral deflection, for certain forms of the flexural rigidity, can be integrated exactly. Thus, the classical boundary conditions of section 2.1.2 can be applied. In the second case there exists an additional distributed axial load, such as selfweight, and the solution, again for some restricted forms of distribution, can only be expressed in terms of the slope $\theta$. Since the deflection $w$ cannot be exactly integrated, similar to those of section 2.7, only columns with zero lateral shear give exact characteristic equations. The solutions to each case can be joined together to form a compound column. These compound columns will not be discussed, not because they are unimportant, but because the matching method has been well described in the previous section. Earlier references for columns of variable cross section are found in Bleich (1952), Timoshenko and Gere (1961), and a recent selective review by Elishakoff (2000).

## 2.8.2 Columns under End Concentrated Load

For columns with variable cross-section, the moment of inertia $I$ is a function of position along the column of length $L$. If there is no distributed axial load, similar to section 2.1, one can show the equation governing the lateral displacement is

$$\frac{d^2}{dx^2}\left(EI\left(x\right)\frac{d^2w}{dx^2}\right) + P\frac{d^2w}{dx^2} = 0 \qquad (2.8.1)$$

where $P \neq 0$ is the end load. Integrating twice, we obtain

$$EI\left(x\right)\frac{d^2w}{dx^2} + Pw = C_1 + C_2 x \qquad (2.8.2)$$

where the value of $C_2$ can be identified with the shear. Thus, the general solution is

$$w = \frac{C_1}{P} + \frac{C_2}{P}x + w_h \qquad (2.8.3)$$

where $w_h$ is the homogeneous solution satisfying

$$EI\left(x\right)\frac{d^2 w_h}{dx^2} + Pw_h = 0 \qquad (2.8.4)$$

Depending on the form of $EI(x)$, there exist a number of exact solutions of Eq. (2.8.4). For example, one can specify $EI(x)$ such that the ordinary differential equation conforms to those with closed form solutions as listed in Kamke (1948) or Murphy (1960). However, most of the exact solutions do not have any physical relevance. Suppose the two independent solutions to Eq. (2.8.4) are found to be $U(z)$ and $V(z)$ where $z = z(x)$. Then the general solution is

$$w = \frac{C_1}{P} + \frac{C_2}{P}x + C_3 U\left(z\right) + C_4 V\left(z\right), \quad z = z\left(x\right) \qquad (2.8.5)$$

Let

$$z_0 = z(0), \quad z_1 = z(L), z_0' = Lz'(0), z_1' = Lz'(L) \qquad (2.8.6)$$

$$U_0 = U(z_0), V_0 = V(z_0), U_0' = U'(z_0), V_0' = V'(z_0) \qquad (2.8.7)$$

$$U_1 = U(z_1), V_1 = V(z_1), U_1' = U'(z_1), V_1' = V'(z_1) \qquad (2.8.8)$$

The stability criteria for the five cases of classical boundary conditions are listed in Table 2.16.

**Table 2.16:** Stability criteria for five cases of classical boundary conditions.
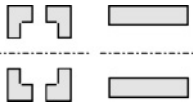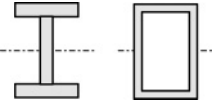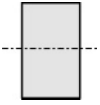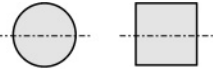
| Figure | Cases | Stability Criteria |
|---|---|---|
|  | 1. Bottom end fixed, top end free | $U_1 V_0' - V_1 U_0' = 0$ |
|  | 2. Both ends pinned | $U_1 V_0 - V_1 U_0 = 0$ |
|  | 3. Bottom end fixed, top end pinned | $U_1(V_0 + z_0' V_0') - V_1(U_0 + z_0' U_0')$ |
|  | 4. Both ends fixed | $(U_1 - U_0 - z_1' U_1')(z_1' V_1' - z_0' V_0') -$ $(V_1 - V_0 - z_1' V_1')(z_1' U_1' - z_0' U_0') = 0$ |
|  | 5. Bottom end fixed, top end sliding | $U_1' V_0' - V_1' U_0' = 0$ |

Gere and Carter (1962) listed the relation between a varying cross-sectional area dimension $h(x)$ and the second moment of inertia $I(x)$ for some meaningful cross-sections where

$$I(x) = Ch(x)^n \qquad (2.8.9)$$

Here $C$ and $n$ are positive constants. The value of $n$ ranges from 1 to 4 and the corresponding physical cross-sectional shapes are shown in Table 2.17.

**Table 2.17:** Various cross-sectional shapes.

| Shape | Description | $n$ |
|---|---|---|
|  | Flat rectangular section<br>Thickness constant, width varies | $n = 2$ |
|  | Open web section or tower section<br>Area constant, depth varies | $n = 2$ |
|  | I-section or box section<br>Width constant, depth varies | $n = 2.1$ to $2.6$ |
|  | Solid rectangular section<br>Width constant, depth varies | $n = 3$ |
|  | Solid similar section<br>Both width and depth vary | $n = 4$ |

Given any $EI(x)$ and cross-sectional characteristics, one can always find the depth variation $h(x)$ by taking the $n$th root, but there are only a few relevant forms of practical interest. Here we shall consider the two more important classes of $EI(x)$ which can be applied to columns of exponential taper and linear taper.

Dinnik (1929) first considered the class of columns whose flexural rigidity is exponential, given by

$$EI(x) = \alpha e^{-ax} \qquad (2.8.10)$$

The solution to Eq. (2.8.4) (Murphy, 1960) consists of Bessel functions of order zero. The general solution is

$$w = \frac{C_1}{P} + \frac{C_2}{P}x + C_3 J_0(z) + C_4 Y_0(z) \qquad (2.8.11)$$

where

$$z = \frac{2}{a}\sqrt{\frac{P}{\alpha}}\, e^{ax/2} \qquad (2.8.12)$$

Thus

$$U(z) = J_0(z), \quad V(z) = Y_0(z) \qquad (2.8.13)$$

and

$$z_0 = \frac{2}{a}\sqrt{\frac{P}{\alpha}}, \quad z_1 = \frac{2}{a}\sqrt{\frac{P}{\alpha}}\, e^{aL/2} \qquad (2.8.14)$$

The stability criteria for the five classical boundary conditions are then obtained from Table 2.16. Given $aL$, some typical values for the normalized buckling load $PL^2/\alpha$ are given in Table 2.18. When $aL = 0$, the buckling loads correspond to those of the uniform column.

**Table 2.18:** Normalized buckling load $PL^2/\alpha$ for exponential columns.

| $aL$ | Case 1 | Case 2 | Case 3 | Case 4 | Case 5 |
|------|--------|--------|--------|--------|--------|
| 0.0 | 2.467 | 9.870 | 9.870 | 20.19 | 39.48 |
| 0.1 | 2.394 | 9.380 | 9.390 | 19.20 | 37.55 |
| 0.5 | 2.110 | 7.634 | 7.683 | 15.64 | 30.60 |
| 1.0 | 1.782 | 5.827 | 5.973 | 11.99 | 23.49 |
| 1.5 | 1.480 | 4.389 | 4.633 | 9.098 | 17.86 |
| 2.0 | 1.209 | 3.264 | 3.580 | 6.839 | 13.46 |

Next, consider the class of flexural rigidity given by the power function (Dinnik, 1932; Gere and Carter, 1962)

$$EI(x) = \alpha(1 - bx)^a \qquad (2.8.15)$$

where $\alpha$ and $a$ are positive constants and $bL \leq 1$. For $a \neq 2$, let

$$c = \left| \frac{1}{2 - a} \right|, \quad k = \frac{P}{\alpha b^2} \qquad (2.8.16)$$

and

$$z = 1 - bx \qquad (2.8.17)$$

Then the homogeneous solution to Eq.(2.8.4) (Murphy, 1960), is

$$U(z) = \sqrt{z} J_c \left( 2\sqrt{k} c z^{1/2c} \right), \quad V(z) = \begin{cases} \sqrt{z} J_{-c} \left( 2\sqrt{k} c z^{1/2c} \right) \\ \sqrt{z} Y_c \left( 2\sqrt{k} c z^{1/2c} \right) \end{cases} \qquad (2.8.18)$$

where the top form of $V$ is used when $c$ is not an integer, and the bottom form is used otherwise. Note that if $c$ is an integer multiple of $1/2$, the Bessel functions can be expressed as harmonic functions. If $a = 2$ the solution form changes completely. Let

$$r = \sqrt{\left| k - \frac{1}{4} \right|} \qquad (2.8.19)$$

The solution is

$$U(z) = z^{r+1/2}, \quad V(z) = z^{-r+1/2} \quad \text{when } k < 1/4 \qquad (2.8.20)$$
$$U(z) = \sqrt{z}, \quad V(z) = \sqrt{z} \ln z \quad \text{when } k = 1/4 \qquad (2.8.21)$$

If $k > 1/4$ the solution is

$$U(z) = \sqrt{z} \cos(r \ln z), \quad V(z) = \sqrt{z} \sin(r \ln z) \qquad (2.8.22)$$

The stability criteria are then obtained from Table 2.16. For the special case of a pinned–pinned column and $k > 1/4$, Freudenthal (1966) used the $V$ solution in Eq. (2.8.22) to obtain the closed form critical load equivalent to

$$\frac{P}{\alpha b^2} = \frac{1}{4} + \left( \frac{\pi}{\ln(1 - bL)} \right)^2 \qquad (2.8.23)$$

Some typical values for various boundary conditions are listed in Table 2.19. When $a = 0$, the column is uniform. The critical loads for the five cases are 2.4674, 9.8696, 20.1907, 39.4784, 9.8696, respectively.

**Table 2.19:** The critical load $PL^2/\alpha$ for the power function rigidity variation. The five cases correspond to the boundary conditions in Table 2.16.

| Case | $a$ | $bL = 0.1$ | 0.3 | 0.5 | 0.7 | 0.9 |
|------|-----|-----------|-----|-----|-----|-----|
|        | 1 | 2.393 | 2.235 | 2.062 | 1.865 | 1.621 |
|        | 2 | 2.319 | 2.012 | 1.683 | 1.318 | 0.862 |
| Case 1 | 3 | 2.246 | 1.798 | 1.336 | 0.853 | 0.321 |
|        | 4 | 2.175 | 1.595 | 1.029 | 0.498 | 0.080 |
|        | 1 | 9.372 | 8.343 | 7.256 | 6.069 | 4.667 |
|        | 2 | 8.893 | 7.005 | 5.198 | 3.459 | 1.710 |
| Case 2 | 3 | 8.436 | 5.840 | 3.628 | 1.821 | 0.467 |
|        | 4 | 7.994 | 4.836 | 2.467 | 0.888 | 0.099 |
|        | 1 | 19.17 | 17.03 | 14.74 | 12.18 | 9.029 |
|        | 2 | 18.19 | 14.29 | 10.53 | 6.868 | 3.164 |
| Case 3 | 3 | 17.25 | 11.92 | 7.362 | 3.634 | 0.875 |
|        | 4 | 16.35 | 9.893 | 5.048 | 1.817 | 0.202 |
|        | 1 | 37.48 | 33.27 | 28.70 | 23.48 | 16.70 |
|        | 2 | 35.56 | 27.91 | 20.48 | 13.23 | 5.864 |
| Case 4 | 3 | 33.73 | 23.29 | 14.35 | 7.045 | 1.670 |
|        | 4 | 31.98 | 19.34 | 9.869 | 3.553 | 0.395 |
|        | 1 | 9.369 | 8.317 | 7.169 | 5.858 | 4.143 |
|        | 2 | 8.893 | 7.005 | 5.198 | 3.459 | 1.710 |
| Case 5 | 3 | 8.442 | 5.897 | 3.758 | 2.011 | 0.620 |
|        | 4 | 8.012 | 4.960 | 2.700 | 1.121 | 0.166 |

### 2.8.3 Columns under Distributed Axial Load

The only important work was due to Dinnik (1955). He assumed a flexural rigidity and a distributed load (force per length) of the form

$$EI(x) = \alpha \left(1 - \frac{x}{L}\right)^a, \quad \rho(x) = \beta \left(1 - \frac{x}{L}\right)^b \qquad (2.8.24)$$

where $\alpha$, $\beta$, $a$, and $b$ are positive constants. Notice these shapes terminate into a point at the top at $x = L$, and no top load is allowed.

A moment balance as in yields

$$\frac{d}{dx}\left(EI\left(x\right)\frac{d\theta}{dx}\right) + \int_{x}^{L}\rho\left(x\right)dx = 0 \qquad (2.8.25)$$

Eqs. (2.8.24) and (2.8.25) become

$$\frac{d}{dz}\left(z^{a}\frac{d\theta}{dz}\right) + \mu z^{b+1}\theta = 0 \qquad (2.8.26)$$

where

$$z = 1 - \frac{x}{L}, \quad \mu = \frac{\beta L^{3}}{\alpha(b+1)} \qquad (2.8.27)$$

The solution is

$$\theta = C_{1}z^{(1-a)/2}J_{\nu}(u) + C_{2}\begin{cases} z^{(1-a)/2}J_{\nu}(u) \\ \sqrt{z}^{(1-a)/2}Y_{\nu}(u) \end{cases} \qquad (2.8.28)$$

where

$$u = \frac{\sqrt{\mu}}{|\kappa|}z^{\kappa}, \quad \nu = \left|\frac{a-1}{b+3-a}\right|, \quad \kappa = \frac{b+3-a}{2} \qquad (2.8.29)$$

As discussed before, since the displacement cannot be integrated in a closed form, the boundary conditions that yield exact characteristic equations are either zero inclination (fixed or sliding) or zero moment (free).

Lastly, we comment on some exact solutions of very specific forms in the literature which are not included here. The first type is the inverse solution, obtained from assuming a deflection form and adjusting the rigidity and/or axial load distribution to satisfy the differential equation (Elishakoff, 2000). The second type concerns an end load which is completely dependent on the given axial load distribution (e.g., dependent on self weight) (Li et al., 1995).

## 2.9 Timoshenko Columns

### 2.9.1 Columns under End Axial Load

When the column is stocky, or built up (latticed or battened) or of a composite-type construction, the application of Euler (classical) beam theory will overestimate the buckling loads. This is due to the neglect of transverse shear deformation in the Euler beam theory. A more

refined beam theory, known as the first-order shear deformation theory or Timoshenko beam theory, that incorporates the shear deformation effect was proposed by Engesser (1891) and Timoshenko (1921). This first-order shear deformation theory relaxes the normality assumption of the Euler beam theory by allowing the normal to rotate at an angle to the deformed centerline. This assumption amounts to a constant transverse shear strain (and thus constant stress) through the beam thickness. In order to compensate for the actual parabolic distribution of the transverse shear stress through the thickness, a shear correction factor is introduced to calculate the effective shear force. The usual approaches of estimating the shear correction factor are either by matching high-frequency spectra of vibrating beams (e.g., Mindlin and Deresiewicz, 1954; Goodman and Sutherland, 1951) or by using approximation procedures and simplifying assumptions within the linear theory of elasticity (e.g., Cowper, 1966; Stephen and Levinson, 1979).

According to the Engesser–Timoshenko beam theory, the stress–resultant–displacement relations are given by

$$M = EI\frac{d\phi}{d\bar{x}} \tag{2.9.1}$$

$$Q = K_s GA\left(\phi + \frac{d\bar{w}}{d\bar{x}}\right) \tag{2.9.2}$$
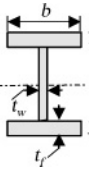
in which $\bar{x}$ is the longitudinal coordinate measured from the column base, $M$ the bending moment, $Q$ the transverse shear force, $\phi$ the rotation in the Engesser–Timoshenko column and $\bar{w}$ the transverse deflection. The shear correction coefficient $K_s$ in Eq. (2.9.2) is introduced to account for the difference in the constant state of shear stress in the Engesser–Timoshenko column theory and the parabolic variation of the actual shear stress through the depth of the cross-section. The values of $K_s$ for various cross-sectional shapes are given in Table 2.20 (Cowper, 1966). The effective shear stiffnesses, $GAK_s$, for various types of built up columns are given in Timoshenko and Gere (1961).

As in the Euler columns, the equilibrium equations are

$$\frac{dM}{d\bar{x}} = Q \tag{2.9.3}$$

$$\frac{dQ}{d\bar{x}} = P\frac{d^2\bar{w}}{d\bar{x}^2} \tag{2.9.4}$$

**Table 2.20:** Shear correction factors $K_s$ for various cross-sectional shapes.

| Section | Description | $K_s$ |
|---------|-------------|-------|
|  | Circle | $\dfrac{6(1+\nu)}{(7+6\nu)}$ |
|  | Hollow cylinder | $\dfrac{6(1+\nu)(1+\frac{b}{a})^2}{(7+6\nu)(1+\frac{b}{a})^2+4(5+3\nu)(\frac{b}{a})^2}$ |
|  | Rectangle | $\dfrac{10(1+\nu)}{12+11\nu}$ |
|  | Semicircle | $\dfrac{(1+\nu)}{1.305+1.273\nu}$ |
|  | Thin-walled circular tube | $\dfrac{2(1+\nu)}{4+\nu}$ |
|  | Thin-walled square tube | $\dfrac{20(1+\nu)}{48+39\nu}$ |
|  | I-beam | $\dfrac{10(1+\nu)(1+3\beta)^2}{\Delta}$ <br><br> $\Delta = 12 + 72\beta + 150\beta^2 + 90\beta^3$ <br> $\quad + \nu(11 + 66\beta + 135\beta^2 + 90\beta^3)$ <br> $\quad + 30\eta^2\beta(1+\beta) + 5\nu\eta^2\beta(8+9\beta)$ <br> $\beta = (2bt_f)/(ht_w), \quad \eta = b/h$ |

where $P$ is the axial compressive load. By substituting Eqs. (2.9.1) and (2.9.2) into Eqs. (2.9.3) and (2.9.4), the governing equations may be expressed as

$$EI\frac{d^2\phi}{d\bar{x}^2} = K_sGA\left(\phi + \frac{d\bar{w}}{d\bar{x}}\right) \qquad (2.9.5)$$

$$K_sGA\left(\frac{d\phi}{d\bar{x}} + \frac{d^2\bar{w}}{d\bar{x}^2}\right) = P\frac{d^2\bar{w}}{d\bar{x}^2} \qquad (2.9.6)$$

By differentiating Eq. (2.9.5) and then using Eq. (2.9.6), we obtain

$$EI\frac{d^3\phi}{d\bar{x}^3} = P\frac{d^2\bar{w}}{d\bar{x}^2} \qquad (2.9.7)$$

and from Eq. (2.9.6),

$$\frac{d\phi}{d\bar{x}} = -\left(1 - \frac{P}{K_sGA}\right)\frac{d^2\bar{w}}{d\bar{x}^2} \qquad (2.9.8)$$

The substitution of Eq. (2.9.8) into Eq. (2.9.7) yields

$$\frac{d^4w}{dx^4} + \bar{k}\frac{d^2w}{dx^2} = 0 \qquad (2.9.9)$$

where $x = \bar{x}/L$, $w = \bar{w}/L$ and

$$\bar{k} = \frac{\frac{PL^2}{EI}}{1 - \frac{P}{K_sGA}} \qquad (2.9.10)$$

By differentiating Eq. (2.9.5) and using Eq. (2.9.7), we can also obtain

$$\frac{d^3\phi}{dx^3} + \bar{k}\frac{d\phi}{dx} = 0 \qquad (2.9.11)$$

The general solutions of Eqs. (2.9.9) and (2.9.11) take the form of

$$w = C_1\sin\sqrt{\bar{k}}x + C_2\cos\sqrt{\bar{k}}x + C_3x + C_4 \qquad (2.9.12a)$$

$$\phi = -C_1\frac{P}{EI\sqrt{\bar{k}}}\cos\sqrt{\bar{k}}x + C_2\frac{P}{EI\sqrt{\bar{k}}}\sin\sqrt{\bar{k}}x - C_3 \qquad (2.9.12b)$$

The boundary conditions for a Timoshenko column are

- Fixed end: $\bar{w} = 0$ and $\phi = 0$ (2.9.13a)

- Pinned end: $\bar{w} = 0$ and $\frac{d\phi}{d\bar{x}} = 0$ (2.9.13b)

- Free end: $\frac{d\phi}{d\bar{x}} = 0$ and $EI\frac{d^2\phi}{d\bar{x}^2} + P\frac{d\bar{w}}{d\bar{x}} = 0$ (2.9.13c)

- Sliding restraint: $\phi = 0$ and $EI\frac{d^2\phi}{d\bar{x}^2} + P\frac{d\bar{w}}{d\bar{x}} = 0$ (2.9.13d)

By substituting Eqs. (2.9.12a, b) into these boundary conditions at the column ends, one obtains the following eigenvalue equation:

$$[A]\{C\} = \begin{bmatrix} a_{11} & a_{12} & a_{13} & a_{14} \\ a_{21} & a_{22} & a_{23} & a_{24} \\ a_{31} & a_{32} & a_{33} & a_{34} \\ a_{41} & a_{42} & a_{43} & a_{44} \end{bmatrix} \begin{Bmatrix} C_1 \\ C_2 \\ C_3 \\ C_4 \end{Bmatrix} = \mathbf{0} \qquad (2.9.14)$$

The vanishing of the determinant of matrix $[A]$ yields the characteristic equation (or stability criterion). The lowest root of the characteristic equation is the critical buckling load. Table 2.21 presents the stability criteria and solutions.

**Table 2.21:** Stability criteria and critical loads of Timoshenko columns under end axial load.

| Boundary Conditions | Stability Criterion | Critical Load |
|---|---|---|
| Fixed–free column | $\cos\sqrt{\bar{k}} = 0$ | $\dfrac{P=\frac{\pi^2 EI}{4L^2}}{1+\frac{\pi^2 EI}{4K_s GAL^2}}$ |
| Pinned–pinned column | $\sin\sqrt{\bar{k}} = 0$ | $\dfrac{P=\frac{\pi^2 EI}{L^2}}{1+\frac{\pi^2 EI}{K_s GAL^2}}$ |
| Fixed–pinned column | $\left(1 - \frac{P}{K_s GA}\right)\sqrt{\bar{k}} = \tan\sqrt{\bar{k}}$ | |
| Fixed–fixed column | $\sin\frac{\sqrt{\bar{k}}}{2} = 0$ | $\dfrac{P=\frac{4\pi^2 EI}{L^2}}{1+\frac{4\pi^2 EI}{K_s GAL^2}}$ |
| Fixed–sliding restraint column | $\cos\frac{\sqrt{\bar{k}}}{2} = 0$ | $\dfrac{P=\frac{\pi^2 EI}{L^2}}{1+\frac{\pi^2 EI}{K_s GAL^2}}$ |

By comparing the stability criteria of the Timoshenko columns with their Euler counterparts in Table 2.1, it is clear that the Timoshenko critical load $P^T$ and the Euler critical load $P^E$ are related by

$$P^T = \frac{P^E}{1 + \frac{P^E}{K_S GA}} \qquad (2.9.15)$$

for all the column end conditions except for the fixed–pinned columns. Note that Ziegler (1982) established that the foregoing relationship (Eq. 2.9.15) and gave the following modified form for the fixed–pinned columns

$$P^T \approx \frac{P^E}{1 + 1.1\frac{P^E}{K_S GA}} \qquad (2.9.16)$$

Banerjee and Williams (1994) showed that the buckling relationship in Eq. (2.9.15) applies as well to hinged–hinged columns with rotational springs of equal stiffness added to their ends.

It is clear from Eq. (2.9.15) that the effect of transverse shear deformation leads to a reduction in the Euler buckling load by the factor found at the denominator of the buckling load relationship. This reduction of the Euler load thus increases with respect to a higher value of Euler load (especially for columns with highly restrained ends or internal restraints) and also with a lower value of shear rigidity.

The critical buckling load formula obtained by Haringx (1942) for helical springs and rubber bearings is given by

$$P^H = \frac{K_s \hat{G} A}{2} \left[ \sqrt{1 + \frac{4P^E}{K_S \hat{G} A}} - 1 \right] \qquad (2.9.17)$$

The correctness of Eqs. (2.9.15) and (2.9.17) for column buckling with allowance for shear deformation has been discussed by a number of researchers (e.g., see Timoshenko and Gere, 1961; Ziegler, 1982). It was pointed out by Bažant (2003) that the two equations are in fact the same after noting that $\hat{G}$ in (2.9.17) is different from $G$ in (2.9.16).

In the Timoshenko beam theory, it is necessary to introduce the shear correction factor $K_s$ to compensate for the error due to the assumption of constant shear strain (or stress) through the beam thickness. The higher-order shear deformation beam theory, proposed by Bickford (1982) and Heyliger and Reddy (1988), does away with the need of the shear correction factor by assuming that the transverse normal to

the centroidal axis deforms into a cubic curve. Using this Bickford–Reddy beam theory, Wang et al. (2000) showed that for pinned ended columns, fixed ended columns and elastic rotationally restrained ended columns, the Bickford–Reddy critical load $P^R$ is related to the Euler critical load $P^E$ by

$$P^R = P^E \left( \frac{1 + \frac{P^E \alpha^2 \bar{D}_{xx}}{GAD_{xx}}}{1 + \frac{P^E \bar{D}_{xx}}{GAD_{xx}}} \right) \tag{2.9.18}$$

where

$$\alpha = \frac{4}{3h^2}, \quad \bar{D}_{xx} = D_{xx} - 2\alpha F_{xx} + \alpha^2 H_{xx}$$

$$(D_{xx}, F_{xx}, H_{xx}) = \int_A (z^2, z^4, z^6) E \, dA \tag{2.9.19}$$

are the higher-order rigidities and $h$ is the height of the column cross-section. For example, for a square cross-section column, Eq. (2.9.18) simplifies to

$$P^R = P^E \left( \frac{1 + \frac{P^E}{70GA}}{1 + \frac{17P^E}{14GA}} \right) \tag{2.9.20}$$

For a circular cross-section, the relationship is given by

$$P^R = P^E \left( \frac{1 + \frac{P^E}{90GA}}{1 + \frac{101P^E}{90GA}} \right) \tag{2.9.21}$$

### 2.9.2 Columns under Intermediate and End Axial Loads

Stability criteria for Timoshenko columns with intermediate and end concentrated axial loads (see Fig. 2.3) are presented in Tables 2.22–2.24 (from Wang et al., 2002). Using the stability criteria presented in Tables 2.22–2.24, one can easily generate numerical results to determine the effect of shear deformation, boundary conditions and the influence of different intermediate load magnitudes and positions on critical loads. The following notation is used in Tables 2.22–2.24.

$$s = \frac{EI}{K_s GAL^2}, \quad \gamma_i = \frac{N_i L^2}{EI}$$

where $N_i$ is the axial compressive force in segment $i$.

**Table 2.22:** Stability criteria for Timoshenko columns subjected to compressive intermediate and end loads.

| Boundary conditions | Stability criteria |
| --- | --- |
| C–F | $1 - \sqrt{\beta}\tan(k_1 a)\tan\left[(1-a)k_1\sqrt{\beta}\right] = 0$ |
| P–P | $\eta\left[(1-a)\eta + a\right]\tan(k_1 a)$ $+\sqrt{\beta}\left[(1-a)\eta^2 + a\eta - \frac{k_1}{\gamma_1}\eta(\eta-1)^2\tan(k_1 a)\right]\tan\left[(1-a)k_1\sqrt{\beta}\right] = 0$ |
| C–P | $(1-a)\gamma_1\eta + a\gamma_1 + \sqrt{\beta}\left[k_1(\eta^2 - 2\eta + 2) + \left\{2k_1(\eta-1)\sec(k_1 a)\right.\right.$ $\left.\left. +\gamma_1\left[(1-a)\eta + a\right]\tan(k_1 a)\right\}\right]\tan\left[(1-a)k_1\sqrt{\beta}\right] - k_1\tan(k_1 a) = 0$ |
| P–C | $\left\{-k_1\beta\left[(1-a) + a\beta\right]\right.$ $+\left\{2 - 2\beta + \beta^2 - 2(1-\beta)\sec\left[(1-a)k_1\sqrt{\beta}\right]\right\}\tan(k_1 a)\Big\}$ $-\left\{\beta + k_1\beta\left[(1-a) + a\beta\right]\tan(k_1 a)\right\}\tan\left[(1-a)k_1\sqrt{\beta}\right] = 0$ |
| C–C | $2k_1\sqrt{\beta}\Big\{\eta^2 - \eta + 1 + (\eta-1)\sec(\lambda_1 a) - \eta\left[\eta - 1 + \sec(k_1 a)\right]$ $\times\sec\left[(1-a)k_1\sqrt{\beta}\right]\Big\} + \sqrt{\beta}\eta\gamma_1\left[(1-a) + \frac{a}{\eta}\right]\tan(k_1 a)$ $+\left[(1-a)\gamma_1\eta + a\gamma_1 - k_1(\beta\eta^2 + 1)\tan(k_1 a)\right]\tan\left[(1-a)k_1\sqrt{\beta}\right] = 0$ |

Note that $k_1^2 = \gamma_1/(1 - s\gamma_1)$, $k_2^2 = \gamma_2/(1 - s\gamma_2)$, $\beta = k_2^2/k_1^2$, $\eta = \gamma_1/\gamma_2$.

**Table 2.23:** Stability criteria for columns subjected to tensile intermediate load and compressive end load.

| Boundary conditions | Stability criteria |
| --- | --- |
| C–F | $1 - \sqrt{\beta}\tanh(k_1 a)\tan\left[(1-a)k_1\sqrt{\beta}\right] = 0$ |
| P–P | $\sqrt{\beta}\gamma_1\left[a - (1-a)\eta\right]\tan\left[(1-a)k_1\sqrt{\beta}\right] + \Big\{\gamma_1\left[(1-a)\eta - a\right]$ $-k_1\sqrt{\beta}(1+\eta)^2\tan\left[(1-a)k_1\sqrt{\beta}\right]\Big\}\tanh(k_1 a) = 0$ |

Table 2.23 is continued from the previous page.

| Boundary conditions | Stability criteria |
|---|---|
| C–P | $a - (1-a)\eta + \frac{k_1\sqrt{\beta}}{\gamma_1}\left[\eta^2 + 2\eta + 2 - 2(1+\eta)\mathrm{sech}(k_1 a)\right]\tan\left[(1-a)k_1\sqrt{\beta}\right]$ $+ \left\{-\frac{k_1}{\gamma_1} + \sqrt{\beta}\left[(1-a)\eta - a\right]\tan\left[(1-a)k_1\sqrt{\beta}\right]\right\}\tanh(k_1 a) = 0$ |
| P–C | $\sqrt{\beta}\left\{a\gamma_1 - (1-a)\gamma_1\eta + k_1\sqrt{\beta}\eta^2\tan\left[k_1\sqrt{\beta}(1-a)\right]\right\}$ $- \left\{k_1\sqrt{\beta}\left\{2\eta^2 + 2\eta + 1 - 2\eta(1+\eta)\sec\left[k_1\sqrt{\beta}(1-a)\right]\right\}\right.$ $+ \gamma_1\left[(1-a)\eta - a\right]\tan\left[k_1\sqrt{\beta}(1-a)\right]\right\}\tanh(k_1 a) = 0$ |
| C–C | $-2(1+\eta+\eta^2) + 2\left\{1+\eta - \eta\sec\left[k_1\sqrt{\beta}(1-a)\right]\right\}\mathrm{sech}(k_1 a)$ $+ \eta\left\{2(1+\eta)\sec\left[k_1\sqrt{\beta}(1-a)\right] + \frac{\gamma_1}{k_1\sqrt{\beta}}\left[\frac{a}{\eta} - (1-a)\right]\tan\left[k_1\sqrt{\beta}(1-a)\right]\right\}$ $+ \left\{-\frac{(1-a)}{k_1}\gamma_1\eta + \frac{a\gamma_1}{k_1} + \frac{(\beta\eta^2-1)}{\sqrt{\beta}}\tan\left[k_1\sqrt{\beta}(1-a)\right]\right\}\tanh(k_1 a) = 0$ |

Note that $k_1^2 = \gamma_1/(1+s\gamma_1)$, $k_2^2 = \gamma_2/(1+s\gamma_2)$, $\beta = k_2^2/k_1^2$, $\eta = \gamma_1/\gamma_2$.

**Table 2.24:** Stability criteria for columns with only compressive intermediate load.

| Boundary conditions | Stability criteria |
|---|---|
| C–F | $\cos(k_1 a) = 0$ |
| P–P | $3(1-a)^2\gamma_1\cos(k_1 a) +$ $k_1\left\{3(2-a) - (1-a)\gamma_1[3s + (1-a)^2]\right\}\sin(k_1 a) = 0$ |
| C–P | $k_1\gamma_1\left\{-6(1-a) + \left\{3(2-a) - (1-a)\gamma_1\left[3s + (1-a)^2\right]\right\}\cos(k_1 a)\right\}$ $-3\left[k_1^2 + (1-a)^2\gamma_1^2\right]\sin(k_1 a) = 0$ |
| P–C | $4\gamma_1\left\{3a - (1-a)\gamma_1\left[3s + (1-a)^2\right]\right\}\cos(k_1 a) +$ $k_1\left\{-12\left[1 + \gamma_1(1-a)\right] + (1-a)^2\gamma_1^2\left[12s + (1-a)^2\right]\right\}\sin(k_1 a) = 0$ |
| C–C | $12k_1\left[2 + \gamma_1(1-a)^2\right] + k_1\left\{-24 - 12\gamma_1(1-a) +\right.$ $\left. + \gamma_1^2(1-a)^2\left[12s + (1-a)^2\right]\right\}\cos(k_1 a)$ $+ 4\left\{3k_1^2(1-a) - 3a\gamma_1 + k_1^2(1-a)\left[3s + (1-a)^2\right]\right\}\sin(k_1 a) = 0$ |

Note that $k_1^2 = \gamma_1/(1 - s\gamma_1)$.

## 2.10 Flexural–Torsional Buckling of Columns

Thin-walled open-section columns subjected to a compressive load may be buckled by twisting, as shown in Fig. 2.17 for a cruciform section, or by combined bending and twisting. When this type of buckling takes place, the twisting of the column causes the axial compressive stresses to exert a disturbing torque which is opposed by the torsional resistance of the column section.

For members of doubly symmetric cross-section, a twisted equilibrium position is possible when the disturbing torque $T$ exactly balances the internal resisting torque $M_z$ (Trahair and Bradford, 1991)

$$M_z = GJ\frac{d\phi}{d\bar{z}} - EI_w\frac{d^3\phi}{d\bar{z}^3} \tag{2.10.1}$$

in which $GJ$ is the torsional rigidity, $EI_w$ the warping rigidity, and $\phi$ the angle of twist. For the column under an axial compressive force $P$, the disturbing torque is given by

$$T = \frac{P}{A}r_0^2\frac{d\phi}{d\bar{z}} \tag{2.10.2}$$

where $r_0^2 = (I_x + I_y)/A$.
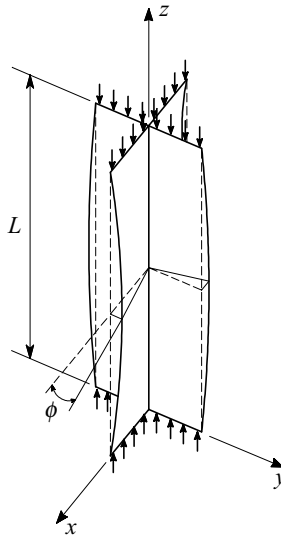


**Figure 2.17:** Torsional buckling of a cruciform section.

In view of Eqs. (2.10.1) and (2.10.2), the governing equation for the torsional buckling of column, is given by

$$EI_w \frac{d^3\phi}{d\bar{z}^3} + \left(\frac{P}{A}r_0^2 - GJ\right)\frac{d\phi}{d\bar{z}} = 0 \qquad (2.10.3)$$

The solution of this equation which satisfies the boundary conditions of end twisting prevented, $\phi|_{\bar{z}=0,L} = 0$, and ends free to warp, $d^2\phi/d\bar{z}^2|_{\bar{z}=0,L} = 0$, is

$$\phi = \phi|_{\bar{z}=L/2} \sin\frac{\pi\bar{z}}{L} \qquad (2.10.4)$$

in which $\phi|_{\bar{z}=L/2}$ is the undetermined magnitude of the angle of twist at the midlength of the column. Thus, the critical torsional buckling load is given by

$$P_{cr} = \frac{GJ}{r_0^2}\left(1 + \frac{\pi^2 EI_w}{GJL^2}\right) \qquad (2.10.5)$$

The above solution may be generalized for columns with other end conditions by expressing it as

$$P_{cr} = \frac{GJ}{r_0^2}\left(1 + \frac{\pi^2 EI_w}{GJl^2}\right) \qquad (2.10.6)$$

where $l$ is the distance between inflection points in the twisted shape.

Monosymmetric and asymmetric section members (such as angles and tees) may buckle in a combined mode by twisting and deflecting. This action takes place because the axis of twist through the shear center does not coincide with the loading axis through the centroid, and any twisting which occurs causes the centroidal axis to deflect. For pinned ended members, it can be shown that the critical buckling load $P_c$ is the lowest root of the cubic equation

$$P_c^3 \left(r_1^2 - x_0^2 - y_0^2\right) - P_c^2 \left[(P_x + P_y + P_z)r_1^2 - P_y x_0^2 - P_x y_0^2\right] \\ + P_c r_1^2 (P_x P_y + P_y P_z + P_x P_z) - P_x P_y P_z r_1^2 = 0 \qquad (2.10.7)$$

where

$$P_x = \frac{\pi^2 EI_x}{L^2}, \quad P_y = \frac{\pi^2 EI_y}{L^2}, \quad P_z = \frac{GJ}{r_1^2}\left(1 + \frac{\pi^2 EI_w}{GJL^2}\right) \qquad (2.10.8)$$

$$r_1^2 = r_0^2 + x_0^2 + y_0^2, \quad r_0^2 = \frac{I_x + I_y}{A} \tag{2.10.9}$$

and $x_0$, $y_0$ are the shear center coordinates measured from the centroid.

## 2.11 Inelastic Buckling of Columns

In the previous sections of this chapter, the buckling loads were determined using the linear material (i.e., stress-strain) response and linear kinematic (i.e., strain-displacement) relations. The assumption of linear elastic behavior is valid if the buckling stress falls below the proportionality limit. This is generally valid for slender columns and the Euler load represents the correct buckling load of such members. On the other hand, the axial stress in a stocky column will exceed the proportionality limit of the material before the applied load reaches the Euler load. Consequently, the results of the linear elastic analysis are not valid for stocky columns. The buckling load of stocky columns must be determined by taking into consideration the inelastic behavior.

Here, we consider buckling of columns in an inelastic range. According to Engesser's tangent modulus theory (1889), the buckling formulas derived for linear elastic range are applicable to the inelastic range provided we replace the modulus $E$ with an effective modulus $E_{\text{eff}}$:

$$P_{\text{cr}} = \frac{\pi^2 E_{\text{eff}} I}{L_{\text{eff}}^2} \tag{2.11.1}$$

where $L_{\text{eff}}$ is the effective length whose value depends on the boundary conditions of the column.

The value of $E_{\text{eff}}$ is calculated in a number of alternative ways. These are given in the next two equations.

1. *Tangent modulus theory* (Engesser, 1889)

$$E_{\text{eff}} = E_T, \quad E_T = \frac{d\sigma}{d\varepsilon} \tag{2.11.2}$$

2. *Reduced (or Double) modulus theory* (Engesser, 1895)

$$E_{\text{eff}} = E_R, \quad E_R = \begin{cases} \frac{4EE_T}{\left(\sqrt{E}+\sqrt{E_T}\right)^2}, & \text{for rectangular cross-section} \\ \frac{2EE_T}{E+E_T}, & \text{for idealized I-section} \end{cases} \tag{2.11.3}$$

An idealized (bi-symmetric) I-section is one in which the web is neglected (because of the negligible thickness of the web). The tangent modulus theory does not allow for load (strain) reversal, while the reduced-modulus theory allows for it.

Shanley (1947) showed that the tangent modulus load is a lower bound and the reduced-modulus load is an unattainable upper bound. The true buckling load lies somewhere between these two extremes. Interested readers may consult Shanley (1947) or Timoshenko and Gere (1961) for details. Exact inelastic stability criteria have also been derived (Groper and Kenig, 1987) for stepped columns shown in Figs. 2.18(a) and 2.18(b).

First, consider the column shown in Fig. 2.18(a). There are three cases to consider: Case 1: both segments behave elastically; Case 2: the top segment behaves inelastically while the bottom segment behaves elastically; and Case 3: both segments behave inelastically. Case 1 has been treated in Section 2.7.3. Here we consider Cases 2 and 3.

**Case 2.** The stability criterion is given by

$$\tan\left(\sqrt{\frac{P_c}{E_T I_1}} aL\right) \tan\left(\sqrt{\frac{P_c}{E I_2}}(1-a)L\right) = \sqrt{\frac{E I_2}{E_T I_1}} \qquad (2.11.4)$$

The critical load $P_c$ may be obtained upon supplying $E, E_T, I_1, I_2, a$ and $L$.
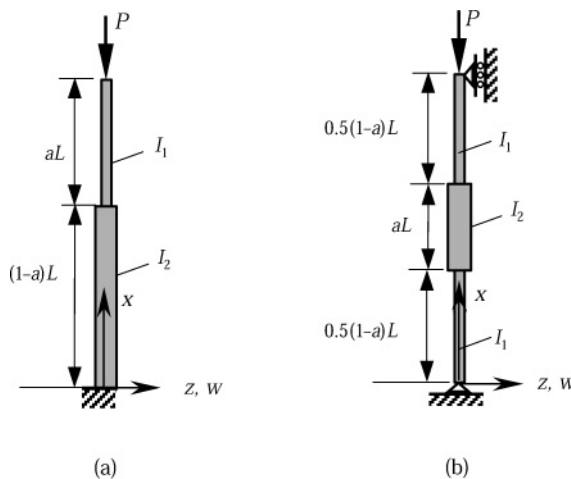


Figure 2.18: Stepped columns under end axial load.

**Case 3.** The stability criterion for this case is

$$\tan\left(\sqrt{\frac{P_c}{E_{T1}I_1}}aL\right)\tan\left(\sqrt{\frac{P_c}{E_{T2}I_2}}(1-a)L\right) = \sqrt{\frac{E_{T2}I_2}{E_{T1}I_1}} \qquad (2.11.5)$$

Next, consider the column shown in Fig. 2.18(b).

**Case 2.** The stability criterion is

$$\tan\left(\sqrt{\frac{P_c}{E_TI_1}}\frac{(1-a)L}{2}\right)\tan\left(\sqrt{\frac{P_c}{EI_2}}\frac{aL}{2}\right) = \sqrt{\frac{EI_2}{E_TI_1}} \qquad (2.11.6)$$

**Case 3.** The stability criterion for this case is

$$\tan\left(\sqrt{\frac{P_c}{E_{T1}I_1}}\frac{(1-a)L}{2}\right)\tan\left(\sqrt{\frac{P_c}{E_{T2}I_2}}\frac{aL}{2}\right) = \sqrt{\frac{E_{T2}I_2}{E_{T1}I_1}} \qquad (2.11.7)$$

Note that Eqs. (2.11.4)–(2.11.7) are transcendental equations and their solutions are obtained by iterative methods such as the Newton method or bisection method.

This completes the discussion on inelastic buckling of columns as per the Euler–Bernoulli beam theory.

## REFERENCES

Abramowitz, M. and Stegun, I. A. (1965), *Handbook of Mathematical Functions*, 2nd ed., Dover, New York.

Banerjee, J. R. and Williams, F. W. (1994), "The effect of shear deformation on the critical buckling of columns," *Journal of Sound and Vibration*, **174**(5), 607–616.

Bažant, Z. P. (2003), "Shear buckling of sandwich, fiber composite and lattice columns, bearings and helical springs: paradox resolved," *Journal of Applied Mechanics,* **70**(1), 75–83.

Bažant, Z. P. and Cedolin, L. (1991), *Stability Structures. Elastic, Inelastic Fracture and Damage Theories,* Oxford University Press, New York.

Bickford, W. B. (1982), "A consistent higher order beam theory," *Developments in Theoretical and Applied Mechanics,* **11**, 137–150.

Bleich, F. (1952), *Buckling Strength of Metal Structures*, McGraw-Hill, New York.

Cowper, G. R. (1966), "The shear coefficient in Timoshenko's beam theory," *Journal of Applied Mechanics*, **33**, 335–340.

Dinnik, A. N. (1929), "Design of columns of varying cross section," *Trans. ASME*, **51**, 165–171.

Dinnik, A. N. (1932), "Design of columns of varying cross sections," *Trans. ASME*, **54**, 105–109.

Dinnik, A. N. (1955), "Buckling and Torsion," *Acad. Nauk. CCCP*, Moscow (in Russian).

Elishakoff, I. (2000), "A selective review of direct, semi-inverse and inverse eigenvalue problems for structures described by differential equations with variable coefficients," *Archives of Computer Methods in Engineering,* **7**(4), 451–526.

Engesser, F. (1889), "Uber die knickfestigkeit gerader stäbe," *Z. Architekten Ing. Vereins zu Hannover,* **35**, 455–462.

Engesser, F. (1891), "Die knickfestigkeit gerader stäbe," *Zentralbl Bauverwaltung,* **11**, 483–486.

Engesser, F. (1895), "Über Knickfragen," *Schweizer. Bauzeitung,* **26**, 24–26.

Freudenthal, A. M. (1966), *Introduction to the Mechanics of Solids*, Wiley, New York.

Gere, J. M. and Carter, W. O. (1962), "Critical buckling loads for tapered columns," *Journal of Structural Division Proceedings*, **88**(1), 1-11.

Greenhill, M. A. (1881), "Determination of the greatest height consistent with stability that a vertical pole or mast can be made, and of the greatest height to which a tree of given proportions can grow," *Cambridge Philosophical Society Proceedings,* **4**, 65–73.

Goodman, L. E. and Sutherland, J. G. (1951), "Discussion of 'natural frequencies of continuous beams of uniform span length'," by R. S. Ayre and L. S. Jacobsen, *Journal of Applied Mechanics,* **18**, 217–218.

Groper, M. and Kenig, M. J. (1987), "Inelastic buckling of non-prismatic columns," *Journal of Engineering Mechanics,* **113**(8), 1233–1239.

Haringx, J. A. (1942), "On the buckling and lateral rigidity of helical springs," *Proc. Konink. Nederl. Akad. Wet.,* **45**, 533.

Hetenyi, M. (1948), *Beams on Elastic Foundation,* University of Michigan Press, Ann Arbor, MI.

Heyliger, P. R. and Reddy, J. N. (1988), "A higher-order beam finite element for bending and vibration problems," *Journal of Sound and Vibration,* **126**(2), 309–326.

Kamke, E. (1948), *Differentialgleichungen Losungsmethoden und Losungen*, Vol. 1, Chelsea, New York.

Kitipornchai, S. and Finch, D. L. (1986), "Stiffness requirements for cross-bracing," *Journal of Structural Engineering*, **112**(12), 2702–2707.

Krawczuk, M. and Ostachowicz, W. (1995), "Modeling and vibration analysis of a cantilever composite beam with a transverse open crack," *Journal of Sound and Vibration,* **183**(1), 69–89.

Li, Q. S., Cao, H. and Li, G. Q. (1995), "Stability analysis of bars with varying cross-section," *International Journal of Solids and Structures*, **32**, 3217–3228.

Mau, S. T. (1989), "Buckling and postbuckling analyses of struts with discrete supports," *Journal of Engineering Mechanics*, **115**(4), 721–739.

Mindlin, R. D. and Deresiewicz, H. (1954), "Timoshenko's shear coefficient for flexural vibrations of beams," *Proc. Second U.S. National Congress of Applied Mechanics*, 175–178.

Murphy, G. M. (1960), *Ordinary Differential Equations*, Van Nostrand, Princeton, NJ.

Mutton, B. R. and Trahair, N. S. (1973), "Stiffness requirements for lateral bracing," *Journal of the Structural Division*, **99**(ST10), 2167–2182.

Olhoff, N. and Akesson, B. (1991), "Minimum stiffness of optimally located supports for maximum value of column buckling loads," *Structural Optimization*, **3**, 163–175.

Reddy, J. N. (1984), *Energy and Variational Methods in Applied Mechanics,* John Wiley, New York.

Reddy, J. N. (2002), *Energy Principles and Variational Methods in Applied Mechanics,* 2nd ed., John Wiley, New York.

Rozvany, G. I. N. and Mröz, Z. (1977), "Column design: optimization of support conditions and segmentation," *Journal of Structural Mechanics*, **5**(3), 279–290.

Shanley, F. R. (1947), "Inelastic column theory," *J. Aeronautical Sciences,* **14**, 261–264.

Stephen, N. G. and Levinson, M. (1979), "A second order beam theory," *Journal of Sound and Vibration*, **67**, 293–305.

Stoman, S. H. (1988), "Stability criteria for X-bracing systems," *Journal of Engineering Mechanics*, **114**(8), 1426–1434.

Thevendran, V. and Wang, C. M. (1993), "Stability of nonsymmetric cross-bracing systems," *Journal of Structural Engineering*, **119**(1), 169–180.

Timoshenko, S. P. (1921), "On the correction for shear of the differential equation for transverse vibrations of prismatic bars," *Philosophical Magazine*, **41**, 744–746.

Timoshenko, S. P. and Gere, J. M. (1961), *Theory of Elastic Stability*, McGraw-Hill, New York.

Trahair, N. S. and Bradford, M. A. (1991), *The Behavior and Design of Steel Structures*, Revised 2nd ed., Chapman and Hall, Great Britain.

Wang, C. M. and Ang, K. K. (1988), "Buckling capacities of braced heavy columns under an axial load," *Computers and Structures*, **28**(5), 563–571.

Wang, C. M., Kitipornchai, S. and Al-Bermani, F. G. A. (1991), "Buckling of columns: allowance for axial shortening," *International Journal of Mechanical Sciences*, **33**(8), 613–622.

Wang, C. M. and Liew, K. M. (1991), "Buckling of columns with overhang," *Journal of Engineering Mechanics*, **117**(11), 2492–2508.

Wang, C. M., Reddy, J. N. and Lee, K. H. (2000), *Shear Deformable Beams and Plates: Relationships with Classical Solutions,* Elsevier, Oxford, UK.

Wang, C. M., Ng, K. H. and Kitipornchai, S. (2002), "Stability criteria for Timoshenko columns with intermediate and end concentrated axial loads," *Journal of Constructional Steel Research*, **58**, 1177–1193.

Wang, C. M., Wang, C. Y. and Nazmul, I. M. (2003), "Stability criteria for Euler columns with intermediate and end axial loads," *Journal of Engineering Mechanics*, **129**(4), 468–472.

Wang, C. Y. and Drachman, B. (1981), "Stability of a heavy column with an end load," *Journal of Applied Mechanics*, **48**, 668–669.

Wang, C. Y. (1983), "Buckling and postbuckling of a long hanging elastic column due to a bottom load," *Journal of Applied Mechanics*, **50**, 311–314.

Wang, C. Y. (1987a), "Optimum location of an interior hinge on a column," *Journal of Structural Engineering,* **113**(1), 161–165.

Wang, C. Y. (1987b), "Approximate formulas for buckling of heavy column with end load," *Journal of Structural Engineering,* **113**(10), 2316–2320.

Wang, C. Y. (1987c), "Buckling and postbuckling of heavy columns," *Journal of Engineering Mechanics, ASCE,* **113**, 1229–1233.

Wang, C. Y. (1987d), Stability of the partially submerged standing column, *Mechanics of Structures & Machines,* **15**(2), 233–240.

Wang, C. Y. (1991), "Elastic stability of a floating vertical column with a bottom load," *Z. Angew. Math. Mech.,* **71**, 58–59.

Ziegler, H. (1982), "Arguments for and against Engesser's buckling formulas," *Ingenieur-Archiv,* **52**, 105–113.

Zyczkowski, M. (ed.) (1991), *Strength of Structural Elements,* PWN–Polish Scientific Publishers, Warsaw, Poland.

CHAPTER 3

# BUCKLING OF BEAMS, ARCHES AND RINGS

## 3.1 Flexural–Torsional Buckling of Beams

### 3.1.1 Introduction

Beams that have relatively small lateral and torsional stiffnesses compared to their stiffness in the plane of loading or that have inadequate lateral restraints may buckle out of plane of the transverse load. For a perfectly straight, elastic beam, there are no out-of-plane deformations until the applied load reaches a critical value, at which point the beam buckles by deflecting laterally and twisting. The lateral deflection and twisting are interdependent. When the beam deflects laterally, the induced moment exerts a component torque about the deflected longitudinal axis which causes the beam to twist. Such buckling behavior has been referred to as *flexural–torsional buckling* or simply *lateral buckling.*

For flexural–torsional buckling of beams, exact buckling solutions can only be obtained for a simply supported beam under uniform moment or simple loading condition such as a midspan concentrated load. This section will focus on only these boundary and load conditions.

### 3.1.2 Beams of Rectangular Cross-Section

Consider a simply supported, narrow beam of uniform rectangular cross-section with width $b$, depth $h$ and span $L$ as shown in Fig. 3.1a. The differential equilibrium equations of minor axis bending and torsion of the buckled beam are

$$EI_y \frac{d^2u}{dz^2} = -M_x\phi \tag{3.1.1}$$

$$GJ \frac{d\phi}{dz} = M_x \frac{du}{dz} + M_z \tag{3.1.2}$$

where $u$ is the lateral displacement, $\phi$ the angle of twist, $z$ the horizontal distance along the length of the beam, $EI_y = Ehb^3/12$ the flexural rigidity about the minor $y$-axis, $GJ = Ghb^3/3$ the torsional rigidity, and $M_x$ and $M_z$ the internal moments in the buckled beam acting about the $x$- and $z$-axes, respectively.

© 2005 by CRC Press LLC
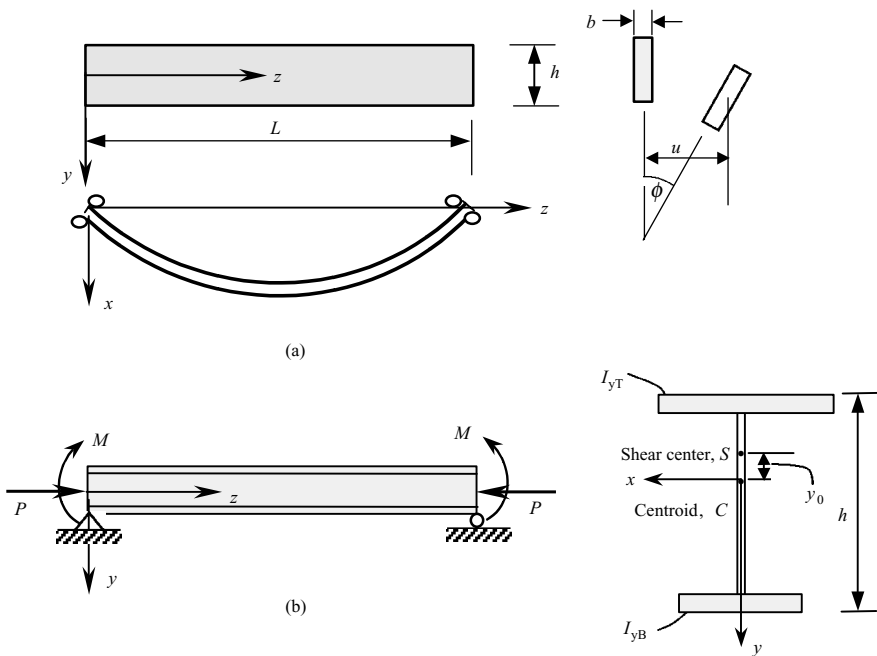
**Figure 3.1:** (a) Geometry of a rectangular section beam. (b) A simply supported, monosymmetric I-beam.

*For a beam that is subjected to only equal end moments M about the x-axis*, we have $M_x = M$ and $M_z = 0$. Thus, Eqs. (3.1.1) and (3.1.2) reduce to

$$EI_y \frac{d^2 u}{dz^2} = -M\phi \tag{3.1.3}$$

and

$$GJ \frac{d\phi}{dz} = M \frac{du}{dz} \tag{3.1.4}$$

Eliminating $u$ from Eqs. (3.1.3) and (3.1.4) we obtain the following single differential equation:

$$\frac{d^2 \phi}{dz^2} + \frac{M^2}{EI_y GJ} \phi = 0 \tag{3.1.5}$$

For the case where the ends of the beam are restrained against rotation $\phi$ about the longitudinal axis of the beam, $\phi = 0$ at both ends of the beam, i.e., at $z = 0, L$.

The smallest root of Eq. (3.1.5), other than the trivial zero, yields the exact buckling moment $M_c$

$$M_c = \frac{\pi\sqrt{EI_yGJ}}{L} \tag{3.1.6}$$

and the corresponding buckled shape is given by

$$\phi = C \sin \frac{\pi z}{L} \tag{3.1.7}$$

where $C$ is an arbitrary amplitude of a small magnitude.

Consider next *a rectangular beam of constant width b but linearly tapered depth*, defined by

$$h = \left(1 + \frac{z}{L}\delta\right) h_0 \tag{3.1.8}$$

where $h_0$ is the depth of the beam at $z = 0$ and $(1 + \delta)$ is the ratio of the height of the tapered beam at $z = L$ to the height at $z = 0$.

The governing equations for buckling of such a tapered beam are still given by Eqs. (3.1.3) and (3.1.4) with

$$EI_y = \frac{Eh_0b^3}{12}\left(1 + \frac{z}{L}\delta\right) \equiv EI_0\eta \tag{3.1.9a}$$

$$GJ = G\frac{h_0b^3}{3}\left(1 + \frac{z}{L}\delta\right) \equiv GJ_0\eta \tag{3.1.9b}$$

where

$$\eta = 1 + \frac{z}{L}\delta \tag{3.1.9c}$$

Note that

$$\frac{d\phi}{dz} = \frac{d\phi}{d\eta}\frac{d\eta}{dz} = \frac{\delta}{L}\frac{d\phi}{d\eta}, \quad \frac{d^2\phi}{dz^2} = \left(\frac{\delta}{L}\right)^2 \frac{d^2\phi}{d\eta^2} \tag{3.1.9d}$$

Elimination of $u$ from Eqs. (3.1.3) and (3.1.4) [making use of (3.1.9d)] results in

$$\eta^2 \frac{d^2\phi}{d\eta^2} + \eta\frac{d\phi}{d\eta} + k^2\phi = 0 \tag{3.1.10a}$$

where

$$k^2 = \frac{M^2 L^2}{EI_0 GJ_0 \delta^2} \tag{3.1.10b}$$

The general solution of Eq. (3.1.10) is (Lee, 1959)

$$\phi = C_1 \sin(k \ln \eta) + C_2 \cos(k \ln \eta) \tag{3.1.11}$$

For a restrained beam with ends restrained against twisting, $\phi = 0$ at $z = 0$ and $z = L$. By solving this eigenvalue problem, the critical buckling moment is given by

$$M_c = \frac{\delta}{\ln(1 + \delta)} \frac{\pi \sqrt{EI_0 GJ_0}}{L} \tag{3.1.12}$$

and the corresponding buckled shape is given by

$$\phi = C \sin\left[ \frac{\ln \eta}{\ln(1 + \delta)} \pi \right] \tag{3.1.13}$$

*For a simply supported beam subjected to a concentrated load $P$ at the midspan*, i.e., $z = L/2$, we have (Timoshenko and Gere, 1961)

$$M_x = \frac{Pz}{2} \tag{3.1.14a}$$

and

$$M_z = \frac{P}{2} (u^* - u) \tag{3.1.14b}$$

where $u^*$ represents the lateral deflection of the centroid of the middle cross-section and $u$ the lateral deflection at any cross-section.

By substituting Eqs. (3.1.14a) and (3.1.14b) into Eqs. (3.1.1) and (3.1.2), eliminating the lateral displacement $u$, and noting that $du^*/dz = 0$, one obtains

$$\frac{d^2\phi}{dz^2} + \frac{P^2 z^2}{4EI_y GJ}\phi = 0 \tag{3.1.15}$$

By letting $\eta = z/L$ and using the notation

$$\zeta = \sqrt{\frac{P^2 L^4}{4EI_y GJ}}$$

Eq. (3.1.15) may be expressed as

$$\frac{d^2\phi}{d\eta^2} + \zeta^2\eta^2\phi = 0 \qquad (3.1.16)$$

The general solution for Eq. (3.1.16) is

$$\phi = \sqrt{\eta}\left[C_1 J_{1/4}\left(\frac{\zeta\eta^2}{2}\right) + C_2 J_{-1/4}\left(\frac{\zeta\eta^2}{2}\right)\right] \qquad (3.1.17)$$

where $J_{1/4}$ and $J_{-1/4}$ are Bessel functions of the first kind of order $1/4$ and $-1/4$, respectively. The boundary conditions are

$$\phi = 0 \text{ at } \eta = 0 \text{ and } \frac{d\phi}{d\eta} = 0 \text{ at } \eta = \frac{1}{2} \qquad (3.1.18)$$

By solving Eq. (3.1.17) together with the boundary conditions in Eq. (3.1.18), one obtains

$$J_{-3/4}\left(\zeta/8\right) = 0 \quad \Rightarrow \quad \frac{\zeta}{8} = 1.0585 \quad \Rightarrow \quad P_c = \frac{16.94}{L^2}\sqrt{EI_yGJ} \quad (3.1.19)$$

*For a cantilever beam of length L and carrying a concentrated load P at its tip (z = L)*, the governing equation and solution take similar forms as (3.1.16) and (3.1.17) by defining

$$\eta = 1 - \frac{z}{L}, \quad \zeta = \sqrt{\frac{P^2 L^4}{EI_yGJ}}$$

The boundary conditions for the cantilever beam are

$$\phi = 0 \text{ at } \eta = 1 \text{ and } \frac{d\phi}{d\eta} = 0 \text{ at } \eta = 0 \qquad (3.1.20)$$

By solving Eq. (3.1.17) subject to the boundary conditions in (3.1.20), we obtain

$$J_{-1/4}(\zeta/2) = 0 \quad \Rightarrow \quad \frac{\zeta}{2} = 2.0063 \quad \Rightarrow \quad P_c = \frac{4.0126}{L^2}\sqrt{EI_yGJ} \qquad (3.1.21)$$

### 3.1.3 I-Beams

Consider a simply supported, monosymmetric I-beam subjected to equal end moments $M$ about the $x$-axis and axial load $P$ acting

through the centroidal axis as shown in Fig. 3.1(b). Note that the sign conventions for $P$ and $M$ are adopted as follows: $P$ is positive when compressive and negative when tensile; $M$ is positive for sagging moment and negative for hogging moment.

The governing differential equations of minor axis bending and torsion are, respectively, given by (Wang and Kitipornchai, 1989)

$$EI_y \frac{d^4u}{dz^4} = -\left(M + Py_0\right) \frac{d^2\phi}{dz^2} - P\frac{d^2u}{dz^2} \qquad (3.1.22)$$

and

$$\left(GJ - Pr_1^2 + M\beta_x\right) \frac{d\phi}{dz} - EI_w \frac{d^3\phi}{dz^3} = M\frac{du}{dz} \qquad (3.1.23)$$

where $EI_y$ is the flexural rigidity about the minor axis; $GJ$ the torsional rigidity; $EI_w = EI_y\rho(1-\rho)h^2$ the warping rigidity; $\rho = I_{yT}/(I_{yT}+I_{yB}) = I_{yT}/I_y$ the degree of beam monosymmetry; $I_{yT}$ and $I_{yB}$ are the second moments of area about the $y$-axis of the top flange and bottom flange, respectively; $y_0$ is the coordinate of the shear center; and $\beta_x$ is the monosymmetric parameter defined as (Kitipornchai et al., 1986)

$$\beta_x = \frac{1}{I_x}\left(\int_A x^2 y\,dA + \int_A y^3\,dA\right) - 2y_0 \qquad (3.1.24)$$

where $x$, $y$ are coordinates with respect to the centroid (see Fig. 3.1(b)) and $r_1$ is the polar radius of gyration about the shear center

$$r_1^2 = \frac{I_x + I_y}{A} + y_0^2 \qquad (3.1.25)$$

For beams restrained at the ends such that twist is prevented but the ends are free to warp (i.e., $\phi = 0$ and $d^2\phi/dz^2 = 0$ at both ends), $u$ and $\phi$ take on half-sine waves. Therefore, Eqs. (3.1.22) and (3.1.23) yield a closed-form solution for the critical values of $P$ and $M$ (Cuk and Trahair, 1981; Trahair and Nethercot, 1984)

$$\left(M + Py_0\right)^2 = r_1^2 P_z P_E \left(1 - \frac{P}{P_E}\right)\left(1 - \frac{P}{P_z} + \frac{M\beta_z}{r_1^2 P_z}\right) \qquad (3.1.26)$$

where $P_E$ is the flexural Euler buckling load

$$P_E = \frac{\pi^2 EI_y}{L^2} \qquad (3.1.27)$$

and

$$P_z = \frac{GJ}{r_1^2} \left( 1 + \frac{\pi^2 EI_w}{GJL^2} \right) \tag{3.1.28}$$

Using the following nondimensional parameters proposed by Wang and Kitipornchai (1989)

$$\rho = \frac{I_{yT}}{I_{yT} + I_{yB}}, \quad \bar{K} = \sqrt{\frac{\pi^2 EI_y h^2}{4GJL^2}}, \quad \eta = \frac{4}{h^2} \left( \frac{I_x + I_y}{A} \right), \quad v = \frac{2y_0}{h},$$

$$\Lambda = \frac{P}{P_E}, \quad \lambda = \left[ -v\Lambda + \frac{\beta_x}{h}(1 - \Lambda) \right] \bar{K}, \quad \gamma = \frac{ML}{\sqrt{EI_y GJ}} \tag{3.1.29}$$

where $h$ is the distance between the centroids of the flanges and $\bar{K}$ the beam parameter, Eq. (3.1.26) may be rewritten as

$$\gamma = \pi \left[ \lambda \pm \sqrt{\lambda^2 - v^2 \bar{K}^2 \Lambda + (1 - \Lambda) \left\{ 1 + \bar{K}^2 \left[ 4\rho(1 - \rho) - \eta\Lambda \right] \right\}} \right] \tag{3.1.30}$$

The exact closed-form expression of the nondimensional elastic buckling moment given by Eq. (3.1.30) is rather compact and may be applied to any monosymmetric beam-columns/tie-beams. Note that Eq. (3.1.30) has two roots, one with the positive sign in front of the square root term and the other with the negative sign.

The above general solution can be shown to reduce to the following special cases:

*Case 1: Buckling of Monosymmetric I-Beams under Equal End Moments*

When there is no axial force ($P = \Lambda = 0$), Eq. (3.1.30) reduces to

$$\gamma = \pi \left[ \frac{\beta_x}{h} \bar{K} + \sqrt{1 + 4\rho(1 - \rho)\bar{K}^2 + \left( \frac{\beta_x}{h} \bar{K} \right)^2} \right] \tag{3.1.31}$$

In the case where the flanges are of equal size, $\rho = 1/2$ and $\beta_x = 0$. Thus, the critical buckling moment for a doubly symmetric I-beam under equal end moments is given by (Kitipornchai and Dux, 1987; Timoshenko and Gere, 1961; Trahair, 1977)

$$\gamma = \pi \sqrt{1 + \bar{K}^2} \tag{3.1.32}$$

*Case 2: Buckling of Doubly Symmetric Beam-Columns/Tie-Beams*

For doubly symmetric columns in which $\rho = 1/2$ and $\beta_x = 0$, Eq. (3.1.30) reduces to (Kitipornchai and Wang, 1988)

$$\gamma = \pi\sqrt{(1 - \Lambda)\left[1 + (1 - \eta\Lambda)\bar{K}^2\right]} \tag{3.1.33}$$

*Case 3: Buckling of Monosymmetric I-Columns*

For I-columns under axial compressive load acting through the centroidal axis, i.e., $\gamma = 0$, Eq. (3.1.30) furnishes the flexural–torsional buckling load ratio $\Lambda_0$ (Chajes and Winter, 1965; Pekoz and Winter, 1969; Vlasov, 1961)

$$\Lambda_0 = \chi_1 \pm \sqrt{\chi_1^2 - \chi_2} \tag{3.1.34}$$

in which

$$\chi_1 = \frac{1}{2}\left(1 + \chi_2 + \frac{v^2}{\eta}\right) \tag{3.1.35}$$

$$\chi_2 = \frac{1 + 4\rho(1 - \rho)\bar{K}^2}{\eta\bar{K}^2} \tag{3.1.36}$$

The lower root gives the buckling load for the column.

In the case of axial compressive load $P$ acting at a distance $e_0$ (positive in the $y$-direction) away from the centroidal axis, the eccentric load can be replaced by a concentric load and a moment $(Pe_0)$. The nondimensional buckling moment $\gamma$ may now be expressed as

$$\gamma = -\pi\Lambda\bar{K}\epsilon \tag{3.1.37}$$

in which $\epsilon = 2e_0/h$ is the eccentricity parameter. Combining Eqs. (3.1.30) and (3.1.37) leads to Eq. (3.1.34) with

$$\chi_1 = \frac{1}{2}\left[1 + \chi_2 + \frac{v^2 + \epsilon(\epsilon - 2v)}{\eta + \epsilon\left(2v + \frac{2\beta_x}{h} - \epsilon\right)}\right] \tag{3.1.38}$$

and

$$\chi_2 = \frac{1 + 4\rho(1 - \rho)\bar{K}^2}{\left[\eta + \epsilon\left(2v + \frac{2\beta_x}{h} - \epsilon\right)\right]\bar{K}^2} \tag{3.1.39}$$

## 3.2 In-plane Buckling of Rings and Arches

### 3.2.1 Governing Equations

Consider thin, elastic, inextensible curved structural members in static equilibrium with applied distributive forces. Since most undeformed funicular shapes cannot be described by exact expressions, their stability equations are also not exact. Thus, the only equilibrium shape that yields exact stability criteria is the circular ring or arch loaded by evenly distributed radial stress. How this stress behaves after deformation is also important. For a constant hydrostatic pressure, the stress is constant and is always normal to the deformed surface. For tethered or elastically supported rings, the stresses vary with displacement. In the literature, there seems to be an overemphasis on the constant radially directed stress. Since such a stress state is unrealistic (springs with one end attached to the center of a ring have the right direction, but their magnitude would not be constant in deformation), we shall ignore this situation and consider the stability of circular rings or arches due to constant pressure only. Rings and arches can also be regarded as long (two-dimensional) shells.

Figure 3.2 shows the equilibrium of an elemental segment of the ring or arch. By balancing the forces in the normal and tangential directions, we find

$$T d\theta - dS - \bar{q}_n d\bar{s} = 0 \qquad (3.2.1)$$

$$\bar{q}_t d\bar{s} + S d\theta + dT = 0 \qquad (3.2.2)$$

Here $T$ is the tension, $S$ the shear, $\bar{q}_n$ and $\bar{q}_t$ are the normal and tangential stresses on the surface, $\theta$ is the local inclination, and $\bar{s}$ the arc length. A local moment balance gives

$$dM - S d\bar{s} = 0 \qquad (3.2.3)$$

The Euler–Bernoulli law yields

$$M = D \frac{d\theta}{d\bar{s}} \qquad (3.2.4)$$

where $D$ is the flexural rigidity. Eliminating $T$, $S$ and $M$ from Eqs. (3.2.1)–(3.2.4), the following nonlinear equilibrium equation is obtained

$$\frac{d\theta}{ds} \frac{d^4\theta}{ds^4} - \frac{d^2\theta}{ds^2} \frac{d^3\theta}{ds^3} + \left[ \left( \frac{d\theta}{ds} \right)^3 - q_n \right] \frac{d^2\theta}{ds^2} + q_t \left( \frac{d\theta}{ds} \right)^2 + \frac{dq_n}{ds} \frac{d\theta}{ds} = 0 \quad (3.2.5)$$
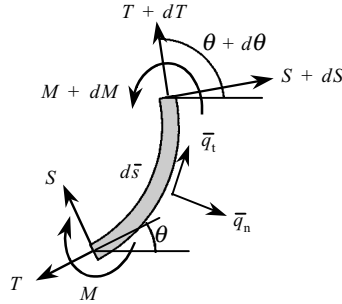
**Figure 3.2:** Equilibrium of an elemental segment of a ring/arch.

where $s = \bar{s}/R$ is the normalized arc length, $q = \bar{q}R^3/D$ the normalized stress, and $R$ is some length scale, usually the undeformed radius of curvature.

The normalized Cartesian coordinates $(x, y)$ are related to $\theta$ by

$$\frac{dx}{ds} = \cos\theta, \quad \frac{dy}{ds} = \sin\theta \tag{3.2.6}$$

In the unbuckled state for a circular ring or arch, $q_t = 0$ and

$$\theta = s + \frac{\pi}{2}, \quad x = \cos s, \quad y = \sin s \tag{3.2.7}$$

Depending on the assumed variation of $q_n$ and $q_t$, Eq. (3.2.5) can be linearized to yield the stability criterion as shown in the next section.

### 3.2.2 Circular Rings under Uniform Pressure

For circular rings under uniform pressure, we set $q_t = 0$ and $q_n = -p$ where $p$ is the constant pressure. Let

$$\theta = s + \frac{\pi}{2} + \psi \tag{3.2.8}$$

where $\psi$ is a small perturbation. Eq. (3.2.5) linearizes to

$$\frac{d^4\psi}{ds^4} + (1+p)\frac{d^2\psi}{ds^2} = 0 \tag{3.2.9}$$

For full rings the perturbation $\psi$ must be $2\pi$ periodic in $s$, or

$$1 + p = N^2 \qquad (3.2.10)$$

where $N$ is a positive integer that denotes the number of full waves formed around the ring. We discard the case for $N = 1$, which represents a rigid translation. Thus, the critical pressure is $p = 3$ ($N = 2$, twofold collapse of ring); see Lévy (1884). For large numbers of waves that might be formed if the ring was restrained by a very stiff elastic medium, $p$ is approximately proportional to $N^2$.

### 3.2.3 Circular Rings with Hinges

Figure 3.3 shows a circular ring with one weakened spot represented by a hinge with a torsional restraint. The figure also represents a weakened longitudinal seam on a long cylindrical shell.

The governing equation for the perturbed angle is given by Eq. (3.2.9), which has the general solution

$$\psi = C_1 + C_2 s + C_3 \cos\left(rs\right) + C_4 \sin\left(rs\right) \qquad (3.2.11)$$

with

$$r = \sqrt{1 + p} \qquad (3.2.12)$$

Let $(\xi, \eta)$ denote the displacements

$$x = \cos s + \xi(s), \quad y = \sin s + \eta(s) \qquad (3.2.13)$$
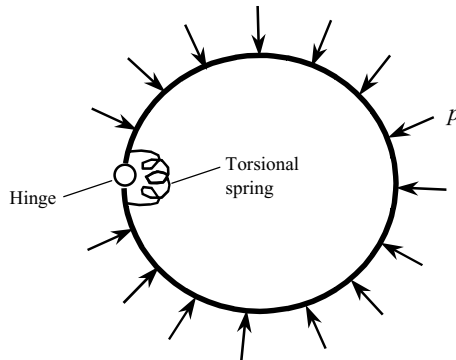


**Figure 3.3:** Circular ring with a hinge.

Equations (3.2.6) and (3.2.8) yield the linearized equations

$$\frac{d\xi}{ds} = -\psi \cos s, \quad \frac{d\eta}{ds} = -\psi \sin s \qquad (3.2.14)$$

For symmetric buckling about the hinge, we retain only the odd terms in Eq. (3.2.11). The other condition is that there are no vertical displacements $\eta$ at $s = 0$ and $s = \pi$, or

$$\int_0^\pi \psi \sin s \; ds = 0 \qquad (3.2.15)$$

This gives

$$C_2\pi + C_4\frac{\sin(r\pi)}{1 - r^2} = 0 \qquad (3.2.16)$$

Now at the hinge, the total angle change is resisted by an additional moment with a torsional spring constant $\bar{k}$, i.e.,

$$D\left(\frac{d\theta}{d\bar{s}} - \frac{1}{R}\right) = \bar{k}\Delta\theta \qquad (3.2.17)$$

or in nondimensional terms as

$$\frac{d\psi}{ds}(\pi) + k\psi(\pi) = 0 \qquad (3.2.18)$$

where $k = \bar{k}R/D$ is the nondimensional spring constant. Using the odd form of $\psi$, Eq. (3.2.18) yields

$$C_2(1 + 2k\pi) + C_4\left[r\cos(r\pi) + 2\sin(r\pi)\right] = 0 \qquad (3.2.19)$$

The characteristic equation for Eqs. (3.2.16) and (3.2.19) is

$$(1 + 2k\pi)\sin(r\pi) + \pi(r^2 - 1)[r\cos(r\pi) + 2k\sin(r\pi)] = 0 \qquad (3.2.20)$$

For a given $k$, the lowest $r > 1$ solution to Eq. (3.2.20) is sought. Then the critical pressure $p$ is obtained from Eq. (3.2.12). Numerical results for $p$ as a function of $k$ are presented in Table 3.1.

When $k = 0$ the hinge has no torsional resistance, and the buckling pressure agrees with that of Wang (1985). When $k = \infty$, the hinge is absent, and the buckling pressure is that for the complete ring described in Sec 3.2.2.

**Table 3.1:** Critical pressure for the ring with a torsionally resistant hinge.

| $k$ | 0 | 0.5 | 1 | 2 | 4 | 10 | 20 | $\infty$ |
|---|---|---|---|---|---|---|---|---|
| $p$ | 1.3923 | 1.7770 | 2.0322 | 2.3331 | 2.5989 | 2.8210 | 2.9075 | 3 |

For the ring with $N$ evenly placed hinges without torsional resistance, Wang (1985) showed the characteristic equation is

$$\pi p \frac{r}{N} + \tan\left(\pi \frac{r}{N}\right) = 0 \tag{3.2.21}$$

For $N = 1, 2, 3$, Eq. (3.2.21) shows the critical pressure is 1.39232, 0.79897, and 2.05564, respectively. For two arbitrarily placed hinges on a ring, Wang (1993) showed the characteristic equation is complicated but is still exact. As the two hinges are separated, the critical pressure increases from the one-hinge value of 1.39232, reaches a maximum at 3 (where the hinges are at the adjacent inflection points of the buckled hingeless ring), and then decreases to the two-opposite-hinge value of 0.79897.

### 3.2.4 Circular Rings with Distributed Resistance

Consider a pressurized circular ring on an elastic (Winkler) foundation. Using the perturbation displacements defined in Eq. (3.2.13), the normal displacement is $(\xi \cos\ s + \eta \sin\ s)$. Thus, the linearized normal stress is

$$q_n = -p - k\left(\xi \cos s + \eta \sin s\right) \tag{3.2.22}$$

where $k$ is the normalized spring constant (force per arc length). Eq. (3.2.5) then linearizes to

$$\frac{d^4\psi}{ds^4} + (p+1)\frac{d^2\psi}{ds^2} - k\frac{d}{ds}\left(\xi \cos s + \eta \sin s\right) = 0 \tag{3.2.23}$$

We assume the buckled shape has $N > 1$ complete waves with the leading harmonic being

$$\psi = C\sin(Ns) \tag{3.2.24}$$

Since due to periodicity

$$\eta(0) = 0, \quad \xi(0) = (\xi \cos\, s + \eta \sin\, s)|_{s=2\pi/N} \qquad (3.2.25)$$

Eqs. (3.2.14) and (3.2.25) integrate out to be

$$\xi = \frac{C}{2} \left\{ \frac{\cos[(N-1)s]}{N-1} + \frac{\cos[(N+1)s]}{N+1} \right\} \qquad (3.2.26)$$

$$\eta = -\frac{C}{2} \left\{ \frac{\sin[(N-1)s]}{N-1} - \frac{\sin[(N+1)s]}{N+1} \right\} \qquad (3.2.27)$$

The substitution of Eqs. (3.2.24), (3.2.26) and (3.2.27) into Eq. (3.2.23) gives

$$C \sin(Ns) \left( -N^2 + p + 1 - \frac{k}{N^2 - 1} \right) = 0 \qquad (3.2.28)$$

or the critical pressure is

$$p = N^2 - 1 + \frac{k}{N^2 - 1} \qquad (3.2.29)$$

When $k$ is zero, the critical pressure is 3 with $N = 2$ fold collapse. For a larger spring constant $k$, the buckling pressure increases and may correspond to a higher fold collapse. We find $N$-fold collapse occurs when

$$N(N^2 - 1)(N - 2) < k < N(N^2 - 1)(N + 2) \qquad (3.2.30)$$

For a given $k$, we first determine $N$ from Eq. (3.2.30) and then $p$ from Eq. (3.2.29). It is to be noted that this criterion is also valid for the buckling of tethered rings under external pressure (Wang et al., 1983).

### 3.2.5 General Circular Arch

Arches differ from complete rings in the sense that the arch base is restricted. A pressurized circular arch with opening angle $2\alpha$ and general rotational restraints at the base is shown in Fig. 3.4. The general solution is given by Eq. (3.2.11) subjected to restraint conditions similar to Eq. (3.2.18)

$$\frac{d\psi}{ds}(\alpha) + k_1 \psi(\alpha) = 0 \qquad (3.2.31)$$

$$\frac{d\psi}{ds}(-\alpha) - k_2 \psi(-\alpha) = 0 \qquad (3.2.32)$$
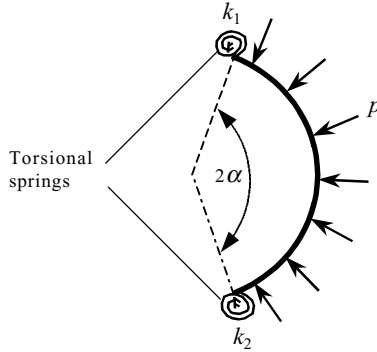
**Figure 3.4:** A pressurized circular arch.

where $k_1$ and $k_2$ are normalized torsional spring constants. The immovability of the base requires $\eta(\alpha) = \eta(-\alpha) = 0$ and $\xi(\alpha) = \xi(-\alpha) = 0$ or

$$\int_{-\alpha}^{\alpha} \psi \sin s \ ds = 0 \tag{3.2.33}$$

$$\int_{-\alpha}^{\alpha} \psi \cos s \ ds = 0 \tag{3.2.34}$$

These integrals also assure the inextensibility condition. These four conditions determine the following general characteristic equation for the buckling pressure:

$$
\begin{vmatrix}
k_1 & k_1\alpha + 1 & k_1\cos(r\alpha) - r\sin(r\alpha) & k_1\sin(r\alpha) + r\cos(r\alpha) \\
-k_2 & k_2\alpha + 1 & -k_2\cos(r\alpha) + r\sin(r\alpha) & k_2\sin(r\alpha) + r\cos(r\alpha) \\
2\sin\alpha & 0 & \frac{1}{r-1}\sin[\alpha(r-1)] & 0 \\
 & & +\frac{1}{r+1}\sin[\alpha(r+1)] & \\
0 & 2\sin\alpha & 0 & \frac{1}{r-1}\sin[\alpha(r-1) \\
 & -2\alpha\cos\alpha & & -\frac{1}{r+1}\sin[\alpha(r+1)]
\end{vmatrix} = 0
\tag{3.2.35}
$$

In the special case of one base fixed and one base hinged, we set $k_1 = \infty$ and $k_2 = 0$. The characteristic equation reduces to

$$
\begin{aligned}
&[-2r\cos(r\alpha)\sin\alpha + 2\cos\alpha\sin(r\alpha)] \\
&\times \left\{ -r\cos(r\alpha)\sin\alpha + \left[\cos\alpha + \alpha(r^2 - 1)\sin\alpha\right]\sin(r\alpha) \right\} \\
&- (r^2 - 1)(\alpha\cos\alpha - \sin\alpha)\left\{ \left[1 + (2r^2 - 1)\cos(2r\alpha)\right] \right. \\
&\times \sin\alpha - r\cos\alpha\sin(2r\alpha) \right\} = 0
\end{aligned}
\tag{3.2.36}
$$

The results are presented in Table 3.2. We note that the critical pressure for an opening angle of $2\pi$ has the same value as the symmetric buckling of a ring with a free hinge.

**Table 3.2:** Critical pressure for arch with one base fixed and one base hinged.

| $2\alpha$ | 30° | 60° | 90° | 120° | 150° |
|---|---|---|---|---|---|
| $p$ | 205.00 | 50.701 | 22.135 | 12.145 | 7.5322 |

| $2\alpha$ | 180° | 225° | 270° | 315° | 360° |
|---|---|---|---|---|---|
| $p$ | 5.0401 | 3.0343 | 2.0064 | 1.5056 | 1.3923 |

### 3.2.6 Symmetrical Circular Arch

Circular arches with symmetrical boundary conditions were considered by previous authors (e.g., Timoshenko and Gere, 1961; Oran and Reagan, 1969). Due to symmetry of the prebuckling geometry, the arch buckles either symmetrically or antisymmetrically. This fact simplifies greatly the stability analysis. Of course one should always check the buckling pressures for both forms in order to determine the lowest critical pressure.

For symmetrical buckling, the perturbation angle $\psi$ is odd in the arc length $s$ and thus we can set

$$\psi = C_2 s + C_4 \sin(rs) \tag{3.2.37}$$

From Eq. (3.2.14) the vertical displacement $\eta$ is also odd in $s$. Thus $\eta(0) = \eta(\alpha) = 0$ or

$$\int_0^\alpha \psi \sin\ s\ ds = 0 \tag{3.2.38}$$

By integrating Eq. (3.2.38), we obtain

$$C_2(\sin\alpha - \alpha\cos\alpha) + C_4[\cos\alpha\sin(r\alpha) - r\sin\alpha\cos(r\alpha)]/(r^2 - 1) = 0 \tag{3.2.39}$$

On the other hand, if the buckling is antisymmetrical, we set

$$\psi = C_1 + C_3 \cos(rs) \tag{3.2.40}$$

By noting that $\xi$ is odd and $\xi(0) = \xi(\alpha) = 0$, we have

$$\int_0^\alpha \psi \cos\ s\ ds = 0 \qquad (3.2.41)$$

or

$$C_1 \sin\alpha + C_3[r\cos\alpha\sin(r\alpha) - \sin\alpha\cos(r\alpha)]/(r^2 - 1) = 0 \qquad (3.2.42)$$

Now consider the arch with symmetrical torsional springs at the base. The boundary condition is

$$\frac{d\psi}{ds}(\alpha) + k\psi(\alpha) = 0 \qquad (3.2.43)$$

If the buckling is symmetric, Eq. (3.2.43) gives

$$C_2(1 + k\alpha) + C_4[r\cos(r\alpha) + k\sin(r\alpha)] = 0 \qquad (3.2.44)$$

Together with Eq. (3.2.39), the characteristic equation is

$$\begin{aligned}(r^2 - 1)[r\cos(r\alpha) + k\sin(r\alpha)](\sin\alpha - \alpha\cos\alpha) - \\ (1 + k\alpha)[\cos\alpha\sin(r\alpha) - r\sin\alpha\cos(r\alpha)] = 0\end{aligned} \qquad (3.2.45)$$

Similarly, if the buckling is antisymmetric, Eq. (3.2.43) gives

$$C_1 k + C_3[k\cos(r\alpha) - r\sin(r\alpha)] = 0 \qquad (3.2.46)$$

This, with Eq. (3.2.42), yields

$$(r^2 - 1)\sin\alpha[r\sin(r\alpha)/k - \cos(r\alpha)] + r\cos\alpha\sin(r\alpha) - \sin\alpha\cos(r\alpha) = 0 \qquad (3.2.47)$$

For an arch with torsional springs at the base, we find the antisymmetric buckling mode prevails, except for an arch with a very large opening angle for which the symmetric mode yields the lowest critical pressure. Critical pressures for the antisymmetric mode are presented in Table 3.3. The results in Table 3.3 are an extension of those given by Timoshenko and Gere (1961) for the case where the base is hinged ($k = 0$) and the case where the base is fixed ($k = \infty$).

For $k = 0$ Eq. (3.2.47) reduces to

$$\sin(r\alpha) = 0 \qquad (3.2.48)$$

giving the exact value

$$p = \frac{\pi^2}{\alpha^2} - 1 \tag{3.2.49}$$

The critical pressure tends to zero as the opening angle approaches $360°$. But we cannot accept zero buckling pressure, since it only represents a rigid rotation. When $k = \infty$ the characteristic equation reduces to

$$\cos \alpha \sin(r\alpha) - r \sin \alpha \cos(r\alpha) = 0 \tag{3.2.50}$$

For general $k$, Oran and Reagan (1969) gave some graphical results. In Table 3.3 the critical pressure for the $2\alpha = 360°$ column should be replaced by the lower symmetric buckling value given in Table 3.1, which is for a ring with a single torsional hinge. A closer study shows the switch from antisymmetric mode to symmetric mode occurs when the opening angle is between $325°$ and $360°$. A typical comparison is shown in Table 3.4 for $k = 1$, where the switch occurs at slightly larger than $330°$.

**Table 3.3:** Critical pressure for arch with torsional springs
at the base, antisymmetric mode.

| $k$ | $2\alpha = 30°$ | $60°$ | $90°$ | $120°$ | $150°$ |
|-----|------|------|------|------|------|
| 0.0 | 143.00 | 35.000 | 15.000 | 8.0000 | 4.7600 |
| 0.5 | 146.77 | 36.888 | 16.280 | 8.9924 | 5.5967 |
| 1.0 | 150.40 | 38.633 | 17.417 | 9.8394 | 6.2822 |
| 2.0 | 157.23 | 41.742 | 19.333 | 11.191 | 7.3172 |
| 4.0 | 169.42 | 46.725 | 22.118 | 12.983 | 8.5744 |
| 10 | 196.86 | 55.692 | 26.319 | 15.325 | 10.028 |
| 20 | 224.24 | 62.282 | 28.863 | 16.564 | 10.722 |
| $\infty$ | 294.26 | 73.327 | 32.431 | 18.138 | 11.548 |

| $k$ | $2\alpha = 180°$ | $225°$ | $270°$ | $315°$ | $360°$ |
|-----|------|------|------|------|------|
| 0.0 | 3.0000 | 1.5600 | 0.7778 | 0.3061 | 0 or 3* |
| 0.5 | 3.7523 | 2.2761 | 1.5767 | 1.5059 | 3* |
| 1.0 | 4.3425 | 2.7986 | 2.1054 | 2.1362 | 3* |
| 2.0 | 5.1842 | 3.4746 | 2.7002 | 2.6283 | 3* |
| 4.0 | 6.1211 | 4.1274 | 3.1731 | 2.8986 | 3* |
| 10 | 7.0910 | 4.7028 | 3.5182 | 3.0360 | 3* |
| 20 | 7.5174 | 4.9294 | 3.6399 | 3.0818 | 3* |
| $\infty$ | 8.0000 | 5.1709 | 3.7627 | 3.1260 | 3* |

* Buckling occurs with a symmetric mode.

**Table 3.4:** Comparison of antisymmetric and symmetric buckling pressures for the case $k = 1$.

| $2\alpha$ | 315° | 320° | 330° | 340° | 350° | 360° |
|---|---|---|---|---|---|---|
| $p_{antisym}$ | 2.1362 | 2.2105 | 2.4231 | 2.7014 | 2.9289 | 3.0000 |
| $p_{sym}$ | 2.6864 | 2.5965 | 2.4307 | 2.2823 | 2.1498 | 2.0322 |

### 3.2.7 Symmetrical Arches with a Central Torsional Hinge

Figure 3.5 shows a symmetrical arch with torsionally resistant base and a central torsional hinge. This situation models closed curved doors under external pressure.

Since the prebuckling geometry is symmetric, the buckling analysis can be simplified to the study of antisymmetric and symmetric modes. The condition at the center is similar to Eq. (3.2.17)

$$D\left(\frac{d\theta}{ds} - \frac{1}{R}\right) = \bar{k}_1 \Delta\theta \tag{3.2.51}$$

We note the antisymmetric solution of the previous section, Eq. (3.2.40), is even. Thus, the moment (derivative of $\psi$) is automatically zero at the center, and due to continuity, the difference in the local angles is also zero there. Thus, Eq.(3.2.51) is automatically satisfied and we can use Table 3.3 as the buckling pressure for the antisymmetric mode for the present problem.
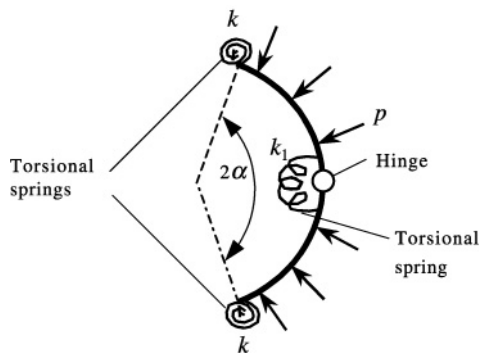


**Figure 3.5:** A symmetrical arch with torsionally resistant base and a central torsional hinge.

For the symmetric mode, we cannot assume $\psi$ is odd since it has a discontinuity at the center. The full form of Eq. (3.2.11) must be used. The boundary conditions are: the perturbed Eq. (3.2.51)

$$\frac{d\psi}{ds}(0) - k_1\psi(0) = 0, \quad k_1 = 2\bar{k}_1 R/D \tag{3.2.52}$$

the vertical displacement condition Eq. (3.2.38), the base torsional spring condition Eq. (3.2.43), and the zero horizontal force condition at the center

$$(S\sin\theta + T\cos\theta)|_{s=0} = 0 \tag{3.2.53}$$

Using Eqs. (3.2.1), (3.2.3), (3.2.4) and (3.2.8), the perturbed Eq. (3.2.53) can be expressed as

$$\frac{d^2\psi}{ds^2}(0) + p\psi(0) = 0 \tag{3.2.54}$$

The four boundary conditions give the following characteristic equation

$$\begin{vmatrix} -k_1 & 1 & -k_1 & r \\ 1-\cos\alpha & \sin\alpha - \alpha\cos\alpha & \beta_1 & \beta_2 \\ k & k\alpha + 1 & k\cos(r\alpha) - r\sin(r\alpha) & k\sin(r\alpha) + r\cos(r\alpha) \\ r^2 - 1 & 0 & -1 & 0 \end{vmatrix}$$
$$= 0 \tag{3.2.55a}$$

where
$$\beta_1 = \frac{\cos\alpha\cos(r\alpha) + r\sin\alpha\sin(r\alpha) - 1}{r^2 - 1}$$
$$\beta_2 = \frac{\cos\alpha\sin(r\alpha) - r\sin\alpha\cos(r\alpha)}{r^2 - 1} \tag{3.2.55b}$$

The results for a free hinge at the center ($k_1 = 0$) and various base spring constants $k$ are shown in Table 3.5.

The values for the case when $k$ is zero (the three-hinged arch) and when $k$ is infinity (the one-hinged arch) extend those given by Timoshenko and Gere (1961). Comparison of Table 3.5 and Table 3.3 shows the symmetric mode prevails, except the cases which have asterisked values. This change in mode for the three-hinged arch is also noted in Farshad (1994). Actually, there is a range of high opening angles and small spring constants where the antisymmetric mode gives the critical pressure.

## 3.3 Flexural–Torsional Buckling of Arches under Equal End Moments

Consider the flexural–torsional buckling problem of a simply supported, circular arch of radius $R$ and arc length $L$ subjected to two equal and opposite end moments $M$, as shown in Fig. 3.6. For an I-section arch, Papangelis and Trahair (1987) derived a solution using half waves for the lateral displacement $u$ and the angle of twist $\phi$

$$u = C_1 \sin \frac{\pi s}{L}, \quad \phi = C_2 \sin \frac{\pi s}{L} \qquad (3.3.1)$$

where $s$ is the distance along the center line of the arch. The critical flexural–torsional buckling moment $M_c$ of the arch may be expressed as

$$\frac{M_c}{M_0} = \frac{ba^3}{2} - \frac{a}{2b} - ab + \sqrt{\left(\frac{ba^3}{2} - \frac{a}{2b} - ab\right)^2 + (1 - a^2)^2} \qquad (3.3.2)$$

**Table 3.5:** Buckling pressure for an arch with a free hinge at the center and torsional springs at the base (symmetric mode).

| $k$ | $2\alpha = 30°$ | $60°$ | $90°$ | $120°$ | $150°$ |
|---|---|---|---|---|---|
| 0.0 | 108.36 | 27.077 | 12.025 | 6.7578 | 4.3216 |
| 0.5 | 109.37 | 27.584 | 12.366 | 7.0195 | 4.5381 |
| 1.0 | 110.36 | 28.056 | 12.673 | 7.2459 | 4.7185 |
| 2.0 | 112.21 | 28.905 | 13.198 | 7.6165 | 5.0005 |
| 4.0 | 115.56 | 30.304 | 13.996 | 8.1385 | 5.3711 |
| 10 | 123.37 | 33.017 | 15.336 | 8.9181 | 5.8719 |
| 20 | 131.80 | 35.294 | 16.287 | 9.4083 | 6.1585 |
| $\infty$ | 160.43 | 40.212 | 17.952 | 10.165 | 6.5647 |

| $k$ | $2\alpha = 180°$ | $225°$ | $270°$ | $315°$ | $360°$ |
|---|---|---|---|---|---|
| 0.0 | 3.0000 | 1.9227* | 1.3438* | 1.0040* | 0.7990 |
| 0.5 | 3.1891 | 2.0894 | 1.5027 | 1.1673 | 0.9807 |
| 1.0 | 3.3405 | 2.2147 | 1.6137 | 1.2713 | 1.0826 |
| 2.0 | 3.5666 | 2.3887 | 1.7561 | 1.3930 | 1.1882 |
| 4.0 | 3.8446 | 2.5828 | 1.9001 | 1.5034 | 1.2724 |
| 10 | 4.1887 | 2.7967 | 2.0425 | 1.6015 | 1.3392 |
| 20 | 4.3711 | 2.8998 | 2.1058 | 1.6420 | 1.3648 |
| $\infty$ | 4.6138 | 3.0275 | 2.1800 | 1.6874 | 1.3923 |

* The antisymmetric mode has lower buckling pressure.
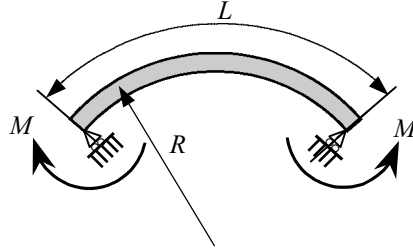
**Figure 3.6:** Circular arch under equal end moments.

in which

$$a = \frac{L}{\pi R}, \quad b = \frac{\pi M_0}{P_y L}, \quad M_0 = \sqrt{P_y \left( GJ + \frac{\pi^2 EI_w}{L^2} \right)}, \quad P_y = \frac{\pi^2 EI_y}{L^2}$$

$$(3.3.3)$$

and $P_y$ is the flexural buckling load of a straight column, $EI_w = EI_y h^2/4$ the warping rigidity, and $h$ the height of the I-beam section. For a straight beam $(R = \infty)$, Eq. (3.3.2) reduces to Eq. (3.1.32). For a narrow rectangular beam, the critical buckling moment is given by Eq. (3.3.2) with the warping section constant $I_w = 0$.

Note that the resulting exact solution differs from the one presented in Eq. (7.33) of Timoshenko and Gere (1961). The reason for this difference is due to the fact that Timoshenko and Gere (1961) neglected the internal torsional component in the principal $yz$-plane and the internal bending component in the direction of the arch centerline in deriving the equilibrium equations. According to Y. L. Pi (University of New South Wales, Australia), the improved equilibrium equations corresponding to Eq. (g) of Timoshenko and Gere (1961) should be

$$\phi M_0 = EI_x \left( \frac{\phi}{R} - \frac{d^2 v}{ds^2} \right) + C \left( \frac{d\phi}{ds} + \frac{1}{R} \frac{dv}{ds} \right) \frac{1}{R} \qquad (3.3.4)$$

$$M_0 \frac{dv}{ds} = -EI_x \left( \frac{\phi}{R} - \frac{d^2 v}{ds^2} \right) \frac{1}{R} + C \left( \frac{d\phi}{ds} + \frac{1}{R} \frac{dv}{ds} \right) \qquad (3.3.5)$$

where $C$ is the torsional rigidity and $v$ the lateral displacement.

# REFERENCES

Chajes, A. and Winter, G. (1965), "Torsional–flexural buckling of thin–walled members," *Journal of Structural Division*, **91**(ST4), 103–124.

Cuk, P. E. and Trahair, N. S. (1981), "Elastic buckling of beam–columns with unequal end moments," *Civil Engineering Transactions*, Institution of Engineers, Australia, **CE23**(3), 166–171.

Farshad, M. (1994), *Stability of Structures*, Elsevier, Amsterdam.

Kitipornchai, S. and Dux, P. F. (1987), "Buckling and bracing of elastic beams and cantilevers," *Civil Engineering Practice, Vol. 1: Structures*, Cheremisinoff/Cheremisinoff/Cheng (eds.), Technomic Publishing Co., Lancaster, PA, 501–520.

Kitipornchai, S., Wang, C. M. and Trahair, N. S. (1986), "Buckling of monosymmetric I-beams under moment gradient," *Journal of Structural Engineering*, **112**(4), 781–799.

Kitipornchai, S. and Wang, C. M. (1988), "Out-of-plane buckling formulae for beam-columns and tie-beams," *Journal of Structural Engineering,* **114**(12), 2773–2789.

Lee, L. H. N. (1959), "On the lateral buckling of a tapered narrow rectangular beam," *Journal of Applied Mechanics*, **26**, 457–458.

Lévy, M. (1884), "Memoire sur un nouveau cas integrable du probleme de l'elastique et l'une de ses applications," *J. d. Math.* Ser. 3, **10**, 5–42.

Oran, C. and Reagan R. S. (1969), "Buckling of uniformly compressed circular arches," *Journal of Engineering Mechanics, ASCE,* **95**(EM4), 879–895.

Papangelis, J. P. and Trahair, N. S. (1987), "Flexural–torsional buckling of arches," *Journal of Structural Engineering,* **113**(4), 889–906.

Pekoz, T. B. and Winter, G. (1969), "Torsional–flexural buckling of thin–walled sections under eccentric load," *Journal of Structural Division, ASCE*, **95**(ST5), 941–963.

Schmidt, R. (1981), "Buckling of a clamped–hinged circular arch under gas pressure and related problems," *Journal of Applied Mechanics,* **48**, 425–426.

Timoshenko, S. P. and Gere, J. M. (1961), *Theory of Elastic Stability*, McGraw-Hill, New York.

Trahair, N. S. (1977), *The Behavior and Design of Steel Structures*, Chapman and Hall, London, England.

Trahair, N. S. and Nethercot, D. A. (1984), "Bracing requirements in thin–walled structures," Chapter 3, *Developments in Thin–Walled Structures,* J. Rhodes and A. C. Walker (eds.), Vol. 2, 93–130, Elsevier, London, UK.

Vlasov, V. Z. (1961), *Thin–Walled Elastic Beams,* 2nd ed., Israel Program for Scientific Translation, Jerusalem, Israel.

Wang, C. M. and Kitipornchai, S. (1989), "New set of buckling parameters for monosymmetric beam-columns/tie-beams," *Journal of Structural Engineering, ASCE*, **115**(6), 1497–1513.

Wang, C. Y. (1985), "Symmetric buckling of hinged ring under uniform pressure," *Journal of Engineering Mechanics,* **111**, 1423–1427.

Wang, C. Y. (1993), "Elastic stability of an externally pressurized ring with two hinges," *Zeit. Angew. Math. Mech.,* **73**, 301–305.

Wang, C. Y., Watson, L. T. and Kamat, M. P. (1983), "Buckling, postbuckling and the flow through a tethered elastic cylinder," *Journal of Applied Mechanics,* **50**, 13–18.

# BUCKLING OF PLATES

## 4.1 Preliminary Comments

The objective of this chapter is to summarize the equations governing buckling of elastic plates and then present exact buckling loads for plates of various geometries (e.g., circular, triangular and rectangular). For the derivation of the governing equations, the reader may consult Timoshenko and Woinowsky-Krieger (1970), Bulson (1970), McFarland et al. (1972), Szilard (1974), Panc (1975), Ugural (1981) and Reddy (1999, 2002, 2004). Much of the material included here is taken from the textbook by Reddy (1999).

## 4.2 Governing Equations in Rectangular Coordinates

We consider the *classical thin plate theory* (CPT), which is based on the *Kirchhoff hypothesis:*

(a) Straight lines perpendicular to the mid-surface (i.e., transverse normals) before deformation remain straight after deformation.

(b) The transverse normals do not experience elongation (i.e., they are inextensible).

(c) The transverse normals rotate such that they remain perpendicular to the mid-surface after deformation.

The consequence of the Kirchhoff hypothesis is that the transverse strains $(\gamma_{xz}, \gamma_{yz}, \varepsilon_{zz})$ are zero, and consequently, the transverse stresses $(\sigma_{xz}, \sigma_{yz}, \sigma_{zz})$ do not enter the theory.

The equation governing buckling of plates under inplane compressive and shear forces is

$$\frac{\partial^2 M_{xx}}{\partial x^2} + 2\frac{\partial^2 M_{xy}}{\partial y \partial x} + \frac{\partial^2 M_{yy}}{\partial y^2} = \frac{\partial}{\partial x}\left(\hat{N}_{xx}\frac{\partial w}{\partial x} + \hat{N}_{xy}\frac{\partial w}{\partial y}\right)$$
$$+ \frac{\partial}{\partial y}\left(\hat{N}_{xy}\frac{\partial w}{\partial x} + \hat{N}_{yy}\frac{\partial w}{\partial y}\right) \quad (4.2.1)$$

where $(M_{xx}, M_{yy})$ are the bending moments per unit length, $M_{xy}$ is the twisting moment per unit length, and $(\hat{N}_{xx}, \hat{N}_{yy}, \hat{N}_{xy})$ are the applied inplane compressive and shear forces measured per unit length (see Fig. 4.1).
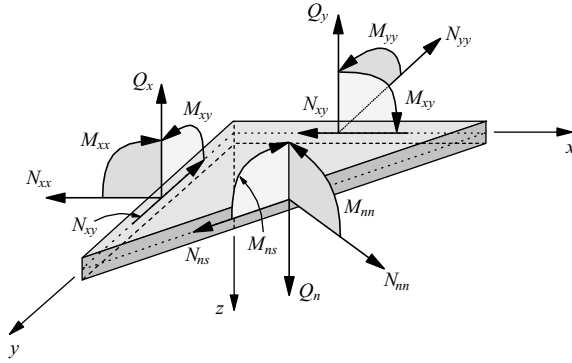
**Figure 4.1:** Applied inplane forces and moments in a plate element.

Equation (4.2.1) must be solved in conjunction with boundary conditions that may be classified as essential and natural:

$$\textit{Essential:}\quad w, \ \frac{\partial w}{\partial n}; \quad \textit{Natural:}\quad V_n, \ M_{nn}$$

where

$$V_n \equiv Q_n + \frac{\partial M_{ns}}{\partial s} - \left( \hat{N}_{xx} \frac{\partial w}{\partial x} + \hat{N}_{xy} \frac{\partial w}{\partial y} \right) n_x$$

$$- \left( \hat{N}_{xy} \frac{\partial w}{\partial x} + \hat{N}_{yy} \frac{\partial w}{\partial y} \right) n_y \tag{4.2.2}$$

$$Q_n \equiv (M_{xx,x} + M_{xy,y})\, n_x + (M_{yy,y} + M_{xy,x})\, n_y \tag{4.2.3}$$

$$M_{nn} = n_x^2 M_{xx} + n_y^2 M_{yy} + 2 n_x n_y M_{xy} \tag{4.2.4}$$

$$M_{ns} = (M_{yy} - M_{xx}) n_x n_y + (n_x^2 - n_y^2) M_{xy} \tag{4.2.5}$$

and $(n_x, n_y)$ are the direction cosines of the unit outward normal vector $\hat{\mathbf{n}}$ that is oriented at an angle $\theta$ from the positive $x$-axis; hence, its direction cosines are: $n_x = \cos\theta$ and $n_y = \sin\theta$. Thus, at every boundary point one must know one element in each of the two pairs: $(w, V_n)$ and $(\partial w/\partial n, M_{nn})$.

Next we discuss some common types of boundary conditions for a rectangular plate with edges parallel to the $x$- and $y$-axes. Here we use the edge at $y = 0$ ($n_x = 0$ and $n_y = -1$) to discuss the boundary conditions. It should be noted that only one element of each of the two pairs may be specified on an edge of a plate. The force boundary conditions may be expressed in terms of the generalized displacements using the plate constitutive equations discussed in the sequel.

**Free edge**, $y = 0$: A free edge is one which is geometrically not restrained in any way. Hence, we have

$$V_y \equiv Q_y + \frac{\partial M_{xy}}{\partial x} - \left( \hat{N}_{xy} \frac{\partial w}{\partial x} + \hat{N}_{yy} \frac{\partial w}{\partial y} \right) = 0, \quad M_{yy} = 0 \qquad (4.2.6)$$

**Fixed** (or *clamped*) **edge**, $y = 0$: A fixed edge is one that is geometrically fully restrained, i.e.,

$$w = 0, \quad \frac{\partial w}{\partial y} = 0 \qquad (4.2.7)$$

**Simply supported edge**, $y = 0$: A simply supported edge is defined as one in which the transverse deflection and normal bending moment are zero:

$$w = 0, \quad M_{yy} = 0 \qquad (4.2.8)$$

For an *orthotropic material* with principal materials axes $(x_1, x_2, x_3)$ coinciding with the plate coordinates $(x, y, z)$, the bending moments are related to the deflection $w(x, y)$ as follows:

$$\left\{ \begin{array}{c} M_{xx} \\ M_{yy} \\ M_{xy} \end{array} \right\} = - \left[ \begin{array}{ccc} D_{11} & D_{12} & 0 \\ D_{12} & D_{22} & 0 \\ 0 & 0 & D_{66} \end{array} \right] \left\{ \begin{array}{c} \frac{\partial^2 w}{\partial x^2} \\ \frac{\partial^2 w}{\partial y^2} \\ 2 \frac{\partial^2 w}{\partial x \partial y} \end{array} \right\} \qquad (4.2.9a)$$

$$D_{11} = \frac{E_1 h^3}{12(1 - \nu_{12}\nu_{21})} \ , \quad D_{12} = \nu_{21} D_{11}$$
$$D_{22} = \frac{E_2}{E_1} D_{11} \ , \quad D_{66} = \frac{G_{12} h^3}{12} \qquad (4.2.9b)$$

The equation of equilibrium (4.2.1) can be expressed in terms of displacement ($w$) by substituting for the moments from Eq. (4.2.9a). For homogeneous plates (i.e., for plates with constant $D$s), the equation of equilibrium takes the form

$$D_{11} \frac{\partial^4 w}{\partial x^4} + 2(D_{12} + 2D_{66}) \frac{\partial^4 w}{\partial x^2 \partial y^2} + D_{22} \frac{\partial^4 w}{\partial y^4}$$
$$+ \frac{\partial}{\partial x} \left( \hat{N}_{xx} \frac{\partial w}{\partial x} + \hat{N}_{xy} \frac{\partial w}{\partial y} \right) + \frac{\partial}{\partial y} \left( \hat{N}_{xy} \frac{\partial w}{\partial x} + \hat{N}_{yy} \frac{\partial w}{\partial y} \right) = 0 \ (4.2.10)$$

## 4.3 Governing Equations in Polar Coordinates

The equations governing circular plates may be obtained using the transformation relations ($x = r\cos\theta$, $y = r\sin\theta$) between the polar coordinates ($r, \theta$) and the rectangular Cartesian coordinates ($x, y$) (see Fig. 4.2). With the help of the transformation relations, one can write the equation of equilibrium (4.2.1) governing the buckling of a circular plate as

$$\frac{1}{r}\left[\frac{\partial}{\partial r}\left(rQ_r\right) + \frac{\partial Q_\theta}{\partial \theta} - \frac{\partial}{\partial r}\left(r\hat{N}_{rr}\frac{\partial w}{\partial r}\right) - \frac{1}{r}\frac{\partial}{\partial \theta}\left(\hat{N}_{\theta\theta}\frac{\partial w}{\partial \theta}\right)\right] = 0 \quad (4.3.1)$$

where ($Q_r, Q_\theta$) are the shear forces, ($M_r, M_\theta, M_{r\theta}$) are the bending moments, and ($\hat{N}_{rr}$, $\hat{N}_{\theta\theta}$, $\hat{N}_{r\theta}$) are the inplane compressive forces (see Fig. 4.3)

$$Q_r = \frac{1}{r}\left[\frac{\partial}{\partial r}\left(rM_{rr}\right) + \frac{\partial M_{r\theta}}{\partial \theta} - M_{\theta\theta}\right] \quad (4.3.2)$$

$$Q_\theta = \frac{1}{r}\left[\frac{\partial}{\partial r}\left(rM_{r\theta}\right) + \frac{\partial M_{\theta\theta}}{\partial \theta} + M_{r\theta}\right] \quad (4.3.3)$$

$$M_{rr} = -\left[D\frac{\partial^2 w}{\partial r^2} + \nu\frac{1}{r}\left(\frac{\partial w}{\partial r} + \frac{1}{r}\frac{\partial^2 w}{\partial \theta^2}\right)\right] \quad (4.3.4\text{a})$$

$$M_{\theta\theta} = -\left[\nu\frac{\partial^2 w}{\partial r^2} + D\frac{1}{r}\left(\frac{\partial w}{\partial r} + \frac{1}{r}\frac{\partial^2 w}{\partial \theta^2}\right)\right] \quad (4.3.4\text{b})$$

$$M_{r\theta} = -\left(1 - \nu\right)D\frac{1}{r}\left[\frac{\partial^2 w}{\partial r\partial \theta} - \frac{1}{r}\frac{\partial w}{\partial \theta}\right] \quad (4.3.4\text{c})$$

The natural (force) boundary conditions can be expressed as

$$\bar{V}_n \equiv V_n - \left[\hat{N}_{rr}\frac{\partial w}{\partial r}n_r + \frac{1}{r}\hat{N}_{\theta\theta}\frac{\partial w}{\partial \theta}n_\theta + \hat{N}_{r\theta}\left(\frac{1}{r}\frac{\partial w}{\partial \theta}n_r + \frac{\partial w}{\partial r}n_\theta\right)\right] \quad (4.3.5)$$

where

$$V_n = Q_n + \frac{\partial M_{ns}}{\partial s}, \quad V_r = Q_r + \frac{1}{r}\frac{\partial M_{r\theta}}{\partial \theta}, \quad V_\theta = Q_\theta + \frac{\partial M_{r\theta}}{\partial r} \quad (4.3.6)$$
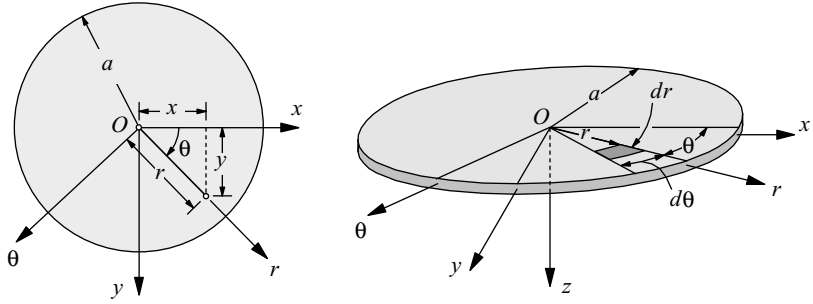
**Figure 4.2:** Transformation between rectangular and polar coordinate systems.
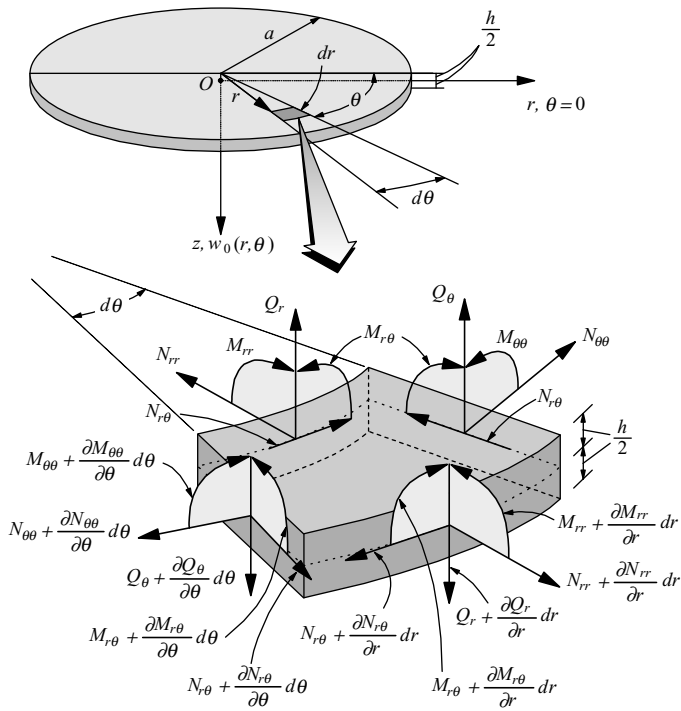


**Figure 4.3:** Moments and shear forces on an element of a circular plate.

The boundary conditions for circular plates involve specifying one quantity in each of the following pairs on positive $r$- and $\theta$-planes:

At $r = \hat{r}$, constant:

$$w = \hat{w} \qquad \text{or} \qquad \hat{r}\bar{V}_r = \hat{r}\hat{\bar{V}}_r \qquad (4.3.7a)$$

$$\frac{\partial w}{\partial r} = \frac{\partial \hat{w}}{\partial r} \qquad \text{or} \qquad \hat{r}M_{rr} = \hat{r}\hat{M}_{rr} \qquad (4.3.7b)$$

At $\theta = \hat{\theta}$, constant:

$$w = \hat{w} \qquad \text{or} \qquad \bar{V}_\theta = \hat{\bar{V}}_\theta \qquad (4.3.8a)$$

$$\frac{1}{r}\frac{\partial w}{\partial \theta} = \frac{1}{r}\frac{\partial \hat{w}}{\partial \theta} \qquad \text{or} \qquad M_{\theta\theta} = \hat{M}_{\theta\theta} \qquad (4.3.8b)$$

where

$$\bar{V}_r = Q_r + \frac{1}{r}\frac{\partial M_{r\theta}}{\partial \theta} - \hat{N}_{rr}\frac{\partial w}{\partial r} - \frac{1}{r}\hat{N}_{r\theta}\frac{\partial w}{\partial \theta} \qquad (4.3.9a)$$

$$\bar{V}_\theta = Q_\theta + \frac{\partial M_{r\theta}}{\partial r} - \frac{1}{r}\hat{N}_{\theta\theta}\frac{\partial w}{\partial \theta} - \hat{N}_{r\theta}\frac{\partial w}{\partial r} \qquad (4.3.9b)$$

The moments are related to the deflection $w$ by

$$M_{rr} = - \left[ D_{11}\frac{\partial^2 w}{\partial r^2} + D_{12}\frac{1}{r}\left( \frac{\partial w}{\partial r} + \frac{1}{r}\frac{\partial^2 w}{\partial \theta^2} \right) \right] \qquad (4.3.10a)$$

$$M_{\theta\theta} = - \left[ D_{12}\frac{\partial^2 w}{\partial r^2} + D_{22}\frac{1}{r}\left( \frac{\partial w}{\partial r} + \frac{1}{r}\frac{\partial^2 w}{\partial \theta^2} \right) \right] \qquad (4.3.10b)$$

$$M_{r\theta} = - 2D_{66}\,\frac{1}{r}\left[ \frac{\partial^2 w}{\partial r \partial \theta} - \frac{1}{r}\frac{\partial w}{\partial \theta} \right] \qquad (4.3.10c)$$

For isotropic plates, we set $D_{11} = D_{22} = D$, $D_{12} = \nu D$ and $2D_{66} = (1 - \nu)D$, and the bending moment–deflection relationships (4.3.10a–c) reduce to

$$M_{rr} = - D\left[ \frac{\partial^2 w}{\partial r^2} + \frac{\nu}{r}\left( \frac{\partial w}{\partial r} + \frac{1}{r}\frac{\partial^2 w}{\partial \theta^2} \right) \right] \qquad (4.3.11a)$$

$$M_{\theta\theta} = - D\left[ \nu\frac{\partial^2 w}{\partial r^2} + \frac{1}{r}\left( \frac{\partial w}{\partial r} + \frac{1}{r}\frac{\partial^2 w}{\partial \theta^2} \right) \right] \qquad (4.3.11b)$$

$$M_{r\theta} = - (1 - \nu)D\,\frac{1}{r}\left( \frac{\partial^2 w}{\partial r \partial \theta} - \frac{1}{r}\frac{\partial w}{\partial \theta} \right) \qquad (4.3.11c)$$

Equation of equilibrium (4.3.4) for an isotropic plate can be written in terms of the displacement with the aid of Eqs. (4.3.11a–c) as

$$
D \left[ \frac{1}{r} \frac{\partial}{\partial r} \left( r \frac{\partial}{\partial r} \right) + \frac{1}{r^2} \frac{\partial^2}{\partial \theta^2} \right] \left[ \frac{1}{r} \frac{\partial}{\partial r} \left( r \frac{\partial w}{\partial r} \right) + \frac{1}{r^2} \frac{\partial^2 w}{\partial \theta^2} \right]
$$
$$
= -\frac{1}{r} \frac{\partial}{\partial r} \left( r \hat{N}_{rr} \frac{\partial w}{\partial r} \right) - \frac{1}{r^2} \frac{\partial}{\partial \theta} \left( \hat{N}_{\theta\theta} \frac{\partial w}{\partial \theta} \right) \tag{4.3.12}
$$

Using the Laplace operator

$$
\nabla^2 = \frac{1}{r} \frac{\partial}{\partial r} \left( r \frac{\partial}{\partial r} \right) + \frac{1}{r^2} \frac{\partial^2}{\partial \theta^2} \tag{4.3.13}
$$

Equation (4.3.12) can be written simply as

$$
D \nabla^2 \nabla^2 w + \frac{1}{r} \frac{\partial}{\partial r} \left( r \hat{N}_{rr} \frac{\partial w}{\partial r} \right) + \frac{1}{r^2} \frac{\partial}{\partial \theta} \left( \hat{N}_{\theta\theta} \frac{\partial w}{\partial \theta} \right) = 0 \tag{4.3.14}
$$

For *axisymmetric buckling* of circular plates, all variables are independent of the angular coordinate $\theta$, and they are only functions of the radial coordinate $r$. Hence, in specializing the governing equations to the axisymmetric case, we omit terms involving differentiation with respect to $\theta$. First, the moment–deflection relationships for the axisymmetric case are

$$
M_{rr} = - \left( D_{11} \frac{d^2 w}{dr^2} + D_{12} \frac{1}{r} \frac{dw}{dr} \right) \tag{4.3.15a}
$$

$$
M_{\theta\theta} = - \left( D_{12} \frac{d^2 w}{dr^2} + D_{22} \frac{1}{r} \frac{dw}{dr} \right) \tag{4.3.15b}
$$

$$
Q_r = -D_{11} \frac{1}{r} \frac{d}{dr} \left( r \frac{d^2 w}{dr^2} \right) + D_{22} \frac{1}{r^2} \frac{dw}{dr} \tag{4.3.16}
$$

Next, the equation of equilibrium for the axisymmetric case can be deduced from Eq. (4.3.4) as

$$
-\frac{1}{r} \frac{d}{dr} (r Q_r) + \frac{1}{r} \frac{d}{dr} \left( r \hat{N}_{rr} \frac{dw}{dr} \right) = 0 \tag{4.3.17}
$$

Using Eq. (4.3.16) for $rQ_r$ in Eq. (4.3.17), we find that

$$D_{11}\frac{1}{r}\frac{d}{dr}\left\{r\frac{d}{dr}\left[\frac{1}{r}\frac{d}{dr}\left(r\frac{dw}{dr}\right)\right]+\left(\frac{D_{11}-D_{22}}{D_{11}}\right)\frac{1}{r}\frac{dw}{dr}\right\}$$
$$+\frac{1}{r}\frac{d}{dr}\left(r\hat{N}_{rr}\frac{dw}{dr}\right)=0 \tag{4.3.18}$$

For isotropic plates $[D_{11}=D_{22}=D]$, Eqs. (4.3.15a, b) and (4.3.16) become

$$M_{rr}=-D\left(\frac{d^2w}{dr^2}+\frac{\nu}{r}\frac{dw}{dr}\right) \tag{4.3.19a}$$

$$M_{\theta\theta}=-D\left(\nu\frac{d^2w}{dr^2}+\frac{1}{r}\frac{dw}{dr}\right) \tag{4.3.19b}$$

$$Q_r=-D\frac{d}{dr}\left[\frac{1}{r}\frac{d}{dr}\left(r\frac{dw}{dr}\right)\right] \tag{4.3.19c}$$

and the equilibrium equation (4.3.18) simplifies to

$$\frac{D}{r}\frac{d}{dr}\left\{r\frac{d}{dr}\left[\frac{1}{r}\frac{d}{dr}\left(r\frac{dw}{dr}\right)\right]\right\}+\frac{1}{r}\frac{d}{dr}\left(r\hat{N}_{rr}\frac{dw}{dr}\right)=0 \tag{4.3.20}$$

The boundary conditions involve specifying

$$w \quad \text{or} \quad r\left(Q_r-\hat{N}_{rr}\frac{dw}{dr}\right) \tag{4.3.21a}$$

and

$$\frac{dw}{dr} \quad \text{or} \quad rM_{rr} \tag{4.3.21b}$$

## 4.4 Circular Plates

### 4.4.1 General Solution for Axisymmetric Buckling

Here we consider exact buckling solutions of circular plates. Consider the shear force–deflection relation (4.3.16):

$$Q_r=-D_{11}\frac{1}{r}\frac{d}{dr}\left(r\frac{d^2w}{dr^2}\right)+D_{22}\frac{1}{r^2}\frac{dw}{dr} \tag{4.4.1}$$

We write the equation in terms of $\phi=(dw/dr)$, which represents the angle between the central axis of the plate and the normal to the deflected surface at any point (see Fig. 4.4), as
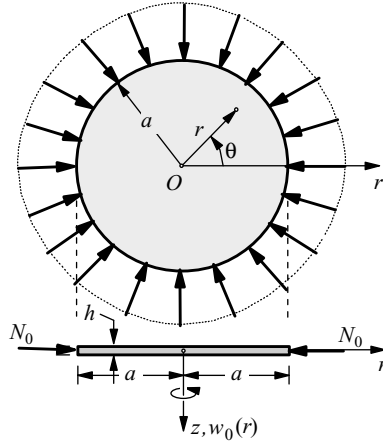
**Figure 4.4:** Buckling of a circular plate under a uniform radial compressive load.

$$Q_r = -D_{11}\frac{1}{r}\frac{d}{dr}\left(r\frac{d\phi}{dr}\right) + D_{22}\frac{\phi}{r^2} \qquad (4.4.2)$$

For a circular plate under the action of uniform radial compressive force $\hat{N}_{rr}$ per unit length, the shear force at any point is given by [an integration of Eq. (4.3.17) gives the result, because $Q_r = 0$ at $r = 0$ for an axisymmetric mode]

$$Q_r = \hat{N}_{rr}\frac{dw}{dr} = \hat{N}_{rr}\phi \qquad (4.4.3)$$

so that the equilibrium equation (4.3.17) can be written as

$$-D_{11}\frac{1}{r}\frac{d}{dr}\left(r\frac{d\phi}{dr}\right) + \frac{D_{22}}{r^2}\phi = \hat{N}_{rr}\phi$$

or

$$r\frac{d}{dr}\left(r\frac{d\phi}{dr}\right) + \left(\frac{\hat{N}_{rr}}{D_{11}}r^2 - \frac{D_{22}}{D_{11}}\right)\phi = 0 \qquad (4.4.4)$$

Equation (4.4.4) can be recast in an alternative form by invoking the transformation

$$\bar{r} = r\sqrt{\frac{\hat{N}_{rr}}{D_{11}}}, \quad n^2 = \frac{D_{22}}{D_{11}} \tag{4.4.5}$$

and the alternative form is

$$\bar{r}\frac{d}{d\bar{r}}\left(\bar{r}\frac{d\phi}{d\bar{r}}\right) + \left(\bar{r}^2 - n^2\right)\phi = 0 \tag{4.4.6}$$

which is recognized as Bessel's differential equation.

The general solution of Eq. (4.4.6) is

$$\phi(\bar{r}) = C_1 J_n(\bar{r}) + C_2 Y_n(\bar{r}) \tag{4.4.7}$$

where $J_n$ is the Bessel function of the first kind of order $n$, $Y_n$ is the Bessel function of the second kind of order $n$, and $C_1$ and $C_2$ are constants to be determined using the boundary conditions. In the case of buckling, we do not actually find these constants but determine the stability criterion. We consider different boundary conditions next.

### 4.4.2 Axisymmetric Buckling of Clamped Plates

For a clamped plate with radius $a$, the boundary conditions are ($dw/dr$ is zero at $r = 0, a$)

$$\phi(0) = 0, \quad \phi(a) = 0 \tag{4.4.8}$$

Using the general solution (4.4.7) for an isotropic ($n = 1$) plate, we obtain

$$C_1 J_1(0) + C_2 Y_1(0) = 0, \quad C_1 J_1(\alpha a) + C_2 Y_1(\alpha a) = 0, \quad \alpha^2 = \frac{\hat{N}_{rr}}{D} \tag{4.4.9}$$

Since $Y_1(0)$ is unbounded, we must have $C_2 = 0$. The fact that $J_1(0) = 0$ reduces the two equations in (4.4.9) to the single condition (since $C_1 \neq 0$ for a nontrivial solution)

$$J_1(\alpha a) = 0 \tag{4.4.10}$$

which is the stability criterion. The smallest root of the condition in (4.4.10) is $\alpha a = 3.8317$. Thus, we have

$$\hat{N}_{\text{cr}} = 14.682\frac{D}{a^2} \tag{4.4.11}$$

### 4.4.3 Axisymmetric Buckling of Simply Supported Plates

For a simply supported plate, the boundary conditions are ($dw/dr$ is zero at $r = 0$ and $M_{rr} = 0$ at $r = a$)

$$\phi(0) = 0, \quad \left[D_{11}\frac{d\phi}{dr} + D_{12}\frac{1}{r}\phi\right]_{r=a} = 0 \tag{4.4.12a}$$

The second boundary condition can be written in terms of $\bar{r}$ as

$$\left[D_{11}\frac{d\phi}{d\bar{r}} + D_{12}\frac{1}{\bar{r}}\phi\right]_{\bar{r}=\alpha a} = 0 \tag{4.4.12b}$$

Using the general solution (4.4.7) for an isotropic plate, we obtain

$$C_1 J_1(0) + C_2 Y_1(0) = 0$$
$$C_1 J_1'(\alpha a) + C_2 Y_1'(\alpha a) + \frac{\nu}{\alpha a}\left[C_1 J_1(\alpha a) + C_2 Y_1(\alpha a)\right] = 0 \tag{4.4.13}$$

The first equation gives $C_2 = 0$, and the second equation, in view of $C_2 = 0$ and the identity

$$\frac{dJ_n}{d\bar{r}} = J_{n-1}(\bar{r}) - \frac{1}{\bar{r}}J_n(\bar{r}) \tag{4.4.14}$$

gives

$$\alpha a J_0(\alpha a) - (1 - \nu)J_1(\alpha a) = 0 \tag{4.4.15}$$

which defines the stability criterion. For $\nu = 0.3$, the smallest root of the transcendental equation (4.4.15) is $\alpha a = 2.05$. Hence, the buckling load becomes

$$\hat{N}_{\text{cr}} = 4.198\frac{D}{a^2} \tag{4.4.16}$$

### 4.4.4 Axisymmetric Buckling of Simply Supported Plates with Rotational Restraint

For a simply supported plate with rotational restraint (see Fig. 4.5), the boundary conditions are

$$\phi(0) = 0, \quad \left[rD_{11}\frac{d\phi}{dr} + D_{12}\phi\right]_{r=a} + K_R a\phi(a) = 0 \tag{4.4.17}$$

where $K_R$ denotes the rotational spring constant. For an isotropic plate, we obtain (Reismann, 1952; Kerr, 1962)
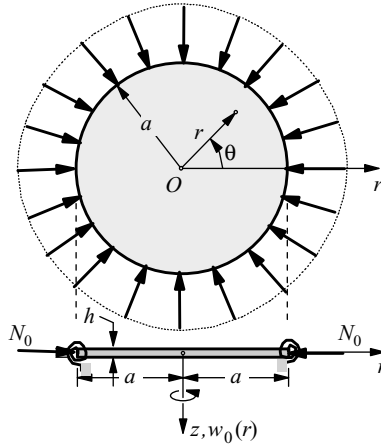
**Figure 4.5:** Buckling of a rotationally restrained circular plate under a uniform radial compressive load.

$$\alpha a J_0'(\alpha a) - (1 - \nu - \beta) J_1(\alpha a) = 0, \quad \beta = \frac{a K_R}{D} \qquad (4.4.18)$$

which is the stability criterion. When $\beta = 0$ we obtain Eq. (4.4.15), and when $\beta = \infty$, we obtain Eq. (4.4.10) as special cases. Table 4.1 contains exact values of the buckling load factor $\bar{N} = \hat{N}_{cr}(a^2/D)$ for various values of the parameter $\beta$ (for $\nu = 0.3$). Additional results can be found in the paper by Thevendran and Wang (1996).

**Table 4.1:** Critical buckling load factors $\bar{N} = \hat{N}_{cr}(a^2/D)$ for rotationally restrained circular plates.

| $\beta$ | 0 | 0.1 | 0.5 | 1 | 5 | 10 | 100 | $\infty$ |
|---------|-------|-------|-------|-------|--------|--------|--------|--------|
| $\bar{N}$ | 4.198 | 4.449 | 5.369 | 6.353 | 10.462 | 12.173 | 14.392 | 14.682 |

### 4.4.5 General Solution for Nonaxisymmetric Buckling

Consider a circular plate of radius $a$ subjected to a uniform radial compressive load $\hat{N}$. The buckling equation is given by (4.3.12) with $\hat{N}_{rr} = \hat{N}_{\theta\theta} = \hat{N}$. The general solution is sought in the form

$$w(r, \theta) = w(r) \cos n\theta \qquad (4.4.19)$$

where $n$ is the number of nodal diameters. Using the nondimensional quantities $\bar{r} = (r/a)$ and $\bar{w} = (w/a)$, the general solution can be written as

$$\bar{w} = C_1 J_n(k\bar{r}) + C_2 Y_n(k\bar{r}) + C_3 \bar{r}^n + C_4 \left\{ \begin{array}{c} \log \bar{r} \\ \bar{r}^{-n} \end{array} \right\} \qquad (4.4.20)$$

where $k^2 = \hat{N}a^2/D$ and $C_i$ are constants to be determined subject to the boundary conditions. In Eq. (4.4.20), the top part of the coefficient $C_4$ is used for $n = 0$ (axisymmetric solution) and the bottom part is used for $n \neq 0$ (nonaxisymmetric).

### 4.4.6 Buckling of Plates with Internal Ring Support

Consider a solid circular plate of radius $a$ with an internal concentric ring support of radius $b$ (Wang and Wang, 2001). Suppose that the edge $r = a$ (or $\bar{r} = 1$) is rotationally restrained, as shown in Fig. 4.6.

The general solution (4.4.20) is valid in both regions, $0 < r < b$ and $b < r < a$, with the solutions $\bar{w}_I$ and $\bar{w}_{II}$ from the two regions $s < \bar{r} < 1$ (outer region) and $0 < \bar{r} < s$ (inner region), respectively, being continuous at $\bar{r} = s$, where $s$ denotes the ratio $s = b/a$. Thus, we have the following continuity conditions

$$\bar{w}_I(s) = \bar{w}_{II}(s), \quad \bar{w}_I'(s) = \bar{w}_{II}'(s), \quad \bar{w}_I''(s) = \bar{w}_{II}''(s) \qquad (4.4.21)$$
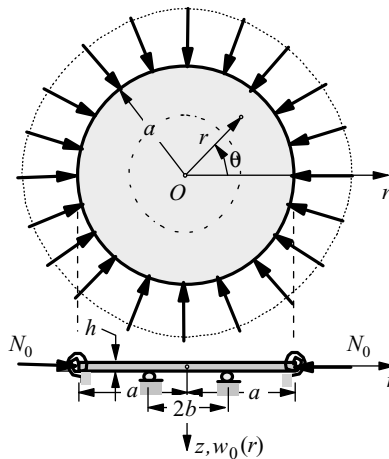


**Figure 4.6:** Buckling of a rotationally restrained circular plate with internal concentric ring support.

The boundary conditions of the plate are

$$\bar{w}_I(1) = 0, \quad \bar{w}_I(s) = 0, \quad \bar{w}_I^{''}(1) + (\nu + \beta)\bar{w}_I^{'}(1) = 0 \qquad (4.4.22)$$

where $\beta = (K_R a/D)$. The solution (4.4.20) is valid in region $I$:

$$\bar{w}_I = C_1 J_n(k\bar{r}) + C_2 Y_n(k\bar{r}) + C_3\bar{r}^n + C_4 \left\{ \begin{matrix} \log \bar{r} \\ \bar{r}^{-n} \end{matrix} \right\} \qquad (4.4.23)$$

Use of the boundary conditions (4.4.22) (all of which apply to the solution in region $I$) in the general solution (4.4.23) results in the following set of equations:

$$C_1 J_n(k) + C_2 Y_n(k) + C_3 + C_4 \left\{ \begin{matrix} 0 \\ 1 \end{matrix} \right\} = 0 \qquad (4.4.24a)$$

$$C_1 \left[ k^2 J_n^{''}(k) + \lambda k J_n^{'}(k) \right] + C_2 \left[ k^2 Y_n^{''}(k) + \lambda k Y_n^{'}(k) \right]$$
$$+ C_3 n(n-1+\lambda) + C_4 \left\{ \begin{matrix} \lambda - 1 \\ n(n+1-\lambda) \end{matrix} \right\} = 0 \qquad (4.4.24b)$$

$$C_1 J_n(ks) + C_2 Y_n(ks) + C_3 s^n + C_4 \left\{ \begin{matrix} \log s \\ s^{-n} \end{matrix} \right\} = 0 \qquad (4.4.24c)$$

where $\lambda = \nu + \beta$.

The general solution (4.4.20) for region $II$ can be simplified using the symmetry conditions, namely, the vanishing of the slope and shear force at $\bar{r} = 0$. These conditions require, to eliminate singularity in the solution, $C_2 = C_4 = 0$ in Eq. (4.4.20) for region $II$:

$$\bar{w}_{II} = C_5 J_n(k\bar{r}) + C_6\bar{r}^n \qquad (4.4.25)$$

Using Eqs. (4.4.23) and (4.4.25) in the continuity conditions (4.4.21), we obtain

$$C_5 J_n(ks) + C_6 s^n = 0 \qquad (4.4.26a)$$

$$C_1 k J_n^{'}(ks) + C_2 k Y_n^{'}(ks) + C_3 n s^{n-1} + C_4 \left\{ \begin{matrix} s^{-1} \\ -ns^{-(n+1)} \end{matrix} \right\}$$
$$- \left[ C_5 k J_n^{'}(ks) + C_6 n s^{n-1} \right] = 0 \qquad (4.4.26b)$$

$$C_1 k^2 J_n^{''}(ks) + C_2 k^2 Y_n^{''}(ks) + C_3 n(n-1) s^{n-2} + C_4 \left\{ \begin{matrix} -s^{-2} \\ n(n+1)s^{-(n+2)} \end{matrix} \right\}$$
$$- \left[ C_5 k^2 J_n^{''}(ks) + C_6 n(n-1) s^{n-2} \right] = 0 \qquad (4.4.26c)$$

Equations (4.4.24a–c) and (4.4.26a–c) provide six equations among $C_i$ ($i = 1, 2, \cdots, 6$). For a nontrivial solution, the determinant of the $6 \times 6$ coefficient matrix of these equations is set to zero. This provides the stability criterion for the problem at hand. The computation of the determinant and roots of the transcendental equations may be carried out by an symbolic manipulator, such as MATHEMATICA.

We have already noted that, at least for solid plates, the stiffness and the Poisson ratio combine to yield the single parameter $\lambda$. Therefore the effect of the rotational elastic constraint on the buckling load is equivalent to a simply supported plate with a higher fictitious Poisson's ratio. Figure 4.7 shows the variation of $k$, the square root of the normalized buckling load, with respect to the ring support radius $s = b/a$, for various values of the combined parameter $\lambda$. For example, the $\lambda = 0.3$ curve may represent either a simply supported plate with a Poisson's ratio $\nu = 0.3$ or an elastically constrained plate with stiffness $\gamma = 0.1$ and a Poisson's ratio $\nu = 0.2$.
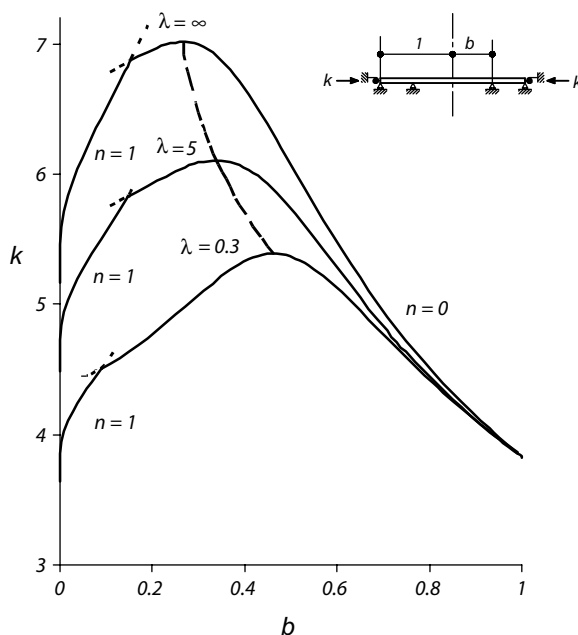


**Figure 4.7:** Buckling load versus radius of the internal ring support.

For a given $\lambda$ value, the buckling load curve is composed of two segments due to the switching of buckling modes. For a larger internal ring support radius $b$, the plate buckles in an axisymmetric mode (i.e., $n = 0$) and the results agree with those of Laura et al. (2000). When $s = b/a \rightarrow 0$, all curves converge to $k = 3.8317$, which is the first root of the stability condition $J_1(k) = 0$ for the clamped plate. Note that two closely spaced simple supports are equivalent to a clamped support. However, for a small ring support of radius $b$, the plate buckles in an asymmetric mode with $n = 1$ and the buckling load decreases dramatically as $b$ decreases in value. This crossover radius varies from $b/a = 0.081$ for $\lambda = 0$ to $b/a = 0.152$ for $\lambda \rightarrow \infty$. When $s \rightarrow 0$, the ring support corresponds to a central, clamped point support for which the plate's theoretical buckling load is given by the root of the equation (see Yamaki, 1958)

$$kJ_1(k) - (1 - \lambda)J_2(k) = 0 \qquad (4.4.27)$$

Of interest in the design of supported circular plates is the optimal location of the internal ring support for the maximum buckling load. Table 4.2 and the locus denoted by the dashed line in Fig. 4.7 show the optimal solutions. It is worth noting that the optimal location of the internal ring support is found at the nodal circle of the second axisymmetric buckling mode of a corresponding circular plate without the internal ring support. Moreover, the buckling load value as well as the eigenfunctions are the same for both these problems. This fact can be proved in a similar manner as reported by Chou et al. (1999) on vibrating circular plates.

**Table 4.2:** Optimal location $s_{opt}$ of ring support and the corresponding buckling load parameter $k_{opt}$ for rotationally restrained circular plates with concentric ring support.

| $\lambda$ | 0 | 0.3 | 1 | 2 | 3 | 5 | 7 | 10 | 20 | 50 | $\infty$ |
|---|---|---|---|---|---|---|---|---|---|---|---|
| $s_{opt}$ | 0.475 | 0.463 | 0.434 | 0.403 | 0.378 | 0.344 | 0.323 | 0.305 | 0.284 | 0.271 | 0.265 |
| $k_{opt}$ | 5.331 | 5.389 | 5.520 | 5.691 | 5.841 | 6.077 | 6.248 | 6.420 | 6.685 | 6.877 | 7.015 |

### 4.4.7 Axisymmetric Buckling of Plates under Intermediate and Edge Radial Loads

Consider an isotropic, circular plate of radius $R$, uniform thickness $h$, Young's modulus $E$, and Poisson's ratio $\nu$. The plate boundary may be either simply supported or clamped. In addition to carrying a uniform edge radial load, it also is subjected to an intermediate radial load acting

at a radius $bR$ as shown in Fig. 4.8. The intermediate load may be introduced using circular piezoelectric actuators.
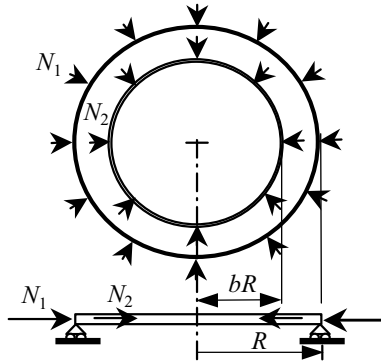


**Figure 4.8:** Buckling of circular plates under intermediate and end radial loads.

**Table 4.3:** Governing differential equations and general solutions for buckling of circular plates under intermediate and edge radial loads ($\bar{w} = w/R$ and $A_i$ and $B_i$ are constants).

| Cases | Governing Differential Equations | | General Solutions | |
|---|---|---|---|---|
| | $1 > \bar{r} > b$ | $b > \bar{r} > 0$ | $1 > \bar{r} > 0$ | $b > \bar{r} > 0$ |
| 1. $N_1 > 0,$ $N_1 + N_2 > 0$ | $\nabla^2(\nabla^2 + k_1^2)\bar{w}_1 = 0$ $k_1^2 = \frac{N_1 R^2}{D}$ | $\nabla^2(\nabla^2 + k_2^2)\bar{w}_2 = 0$ $k_2^2 = \frac{(N_1+N_2)R^2}{D}$ | $\bar{w}_1 = A_1 J_0(k_1\bar{r})$ $+A_2 Y_0(k_1\bar{r})$ $+A_3 \log\bar{r} + A_4$ | $\bar{w}_2 = B_1 J_0(k_2\bar{r})$ $+B_2$ |
| 2. $N_1 > 0,$ $N_1 + N_2 < 0$ | $\nabla^2(\nabla^2 + k_1^2)\bar{w}_1 = 0$ $k_1^2 = \frac{N_1 R^2}{D}$ | $\nabla^2(\nabla^2 - k_2^2)\bar{w}_2 = 0$ $k_2^2 = \frac{(|N_1+N_2|)R^2}{D}$ | $\bar{w}_1 = A_1 J_0(k_1\bar{r})$ $+A_2 Y_0(k_1\bar{r})$ $+A_3 \log\bar{r} + A_4$ | $\bar{w}_2 = B_1 I_0(k_2\bar{r})$ $+B_2$ |
| 3. $N_1 > 0,$ $N_1 + N_2 = 0$ | $\nabla^2(\nabla^2 + k_1^2)\bar{w}_1 = 0$ $k_1^2 = \frac{N_1 R^2}{D}$ | $\nabla^4\bar{w}_2 = 0$ | $\bar{w}_1 = A_1 J_0(k_1\bar{r})$ $+A_2 Y_0(k_1\bar{r})$ $+A_3 \log\bar{r} + A_4$ | $\bar{w}_2 = B_1\bar{r}^2 + B_2$ |
| 4. $N_1 = 0,$ $N_1 + N_2 > 0$ | $\nabla^4\bar{w}_1 = 0$ | $\nabla^2(\nabla^2 + k_2^2)\bar{w}_2 = 0$ $k_2^2 = \frac{(|N_1+N_2|)R^2}{D}$ | $\bar{w}_1 = A_1\bar{r}^2$ $+A_2\bar{r}^2\log\bar{r}$ $+A_3\log\bar{r} + A_4$ | $\bar{w}_2 = B_1 J_0(k_2\bar{r})$ $+B_2$ |
| 5. $N_1 < 0,$ $N_1 + N_2 > 0$ | $\nabla^2(\nabla^2 - k_1^2)\bar{w}_1 = 0$ $k_1^2 = \frac{|N_1|R^2}{D}$ | $\nabla^2(\nabla^2 + k_2^2)\bar{w}_2 = 0$ $k_2^2 = \frac{(|N_1+N_2|)R^2}{D}$ | $\bar{w}_1 = A_1 I_0(k_1\bar{r})$ $+A_2 K_0(k_1\bar{r})$ $+A_3\log\bar{r} + A_4$ | $\bar{w}_2 = B_1 J_0(k_2\bar{r})$ $+B_2$ |

This buckling problem may be solved by considering the plate as one consisting of an outer annular segment $1 > \bar{r} > b$ and an inner circular segment $b > \bar{r} > 0$ $(\bar{r} = r/R)$. The interface of the two segments is where the intermediate radial load is applied. The governing differential equations and general solutions for five different load cases are presented in Table 4.3. Using the general solution and edge conditions and continuity conditions at the interface, we can derive the stability criterion for each load case and boundary conditions. Here we treat simply supported and clamped edge conditions. The stability criterion for each load case is given next.

**Case 1.** $N_1 > 0$ and $(N_1 + N_2) > 0$, implying that both outer segment and inner circular segment are in a state of compression. The stability criterion for the simply supported circular plate is

$$b^2 k_1^3 \pi \sqrt{\beta} J_0(b\sqrt{\beta}k_1) \left[ J_1(bk_1)\Phi - Y_1(bk_1)\Psi \right] +$$
$$\{ J_1(b\sqrt{\beta}k_1)[4(\nu - 1) + b^2 k_1^2 \pi \{ Y_0(bk_1)[k_1\Psi - (\nu - 1)J_2(bk_1)]$$
$$- J_0(bk_1)[k_1\Phi - (\nu - 1)Y_2(bk_1)]\}]\} = 0 \qquad (4.4.28)$$

where $J_n$ and $Y_n$ are the Bessel function of the first kind and the second kind of order $n$, and

$$\Phi = k_1 Y_0(k_1) + (\nu - 1)Y_1(k_1), \quad \Psi = k_1 J_0(k_1) + (\nu - 1)J_1(k_1), \quad \beta = \frac{k_1^2 + k_2^2}{k_1^2} \qquad (4.4.29)$$

The stability criterion for the clamped circular plate is

$$b^2 k_1^3 \pi \sqrt{\beta} J_0(b\sqrt{\beta}k_1)[J_1(bk_1)Y_1(k_1) - J_1(k_1)Y_1(bk_1)]$$
$$+ J_1(b\sqrt{\beta}k_1)[4 + b^2 k_1^2 \pi \{ Y_0(bk_1)[k_1 J_1(k_1) - J_2(bk_1)]$$
$$- J_0(bk_1)[k_1 Y_1(k_1) - Y_2(bk_1)]\}] = 0 \qquad (4.4.30)$$

**Case 2.** $N_1 > 0$ and $(N_1 + N_2) < 0$, implying that the outer annular segment is in a state of compression while the inner segment is in tension. The stability criterion for the simply supported circular plate is

$$I_1(b\sqrt{\beta}k_1)\left[ J_0(bk_1)\Phi - Y_0(bk_1)\Psi \right] + \sqrt{\beta}I_0(b\sqrt{\beta}k_1)\left[ Y_1(bk_1)\Psi - J_1(bk_1)\Phi \right]$$
$$= 0 \qquad (4.4.31)$$

where $I_n$ is the modified Bessel function of the first kind of order $n$. For the clamped circular plate, the stability criterion is

$$b^2 k_1^3 \pi \sqrt{\beta} I_0(b\sqrt{\beta}k_1)[J_1(k_1)Y_1(bk_1) - J_1(bk_1)Y_1(k_1)]$$
$$- I_1(b\sqrt{\beta}k_1)[4 + b^2 k_1^2 \pi \{ Y_0(bk_1)[k_1 J_1(k_1) - J_2(bk_1)]$$
$$- J_0(bk_1)[k_1 Y_1(k_1) - Y_2(bk_1)]\}] = 0 \qquad (4.4.32)$$

**Case 3.** $N_1 > 0$ and $(N_1 + N_2) = 0$, implying that the outer annular segment is in a state of compression while the inner circular segment is in an unloaded state. The stability criterion for the simply supported circular plate is

$$Y_2(bk_1)\Psi - J_2(bk_1)\Phi = 0 \tag{4.4.33}$$

For the clamped circular plate, the stability criterion is

$$J_1(k_1)Y_2(bk_1) - J_2(bk_1)Y_1(k_1) = 0 \tag{4.4.34}$$

**Case 4.** $N_1 = 0$ and $(N_1 + N_2) > 0$, implying that the outer annular segment is in an unloaded state while the inner circular segment is in compression. The stability criterion for the simply supported circular plate is

$$
\begin{aligned}
&k_2 J_0(bk_2)[b^2(1-\nu) + (1+\nu)] + bJ_1(bk_2)\{(1-\nu)[k_2^2(b^2-1) - 2] \\
&+ 2(1+\nu)k_2^2 \log(b)\} = 0
\end{aligned} \tag{4.4.35}
$$

For the clamped circular plate, the stability criterion is

$$(b^2 - 1)k_2 J_0(bk_2) - 2bJ_1(bk_2) = 0 \tag{4.4.36}$$

**Case 5.** $N_1 < 0$ and $(N_1 + N_2) > 0$, implying that the outer annular segment is in tension while the inner circular segment is in a compressive state. The stability criterion for the simply supported circular plate is

$$
\begin{aligned}
&b^2 k_1^3 \sqrt{\beta}\left\{I_1(bk_1)\left[J_2(b\sqrt{\beta}k_1) - J_0(b\sqrt{\beta}k_1)\right]\Omega - 2\Lambda J_0(b\sqrt{\beta}k_1)K_1(bk_1)\right\} \\
&+ J_1(b\sqrt{\beta}k_1)[2(\nu - 1) + b^2 k_1^2\{-2k_1\Lambda K_0(bk_1) \\
&+ I_2(bk_1)\left[k_1\Omega + (\nu - 1)K_0(bk_1)\right] \\
&+ I_0(bk_1)\left[k_1\Omega - (\nu - 1)K_2(bk_1)\right]\}] = 0
\end{aligned} \tag{4.4.37}
$$

where $K_n$ is the modified Bessel function of the second kind of order $n$.

$$\Omega = k_1 K_0(k_1) - (\nu - 1)K_1(k_1), \quad \Lambda = k_1 I_0(k_1) + (\nu - 1)I_1(k_1) \tag{4.4.38}$$

The stability criterion for the clamped circular plate is

$$
\begin{aligned}
&b_2 k_1^3 \sqrt{\beta}\left[J_0(b\sqrt{\beta}k_1) - J_2(b\sqrt{\beta}k_1)\right][I_1(bk_1)K_1(k_1) - I_1(k_1)K_1(bk_1)] \\
&- J_1(b\sqrt{\beta}k_1)[-2 + b^2 k_1^2\{I_2(bk_1)[k_1 K_1(k_1) - K_0(bk_1)] \\
&+ k_1 I_1(k_1)[K_0(bk_1) + K_2(bk_1)] + I_0(bk_1)[k_1 K_1(k_1) + K_2(bk_1)]\}] = 0
\end{aligned} \tag{4.4.39}
$$

Plots of the stability criteria for various intermediate load location $b$ and support conditions are presented in Fig. 4.9.
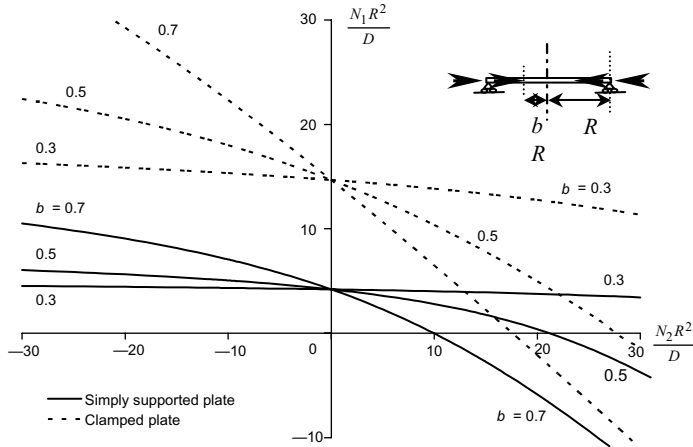


**Figure 4.9:** Stability criteria for circular plates under intermediate and edge radial loads.

### 4.4.8 Buckling of Annular Plates under Uniform Compression

Yamaki (1958) solved the elastic buckling problem of thin annular plates under uniform compression. He presented stability criteria for twelve combinations of standard boundary conditions for the inner and outer edges of the annular plate, buckling results, and discussed the limiting case of a small core.

Consider an annular plate that is compressed by forces uniformly distributed along the inner edge $r = b$ and along the outer edge $r = a$, as shown in Fig. 4.10. By introducing the buckling load parameter $k^2 = Na^2/D$, where $N$ is the intensity of the force, $D$ the flexural rigidity, and by assuming the deflection $w(\bar{r})\cos n\theta$, where $n$ $(= 0, 1, 2, \ldots)$ is the number of nodal diameters and $\bar{r} = r/a$, the solution for the governing buckling equation may be expressed as

$$w = A_0 J_0(k\bar{r}) + B_0 Y_0(k\bar{r}) + C_0 + D_0 \ln \bar{r} \qquad (4.4.40a)$$

for axisymmetric buckling $(n = 0)$ and

$$w = A_n J_n(k\bar{r}) + B_n Y_n(k\bar{r}) + C_n \bar{r}^n + D_n \bar{r}^{-n} \qquad (4.4.40b)$$

for nonaxisymmetric buckling ($n \neq 0$). Here ($A_n$, $B_n$, $C_n$, $D_n$) are constants and ($J_n$, $Y_n$) are the Bessel functions of the first and second kinds, respectively.

The common boundary conditions are given below.

*Clamped edge*

$$w = 0, \quad \frac{\partial w}{\partial \bar{r}} = 0 \tag{4.4.41}$$

*Simply supported edge*

$$w = 0, \quad \frac{\partial^2 w}{\partial \bar{r}^2} + \frac{\nu}{\bar{r}}\left(\frac{\partial w}{\partial \bar{r}} + \frac{1}{\bar{r}}\frac{\partial^2 w}{\partial \theta^2}\right) = 0 \tag{4.4.42}$$

*Free edge*

$$\frac{\partial^2 w}{\partial \bar{r}^2} + \frac{\nu}{\bar{r}}\left(\frac{\partial w}{\partial \bar{r}} + \frac{1}{\bar{r}}\frac{\partial^2 w}{\partial \theta^2}\right) = 0 \tag{4.4.43a}$$

$$\frac{\partial}{\partial \bar{r}}\left(\frac{\partial^2 w}{\partial \bar{r}^2} + \frac{1}{\bar{r}}\frac{\partial w}{\partial \bar{r}} + \frac{1}{\bar{r}^2}\frac{\partial^2 w}{\partial \theta^2}\right) + \frac{1-\nu}{\bar{r}}\frac{\partial}{\partial \theta}\left[\frac{\partial}{\partial \bar{r}}\left(\frac{1}{\bar{r}}\frac{\partial w}{\partial \theta}\right)\right] + k^2\frac{\partial w}{\partial \bar{r}} = 0 \tag{4.4.43b}$$

*Movable (or sliding) edge that cannot rotate*

$$\frac{\partial w}{\partial \bar{r}} = 0, \quad \frac{\partial}{\partial \bar{r}}\left(\frac{\partial^2 w}{\partial \bar{r}^2} + \frac{1}{\bar{r}}\frac{\partial w}{\partial \bar{r}} + \frac{1}{\bar{r}^2}\frac{\partial^2 w}{\partial \theta^2}\right) + \frac{1-\nu}{\bar{r}}\frac{\partial}{\partial \theta}\left[\frac{\partial}{\partial \bar{r}}\left(\frac{1}{\bar{r}}\frac{\partial w}{\partial \theta}\right)\right] = 0 \tag{4.4.44}$$
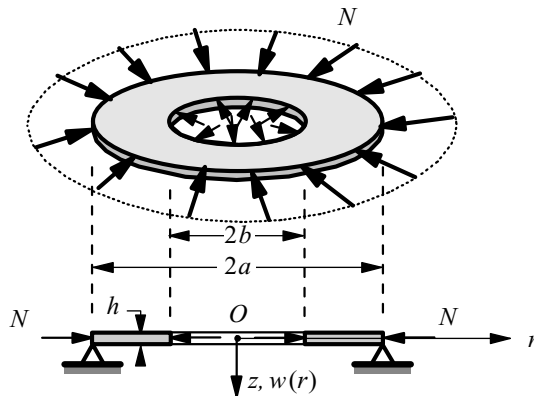


**Figure 4.10:** Annular plate under uniform compression.

By substituting the solution given in Eqs. (4.4.40a, b) into the boundary conditions (4.4.41)–(4.4.44) for the inner and outer edges, we obtain an eigenvalue problem. By solving the eigenvalue problem, stability criteria are obtained for various combinations of boundary conditions for the inner and outer edges of the annular plate. The following quantities are used to write the stability criteria in concise form:

$$\Phi_n(k,s) = J_n(k)Y_n(ks) - J_n(ks)Y_n(k)$$
$$\Psi_n(k,s) = J_n(k)Y_{1+n}(ks) - J_{1+n}(ks)Y_n(k) \qquad (4.4.45)$$
$$\Theta_n(k,s) = J_{1+n}(k)Y_n(ks) - J_n(ks)Y_{1+n}(k)$$

where $s = b/a$. The criteria are listed below.

**Case 1:** Both inner and outer edges clamped

$$(4/\pi k) - ks \ln s\, \Phi_1 + s\Psi_0 - \Theta_0 = 0 \qquad (4.4.46a)$$

$$(8n/\pi k) - ks(s^n - s^{-n})\Phi_{1+n} + 2ns^{1+n}\Psi_n - 2ns^{-n}\Theta_n = 0 \ (n \neq 0)$$
$$(4.4.46b)$$

**Case 2:** Outer edge clamped while inner edge simply supported

$$[4(1-\nu)/\pi k] - ks^2\Phi_0 - (1-\nu)s(k \ln s\, \Phi_1 - \Psi_0)$$
$$+ (k^2s^2 \ln s - 1 + \nu)\Theta_0 = 0 \quad (4.4.47a)$$

$$(8n/\pi k) - 2n(1-\nu)^{-1}ks^{2+n}\Phi_n - ks(s^n - s^{-n})\Phi_{1+n} + 2ns^{1+n}\Psi_n$$
$$+ \left[(1-\nu)^{-1}k^2s^2(s^n - s^{-n}) - 2ns^{-n}\right]\Theta_n = 0 \ \ (n \neq 0) \qquad (4.4.47b)$$

**Case 3:** Outer edge clamped while inner edge free

$$(1-\nu)\Phi_1 - ks\Theta_0 = 0 \ (n = 0) \qquad (4.4.48a)$$

$$(8/\pi k)(n^2 - 1 - n\zeta_n) - 2(1-\nu)^{-1}ks^{2+n}(2n - 2 - \zeta_n)\Phi_n$$
$$- (ks/n)\left[(n^2 - 1 - \zeta_n)s^n - (n^2 - 1 + \zeta_n)s^{-n}\right]\Phi_{1+n}$$
$$+ 2s^{1+n}(n^2 - 1 - \zeta_n)\Psi_n + \{\zeta_n(2n - 2 - \zeta_n)s^n$$
$$- \left[\zeta_n^2 + 2(n^2 - 1 - n\zeta_n)\right]s^{-n}\}\Theta_n = 0 \ (n \neq 0) \qquad (4.4.48b)$$

where $\zeta_n = k^2 s^2/[n(1-\nu)]$.

**Case 4:** Outer edge clamped while inner edge movable

$$\Phi_1 = 0 \quad (n=0) \tag{4.4.49a}$$

$$(8/\pi k) - 2(1-\nu)^{-1}ks^{2+n}\Phi_n - (ks/n)\left[(1+\zeta_n)s^n - (1-\zeta_n)s^{-n}\right]\Phi_{1+n}$$
$$+ 2(1+\zeta_n)s^{1+n}\Psi_n + \left[(s^n - s^{-n})\zeta_n - 2s^{-n}\right]\Theta_n = 0 \ (n \neq 0) \tag{4.4.49b}$$

**Case 5:** Outer edge simply supported while inner edge clamped

$$[4(1-\nu)/\pi k] + k\Phi_0 - (1-\nu)(ks\ln s\,\Phi_1 + \Theta_0) + s(k^2\ln s + 1 - \nu)\Psi_0 = 0 \tag{4.4.50a}$$

$$(8n/\pi k) + 2n(1-\nu)^{-1}ks^{-n}\Phi_n - ks(s^n - s^{-n})\Phi_{1+n} - 2ns^{-n}\Theta_n$$
$$+ s\left[(1-\nu)^{-1}k^2(s^n - s^{-n}) + 2ns^n\right]\Psi_n = 0 \ (n \neq 0) \tag{4.4.50b}$$

**Case 6:** Both edges simply supported

$$[4(1-\nu)/\pi k] - k\left[(1-\nu)^{-1}k^2s^2\ln s + s^2 - 1\right]\Phi_0 - (1-\nu)ks\ln s\,\Phi_1$$
$$+ s(k^2\ln s + 1 - \nu)\Psi_0 + (k^2s^2\ln s - 1 + \nu)\Theta_0 = 0 \tag{4.4.51a}$$

$$(8n/\pi k) - (1-\nu)^{-1}k\left[(2+\xi_n)s^{2+n} - (2+\zeta_n)s^{-n}\right]\Phi_n$$
$$- (ks/n)(s^n - s^{-n})\Phi_{1+n} + s\left[\xi_n(s^n - s^{-n}) + 2s^n\right]\Psi_n$$
$$+ \left[\zeta_n(s^n - s^{-n}) - 2s^{-n}\right]\Theta_n = 0 \quad (n \neq 0) \tag{4.4.51b}$$

where $\xi_n = k^2/[n(1-\nu)]$.

**Case 7:** Outer edge simply supported while inner edge free

$$k^2s\Phi_0 + (1-\nu)^2\Phi_1 - k(1-\nu)(\Psi_0 + s\Theta_0) = 0 \tag{4.4.52a}$$

$$(8/\pi k)(n^2 - 1 - n\zeta_n) - (ks/n)\left[(n^2 - 1 - \zeta_n)s^n - (n^2 - 1 + \zeta_n)s^{-n}\right]\Phi_{1+n}$$
$$- (1-\nu)^{-1}k\{(2+\xi_n)(2n - 2 - \zeta_n)s^{2+n} - [\zeta_n^2 + 2(n^2 - 1 - n\zeta_n)]s^{-n}\}\Phi_n$$
$$+ s\left[(2+\xi_n)(n^2 - 1 - \zeta_n)s^n - \xi_n(n^2 - 1 + \zeta_n)s^{-n}\right]\Psi_n$$
$$+ \{\zeta_n(2n - 2 - \zeta_n)s^n - [\zeta_n^2 + 2(n^2 - 1 - n\zeta_n)]s^{-n}\}\Theta_n = 0 \ (n \neq 0) \tag{4.4.52b}$$

**Case 8:** Outer edge simply supported while inner edge movable

$$(1 - \nu)\Phi_1 - k\Psi_0 = 0 \qquad (4.4.53a)$$

$$
\begin{aligned}
(8/\pi k) &- (1 - \nu)^{-1}k[(2 + \xi_n)s^{2+n} - (2 - \zeta_n)s^{-n}]\Phi_n \\
&- (ks/n)\left[(1 + \zeta_n)s^n - (1 - \zeta_n)s^{-n}\right]\Phi_{1+n} \\
&+ s\left[(2 + \xi_n)(1 + \zeta_n)s^n - \xi_n(1 - \zeta_n)s^{-n}\right]\Psi_n \\
&+ \{\zeta_n(s^n + s^{-n}) - 2s^{-n}\}\Theta_n = 0 \ (n \neq 0) \qquad (4.4.53b)
\end{aligned}
$$

**Case 9:** Outer edge free while inner edge clamped

$$(1 - \nu)\Phi_1 - k\Psi_0 = 0 \qquad (4.4.54a)$$

$$
\begin{aligned}
(8/\pi k)&(n^2 - 1 - n\xi_n) + 2(1 - \nu)^{-1}k(2n - 2 - \xi_n)s^{-n}\Phi_n \\
&- (ks/n)\left[(n^2 - 1 + \xi_n)s^n - (n^2 - 1 - \xi_n)s^{-n}\right]\Phi_{1+n} \\
&+ s\left\{[\xi_n^2 + 2(n^2 - 1 - n\xi_n)]s^n - \xi_n(2n - 2 - \xi_n)s^{-n}\right\}\Psi_n \\
&- 2(n^2 - 1 - \xi_n)s^{-n}\Theta_n = 0 \ (n \neq 0) \qquad (4.4.54b)
\end{aligned}
$$

**Case 10:** Outer edge free while inner edge simply supported

$$k^2 s\Phi_0 + (1 - \nu)^2\Phi_1 - k(1 - \nu)(\Psi_0 + s\Theta_0) = 0 \qquad (4.4.55a)$$

$$
\begin{aligned}
- (ks/n)&\left[(n^2 - 1 - \xi_n)s^n - (n^2 - 1 - \xi_n)s^{-n}\right]\Phi_{1+n} - (1 - \nu)^{-1}k \\
&\times \left\{\left[\xi_n^2 + 2(n^2 - 1 - n\xi_n)\right]s^{2+n} - (2n - 2 - \xi_n)(2 + \zeta_n)s^{-n}\right\}\Phi_n \\
&+ s\left\{\left[\xi_n^2 + 2(n^2 - 1 - n\xi_n)\right]s^n - \xi_n(2n - 2 - \xi_n)s^{-n}\right\}\Psi_n \\
&+ \left[\xi_n(n^2 - 1 + \xi_n)s^{2+n} - (n^2 - 1 - \xi_n)(2 + \zeta_n)s^{-n}\right]\Theta_n \\
&+ (8/\pi k)(n^2 - 1 - n\xi_n) = 0 \ \ (n \neq 0) \qquad (4.4.55b)
\end{aligned}
$$

**Case 11:** Outer edge movable while inner edge clamped

$$\Phi_1 = 0 \ (n = 0) \qquad (4.4.56a)$$

$$
\begin{aligned}
(8/\pi k) &+ 2(1 - \nu)^{-1}ks^{-n}\Phi_n - (ks/n)\left[(1 - \xi_n)s^n - (1 + \xi_n)s^{-n}\right]\Phi_{1+n} \\
&+ s[2s^n - \xi_n(s^n + s^{-n})]\Psi_n - 2(1 + \xi_n)s^{-n}\Theta_n = 0 \ (n \neq 0) \qquad (4.4.56b)
\end{aligned}
$$

**Case 12:** Outer edge movable while inner edge simply supported

$$(1 - \nu)\Phi_1 - ks\Theta_0 = 0 \qquad\qquad (4.4.57a)$$

$$(8/\pi k) - (1 - \nu)^{-1}k\left\{(2 - \xi_n)s^{2+n} - (2 + \zeta_n)s^{-n}\right\}\Phi_n$$
$$- (ks/n)\left[(1 - \xi_n)s^n - (1 + \xi_n)s^{-n}\right]\Phi_{n+1} + s\left[(2 - \xi_n)s^n - \xi_n s^{-n}\right]\Psi_n$$
$$+ \left\{\zeta_n(1 - \xi_n)s^n - 2(1 + \zeta_n)(1 + \xi_n)s^{-n}\right\}\Theta_n = 0 \ (n \neq 0) \qquad (4.4.57b)$$

Critical buckling loads for the above twelve cases are presented in Table 4.4 for various values of ratio $s = b/a$, and the bracketed integers denote the values of $n$. In the calculations, a Poisson ratio of $\nu = 0.3$ was used.

**Table 4.4:** Critical buckling load parameter $k$ and corresponding number of nodal diameters $n$ (Yamaki, 1958).

| Case | $s = 0$ | $s = 0.1$ | $s = 0.3$ | $s = 0.5$ | $s = 0.7$ | $s = 0.9$ |
|------|---------|-----------|-----------|-----------|-----------|-----------|
| 1 | 5.135 (1) | 6.68 (2) | 8.63 (2) | 12.15 (4) | 20.27 (7) | 60.89 (24) |
| 2 | 5.135 (1) | 6.02 (1) | 7.06 (0) | 9.42 (0) | 15.31 (0) | 45.20 (0) |
| 3 | 3.832 (0) | 3.62 (0) | 3.19 (0) | 3.65 (0) | 5.52 (0) | 15.89 (0) |
| 4 | 3.832 (0) | 3.94 (0) | 4.71 (0) | 6.39 (0) | 10.49 (2) | 30.45 (12) |
| 5 | 3.625 (1) | 4.71 (1) | 6.16 (0) | 8.73 (0) | 14.73 (0) | 44.69 (0) |
| 6 | 3.625 (1) | 4.20 (1) | 4.75 (0) | 6.40 (0) | 10.52 (0) | 31.43 (0) |
| 7 | 2.049 (0) | 1.98 (0) | 1.61 (0) | 1.32 (0) | 1.14 (0) | 1.01 (0) |
| 8 | 2.049 (0) | 2.09 (0) | 2.40 (0) | 3.18 (0) | 5.19 (0) | 15.61 (0) |
| 9 | 0.0 (1) | 1.49 (1) | 2.18 (2) | 3.14 (1) | 5.19 (0) | 15.61 (0) |
| 10 | 0.0 (1) | 1.12 (1) | 1.34 (1) | 1.32 (0) | 1.14 (0) | 1.01 (0) |
| 11 | 1.675 (1) | 2.94 (1) | 3.84 (2) | 5.69 (3) | 9.79 (4) | 30.45 (12) |
| 12 | 1.675 (1) | 2.42 (1) | 2.87 (1) | 3.64 (1) | 5.52 (0) | 15.89 (0) |

This completes the discussion of buckling solutions of circular plates.

## 4.5 Buckling of Rectangular Plates
### 4.5.1 Preliminary Comments

Consider a rectangular plate subjected to uniaxial, uniform compressive load $\hat{N}_{xx}$ along the $x$-axis, applied in the middle plane of the plate. The linear load–deflection relationship holds until a certain value of the load $\hat{N}_{xx}$ is reached. At this load, called the *critical buckling load*, the stable state of the plate is disturbed and the plate seeks an alternative equilibrium configuration accompanied by a change in the load–deflection behavior. The magnitude of the buckling load depends, as will be shown shortly, on geometry (i.e., shape as well as boundary conditions) and material properties.

Here we present exact expressions and in some cases numerical results for critical buckling loads of rectangular plates under various boundary conditions and loads. The equation governing buckling deflection $w$ of a biaxially loaded plate (see Fig. 4.11) is given by

$$D_{11}\frac{\partial^4 w}{\partial x^4} + 2\hat{D}_{12}\frac{\partial^4 w}{\partial x^2 \partial y^2} + D_{22}\frac{\partial^4 w}{\partial y^4} + \hat{N}_{xx}\frac{\partial^2 w}{\partial x^2} + \hat{N}_{yy}\frac{\partial^2 w}{\partial y^2} = 0 \quad (4.5.1)$$

where $\hat{D}_{12} = D_{12} + 2D_{66}$, and

$$\hat{N}_{xx} = N_0, \quad \hat{N}_{yy} = \gamma N_0, \quad \gamma = \frac{\hat{N}_{yy}}{\hat{N}_{xx}} \quad (4.5.2)$$
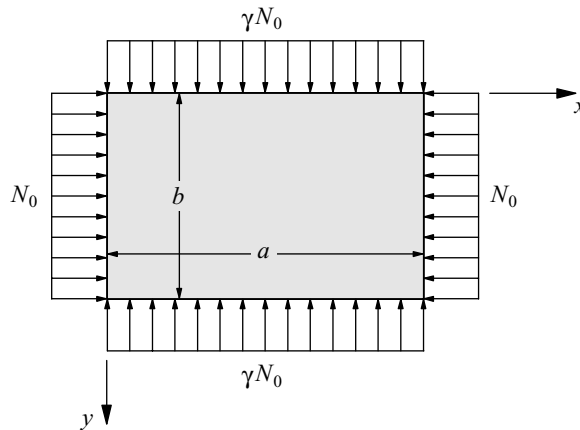


**Figure 4.11:** Biaxial compression of a rectangular plate ($\hat{N}_{xx} = N_0$ and $N_{yy}^0 = \gamma N_0$).

### 4.5.2 Simply Supported Biaxially Loaded Plates

For simply supported plates under biaxial compressive loads, the Navier solution approach can be used to obtain the exact buckling load and mode shape. The simply supported boundary conditions can be expressed as

$$w(0,y) = 0, \quad w(a,y) = 0, \quad w(x,0) = 0, \quad w(x,b) = 0 \qquad (4.5.3a)$$

$$M_{xx}(0,y) = 0, \quad M_{xx}(a,y) = 0, \quad M_{yy}(x,0) = 0, \quad M_{yy}(x,b) = 0 \quad (4.5.3b)$$

The Navier solution approach involves selecting an expansion for $w$ in the series form

$$w(x,y) = \sum_{m=1}^{\infty} \sum_{n=1}^{\infty} W_{mn} \phi_{mn}(x,y) \qquad (4.5.4)$$

where $W_{mn}$ are parameters (amplitudes) to be determined and $\phi_{mn}$ are functions (mode shapes) to be selected such that $w$ satisfies the boundary conditions. The choice

$$\phi_{mn}(x,y) = \sin \alpha_m x \ \sin \beta_n y, \quad \alpha_m = \frac{m\pi}{a} \ , \quad \beta_n = \frac{n\pi}{b} \qquad (4.5.5)$$

clearly satisfies the boundary conditions in Eqs. (4.5.3a, b) for any values of $W_{mn}$. Then the parameters $W_{mn}$ (and the buckling load $\hat{N}_0$) are determined such that $w(x,y)$ of Eq. (4.5.4) also satisfies the governing equation (4.5.1).

By substituting Eq. (4.5.4), with $\phi_{mn}$ given by Eq. (4.5.5), into Eq. (4.5.1), we obtain for any $m$ and $n$ the relation

$$0 = \left[ \left( D_{11}\alpha_m^4 + 2\hat{D}_{12}\alpha_m^2\beta_n^2 + D_{22}\beta_n^4 \right) - (\alpha_m^2 + \gamma\beta_n^2)N_0 \right]$$
$$\times W_{mn} \ \sin \alpha_m x \ \sin \beta_n y \qquad (4.5.6)$$

Since Eq. (4.5.6) must hold for every point $(x,y)$ of the domain for nonzero deflection $w(x,y)$ (i.e., $W_{mn} \neq 0$), the expression inside the square brackets should be zero for every $m$ and $n$. This yields

$$N_0(m,n) = \frac{\pi^2}{b^2} \left( \frac{D_{11}s^4 m^4 + 2\hat{D}_{12}s^2 m^2 n^2 + D_{22}n^4}{s^2 m^2 + \gamma n^2} \right) \qquad (4.5.7)$$

where $s = b/a$ is the plate aspect ratio. Thus, for each choice of $m$ and $n$ there is a unique value of $N_0$. The *critical buckling load* is the smallest of $N_0(m,n)$. For a given rectangular plate, this value is dictated by a particular combination of the values of $m$ and $n$, value of $\gamma$, plate dimensions, and material properties.

**Biaxially Compressed Plate**

For a square orthotropic plate subjected to the same magnitude of uniform compressive forces on both edges (i.e., biaxial compression with $\gamma = 1$), Eq. (4.5.7) yields

$$N_0(m, n) = \frac{\pi^2}{a^2} \left( \frac{m^4 D_{11} + 2m^2 n^2 \hat{D}_{12} + n^4 D_{22}}{m^2 + n^2} \right) \qquad (4.5.8)$$

Now suppose that $D_{11} > D_{22}$. Then $D_{11}m^2$ increases more rapidly than the decrease in $D_{22}/m^2$ with an increase in $m$. Thus, the minimum of $N_0$ occurs when $m = 1$:

$$N_0(1, n) = \left( \frac{\pi^2}{a^2} \right) \left( \frac{D_{11} + 2\hat{D}_{12} n^2 + D_{22} n^4}{1 + n^2} \right). \qquad (4.5.9)$$

The buckling load is a minimum when $n$ is the nearest positive integer to the real number $R$

$$R^2 = -1 + \left( 1 + \frac{D_{11} - 2\hat{D}_{12}}{D_{22}} \right)^{\frac{1}{2}} \qquad (4.5.10)$$

For example, for modulus ratios of $D_{11}/D_{22} = 10$ and $\hat{D}_{12}/D_{22} = 1$, the minimum buckling load occurs at $n = 1$ (because $R = \sqrt{2}$) and it is given by

$$N_{cr} \equiv N_0(1, 1) = 6.5 \left( \frac{\pi^2 D_{22}}{a^2} \right) \qquad (4.5.11)$$

For modulus ratios of $D_{11}/D_{22} = 12$ and $\hat{D}_{12}/D_{22} = 1$, the value of $R$ is 1.52. Hence, the minimum buckling load occurs for $n = 2$

$$N_{cr} = 7.2 \left( \frac{\pi^2 D_{22}}{a^2} \right) \qquad (4.5.12a)$$

and the mode shape is given by

$$W_{12} = \sin \frac{\pi x}{a} \sin \frac{2\pi y}{a} \qquad (4.5.12b)$$

For an isotropic rectangular plate $[D_{11} = D_{22} = D, \; D_{12} = \nu D, \; 2D_{66} = (1 - \nu)D \text{ or } \hat{D}_{12} = D]$ under biaxial compression, the buckling load can be calculated using Eq. (4.5.7):

$$N_0(m, n) = \frac{\pi^2 D}{b^2} \left( m^2 s^2 + n^2 \right), \quad s = \frac{b}{a} \qquad (4.5.13)$$

Clearly, the critical buckling load for this case occurs at $m = n = 1$ and it is equal to

$$N_{cr} = (1 + s^2)\frac{\pi^2 D}{b^2}, \quad s = \frac{b}{a} \tag{4.5.14}$$

and for a square plate it reduces to

$$N_{cr} = \frac{2\pi^2 D}{b^2} \tag{4.5.15}$$

## Biaxially Loaded Plate

When the edges $x = 0, a$ of a square plate are subjected to a compressive load $\hat{N}_{xx} = N_0$ and the edges $y = 0, b$ are subjected to a tensile load $\hat{N}_{yy} = -\gamma N_0$ (see Fig. 4.12), Eq. (4.5.7) becomes

$$N_0(m, n) = \frac{\pi^2}{a^2} \left( \frac{m^4 D_{11} + 2m^2 n^2 \hat{D}_{12} + n^4 D_{22}}{m^2 - \gamma n^2} \right) \tag{4.5.16}$$

when $\gamma n^2 < m^2$. For example, when $\gamma = 0.5$, the minimum buckling load occurs at $m = 1$ and $n = 1$:

$$N_0(1, 1) = \frac{2\pi^2}{a^2} \left( D_{11} + 2\hat{D}_{12} + D_{22} \right) \tag{4.5.17}$$

For a rectangular isotropic plate, the buckling load under biaxial loading ($N_{xx} = N_0$ and $N_{yy} = -\gamma N_0$) becomes

$$N_0(m, n) = \left( \frac{\pi^2 D}{b^2} \right) \frac{(m^2 s^2 + n^2)^2}{m^2 s^2 - \gamma n^2} \tag{4.5.18}$$

and the minimum buckling load occurs for $n = 1$

$$N_0(m, 1) = \left( \frac{\pi^2 D}{b^2} \right) \frac{(m^2 s^2 + 1)^2}{m^2 s^2 - \gamma} \tag{4.5.19}$$

In theory, the minimum of $N_0(m, 1)$ occurs when $m^2 s^2 = 1 + 2\gamma$. For a square isotropic plate with $\gamma = 0.5$, we find

$$N_0(1, 1) = \frac{8\pi^2 D}{a^2}, \quad N_0(2, 1) = 7.1429\frac{\pi^2 D}{a^2} = N_{cr} \tag{4.5.20}$$
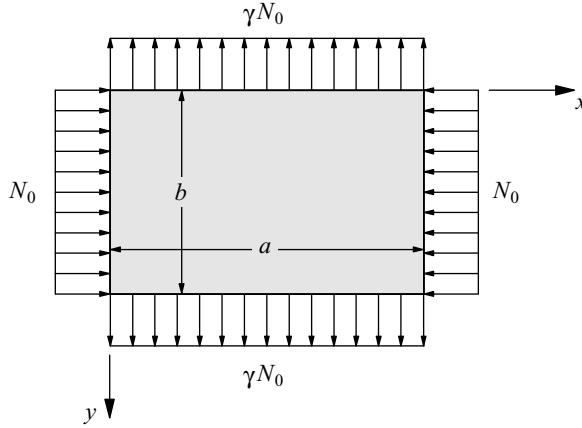
**Figure 4.12:** Plate subjected to uniform compression along $x$ ($\hat{N}_{xx} = N_0$) and uniform tension along $y$ ($\hat{N}_{yy} = -\gamma N_0$).

## Uniaxially Compressed Plate

When a rectangular plate is subjected to a uniform compressive load $N_0$ on edges $x = 0$ and $x = a$ (i.e., when $\gamma = 0$), the buckling load can be calculated using Eq. (4.5.7)

$$N_0(m, n) = \frac{\pi^2}{m^2 s^2 b^2} \left( m^4 s^4 D_{11} + 2 s^2 m^2 n^2 \hat{D}_{12} + n^4 D_{22} \right) \qquad (4.5.21)$$

The smallest value of $N_0$ for any $m$ occurs for $n = 1$:

$$N_0(m, 1) = \frac{\pi^2 D_{22}}{b^2} \left( m^2 s^2 \frac{D_{11}}{D_{22}} + 2 \frac{\hat{D}_{12}}{D_{22}} + \frac{1}{m^2 s^2} \right) \qquad (4.5.22)$$

Thus, the plate buckles in such a way that there can be several ($m \geq 1$) half-waves in the direction of compression but only one ($n = 1$) half-wave in the perpendicular direction. The critical buckling load is then determined by finding the minimum of $N_0 = N_0(m)$ in Eq. (4.5.22) with respect to $m$. We have

$$\frac{dN_0}{dm} = 0 \quad \text{gives} \quad m_c^4 = \frac{1}{s^4} \frac{D_{22}}{D_{11}} \qquad (4.5.23)$$

The second derivative of $N_0$ with respect to $m$ can be shown to be positive. Since the value of $m$ from Eq. (4.5.23) is not always an integer,

the minimum buckling load cannot be predicted by substituting the value of $m_c$ from Eq. (4.5.23) for $m$ into Eq. (4.5.22). The minimum value of $N_0$ is given by Eq. (4.5.22) when $m_c$ is the nearest integer value given by Eq. (4.5.23). Since the value of $m_c$ depends on the ratio of the principal bending stiffnesses $D_{11}$ and $D_{22}$ as well as plate aspect ratio $s = b/a$, one must investigate the variation of $N_0$ with aspect ratio $s$ for different values of $m_c$ for a given rectangular plate.

For an isotropic plate, Eqs. (4.5.21) and (4.5.22) reduce to

$$N_0(m,n) = \frac{\pi^2 a^2 D}{m^2} \left( \frac{m^2}{a^2} + \frac{n^2}{b^2} \right)^2 \tag{4.5.24}$$

$$N_0(m,1) = \frac{\pi^2 D}{a^2} \left( m + \frac{1}{m} \frac{a^2}{b^2} \right)^2 \tag{4.5.25}$$

For a given aspect ratio, two different modes, $m_1$ and $m_2$, will have the same buckling load when $\sqrt{m_1 m_2} = a/b$. In particular, the point of intersection of curves $m$ and $m+1$ occurs for aspect ratios

$$\frac{a}{b} = \sqrt{2}, \ \sqrt{6}, \ \sqrt{12}, \ \sqrt{20}, \ \cdots, \ \sqrt{m^2 + m}$$

Thus, there is a mode change at these aspect ratios from $m$ half-waves to $m+1$ half-waves. Putting $m = 1$ in Eq. (4.5.25), we find

$$N_{cr} = \frac{\pi^2 D}{b^2} \left( \frac{a}{b} + \frac{b}{a} \right)^2 \tag{4.5.26}$$

For a square plate, Eq. (4.5.26) yields

$$N_{cr} = \frac{4\pi^2 D}{b^2} \tag{4.5.27}$$

Table 4.5 contains exact values of the critical buckling load $\bar{N} = N_{cr} b^2/(\pi^2 D_{22})$ of rectangular plates for various load cases ($\gamma = 0$ and $\gamma = 1$), aspect ratios and modulus ratios (orthotropic plates). In all cases, the critical buckling mode is $(m,n) = (1,1)$, except as indicated. The effect of aspect ratio and mode on critical buckling loads of simply supported isotropic plates is shown in Fig. 4.13.

**Table 4.5:** Effect of plate aspect ratio $a/b$ and modulus ratio $E_1/E_2$ on buckling load $\bar{N} = N_{cr}b^2/(\pi^2 D_{22})$ of simply supported rectangular plates under uniform axial compression ($\gamma = 0$) and biaxial compression ($\gamma = 1$).

| $\gamma$ | $\frac{a}{b}$ | $\frac{E_1}{E_2} = 1$ | $\frac{E_1}{E_2} = 3$ | $\frac{E_1}{E_2} = 10$ | $\frac{E_1}{E_2} = 25$ |
|---|---|---|---|---|---|
| 0 | 0.5 | 6.250 | 14.708 | 42.737 | 102.750 |
|   | 1.0 | 4.000 | 6.458 | 13.488 | 28.495 |
|   | 1.5 | $4.340^{(2,1)\dagger}$ | 6.042 | 9.182 | 15.856 |
|   | 2.0 | $4.000^{(2,1)}$ | $6.458^{(2,1)}$ | 8.987 | 12.745 |
|   | 2.5 | $4.134^{(3,1)}$ | $5.941^{(2,1)}$ | 10.338 | 12.745 |
|   | 3.0 | $4.000^{(3,1)}$ | $6.042^{(2,1)}$ | $9.182^{(2,1)}$ | 14.273 |
| 1 | 0.5 | 5.000 | 11.767 | $25.427^{(1,3)}$ | $40.784^{(1,4)}$ |
|   | 1.0 | 2.000 | 3.229 | 6.744 | $10.196^{(1,2)}$ |
|   | 1.5 | 1.444 | 1.859 | 2.825 | 4.879 |
|   | 2.0 | 1.250 | 1.442 | 1.798 | 2.549 |
|   | 2.5 | 1.160 | 1.267 | 1.426 | 1.758 |
|   | 3.0 | 1.111 | 1.179 | 1.260 | 1.427 |

$\dagger$ Denotes mode numbers $(m, n)$ at which the critical buckling load occurred; $(m, n) = (1, 1)$ for all other cases.
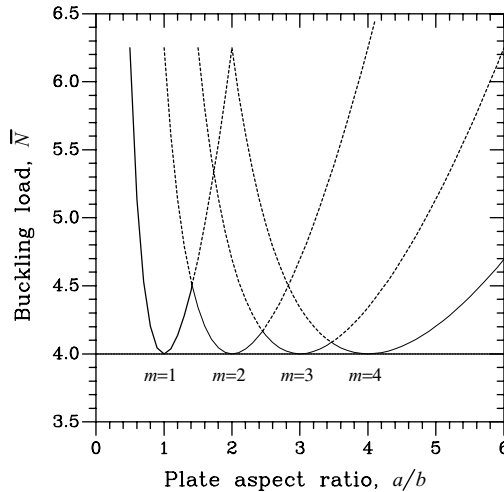


**Figure 4.13:** Nondimensionalized buckling load, $\bar{N} = N_0 b^2/(\pi^2 D)$, versus plate aspect ratio $a/b$ for isotropic SSSS plates.

### 4.5.3 Plates Simply Supported along Two Opposite Sides and Compressed in the Direction Perpendicular to These Sides

Analytical solutions for the buckling loads of uniformly compressed rectangular plates, simply supported along two opposite edges perpendicular to the direction of compression (see Fig. 4.14) and having various edge conditions along the other two sides, may be obtained using the Lévy method of solution. The Lévy method is similar to Navier's method in that we select $\phi_{mn}$ to satisfy the boundary conditions along two of the simply supported edges, $x = 0, a$, thereby reducing the governing partial differential equation (4.5.1) to an ordinary differential equation in $y$. The differential equation in one dimension may then be solved analytically or numerically.
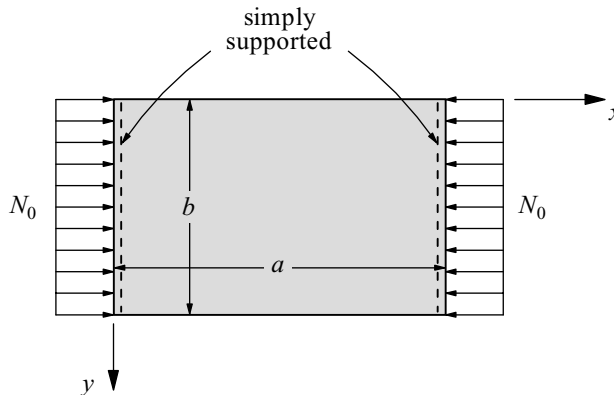


**Figure 4.14:** Rectangular plates, uniformly compressed along $x =$ constant, simply supported along two opposite sides ($x = 0, a$) perpendicular to the direction of compression, and having various boundary conditions along the other two sides ($y = 0, b$).

Here we consider the analytical solution of the one-dimensional problem for isotropic plates. For the case of uniform compression along the $x$-axis, we have $\hat{N}_{xx} = N_0$ and $\hat{N}_{yy} = 0$, and Eq. (4.5.1) reduces to

$$D\left(\frac{\partial^4 w}{\partial x^4} + 2\frac{\partial^4 w}{\partial x^2 \partial y^2} + \frac{\partial^4 w}{\partial y^4}\right) + N_0\frac{\partial^2 w}{\partial x^2} = 0 \qquad (4.5.28)$$

This equation must be solved for the buckling load $N_0$ and mode shape $w$ for any given boundary conditions.

Assuming solution of Eq. (4.5.28) in the form

$$w(x, y) = \sum_{m=1}^{\infty} W_m(y) \, \sin \frac{m\pi x}{a} \qquad (4.5.29)$$

That is, under the action of compressive forces, the plate buckles into $m$ sinusoidal half-waves. The function $W_m(y)$, which is to be determined, represents the buckling shape along the $y$-axis. The assumed solution satisfies the boundary conditions along the simply supported edges $x = 0, a$ of the plate:

$$w = 0, \quad M_{xx} \equiv -D \left( \frac{\partial^2 w}{\partial x^2} + \nu \frac{\partial^2 w}{\partial y^2} \right) = 0 \ \ \text{at } x = 0, a \qquad (4.5.30)$$

By substituting Eq. (4.5.29) into Eq. (4.5.28), we obtain

$$\left( \alpha_m^4 - \frac{N_0}{D} \alpha_m^2 \right) W_m - 2\alpha_m^2 \frac{d^2 W_m}{dy^2} + \frac{d^4 W_m}{dy^4} = 0 \qquad (4.5.31)$$

The form of the solution to Eq. (4.5.31) depends on the nature of the roots $\lambda$ of the equation

$$\lambda^4 - 2\alpha_m^2 \lambda^2 + \left( \alpha_m^4 - \alpha_m^2 \frac{N_0}{D} \right) = 0 \qquad (4.5.32)$$

Owing to the geometric constraints on the edges $y = 0, b$, the buckling load $N_0$ is such that

$$N_0 > D\alpha_m^2 \qquad (4.5.33)$$

Hence, the solution to Eq. (4.5.32) is of the form

$$W(y) = C_1 \cosh \lambda_1 y + C_2 \sinh \lambda_1 y + C_3 \cos \lambda_2 y + C_4 \sin \lambda_2 y \qquad (4.5.34)$$

where

$$(\lambda_1)^2 = \sqrt{\alpha_m^2 \frac{N_0}{D} + \alpha_m^2}, \quad (\lambda_2)^2 = \sqrt{\alpha_m^2 \frac{N_0}{D} - \alpha_m^2} \qquad (4.5.35)$$

We shall consider various cases of boundary conditions next.

A four-letter notation is used to identify rectangular plates with various edge conditions. Since in the present discussion edges $x = 0, a$ are always simply supported, the first two letters will always be SS. The remaining two letters refer to the boundary conditions on edges $y = 0$ and $y = b$. The label SSSF, for example, denotes a rectangular plate whose edges $x = 0, a$ are simply supported (S), edge $y = 0$ is simply supported, and edge $y = b$ is free (F).

**Buckling of SSSF Plates**

Consider buckling of uniformly compressed rectangular plates with side $y = 0$ simply supported (S) and side $y = b$ free (F), as shown in Fig. 4.15. The boundary conditions on the simply supported and free edges are

$$w = 0, \quad M_{yy} = -D \left( \nu \frac{\partial^2 w}{\partial x^2} + \frac{\partial^2 w}{\partial y^2} \right) = 0 \ \text{ at } \ y = 0 \qquad (4.5.36)$$

$$M_{yy} = 0, \quad V_y = -D \left[ \frac{\partial^3 w}{\partial y^3} + (2 - \nu) \frac{\partial^3 w}{\partial x^2 \partial y} \right] = 0 \ \text{ at } \ y = b \quad (4.5.37)$$

Using the boundary conditions (4.5.36), we obtain $C_1 = C_3 = 0$. Boundary conditions (4.5.37) yield the following two linear relations among $C_2$ and $C_4$:
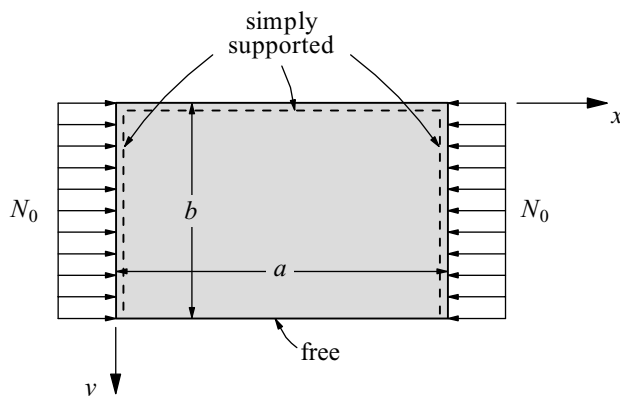


**Figure 4.15:** Uniformly compressed rectangular plate simply supported along two opposite sides $(x = 0, a)$ perpendicular to the direction of compression, and simply supported on side $y = 0$ and free on side $y = b$ (SSSF).

$$\left(\nu\alpha_m^2 - \lambda_1^2\right)C_2 \sinh\lambda_1 b + \left(\nu\alpha_m^2 + \lambda_2^2\right)C_4 \sin\lambda_2 b = 0$$

$$\lambda_1\left[(2-\nu)\alpha_m^2 - \lambda_1^2\right]C_2 \cosh\lambda_1 b + \lambda_2\left[(2-\nu)\alpha_m^2 + \lambda_2^2\right]C_4 \cos\lambda_2 b = 0$$

$$(4.5.38)$$

For the nontrivial solution (i.e., not both $C_2 \neq 0$ and $C_4 \neq 0$ are zero), we require that the determinant of the two linear equations in (4.5.38) be zero:

$$\lambda_2\Omega_1^2 \sinh\lambda_1 b \ \cos\lambda_2 b - \lambda_1\Omega_2^2 \cosh\lambda_1 b \ \sin\lambda_2 b = 0 \qquad (4.5.39)$$

where $\Omega_1$ and $\Omega_2$ are defined by

$$\Omega_1 = \left(\lambda_1^2 - \nu\alpha_m^2\right), \quad \Omega_2 = \left(\lambda_2^2 + \nu\alpha_m^2\right) \qquad (4.5.40)$$

Since $\lambda_1$ and $\lambda_2$ contain $N_0$ [see Eq. (4.5.35)], Eq. (4.5.39) can be solved, using an iterative scheme, for the smallest $N_0$, denoted $N_{cr}$, once the geometric and material parameters of the plate are known. The critical buckling load may be written as

$$N_{cr} = \kappa \frac{\pi^2 D}{b^2} \qquad (4.5.41)$$

where $\kappa$ is a numerical factor depending on the plate aspect ratio $b/a$ and material properties. The general mode shape is given by

$$w(x,y) = (\Omega_1 \sinh\lambda_1 b \sin\lambda_2 y + \Omega_2 \sinh\lambda_1 y \sin\lambda_2 b) \sin\alpha_m x \qquad (4.5.42)$$

Table 4.6 contains buckling loads of isotropic ($\nu = 0.25$) plates (SSSF) for various values of $a/b$ and modes $m = 1, 2$. The critical buckling load occurs in mode $m = 1$ with aspect ratio $0 < a/b \leq 6$. The mode shape associated with the critical buckling load is

$$w(x,y) = (\Omega_1 \sinh\lambda_1 b \sin\lambda_2 y + \Omega_2 \sinh\lambda_1 y \sin\lambda_2 b) \ \sin\frac{\pi x}{a}$$

**Table 4.6:** Effect of plate aspect ratio on the nondimensionalized buckling loads $\bar{N} = N_0 b^2/(\pi^2 D)$ of rectangular plates (SSSF) under uniform compression $\hat{N}_{xx} = -N_0$.

| $\frac{a}{b}$ | $m = 1$ | $m = 2$ | $\frac{a}{b}$ | $m = 1$ | $m = 2$ |
|------|--------|---------|------|--------|--------|
| 0.4  | 6.6367 | 25.2899 | 3.0  | 0.5630 | 0.8879 |
| 0.6  | 3.1921 | 11.4675 | 3.5  | 0.5345 | 0.7726 |
| 0.8  | 1.9894 | 6.3667  | 4.0  | 0.5161 | 0.6979 |
| 1.0  | 1.4342 | 4.4036  | 4.5  | 0.5034 | 0.6469 |
| 1.5  | 0.8880 | 2.2022  | 5.0  | 0.4944 | 0.6104 |
| 2.0  | 0.6979 | 1.4342  | 5.5  | 0.4877 | 0.5835 |
| 2.5  | 0.6104 | 1.0798  | 6.0  | 0.4826 | 0.5630 |

### Buckling of SSCF Plates

Here we consider buckling of uniformly compressed rectangular plates with side $y = 0$ clamped and side $y = b$ free (see Fig. 4.16). The boundary conditions are

$$w = 0, \quad \frac{\partial w}{\partial y} = 0 \ \text{ at } \ y = 0 \tag{4.5.43a}$$

$$M_{yy} = 0, \quad V_y = -D\left[\frac{\partial^3 w}{\partial y^3} + (2 - \nu)\frac{\partial^3 w}{\partial x^2 \partial y}\right] = 0 \ \text{ at } \ y = b \tag{4.5.43b}$$
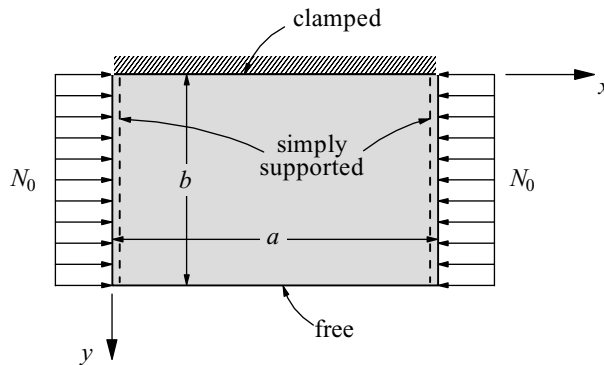


**Figure 4.16:** Uniformly compressed rectangular plate which is simply supported along two opposite sides $(x = 0, a)$, clamped on side $y = 0$, and free on side $y = b$.

which give $C_3 = -C_1$, $C_4 = -(\lambda_1/\lambda_2)C_2$, and

$$-\Omega_1 \left(C_1 \cosh \lambda_1 b + C_2 \sinh \lambda_1 b\right) + \Omega_2 \left(C_3 \cos \lambda_2 b + C_4 \sin \lambda_2 b\right) = 0$$
$$-\lambda_1 \Omega_1 \left(C_1 \sinh \lambda_1 b + C_2 \cosh \lambda_1 b\right) + \lambda_2 \Omega_2 \left(-C_3 \sin \lambda_2 b + C_4 \cos \lambda_2 b\right) = 0$$
$$(4.5.44)$$

Setting the determinant of these equations to zero, and after substituting for $C_3 = -C_1$ and $C_4 = -(\lambda_1/\lambda_2)C_2$, we obtain

$$2\Omega_1\Omega_2 + \left(\Omega_1^2 + \Omega_2^2\right) \cosh \lambda_1 b \, \cos \lambda_2 b$$
$$- \frac{1}{\lambda_1 \lambda_2} \left(\lambda_1^2 \Omega_2^2 - \lambda_2^2 \Omega_1^2\right) \sinh \lambda_1 b \, \sin \lambda_2 b = 0 \quad (4.5.45)$$

where $\Omega_1$ and $\Omega_2$ are defined in Eq. (4.5.40).

Nondimensional critical buckling loads $\bar{N} = N_0 b^2/(\pi^2 D)$ of SSCF plates are presented in Table 4.7 for isotropic ($\nu = 0.25$) plates for various aspect ratios. Fig. 4.17 contains plots of nondimensional buckling load versus plate aspect ratio for modes $m = 1, 2, 3$ of isotropic plates. It is seen that at the beginning, the buckling load of an isotropic plate decreases with an increase in the aspect ratio $a/b$. The minimum value of the buckling load $\bar{N}_{cr} = 1.329$ occurs at $a/b = 1.635$. There is a mode change at $a/b = 2.3149$ from $m = 1$ and $m = 2$, and the buckling load for this aspect ratio is $\bar{N}_{cr} = 1.503$. The minimum buckling load ($\bar{N}_{cr} = 1.329$) for mode $m = 2$ occurs at $a/b = 3.27$. For comparatively long isotropic plates, the critical buckling load can be taken with sufficient accuracy as $\bar{N}_{cr} = 1.329$.

**Table 4.7:** Nondimensionalized buckling loads $\bar{N}$ of SSCF rectangular plates under uniform axial compression $\hat{N}_{xx} = N_0$.

| $\frac{a}{b}$ | $\bar{N}$ | $\frac{a}{b}$ | $\bar{N}$ | $\frac{a}{b}$ | $\bar{N}$ | $\frac{a}{b}$ | $\bar{N}$ |
|---|---|---|---|---|---|---|---|
| 0.5 | 4.518 | 2.0 | 1.386 | 3.5 | 1.336 | 5.0 | 1.329 |
| 1.0 | 1.698 | 2.5 | 1.432† | 4.0 | 1.386 | 5.5 | 1.347 |
| 1.5 | 1.339 | 3.0 | 1.339 | 4.5 | 1.339† | 6.0 | 1.339† |

† Denotes change to next higher mode.
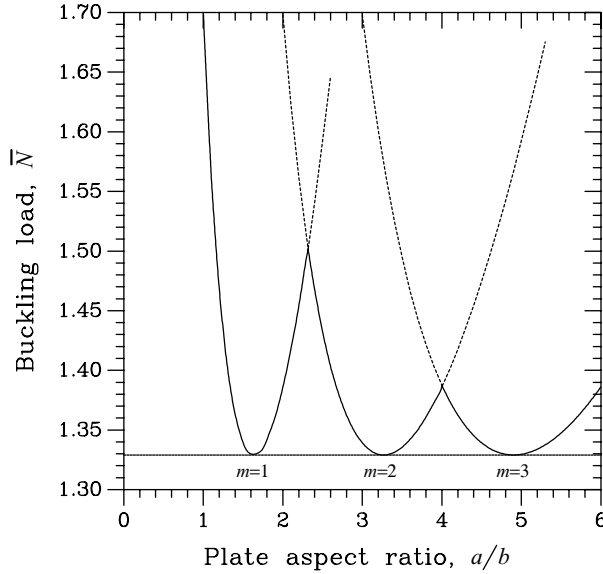
**Figure 4.17:** Nondimensionalized buckling load, $\bar{N} = N_0 b^2 / (\pi^2 D)$, versus plate aspect ratio $a/b$ for isotropic SSCF plates.

## Buckling of SSCC Plates

Here we consider buckling of uniformly compressed rectangular plates with sides $y = 0, b$ clamped (see Fig. 4.18). The boundary conditions are

$$w = 0, \quad \frac{\partial w}{\partial y} = 0 \ \text{ at } \ y = 0, b \tag{4.5.46}$$

The boundary conditions yield $C_3 = C_4 = 0$, and

$$C_1 \left(\cosh \lambda_1 b - \cos \lambda_2 b\right) + C_2 \left(\sinh \lambda_1 b - \frac{\lambda_1}{\lambda_2} \sin \lambda_2 b\right) = 0,$$
$$C_1 \left(\lambda_1 \sinh \lambda_1 b + \lambda_2 \sin \lambda_2 b\right) + C_2 \lambda_1 \left(\cosh \lambda_1 b - \cos \lambda_2 b\right) = 0 \tag{4.5.47}$$

The determinant of these equations is

$$2 \left(1 - \cosh \lambda_1 b \ \cos \lambda_2 b\right) + \left(\frac{\lambda_1}{\lambda_2} - \frac{\lambda_2}{\lambda_1}\right) \sinh \lambda_1 b \ \sin \lambda_2 b = 0 \tag{4.5.48}$$
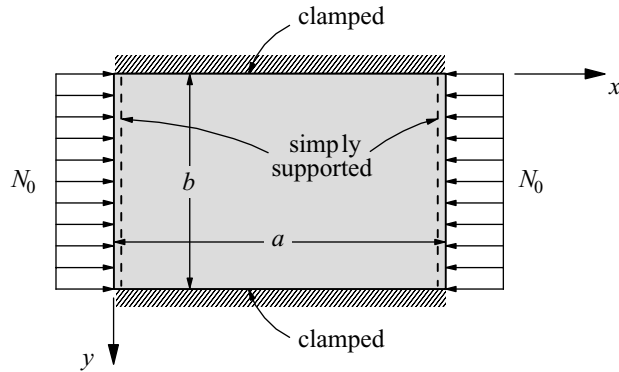
**Figure 4.18:** Uniformly compressed SSCC rectangular plate.

Nondimensional critical buckling loads $\bar{N}_{cr} = N_{cr}b^2/(\pi^2 D)$ of SSCC plates are presented in Table 4.8 for isotropic ($\nu = 0.25$) plates for various aspect ratios. Figure 4.19 contains plots of buckling load versus plate aspect ratio for modes $m = 1, 2, 3$ of isotropic plates. The minimum value of the buckling load $\bar{N}_{cr} = 0.697$ occurs at $a/b = 0.661$. There is a mode change at $a/b = 0.9349$ from $m = 1$ to $m = 2$, and the buckling load for this aspect ratio is $\bar{N}_{cr} = 8.097$. The minimum buckling load ($\bar{N}_{cr} = 0.697$) for mode $m = 2$ occurs at $a/b = 1.322$.

**Table 4.8:** Buckling loads $\bar{N}_{cr}$ of SSCC rectangular plates under uniform axial compression $\hat{N}_{xx} = -N_0$.

| $\frac{a}{b}$ | $\bar{N}$ | $\frac{a}{b}$ | $\bar{N}$ | $\frac{a}{b}$ | $\bar{N}$ |
|------|--------|------|----------------|------|----------|
| 0.4 | 9.448 | 1.0 | 7.691[†] | 1.6 | 7.304 |
| 0.6 | 7.055 | 1.2 | 7.055 | 1.8 | 7.055† |
| 0.8 | 7.304 | 1.4 | 7.001 | 2.0 | 6.972 |

[†] Denotes change to next higher mode.
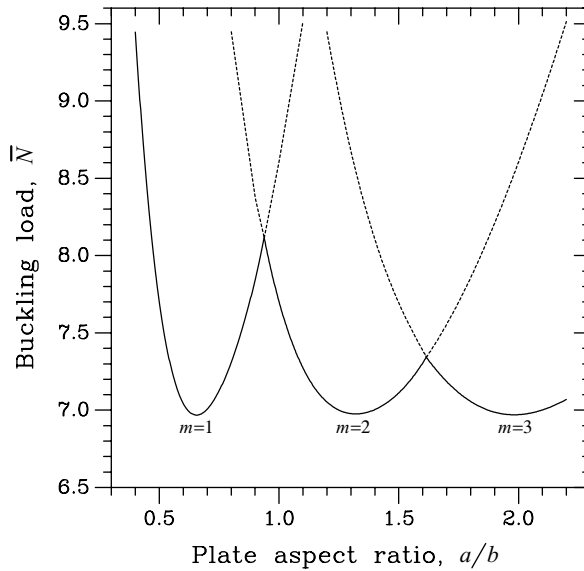
**Figure 4.19:** Nondimensionalized buckling load, $\bar{N} = N_0 b^2 / (\pi^2 D)$, versus plate aspect ratio $a/b$ for isotropic SSCC plates.

### 4.5.4 Plates with Abrupt Changes in Geometry or Material Properties

Consider an elastic, rectangular thin plate of length $a$ and width $b$. The origin of the coordinate system is set at the center of the lower plate edge as shown in Fig. 4.20. The plate is simply supported along two opposite edges that are parallel to the $x$-axis, i.e., edges AD and BC. The other two edges AB and CD may have any combination of free, simply supported and clamped edge conditions. The plate has abrupt changes along $(n-1)$th lines that are perpendicular to the simply supported edges. These abrupt changes could be due to a change in plate thickness, presence of an internal line hinge, a change in shear force due to an internal line support, a change in material properties, or the presence of an intermediate uniaxial load.

Harik and Andrade (1989), Xiang et al. (1996), and Liew et al. (1996) developed an analytical approach for determining the exact buckling solutions for such rectangular plates with abrupt changes. The approach involves

- the Lévy solution technique to convert the partial differential equation into a fourth-order ordinary differential equation,
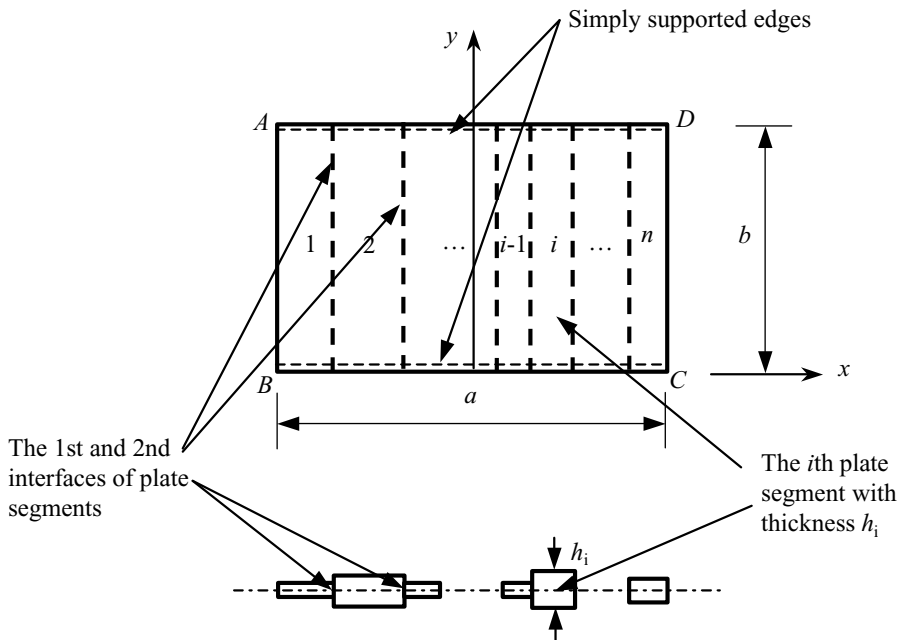
**Figure 4.20:** Geometry and coordinates system for a multisegment rectangular plate.

- the domain decomposition technique to handle the different properties in the plate segments bounded by the simply supported edges and the boundaries of the abrupt changes, and finally
- the state space technique to convert the fourth-order differential equation that governs each segment problem into a set of first-order differential equations which can then be solved in a straightforward manner.

The approach will be briefly described below and sample exact buckling solutions for rectangular plates with various kinds of abrupt changes are presented. Based on the classical thin plate theory, the governing partial differential equation for the elastic buckling of the $i$th region of the plate when the plate is subjected to an in-plane compressive stress resultant $\bar{N}_i = (\sigma_x)_i h_i$ per unit length in the $x$-direction is given by

$$D_i \left( \frac{\partial^4 w_i}{\partial x^4} + 2 \frac{\partial^4 w_i}{\partial x^2 \partial y^2} + \frac{\partial^4 w_i}{\partial y^4} \right) + \bar{N}_i \frac{\partial^2 w_i}{\partial x^2} = 0, \quad i = 1, 2, \cdots, n \quad (4.5.49)$$

in which $w_i(x,y)$ is the transverse displacement in the $i$th region of the plate, $x$ and $y$ are the rectangular Cartesian coordinates, $D_i =$

$E_i h_i^3/[12(1 - \nu_i^2)]$ is the flexural rigidity, $h_i$ is the thickness, and $E_i$ and $\nu_i$ are the elastic modulus and the Poisson ratio.

The essential and natural boundary conditions for the two simply supported edges at $y = 0$ and $y = b$ associated with the $i$th plate segment are

$$w_i = 0 \quad \text{and} \quad (M_y)_i \equiv D_i \left( \frac{\partial^2 w_i}{\partial y^2} + \nu_i \frac{\partial^2 w_i}{\partial x^2} \right) = 0 \qquad (4.5.50)$$

where $(M_y)_i$ is the bending moment. As for the other two edges at $x = -a/2$ and $x = a/2$ (see Fig. 4.20), the boundary conditions are

$$w_i = 0 \quad \text{and} \quad (M_x)_i \equiv D_i \left( \frac{\partial^2 w_i}{\partial x^2} + \nu_i \frac{\partial^2 w_i}{\partial y^2} \right) = 0 \qquad (4.5.51)$$

if the edge is simply supported $(S)$,

$$w_i = 0 \quad \text{and} \quad \frac{\partial w_i}{\partial x} = 0 \qquad (4.5.52)$$

if the edge is clamped $(C)$, and

$$(M_x)_i \equiv D_i \left( \frac{\partial^2 w_i}{\partial x^2} + \nu_i \frac{\partial^2 w_i}{\partial y^2} \right) = 0$$

$$(V_x)_i \equiv D_i \left[ \frac{\partial^3 w_i}{\partial x^3} + (2 - \nu_i) \frac{\partial^3 w_i}{\partial x \partial y^2} \right] + \bar{N}_i \frac{\partial w_i}{\partial x} = 0 \quad (4.5.53)$$

if the edge is free $(F)$. The subscript $i$ takes the value of either 1 or $n$ and $V_x$ is the effective shear force.

Adopting the Lévy technique, the displacement function for the $i$th segment of the plate can be expressed as

$$w_i(x, y) = X_i(x) \sin \frac{m\pi y}{b}, \quad i = 1, 2, \cdots, n \qquad (4.5.54)$$

where $m$ is the number of half-waves of the buckling mode in the $y$-direction and $X_i(x)$ is an unknown function to be determined. Equation (4.5.54) satisfies the boundary conditions given by Eqs. (4.5.50).

Using the state–space technique, a homogenous differential equation system for the $i$th plate segment can be derived, in view of Eqs. (4.5.49) and (4.5.54), as

$$\boldsymbol{\Psi}_i' - \mathbf{H}_i \boldsymbol{\Psi}_i = \mathbf{0}, \quad i = 1, 2, \cdots, n \qquad (4.5.55)$$

in which $\boldsymbol{\Psi}_i = \{X_i \; X_i' \; X_i'' \; X_i'''\}^{\mathrm{T}}$ and the prime denotes differentiation with respect to $x$, $\boldsymbol{\Psi}_i'$ is the first derivative of $\boldsymbol{\Psi}_i$, and $\mathbf{H}_i$ is a $4 \times 4$ matrix. The nonzero elements of $\mathbf{H}_i$ are

$$(H_{12})_i = (H_{23})_i = (H_{34})_i = 1, \quad (H_{41})_i = -\left(\frac{m\pi}{b}\right)^4$$

$$(H_{43})_i = 2\left(\frac{m\pi}{b}\right)^2 - \frac{\bar{N}_i}{D_i}$$

(4.5.56)

The solution for Eq. (4.5.55) may be expressed as

$$\boldsymbol{\Psi}_i = \mathbf{e}^{\mathbf{H}_i x}\mathbf{c}_i = \mathbf{F}_i(x)\mathbf{F}_i^{-1}(0)\mathbf{c}_i \tag{4.5.57}$$

in which $\mathbf{e}^{\mathbf{H}_i x}$ is a general matrix solution for Eq. (4.5.55) and $\mathbf{c}_i$ is a $(4 \times 1)$ constant column matrix that is to be determined using the plate boundary conditions and interface conditions between the adjacent plate segments. The function $\mathbf{F}_i(x)$ in Eq. (4.5.57) is related to the eigenvalues and eigenvectors of $\mathbf{H}_i$ (see Braun, 1993). For example, if all eigenvalues of $\mathbf{H}_i$ are real and distinct, then $\mathbf{F}_i(x) = [\mathbf{f}_1(x) \; \mathbf{f}_2(x) \; \mathbf{f}_3(x) \; \mathbf{f}_4(x)]$ where $\mathbf{f}_j(x) = e^{\lambda_j x}\mathbf{v}_j$, $\lambda_j$ is the $j$th eigenvalue and $\mathbf{v}_j$ is the $j$th eigenvector. If the eigenvalues of $\mathbf{H}_i$ include complex values or repeated roots, the readers are referred to Braun (1993) and Xiang et al. (1996) for determining $\mathbf{F}_i(x)$ in Eq. (4.5.57).

Along the interface between the $i$th segment and the $(i+1)$th segment of the plate, the following continuity conditions must be satisfied.

*For plates with abrupt changes in plate thickness, material properties and intermediate uniaxial load:*

$$w_i = w_{i+1}, \quad \frac{\partial w_i}{\partial x} = \frac{\partial w_{i+1}}{\partial x} = 0, \quad (V_x)_i + \bar{N}_i\frac{\partial w_i}{\partial x} = (V_x)_{i+1} + \bar{N}_{i+1}\frac{\partial w_{i+1}}{\partial x}$$

(4.5.58)

*For plates with abrupt changes in shear force due to the presence of an internal line support:*

$$w_i = 0, \quad w_{i+1} = 0, \quad \frac{\partial w_i}{\partial x} = \frac{\partial w_{i+1}}{\partial x} = 0, \quad (M_x)_i = (M_x)_{i+1} \tag{4.5.59}$$

*For plates with abrupt changes in slope due to the presence of an internal line hinge:*

$$w_i = w_{i+1}, \quad (M_x)_i = 0, \quad (M_x)_{i+1} = 0$$

$$(V_x)_i + \bar{N}_i\frac{\partial w_i}{\partial x} = (V_x)_{i+1} + \bar{N}_{i+1}\frac{\partial w_{i+1}}{\partial x}$$

(4.5.60)

In view of Eq. (4.5.55), a homogeneous system of equations can be derived by implementing the boundary conditions of the plate along the two edges parallel to the $y$-axis [Eqs. (4.5.51) to (4.5.53)] and the interface conditions between two plate segments [Eqs. (4.5.58) to (4.5.59)] when assembling the segments to form the entire plate

$$\mathbf{K}\{\mathbf{c}\} = \{\mathbf{0}\} \qquad (4.5.61)$$

where $\mathbf{K}$ is a $4n \times 4n$ matrix. The buckling load is evaluated by setting the determinant of $\mathbf{K}$ in Eq. (4.5.61) to be zero.

The proposed method is used to determine exact buckling solutions for rectangular plates with abrupt property changes. For brevity, letters $F$, $S$ and $C$ are used to denote a free edge, a simply supported edge, and a clamped edge, respectively. A two-letter symbol is used to denote the left and right edge support conditions in a plate. For example, an SF plate has a simply supported left edge and a free right edge, while the other two remaining edges are simply supported.

**Plates with Two Different Thicknesses**

Consider an SS plate with two segments, each with a different uniform thicknesses, as shown in Table 4.9. The plate is subjected to a uniaxial inplane compressive load $N$ in the $x$-direction (Xiang and Wang, 2002). The exact results are compared in Table 4.9 with the very accurate ones computed by Eisenberger and Alexandrov (2000), who used exact beam stability functions in the stiffness method and performed the analysis in two directions in cycles. The two sets of results are in excellent agreement, with the exception of the case $h_2/h_1 = 0.4$. The exception is attributed to the fact that Eisenberger and Alexandrov (2000) obtained the buckling load factor that corresponds to the third buckling mode while Xiang and Wang (2002) obtained the correct value for the first buckling mode. Results for stepped laminated plates can be found in Xiang and Reddy (2001).

**Plates with an Internal Line Hinge**

Consider an isotropic plate with an internal line hinge as shown in Table 4.10. Using the proposed method, the buckling factors for SS, FF and CC square plates subjected to uniaxial inplane compressive load $N$ in the $x$-direction are obtained (Xiang et al., 2001). Results for shear deformable laminated plates may be found in Gupta and Reddy (2002).

**Table 4.9:** Comparison of buckling load factors $Nb^2/(\pi^2 D_1)$ for a stepped, SS rectangular plate subjected to uniaxial inplane load ($a/b = 2.0$, $c/a = 0.5$, $E_1 = E_2$, $\nu_1 = \nu_2 = 0.25$).
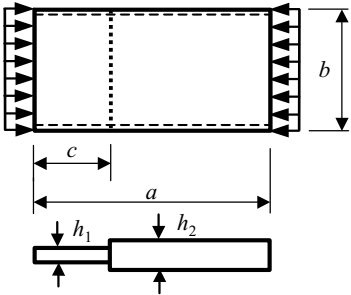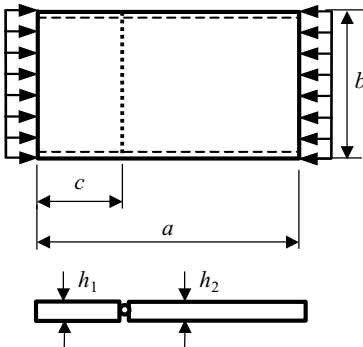
| Stepped plate with two thicknesses | $\frac{h_2}{h_1}$ | Eisenberger and Alexandrov (2000) | Xiang and Wang (2002) |
|---|---|---|---|
| | 0.4 | 0.8619 | 0.3083 |
| | 0.6 | 1.0245 | 1.0246 |
| | 0.8 | 2.3442 | 2.3442 |
| | 1.0 | 4.0000 | 4.0000 |
| | 1.2 | 4.5324 | 4.5325 |
| | 1.4 | 4.6663 | 4.6663 |
| | 1.6 | 4.7292 | 4.7292 |
| | 1.8 | 4.7652 | 4.7652 |
| | 2.0 | 4.7877 | 4.7878 |
| | 2.2 | 4.8026 | 4.8027 |
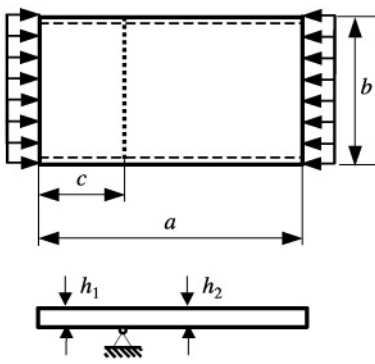


**Table 4.10:** Buckling load factors $Nb^2/(\pi^2 D_1)$ for SS, FF and CC square plates having an internal line hinge and subjected to uniaxial inplane load ($a/b = 1.0$, $h_1 = h_2$, $E_1 = E_2$, $\nu_1 = \nu_2 = 0.3$).

| Plate with an internal line hinge | $\frac{c}{a}$ | SS | FF | CC |
|---|---|---|---|---|
| | 0.001 | 1.4017 | 1.4000 | 4.8497 |
| | 0.1 | 1.5770 | 1.4216 | 5.1550 |
| | 0.2 | 1.7474 | 1.4676 | 5.1799 |
| | 0.3 | 1.8969 | 1.5206 | 3.5428 |
| | 0.4 | 2.0035 | 1.5645 | 2.8066 |
| | 0.5 | 2.0429 | 1.5820 | 2.6261 |



## Plates with Internal Line Supports

Table 4.11 contains the exact buckling solutions for SS, FF and CC square plates having one internal line support and subjected to uniaxial inplane load (Xiang 2003).

**Table 4.11:** Buckling load factors $Nb^2/(\pi^2 D_1)$ for SS, FF and CC square plates having an internal line support and subjected to uniaxial inplane load ($a/b = 1.0$, $h_1 = h_2$, $E_1 = E_2$, $\nu_1 = \nu_2 = 0.3$).

| Plate with an internal line support | $\frac{c}{a}$ | SS | FF | CC |
|---|---|---|---|---|
| | 0.001 | 4.8489 | 2.3660 | 6.7481 |
| | 0.1 | 5.0467 | 2.3891 | 7.3051 |
| | 0.2 | 5.3165 | 2.3966 | 8.0315 |
| | 0.3 | 5.6652 | 2.2564 | 8.9336 |
| | 0.4 | 6.0482 | 2.0936 | 9.8920 |
| | 0.5 | 6.2500 | 2.0429 | 10.386 |



## Plates with Intermediate Inplane Load

The geometry and load configuration for a plate subjected to an intermediate inplane load is given in Fig. 4.21. Table 4.12 contains the buckling intermediate load factor $N_2 b^2/(\pi^2 D_1)$ for square and rectangular SS, FF and CC plates when the end load $N_1 = 0$ (see Xiang, et al., 2003; and Wang, et al., 2004).
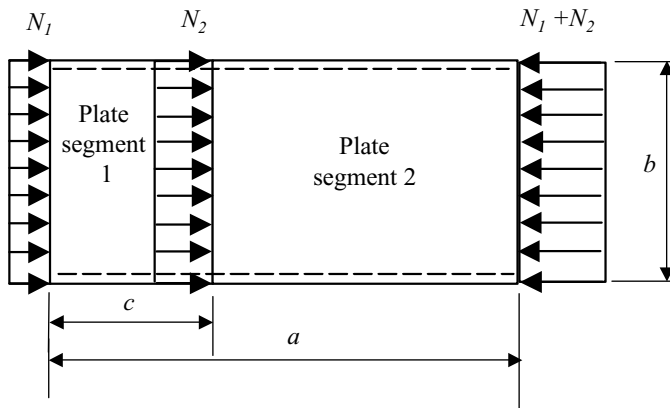


**Figure 4.21:** Rectangular plate subjected to an intermediate inplane load.
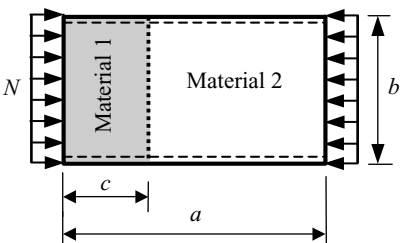
**Table 4.12:** Buckling intermediate load factors $N_2 b^2/(\pi^2 D_1)$ with $N_1 = 0$ ($h_1 = h_2$, $E_1 = E_2$, $\nu_1 = \nu_2 = 0.3$).

| | $a/b = 1$ | | | $a/b = 2$ | | |
|---|---|---|---|---|---|---|
| $\frac{c}{a}$ | SS | FF | CC | SS | FF | CC |
| 0.3 | 5.3134 | 2.2511 | 8.4730 | 4.3540 | 2.3145 | 5.2077 |
| 0.5 | 6.3779 | 2.3282 | 12.050 | 4.5430 | 2.3254 | 5.9609 |
| 0.7 | 6.6443 | 2.6384 | 13.307 | 5.8152 | 2.3389 | 8.8086 |

## Plates with Different Materials

The proposed method may also be used to solve the buckling problem of rectangular plates with multiple material properties. The buckling load factors for square plates having two materials and subjected to uniaxial inplane compressive load $N$ in the $x$-direction are presented in Table 4.13. As expected, the buckling factors decrease as the portion of material 1 (weaker material) increases.

**Table 4.13:** Buckling load factors $N b^2/(\pi^2 D_1)$ for SS, FF and CC plates having two different materials and subjected to uniaxial inplane load ($a/b = 1.0$, $h_1 = h_2$, $E_2 = 2E_1$, $\nu_1 = 0.3$, $\nu_2 = 0.25$).

| Plate with two materials | | $\frac{c}{a}$ | SS | FF | CC |
|---|---|---|---|---|---|
|  | | 0.001 | 7.7623 | 4.2153 | 13.079 |
| | | 0.1 | 7.3876 | 3.6301 | 12.131 |
| | | 0.3 | 6.0912 | 2.6981 | 10.999 |
| | | 0.5 | 5.1983 | 2.3859 | 8.7850 |
| | | 0.7 | 4.6749 | 2.2997 | 7.8682 |
| | | 0.9 | 4.2507 | 2.2345 | 7.1064 |
| | | 0.999 | 4.0030 | 2.0478 | 6.7464 |

## 4.6 Simply Supported Isosceles Triangular Plates

Han (1960) presented buckling of a simply supported, isosceles triangular plate of height $a$ and base $2as$, and subjected to a normal compressive force $\hat{N}_0$ along the boundaries, as shown in Fig. 4.22. The

governing equation is given by [see Eq. (4.5.28)]

$$D\nabla^4 w + \hat{N}_0 \nabla^2 w = 0. \tag{4.6.1}$$

The simply supported boundary conditions require

$$w = 0, \quad \nabla^2 w = 0. \tag{4.6.2}$$
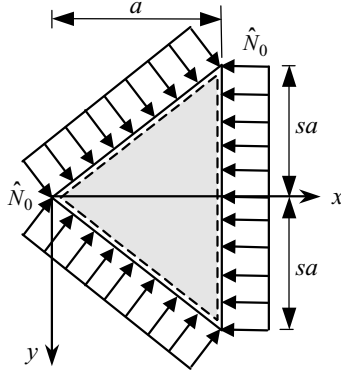


**Figure 4.22:** An isosceles triangular plate.

Han (1960) approximated the displacement function as

$$w \approx \sum_{n=1} C_n F_n(x), \quad F_n = 2\sin\frac{n\pi x}{a}\cos\frac{n\pi y}{as} - \sin\frac{2n\pi x}{a} \tag{4.6.3}$$

where $C_n$ are arbitrary constants, and used the Ritz method to minimize the energy functional associated with Eq. (4.6.1). Clearly, the assumed approximation satisfies the boundary conditions in (4.6.2). This yields $\hat{N}_0$ as a function of $n$, which is then minimized with respect to $n$ to obtain the critical buckling load

$$\hat{N}_0 = \frac{2\pi^2 D}{a^2}\left(1 + \frac{1}{3s^2}\right) \tag{4.6.4}$$

Although this is an approximate solution for arbitrary $s < 1.0$, it is exact for $s = 1/\sqrt{3}$, which corresponds to the case of an equilateral triangle. For this case the critical buckling load is

$$\hat{N}_0 = \frac{4\pi^2 D}{a^2} \tag{4.6.5}$$

For the following alternative choice of $F_n$ in Eq. (4.6.3), when $s \geq 1.0$,

$$F_n = \cos \frac{(m+n)\pi x}{2a} \cos \frac{(m-n)\pi y}{2as} - \cos \frac{(m-n)\pi x}{2a} \cos \frac{(m+n)\pi y}{2as}$$
(4.6.6)

the approximate critical buckling load is given by

$$\hat{N}_0 = \frac{5\pi^2 D}{4a^2} \left( 1 + \frac{1}{s^2} \right)$$
(4.6.7)

This is exact when $s = 1$, and the value is given by

$$\hat{N}_0 = \frac{5\pi^2 D}{2a^2}$$
(4.6.8)

Accurate buckling formulas for simply supported and clamped isosceles triangular plates can be found in the paper by Wang and Liew (1994).

## 4.7 First-Order Shear Deformation Theory of Plates

### 4.7.1 Governing Equations of Rectangular Plates

The simplest shear deformation plate theory is the first-order shear deformation plate theory (or FSDT), also referred to as the Mindlin plate theory (Mindlin, 1951), and it is based on the displacement field

$$u(x, y, z) = z\phi_x(x, y)$$
(4.7.1a)
$$v(x, y, z) = z\phi_y(x, y)$$
(4.7.1b)
$$w(x, y, z) = w(x, y)$$
(4.7.1c)

where $\phi_x$ and $-\phi_y$ denote rotations about the $y$- and $x$-axes, respectively. In FSDT, shear correction factors are introduced to correct the discrepancy between the actual transverse shear force distributions and those computed using the kinematic relations of FSDT. The shear correction factors depend not only on the geometric parameters but also on the loading and boundary conditions of the plate.

The equations of equilibrium of the first-order plate theory are given by

$$-\left( \frac{\partial Q_x}{\partial x} + \frac{\partial Q_y}{\partial y} \right) + \frac{\partial}{\partial x} \left( \hat{N}_{xx} \frac{\partial w}{\partial x} + \hat{N}_{xy} \frac{\partial w}{\partial y} \right)$$
$$+ \frac{\partial}{\partial y} \left( \hat{N}_{xy} \frac{\partial w}{\partial x} + \hat{N}_{yy} \frac{\partial w}{\partial y} \right) = 0, \quad (4.7.2a)$$

$$-\left( \frac{\partial M_{xx}}{\partial x} + \frac{\partial M_{xy}}{\partial y} \right) + Q_x = 0, \quad (4.7.2b)$$

$$-\left( \frac{\partial M_{xy}}{\partial x} + \frac{\partial M_{yy}}{\partial y} \right) + Q_y = 0, \quad (4.7.2c)$$

where $(\hat{N}_{xx}, \hat{N}_{yy}, \hat{N}_{xy})$ are applied inplane compressive and shear forces per unit length,$(M_{xx}, M_{yy}, M_{xy})$ are the moments, and $(Q_x, Q_y)$ the transverse shear forces per unit length (see Fig. 4.1).

The primary and secondary variables of the theory are

$$\text{primary variables:} \quad w, \ \phi_n, \ \phi_s$$
$$\text{secondary variables:} \quad Q_n, \ M_{nn}, \ M_{ns} \qquad (4.7.3)$$

where

$$\phi_x = n_x \phi_n - n_y \phi_s , \quad \phi_y = n_y \delta \phi_n + n_x \delta \phi_s \qquad (4.7.4a)$$

$$Q_n \equiv Q_x n_x + Q_y n_y \qquad (4.7.4b)$$

The boundary conditions involve specifying one element of each of the following pairs:

$$(w, Q_n), \quad (\phi_n, M_{nn}), \quad (\phi_s, M_{ns})$$

Assuming that the plate material is orthotropic and obeys Hooke's law, we can express the stress resultants of Eqs. (4.7.2a–c) in terms of the displacements $(w, \phi_x, \phi_y)$ as

$$\left\{ \begin{array}{c} M_{xx} \\ M_{yy} \\ M_{xy} \end{array} \right\} = \left[ \begin{array}{ccc} D_{11} & D_{12} & 0 \\ D_{12} & D_{22} & 0 \\ 0 & 0 & D_{66} \end{array} \right] \left\{ \begin{array}{c} \frac{\partial \phi_x}{\partial x} \\ \frac{\partial \phi_y}{\partial y} \\ \frac{\partial \phi_x}{\partial y} + \frac{\partial \phi_y}{\partial x} \end{array} \right\} \qquad (4.7.5a)$$

$$\left\{ \begin{array}{c} Q_y \\ Q_x \end{array} \right\} = K_s \left[ \begin{array}{cc} A_{44} & 0 \\ 0 & A_{55} \end{array} \right] \left\{ \begin{array}{c} \frac{\partial w}{\partial y} + \phi_y \\ \frac{\partial w}{\partial x} + \phi_x \end{array} \right\} \qquad (4.7.5b)$$

where $K_s$ denotes the shear correction factor, $D_{ij}$ are defined in Eq. (4.2.9b), and

$$D_{11} = \frac{E_1 h^3}{12(1 - \nu_{12}\nu_{21})}, \quad D_{22} = \frac{E_2}{E_1} D_{11}, \quad D_{12} = D_{11}\nu_{21}, \quad D_{66} = \frac{G_{12} h^3}{12}$$

$$A_{44} = G_{23} h, \quad A_{55} = G_{12} h. \qquad (4.7.6)$$

In view of the relations (4.7.5a, b), the equations of equilibrium (4.7.2a–c) can be expressed in terms of displacements $(w, \phi_x, \phi_y)$ as

$$K_s A_{55} \left( \frac{\partial^2 w}{\partial x^2} + \frac{\partial \phi_x}{\partial x} \right) + K_s A_{44} \left( \frac{\partial^2 w}{\partial y^2} + \frac{\partial \phi_y}{\partial y} \right)$$

$$= \frac{\partial}{\partial x} \left( \hat{N}_{xx} \frac{\partial w}{\partial x} + \hat{N}_{xy} \frac{\partial w}{\partial y} \right) + \frac{\partial}{\partial y} \left( \hat{N}_{xy} \frac{\partial w}{\partial x} + \hat{N}_{yy} \frac{\partial w}{\partial y} \right) \qquad (4.7.7)$$

$$D_{11}\frac{\partial^2 \phi_x}{\partial x^2} + D_{12}\frac{\partial^2 \phi_y}{\partial y \partial x} + D_{66}\left(\frac{\partial^2 \phi_x}{\partial y^2} + \frac{\partial^2 \phi_y}{\partial y \partial x}\right)$$
$$- K_s A_{55}\left(\frac{\partial w}{\partial x} + \phi_x\right) = 0 \qquad (4.7.8)$$

$$D_{66}\left(\frac{\partial^2 \phi_x}{\partial x \partial y} + \frac{\partial^2 \phi_y}{\partial x^2}\right) + D_{12}\frac{\partial^2 \phi_x}{\partial x \partial y} + D_{22}\frac{\partial^2 \phi_y}{\partial y^2}$$
$$- K_s A_{44}\left(\frac{\partial w}{\partial y} + \phi_y\right) = 0 \qquad (4.7.9)$$

### 4.7.2 Buckling Loads of Rectangular Plates

As in the case of the classical thin plate theory, analytical solutions of the first-order shear deformation plate theory can be developed using Navier's and Lévy's methods. Here, we limit our discussion to the Navier method of solution for the pure bending case (i.e., omit stretching deformation). The Lévy method of analysis for the first-order shear deformation plate theory is more involved than the classical plate theory, and the buckling loads can be determined only numerically by solving the eigenvalue problem numerically. Additional details on the Lévy method can be found in the books by Reddy (1999, 2002, 2004).

The simply supported boundary conditions for the first-order shear deformation plate theory (FSDT) can be expressed as (see Fig. 4.23)

$$w(x,0) = 0, \quad w(x,b) = 0, \quad w(0,y) = 0, \quad w(a,y) = 0 \qquad (4.7.10a)$$
$$\phi_x(x,0) = 0, \quad \phi_x(x,b) = 0, \quad \phi_y(0,y) = 0, \quad \phi_y(a,y) = 0 \quad (4.7.10b)$$
$$M_{yy}(x,0) = 0, \quad M_{yy}(x,b) = 0, \quad M_{xx}(0,y) = 0, \quad M_{xx}(a,y) = 0$$
$$(4.7.10c)$$

where $a$ and $b$ denote the dimensions of the rectangular plate. The boundary conditions in Eqs. (4.7.10a–c) are satisfied by the following expansions:

$$w(x,y) = \sum_{n=1}^{\infty}\sum_{m=1}^{\infty} W_{mn} \sin\frac{m\pi x}{a} \sin\frac{n\pi y}{b} \qquad (4.7.11a)$$

$$\phi_x(x,y) = \sum_{n=1}^{\infty}\sum_{m=1}^{\infty} X_{mn} \cos\frac{m\pi x}{a} \sin\frac{n\pi y}{b} \qquad (4.7.11b)$$

$$\phi_y(x,y) = \sum_{n=1}^{\infty}\sum_{m=1}^{\infty} Y_{mn} \sin\frac{m\pi x}{a} \cos\frac{n\pi y}{b} \qquad (4.7.11c)$$

At top of figure (boundary conditions):
$w_0 = \phi_x = 0$, $M_{yy} = 0$
$a$
$x$
$w_0 = \phi_y = 0$, $M_{xx} = 0$
$b$
$w_0 = \phi_y = 0$, $M_{xx} = 0$
$w_0 = \phi_x = 0$, $M_{yy} = 0$
$y$
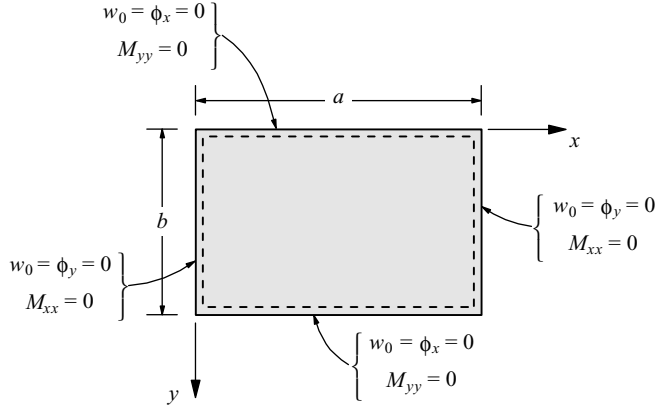
**Figure 4.23:** The simply supported boundary conditions of the first-order shear deformation theory.

The substitution of Eqs. (4.7.11a–c) into Eqs. (4.7.7)–(4.7.9), with $\hat{N}_{xy} = 0$, yields the following equations for the coefficients $(W_{mn}, X_{mn}, Y_{mn})$:

$$
\begin{bmatrix}
s_{11} - \bar{s}_{11} & s_{12} & s_{13} \\
s_{12} & s_{22} & s_{23} \\
s_{13} & s_{23} & s_{33}
\end{bmatrix}
\begin{Bmatrix}
W_{mn} \\
X_{mn} \\
Y_{mn}
\end{Bmatrix}
=
\begin{Bmatrix}
0 \\
0 \\
0
\end{Bmatrix}
\qquad (4.7.12)
$$

where $s_{ij}$ are defined by (for orthotropic plates)

$$s_{11} = K_s(A_{55}\alpha_m^2 + A_{44}\beta_n^2), \quad \bar{s}_{11} = \hat{N}_{xx}\alpha_m^2 + \hat{N}_{yy}\beta_n^2$$

$$s_{12} = K_s A_{55}\alpha_m, \quad s_{13} = K_s A_{44}\beta_n, \quad s_{22} = (D_{11}\alpha_m^2 + D_{66}\beta_n^2 + K_s A_{55})$$

$$s_{23} = (D_{12} + D_{66})\alpha_m\beta_n, \quad s_{33} = (D_{66}\alpha_m^2 + D_{22}\beta_n^2 + K_s A_{44}) \qquad (4.7.13)$$

and $\alpha_m = m\pi/a$ and $\beta_n = n\pi/b$.

Suppose that the only applied loads are the inplane compressive forces

$$\hat{N}_{xx} = N_0, \quad \hat{N}_{yy} = \gamma N_0, \quad \gamma = \frac{\hat{N}_{yy}}{\hat{N}_{xx}} \qquad (4.7.14)$$

and all other loads are zero. From Eq. (4.7.12) we have

$$
\begin{bmatrix}
s_{11} - N_0\left(\alpha_m^2 + \gamma\beta_n^2\right) & s_{12} & s_{13} \\
s_{12} & s_{22} & s_{23} \\
s_{13} & s_{23} & s_{33}
\end{bmatrix}
\begin{Bmatrix}
W_{mn} \\
X_{mn} \\
Y_{mn}
\end{Bmatrix}
=
\begin{Bmatrix}
0 \\
0 \\
0
\end{Bmatrix}
\qquad (4.7.15)
$$

For a nontrivial solution the determinant of the coefficient matrix in Eq. (4.7.15) must be zero. This gives the following expression for the buckling load:

$$N_0 = \left(\frac{1}{\alpha_m^2 + \gamma\beta_n^2}\right)\left[\frac{c_0 + \left(\frac{\alpha_m^2}{K_s A_{44}} + \frac{\beta_n^2}{K_s A_{55}}\right)c_1}{1 + \frac{c_1}{K_s^2 A_{44} A_{55}} + \frac{c_2}{K_s A_{55}} + \frac{c_3}{K_s A_{44}}}\right] \quad (4.7.16a)$$

$$c_0 = D_{11}\alpha_m^4 + 2\left(D_{12} + 2D_{66}\right)\alpha_m^2\beta_n^2 + D_{22}\beta_n^4, \quad c_1 = c_2 c_3 - (c_4)^2 > 0$$

$$c_2 = D_{11}\alpha_m^2 + D_{66}\beta_n^2, \; c_3 = D_{66}\alpha_m^2 + D_{22}\beta_n^2, \quad c_4 = \left(D_{12} + D_{66}\right)\alpha_m\beta_n$$
$$(4.7.16b)$$

Table 4.14 contains the critical buckling loads $\bar{N} = N_{cr}b^2/(\pi^2 D_{22})$ as a function of the plate aspect ratio $a/b$, side-to-thickness ratio $b/h$, and modulus ratio $E_1/E_2$ for uniaxial ($\gamma = 0$) and biaxial ($\gamma = 1$) compression. The classical plate theory (CPT) results are also included for comparison. The effect of transverse shear deformation is significant for lower aspect ratios, thick plates and larger modulus ratios. For thin plates, irrespective of the aspect ratio and modular ratio, the critical loads predicted by the shear deformation plate theory are very close to those of the classical plate theory.

For isotropic, simply supported, rectangular plates on (Pasternak) elastic foundation, the critical buckling load is given by (Xiang et al., 1994)

$$\underset{m,n}{\text{Minimize}} \; N(m,n) = \frac{\frac{\lambda_{mn}D}{1+\frac{\lambda_{mn}D}{K_s Gh}} + \frac{k}{\lambda_{mn}} + G_b}{1 - \frac{\beta_n^2(1-\gamma)}{\lambda_{mn}}} \quad (4.7.17)$$

where $k$ is the modulus of the subgrade reaction, $G_b$ is the shear modulus of the subgrade, and $\lambda_{mn} = \alpha_m^2 + \beta_n^2$.

### 4.7.3 Buckling Loads of Circular Plates

Here we present critical buckling loads of circular plates using the relationships between the classical and first-order shear deformation plate theories (see Wang et al., 2000). Consider an elastic, isotropic circular plate of radius $R$, uniform thickness $h$, Young's modulus $E$, shear modulus $G$ and Poisson's ratio $\nu$ subjected to a uniform radial compressive load $N$.

**Table 4.14:** Critical buckling loads $\bar{N}$ of simply supported plates under in-plane uniform uniaxial ($\gamma = 0$) and biaxial ($\gamma = 1$) compression.

| $\gamma$ | $\frac{a}{b}$ | $\frac{h}{b}$ | $\frac{E_1}{E_2} = 1$ | $\frac{E_1}{E_2} = 3$ | $\frac{E_1}{E_2} = 10$ | $\frac{E_1}{E_2} = 25$ |
|---|---|---|---|---|---|---|
| 0 | 0.5 | 10 | 5.523 | 11.583 | 23.781 | 34.701 |
| | | 20 | 6.051 | 13.779 | 35.615 | 68.798 |
| | | 100 | 6.242 | 14.669 | 42.398 | 100.750 |
| | | CPT | 6.250 | 14.708 | 42.737 | 102.750 |
| | 1.0 | 10 | 3.800 | 5.901 | 11.205 | 19.252 |
| | | 20 | 3.948 | 6.309 | 12.832 | 25.412 |
| | | 100 | 3.998 | 6.452 | 13.460 | 28.357 |
| | | CPT | 4.000 | 6.458 | 13.488 | 28.495 |
| | 1.5 | 10 | $4.045^{(2,1)\dagger}$ | 5.664 | 8.354 | 13.166 |
| | | 20 | $4.262^{(2,1)}$ | 5.942 | 8.959 | 15.077 |
| | | 100 | $4.337^{(2,1)}$ | 6.037 | 9.173 | 15.823 |
| | | CPT | $4.340^{(2,1)}$ | 6.042 | 9.182 | 15.856 |
| | 3.0 | 10 | $3.800^{(3,1)}$ | $5.664^{(2,1)}$ | $8.354^{(2,1)}$ | $13.166^{(2,1)}$ |
| | | 20 | $3.948^{(3,1)}$ | $5.942^{(2,1)}$ | $8.959^{(2,1)}$ | 14.052 |
| | | 100 | $3.998^{(3,1)}$ | $6.037^{(2,1)}$ | $9.173^{(2,1)}$ | 14.264 |
| | | CPT | $4.000^{(3,1)}$ | $6.042^{(2,1)}$ | $9.182^{(2,1)}$ | 14.273 |
| 1 | 0.5 | 10 | 4.418 | 9.405 | $15.191^{(1,3)}$ | $17.773^{(1,3)}$ |
| | | 20 | 4.841 | 11.070 | $21.565^{(1,3)}$ | $30.073^{(1,4)}$ |
| | | 100 | 4.993 | 11.737 | $25.241^{(1,3)}$ | $40.157^{(1,4)}$ |
| | | CPT | 5.000 | 11.767 | $25.427^{(1,3)}$ | $40.784^{(1,4)}$ |
| | 1.0 | 10 | 1.900 | 3.015 | 5.662 | $7.518^{(1,2)}$ |
| | | 20 | 1.974 | 3.173 | 6.433 | $9.308^{(1,2)}$ |
| | | 100 | 1.999 | 3.227 | 6.731 | $10.156^{(1,2)}$ |
| | | CPT | 2.000 | 3.229 | 6.744 | $10.196^{(1,2)}$ |
| | 1.5 | 10 | 1.391 | 1.788 | 2.614 | 4.093 |
| | | 20 | 1.431 | 1.841 | 2.769 | 4.651 |
| | | 100 | 1.444 | 1.858 | 2.823 | 4.869 |
| | | CPT | 1.444 | 1.859 | 2.825 | 4.879 |
| | 3.0 | 10 | 1.079 | 1.151 | 1.227 | 1.375 |
| | | 20 | 1.103 | 1.172 | 1.251 | 1.414 |
| | | 100 | 1.111 | 1.179 | 1.259 | 1.426 |
| | | CPT | 1.111 | 1.179 | 1.260 | 1.427 |

$\dagger$ Denotes mode numbers $(m,n)$ at which the critical buckling load occurred; $(m,n) = (1,1)$ for all other cases.

The governing equations for axisymmetric buckling have the form

$$\frac{d}{dr}(rQ_r) = r\hat{N}_{rr}\nabla^2 w, \quad rQ_r = \frac{d}{dr}(rM_{rr}) - M_{\theta\theta} \qquad (4.7.18a)$$

$$M_{rr} = D\left(\frac{d\phi_r}{dr} + \frac{\nu}{r}\phi_r\right), \quad M_{\theta\theta} = D\left(\nu\frac{d\phi_r}{dr} + \frac{1}{r}\phi_r\right) \qquad (4.7.18b)$$

$$Q_r = K_s Gh\left(\phi_r + \frac{dw}{dr}\right) \qquad (4.7.18c)$$

Equations (4.3.17) and (4.4.1) of the CPT and Eqs. (4.7.18a–c) of the FSDT for isotropic plates can be reduced to

$$\frac{d^3\psi}{dr^3} + \frac{2}{r}\frac{d^2\psi}{dr^2} + \left(\lambda_0 - \frac{1}{r^2}\right)\frac{d\psi}{dr} + \frac{1}{r}\left(\lambda_0 + \frac{1}{r^2}\right)\psi = 0 \qquad (4.7.19)$$

where

$$\psi = \begin{cases} -\frac{dw^C}{dr}, & \text{for CPT} \\[2ex] \phi_r^F, & \text{for FSDT} \end{cases} \qquad (4.7.20a)$$

$$\lambda_0 = \begin{cases} \frac{\hat{N}_{rr}^C}{D}, & \text{for CPT} \\[2ex] \frac{\hat{N}_{rr}^F}{1 - \frac{\hat{N}_{rr}^F}{K_s Gh}}, & \text{for FSDT} \end{cases} \qquad (4.7.20b)$$

where superscripts $C$ and $F$ refer to the CPT and FSDT, respectively. Equation $\psi$ is subject to the boundary conditions

At $r = R$ :

$\psi = 0$ for clamped plates

$\frac{d\psi}{dr} + \frac{\nu}{r}\psi = 0$ for simply supported plates $\qquad$ (4.7.21a)

$\frac{d\psi}{dr} + \frac{\nu}{r}\psi = k_2\psi$ for rotational elastic restraint

At $r = 0$ :

$\psi = 0$ for all boundary conditions $\qquad$ (4.7.21b)

where $k_2$ is the rotational spring constant. In view of the similarity of the governing equations and boundary conditions, we obtain

$$\hat{N}_{rr}^F = \frac{\hat{N}_{rr}^C}{1 + \frac{\hat{N}_{rr}^C}{K_s Gh}} \qquad (4.7.22)$$

The buckling load relationship (4.7.22) also applies to sectorial plates with simply supported edges and to sectorial plates with simply supported radial edges and either a clamped or a free circular edge. The availability of this relationship allows easy and accurate deduction of critical buckling loads based on the FSDT from their corresponding CPT critical buckling loads. For more details, see Wang et al. (2000).

Table 4.15 contains the CPT and FSDT buckling factors $\hat{N}_{rr}R^2/D$ for circular plates with various values of the thickness-to-radius ratio $h/R$, elastic rotational restraint parameter $k_2R/D$ and Poisson's ratio $\nu = 0.3$. Note that the buckling load factor in CPT is independent of $h/R$ due to the neglect of transverse shear deformation. The three-dimensional elasticity solutions of Ye (1995) are also included for comparison.

**Table 4.15:** Comparison of buckling load factors for circular plates based on different theories.

| $\frac{h}{R}$ | $\frac{k_2R}{D}$ | CPT | FSDT | Ye (1995) |
|---|---|---|---|---|
| | 0 | 4.1978 | 4.1853 | |
| 0.05 | 1 | 6.3532 | 6.3245 | |
| | 10 | 12.173 | 12.068 | |
| | $\infty$ | 14.682 | 14.530 | 14.552 |
| | 0 | 4.1978 | 4.1481 | |
| 0.10 | 1 | 6.3532 | 6.2400 | |
| | 10 | 12.173 | 11.764 | |
| | $\infty$ | 14.682 | 14.091 | 14.177 |
| | 0 | 4.1978 | 4.0057 | |
| 0.20 | 1 | 6.3532 | 5.9235 | |
| | 10 | 12.173 | 10.688 | |
| | $\infty$ | 14.682 | 12.572 | 12.824 |
| | 0 | 4.1978 | 3.7893 | |
| 0.30 | 1 | 6.3532 | 5.4625 | |
| | 10 | 12.173 | 9.2792 | |
| | $\infty$ | 14.682 | 10.658 | 11.024 |

## 4.8 Inelastic Buckling of Plates

### 4.8.1 Introduction

Inelastic buckling analysis of plates may be based on incremental (or flow) theory of plasticity (e.g., Handelman and Prager, 1948; Pearson, 1950) or the deformation theory of plasticity (e.g., Kaufmann, 1936; Illyushin, 1947; Stowell, 1948; Bijlaard, 1949; El-Ghazaly and Sherbourne, 1986), or the slip theory (e.g., Bartdorf, 1949; Inoue and Kato, 1993). The success of these is varied. For example, the deformation theory gives a better prediction of critical buckling loads for long simply supported plates while the incremental theory gives better results for cylinders under compression and torsion. Accordingly, some researchers (e.g., Shrivastava, 1979; Ore and Durban, 1989; Tugcu, 1991; and Durban and Zuckerman, 1999) presented the inelastic buckling loads of plates based on both the deformation-type theory and the incremental-type theory. There are, however, other simplified theories such as the one proposed by Bleich (1952). Bleich assumed a two-moduli plate where the modulus in the direction of stress that is likely to exceed the proportional limit be taken as the tangent modulus $E_T$, while in the direction where there is little stress, the elastic modulus $E$ be taken. Furthermore, the factor for the twisting moment curvature relation is arbitrarily chosen as $\sqrt{E_T/E}$. Bleich's simplified theory seems to give results in close agreement with large-scale test results obtained by Kollbrunner (1946).

Apart from the paper by Shrivastava (1979), the aforementioned studies on inelastic buckling analysis of plates adopted the classical thin-plate theory. When dealing with thick plates where buckling occurs in the plastic range, a shear deformable plate theory has to be employed so as to admit the significant effect of transverse shear deformation. Complementing the work of Shrivastava (1979), Wang et al. (2001) adopted the Mindlin plate theory for the inelastic buckling of rectangular thick plates under equibiaxial and uniaxial loading, and of circular thick plates under a uniform radial load.

Following Wang et al. (2001), two plasticity theories are considered here: the incremental theory (IT) of plasticity with the Prandtl–Reuss constitutive equations and the deformation theory (DT) of plasticity with the Hencky stress–strain relation. An important difference between these two theories is that the strain in the former theory depends on the manner in which the state of stress is built up, whereas in the latter theory the strain that corresponds to a certain state of stress is entirely independent of the manner in which this state of stress has been reached. Analytical forms of inelastic stability criteria are presented

for rectangular and circular thick plates for both theories. Critical buckling stress factors, from both theories of plasticity, are tabulated for square and circular plates whose materials exhibit strain hardening characterized by the Ramberg–Osgood stress–strain relation.

## 4.8.2 Governing Equations of Circular Plates

Consider a circular plate with radius $a$ and uniform thickness $h$. The plate is subjected to uniform compressive radial stress of magnitude $\sigma$. According to the Mindlin plate theory, the admissible velocity field for axisymmetric deformation is given by

$$v_r = z\phi; \quad v_\theta = 0; \quad v_z = w \tag{4.8.1}$$

where $\phi$ is the rate of rotation and $w$ the transverse velocity. For axisymmetric buckling, the nonzero strain rates associated with Eqs. (4.8.1) are given by

$$\dot{\varepsilon}_{rr} = z\frac{d\phi}{dr}; \quad \dot{\varepsilon}_{\theta\theta} = z\frac{\phi}{r}; \quad \dot{\gamma}_{rz} = \phi + \frac{dw}{dr} \tag{4.8.2}$$

The constitutive relations are given by (Chakrabarty, 2000)

$$\dot{\sigma}_{rr} = E(\alpha\dot{\varepsilon}_{rr} + \beta\dot{\varepsilon}_{\theta\theta}); \quad \dot{\sigma}_{\theta\theta} = E\left(\beta\dot{\varepsilon}_{rr} + \alpha\dot{\varepsilon}_{\theta\theta}\right); \quad \dot{\tau}_{rz} = K_s G\dot{\gamma}_{rz} \tag{4.8.3}$$

where $E$ is Young's modulus, $K_s$ the shear correction factor, $G$ the effective shear modulus, and the parameters $\alpha$, $\beta$, $\rho$ are given by

$$\alpha = \frac{1}{\rho}\left[4 - 3\left(1 - \frac{E_T}{E_s}\right)\right] \tag{4.8.4a}$$

$$\beta = \frac{1}{\rho}\left[2 - 2\left(1 - 2\nu\right)\frac{E_T}{E} - 3\left(1 - \frac{E_T}{E_s}\right)\right] \tag{4.8.4b}$$

$$\rho = 3\frac{E}{E_s} + \left(1 - 2\nu\right)\left[2 - \left(1 - 2\nu\right)\frac{E_T}{E} - 3\left(1 - \frac{E_T}{E_s}\right)\right] \tag{4.8.4c}$$

and the ratios of the elastic modulus $E$ to the shear modulus $G$, the tangent modulus $E_T$ and the secant modulus $E_s$ at the onset of buckling are expressed by the Ramberg–Osgood elasto–plastic characteristic in the forms of

$$\frac{E}{G} = 2 + \nu + 3\left(\frac{E}{E_s} - 1\right) \tag{4.8.5}$$

$$\frac{E}{E_T} = 1 + ck\left(\frac{\bar{\sigma}}{\sigma_0}\right)^{c-1}; \quad c > 1 \tag{4.8.6}$$

$$\frac{E}{E_s} = 1 + k\left(\frac{\bar{\sigma}}{\sigma_0}\right)^{c-1}; \quad c > 1 \tag{4.8.7}$$

where $\sigma_0$ is a nominal yield stress, $c$ is the hardening index that describes the shape of the stress–strain relationship with $c = \infty$ for elastic–perfectly plastic response, and $k$ is the horizontal distance between the knee of the curve and the intersection of the $c$ curve with the $\sigma/\sigma_0 = 1$ line, as shown in Fig. 4.24. The expressions (4.8.4a–c) for $\alpha, \beta, \rho$ describe the constitutive equations based on the rate form of Hencky's stress–strain relation. By setting $E_s = E$, these expressions reduce to those corresponding to the Prandtl–Reuss constitutive relations.
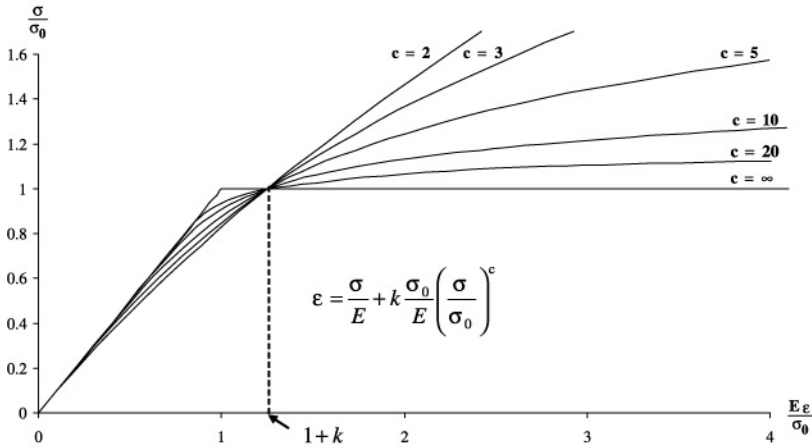


**Figure 4.24:** Ramberg–Osgood stress–strain relation.

To obtain the condition for bifurcation of the plate in the elastic/plastic range, it is assumed that Shanley's concept of continuous loading during buckling is accepted and therefore no unloading takes place. Consider the uniqueness criterion in the form of (Chakrabarty, 2000)

$$\int \left\{ (\dot{\sigma}_{rr}\dot{\varepsilon}_{rr} + \dot{\sigma}_{\theta\theta}\dot{\varepsilon}_{\theta\theta} + \dot{\tau}_{rz}\dot{\gamma}_{rz}) - \sigma \left( \frac{dw}{dr} \right)^2 \right\} dV > 0 \qquad (4.8.8)$$

Using Eqs. (4.8.2) and (4.8.3) and integrating through the thickness of the plate, the condition for uniqueness is reduced to

$$\int \left\{ \frac{\alpha E h^3}{12} \left( \frac{d\phi}{dr} \right) + \frac{\alpha E h^3}{12} \left( \frac{\phi}{r} \right)^2 + \frac{\beta E h^3}{6} \left( \frac{\phi}{r} \right) \left( \frac{d\phi}{dr} \right) \right.$$

$$\left. + K_s G h \left( \phi + \frac{dw}{dr} \right)^2 - \sigma h \left( \frac{dw}{dr} \right)^2 \right\} r\, dr > 0 \qquad (4.8.9)$$

The Euler–Lagrange differential equations associated with the minimization of the functional with respect to arbitrary variations of $w$ and $\phi$ are easily shown to be

$$K_s G h \left( \phi + \frac{dw}{dr} \right) = \sigma h \frac{dw}{dr} \Rightarrow \frac{dw}{dr} = -\frac{\phi}{1 - \frac{\sigma}{K_s G}} \qquad (4.8.10a)$$

and

$$\frac{\alpha E h^3}{12} r \frac{d^2 \phi}{dr^2} + \frac{\alpha E h^3}{12} \frac{d\phi}{dr} - \frac{\alpha E h^3}{12} \frac{\phi}{r} - r K_s G h \left( \phi + \frac{dw}{dr} \right) = 0 \quad (4.8.10b)$$

When the bifurcation occurs in the elastic range (i.e., $E_T = E_s = E$), Eqs. (4.8.10a) and (4.8.10b) reduce to the well-known governing equation for elastic buckling of circular Mindlin plates (Hong et al., 1993).

### 4.8.3 Buckling Solutions of Circular Plates

The elimination of the derivative of $w$ in Eq. (4.8.10b) by using Eq. (4.8.10a) yields

$$r^2 \frac{d^2 \phi}{dr^2} + r \frac{d\phi}{dr} + \left( \xi^2 - 1 \right) \phi = 0 \qquad (4.8.11)$$

where

$$\xi = r \sqrt{\left( \frac{\sigma h}{1 - \frac{\sigma}{K_s G}} \right) \frac{12}{\alpha E h^3}} \qquad (4.8.12)$$

Equation (4.8.11) is a Bessel's differential equation with the general solution

$$\phi = C_1 J_1 \left( \xi \right) + C_2 Y_1 \left( \xi \right) \qquad (4.8.13)$$

where $C_1$ and $C_2$ are constants and $J_1(\xi)$, $Y_1(\xi)$ are first-order Bessel functions of the first kind and second kind, respectively. Since from axisymmetric condition $\phi = 0$ at the plate center (i.e., at $r = \xi = 0$), the constant $C_2$ must vanish in Eq. (4.8.13). Thus, Eq. (4.8.13) reduces to

$$\phi = C_1 J_1(\xi) \qquad (4.8.14)$$

The critical stress would evidently depend on the support condition at the edge at $r = a$.

## Clamped Circular Plate

For a clamped circular plate, the rotation at the edge must vanish at the edge, i.e., $\phi = 0$ at $r = a$. Thus, in view of this boundary condition and Eq. (4.8.14), the bifurcation criterion is given by

$$J_1(\lambda) = 0 \qquad (4.8.15)$$

where, in view of Eqs. (4.8.4a) and (4.8.12),

$$\lambda = a\sqrt{\left(\frac{\sigma h}{1 - \frac{\sigma}{K_s G}}\right)\frac{12}{\alpha E h^3}} \qquad (4.8.16)$$

Since $\lambda$ involves $\sigma/E$ for any given stress–strain curve, the solution must be found by an iterative method, such as the false position method.

## Simply Supported Circular Plate

For a simply supported circular plate, the bending moment in the radial direction must vanish at the edge, i.e., $d\phi/d\xi + (\beta\phi)/(\alpha\xi) = 0$ at $r = a$. Thus, in view of Eqs. (4.8.4a) and (4.8.4b), using Eq. (4.8.13) and noting the fact that $J_1'(\xi) = J_0(\xi) - (1/\xi)J_1(\xi)$, we obtain the bifurcation criterion as

$$\frac{\lambda J_0(\lambda)}{J_1(\lambda)} = 1 - \frac{\beta}{\alpha} \qquad (4.8.17)$$

Since the left-hand side of this stability criterion (4.8.17) depends on the value of $\sigma/E$, the critical stress has to be computed iteratively.

Tables 4.16 and 4.17 contain the critical buckling stress factors for simply supported and clamped circular plates, respectively, for various values of $c$ and thickness-to-radius ratios $h/a$. In the calculations, $K_s = 5/6$ and $\nu = 0.3$ were taken. The elastic critical buckling stress factors, obtained by setting $E_T = E_s = E$, are also given for comparison purposes and these elastic results check out with those obtained by Kanaka Raju and Venkateswara Rao (1983) and Hong et al. (1993).

### 4.8.4 Governing Equations of Rectangular Plates

Consider a flat, rectangular plate whose sides are of lengths $a$ and $b$ and of uniform thickness $h$ as shown in Fig. 4.25. The plate is acted upon by uniform compressive stresses of magnitudes $\sigma_1$ and $\sigma_2$ in the

**Table 4.16:** Critical buckling stress factors $\sigma_c h a^2/(\pi^2 D)$ for simply supported circular plates ($K_s = 5/6, \quad \nu = 0.3, \quad k = 0.25$).

| | | $\sigma_c h a^2/(\pi^2 D)$ | | | | | |
| | | $h/a = 0.025$ | | $h/a = 0.050$ | | $h/a = 0.075$ | |
| $c$ | $E/\sigma_0$ | IT* | DT* | IT | DT | IT | DT |
|---|---|---|---|---|---|---|---|
| Elastic | - | 0.4250 | 0.4250 | 0.4241 | 0.4241 | 0.4225 | 0.4225 |
| 2 | 200 | 0.4185 | 0.4181 | 0.4002 | 0.3988 | 0.3756 | 0.3728 |
| | 300 | 0.4153 | 0.4147 | 0.3902 | 0.3881 | 0.3586 | 0.3549 |
| | 500 | 0.4094 | 0.4084 | 0.3726 | 0.3697 | 0.3317 | 0.3270 |
| | 750 | 0.4024 | 0.4010 | 0.3545 | 0.3507 | 0.3067 | 0.3010 |
| 3 | 200 | 0.4245 | 0.4245 | 0.4167 | 0.4164 | 0.3919 | 0.3907 |
| | 300 | 0.4239 | 0.4239 | 0.4086 | 0.4079 | 0.3665 | 0.3644 |
| | 500 | 0.4220 | 0.4219 | 0.3875 | 0.3861 | 0.3198 | 0.3168 |
| | 750 | 0.4185 | 0.4182 | 0.3589 | 0.3568 | 0.2757 | 0.2720 |
| 5 | 200 | 0.4250 | 0.4250 | 0.4236 | 0.4236 | 0.4121 | 0.4118 |
| | 300 | 0.4250 | 0.4250 | 0.4217 | 0.4217 | 0.3850 | 0.3843 |
| | 500 | 0.4249 | 0.4249 | 0.4087 | 0.4084 | 0.3160 | 0.3146 |
| | 750 | 0.4246 | 0.4246 | 0.3744 | 0.3735 | 0.2518 | 0.2500 |
| 20 | 200 | 0.4250 | 0.4250 | 0.4241 | 0.4241 | 0.4225 | 0.4225 |
| | 300 | 0.4250 | 0.4250 | 0.4241 | 0.4241 | 0.4222 | 0.4221 |
| | 500 | 0.4250 | 0.4250 | 0.4241 | 0.4241 | 0.3425 | 0.3424 |
| | 750 | 0.4250 | 0.4250 | 0.4217 | 0.4217 | 0.2429 | 0.2427 |

\* IT = Incremental theory of plasticity; DT = Deformation theory of plasticity.

$x-$ and $y$-directions, respectively. According to the first-order shear deformation plate theory, the admissible velocity field may be written as

$$v_x = z\dot{\phi}_x, \quad v_y = z\dot{\phi}_y, \quad v_z = \dot{w} \qquad (4.8.18)$$

where $(\dot{\phi}_x, \dot{\phi}_y)$ are the rotation rates about the $y$- and $x$-axes, respectively, and $\dot{w}$ is the transverse velocity. The strain rates corresponding to Eqs. (4.8.18) are given by Eqs. (4.8.19) on page 165.

**Table 4.17:** Buckling stress factors $\sigma_c h a^2/(\pi^2 D)$ for clamped circular plates ($K_s = 5/6$,  $\nu = 0.3$,  $k = 0.25$).

| $c$ | $E/\sigma_0$ | $\sigma_c h a^2/(\pi^2 D)$ | | | | | |
|---|---|---|---|---|---|---|---|
| | | $h/a = 0.025$ | | $h/a = 0.050$ | | $h/a = 0.075$ | |
| | | IT* | DT* | IT | DT | IT | DT |
| | Elastic | 1.484 | 1.484 | 1.472 | 1.472 | 1.453 | 1.453 |
| 2 | 200 | 1.431 | 1.409 | 1.307 | 1.241 | 1.176 | 1.0690 |
| | 300 | 1.408 | 1.377 | 1.252 | 1.166 | 1.105 | 0.9742 |
| | 500 | 1.367 | 1.320 | 1.168 | 1.055 | 1.009 | 0.8483 |
| | 750 | 1.323 | 1.260 | 1.094 | 0.9573 | 0.9326 | 0.7481 |
| 3 | 200 | 1.470 | 1.466 | 1.320 | 1.282 | 1.086 | 1.0010 |
| | 300 | 1.453 | 1.445 | 1.218 | 1.158 | 0.9573 | 0.8458 |
| | 500 | 1.409 | 1.388 | 1.060 | 0.9677 | 0.8072 | 0.6601 |
| | 750 | 1.342 | 1.306 | 0.9296 | 0.8107 | 0.7092 | 0.5311 |
| 5 | 200 | 1.483 | 1.483 | 1.364 | 1.348 | 0.9997 | 0.9467 |
| | 300 | 1.480 | 1.480 | 1.203 | 1.171 | 0.8168 | 0.7388 |
| | 500 | 1.460 | 1.456 | 0.9534 | 0.8941 | 0.6443 | 0.5223 |
| | 750 | 1.390 | 1.377 | 0.7779 | 0.6918 | 0.5638 | 0.3901 |
| 20 | 200 | 1.484 | 1.484 | 1.471 | 1.471 | 0.9316 | 0.9243 |
| | 300 | 1.484 | 1.484 | 1.283 | 1.279 | 0.6689 | 0.6500 |
| | 500 | 1.484 | 1.484 | 0.8550 | 0.8456 | 0.5178 | 0.4112 |
| | 750 | 1.483 | 1.483 | 0.6182 | 0.5925 | 0.5164 | 0.2836 |

*IT = Incremental theory of plasticity; DT = Deformation theory of plasticity.
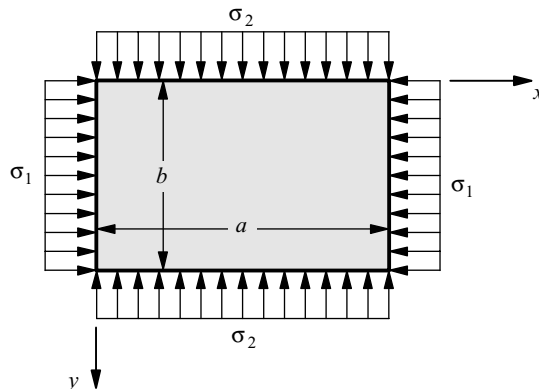


**Figure 4.25:** Plate subjected to uniform compressive stress $\sigma_1$ along the $x$-axis and uniform compression $\sigma_2$ along the $y$-axis.

$$\dot{\varepsilon}_{xx} = z\frac{\partial \dot{\phi}_x}{\partial x}; \quad \dot{\varepsilon}_{yy} = z\frac{\partial \dot{\phi}_y}{\partial y}, \quad \dot{\gamma}_{xy} = z\left(\frac{\partial \dot{\phi}_x}{\partial y} + \frac{\partial \dot{\phi}_y}{\partial x}\right)$$
$$\dot{\gamma}_{xz} = \dot{\phi}_x + \frac{\partial \dot{w}}{\partial x}, \quad \dot{\gamma}_{yz} = \dot{\phi}_y + \frac{\partial \dot{w}}{\partial y} \tag{4.8.19}$$

The constitutive relations of the Prandtl–Reuss type as well as the Hencky type for a linearized elastic/plastic solid that behaves identically under loading and unloading are given by (Chakrabarty, 2000)

$$\dot{\sigma}_{xx} = E\left(\alpha\dot{\varepsilon}_{xx} + \beta\dot{\varepsilon}_{yy}\right); \quad \dot{\sigma}_{yy} = E\left(\beta\dot{\varepsilon}_{xx} + \gamma\dot{\varepsilon}_{yy}\right) \tag{4.8.20a}$$
$$\dot{\tau}_{xy} = G\dot{\gamma}_{xy}; \quad \dot{\tau}_{xz} = K_s G\dot{\gamma}_{xz}; \quad \dot{\tau}_{yz} = K_s G\dot{\gamma}_{yz} \tag{4.8.20b}$$

where $E$ is the elastic modulus, $G$ the effective shear modulus, and $K_s$ is the shear correction factor. The expressions for $(\alpha, \beta, \gamma, \rho)$ and the shear modulus $G$ are given below for the two different plasticity theories.

*Incremental theory of plasticity (IT):*

$$\alpha = \frac{1}{\rho}\left[4 - 3\left(1 - \frac{E_T}{E}\right)\frac{\sigma_1^2}{\bar{\sigma}^2}\right] \tag{4.8.21a}$$

$$\beta = \frac{1}{\rho}\left[2 - 2(1 - 2\nu)\frac{E_T}{E} - 3\left(1 - \frac{E_T}{E}\right)\frac{\sigma_1\sigma_2}{\bar{\sigma}^2}\right] \tag{4.8.21b}$$

$$\gamma = \frac{1}{\rho}\left[4 - 3\left(1 - \frac{E_T}{E}\right)\frac{\sigma_2^2}{\bar{\sigma}^2}\right] \tag{4.8.21c}$$

$$\rho = (5 - 4\nu) + (1 - 2\nu)^2\frac{E_T}{E} - 3(1 - 2\nu)\left(1 - \frac{E_T}{E}\right)\frac{\sigma_1\sigma_2}{\bar{\sigma}^2} \tag{4.8.21d}$$

$$\frac{E}{G} = 2(1 + \nu) \tag{4.8.21e}$$

*Deformation theory of plasticity (DT):*

$$\alpha = \frac{1}{\rho}\left[4 - 3\left(1 - \frac{E_T}{E_s}\right)\frac{\sigma_1^2}{\bar{\sigma}^2}\right] \tag{4.8.22a}$$

$$\beta = \frac{1}{\rho}\left[2 - 2(1 - 2\nu)\frac{E_T}{E} - 3\left(1 - \frac{E_T}{E_s}\right)\frac{\sigma_1\sigma_2}{\bar{\sigma}^2}\right] \tag{4.8.22b}$$

$$\gamma = \frac{1}{\rho}\left[4 - 3\left(1 - \frac{E_T}{E_s}\right)\frac{\sigma_2^2}{\bar{\sigma}^2}\right] \tag{4.8.22c}$$

$$\rho = 3\frac{E}{E_s} + (1 - 2\nu)\left[2 - (1 - 2\nu)\frac{E_T}{E} - 3\left(1 - \frac{E_T}{E_s}\right)\frac{\sigma_1\sigma_2}{\bar{\sigma}^2}\right] \tag{4.8.22d}$$

$$\frac{E}{G} = 2 + 2\nu + 3\left(\frac{E}{E_s} - 1\right) \tag{4.8.22e}$$

wherein the ratios of the elastic modulus $E$ to the tangent modulus $E_T$ and the secant modulus $E_S$ at the onset of buckling are expressed by the Ramberg–Osgood elastoplastic characteristic in the forms of

$$\frac{E}{E_T} = 1 + ck \left( \frac{\bar{\sigma}}{\sigma_0} \right)^{c-1}; \quad c > 1 \tag{4.8.23}$$

$$\frac{E}{E_s} = 1 + k \left( \frac{\bar{\sigma}}{\sigma_0} \right)^{c-1}; \quad c > 1 \tag{4.8.24}$$

The equivalent stress $\bar{\sigma}$ is defined on the basis of the von Mises yield criterion given by

$$\bar{\sigma}^2 = \sigma_1^2 - \sigma_1 \sigma_2 + \sigma_2^2 \tag{4.8.25}$$

Note that by setting the secant modulus $E_s$ in Eqs. (4.8.22a–e) to be equal to the elastic modulus (i.e., $E_s = E$), the expressions of $\alpha, \beta, \gamma, \rho$ of the Hencky deformation theory (DT) reduce to those corresponding to the incremental theory (IT) with Prandtl–Reuss equations.

To obtain the condition for bifurcation of the plate in the inelastic range, consider the uniqueness criterion in the form (Charkrabarty, 2000)

$$\int_V \left\{ (\dot{\sigma}_{xx} \dot{\varepsilon}_{xx} + \dot{\sigma}_{yy} \dot{\varepsilon}_{yy} + \dot{\tau}_{xy} \dot{\gamma}_{xy} + \dot{\tau}_{xz} \dot{\gamma}_{xz} + \dot{\tau}_{yz} \dot{\gamma}_{yz}) \right.$$
$$\left. - \sigma_1 \left( \frac{\partial w}{\partial x} \right)^2 - \sigma_2 \left( \frac{\partial w}{\partial y} \right)^2 \right\} dV > 0 \tag{4.8.26}$$

Using Eqs. (4.8.19) and (4.8.20) and integrating through the thickness of the plate, the condition for uniqueness is reduced to

$$\int_S \left\{ \frac{\alpha E h^3}{12} \left( \frac{\partial \phi_x}{\partial x} \right)^2 + \frac{\gamma E h^3}{12} \left( \frac{\partial \phi_y}{\partial y} \right)^2 + \frac{\beta E h^3}{6} \left( \frac{\partial \phi_x}{\partial x} \right) \left( \frac{\partial \phi_y}{\partial y} \right) \right.$$
$$+ \frac{G h^3}{12} \left( \frac{\partial \phi_x}{\partial x} + \frac{\partial \phi_y}{\partial y} \right)^2 + K_s G h \left[ \left( \phi_x + \frac{\partial w}{\partial x} \right)^2 + \left( \phi_y + \frac{\partial w}{\partial y} \right)^2 \right]$$
$$\left. - \sigma_1 h \left( \frac{\partial w}{\partial x} \right)^2 - \sigma_2 h \left( \frac{\partial w}{\partial y} \right)^2 \right\} dx dy > 0 \tag{4.8.27}$$

The Euler–Lagrange differential equations associated with the minimization of the functional with respect to arbitrary variations of

$(w, \phi_x, \phi_y)$ are easily shown to be

$$K_s Gh \left( \frac{\partial \phi_x}{\partial x} + \frac{\partial \phi_y}{\partial y} + \nabla^2 w \right) = \sigma_1 h \frac{\partial^2 w}{\partial x^2} + \sigma_2 h \frac{\partial^2 w}{\partial y^2} \qquad (4.8.28a)$$

$$\frac{\partial}{\partial x} \left( \frac{\alpha E h^3}{12} \frac{\partial \phi_x}{\partial x} + \frac{\beta E h^3}{12} \frac{\partial \phi_y}{\partial y} \right) + \frac{\partial}{\partial y} \left[ \frac{Gh^3}{12} \left( \frac{\partial \phi_x}{\partial y} + \frac{\partial \phi_y}{\partial x} \right) \right]$$
$$- K_s Gh \left( \phi_x + \frac{\partial w}{\partial x} \right) = 0 \qquad (4.8.28b)$$

$$\frac{\partial}{\partial y} \left( \frac{\gamma E h^3}{12} \frac{\partial \phi_y}{\partial y} + \frac{\beta E h^3}{12} \frac{\partial \phi_x}{\partial x} \right) + \frac{\partial}{\partial x} \left[ \frac{Gh^3}{12} \left( \frac{\partial \phi_x}{\partial y} + \frac{\partial \phi_y}{\partial x} \right) \right]$$
$$- K_s Gh \left( \phi_y + \frac{\partial w}{\partial y} \right) = 0 \qquad (4.8.28c)$$

If the tangent modulus and the secant modulus at the point of bifurcation are the same as the elastic modulus, i.e., $E_T = E_s = E$, we have

$$\alpha = \gamma = \frac{1}{1 - \nu^2}, \quad \beta = \frac{\nu}{1 - \nu^2} \qquad (4.8.29)$$

and Eqs. (4.8.28a–c) would then reduce to the well-known equations governing elastic buckling of Mindlin plates (Brunelle, 1971; Wang, 1995).

### 4.8.5 Buckling Solutions of Rectangular Plates

### Simply Supported Rectangular Plates

For a rectangular plate with simply supported edges, the boundary conditions are

$$w(0, y) = M_{xx}(0, y) = \phi_y(0, y) = 0 \qquad (4.8.30a)$$
$$w(x, 0) = M_{yy}(x, 0) = \phi_x(x, 0) = 0 \qquad (4.8.30b)$$
$$w(a, y) = M_{xx}(a, y) = \phi_y(a, y) = 0 \qquad (4.8.30c)$$
$$w(x, b) = M_{yy}(x, b) = \phi_x(x, b) = 0 \qquad (4.8.30d)$$

where the bending moment rates are

$$M_{xx} = \frac{Eh^3}{12} \left( \alpha \frac{\partial \phi_x}{\partial x} + \beta \frac{\partial \phi_y}{\partial y} \right)$$
$$M_{yy} = \frac{Eh^3}{12} \left( \beta \frac{\partial \phi_x}{\partial x} + \gamma \frac{\partial \phi_y}{\partial y} \right) \qquad (4.8.31)$$

The rates of displacement and rotations that satisfy the foregoing boundary conditions are given by

$$w = C_{mn}^{w} \sin\left(\frac{m\pi x}{a}\right) \sin\left(\frac{n\pi y}{b}\right) \tag{4.8.32a}$$

$$\phi_x = C_{mn}^{\phi_x} \cos\left(\frac{m\pi x}{a}\right) \sin\left(\frac{n\pi y}{b}\right) \tag{4.8.32b}$$

$$\phi_y = C_{mn}^{\phi_y} \sin\left(\frac{m\pi x}{a}\right) \cos\left(\frac{n\pi y}{b}\right) \tag{4.8.32c}$$

where $C_{mn}^{w}$, $C_{mn}^{\phi_x}$, and $C_{mn}^{\phi_y}$ ($m, n = 1, 2, \cdots$) are constants. The substitution of Eqs. (4.8.32a–c) into Eqs. (4.8.28a–c) results in the following three homogeneous equations which may be expressed as

$$\begin{bmatrix} A_{11} & A_{12} & A_{13} \\ & A_{22} & A_{23} \\ sym & & A_{33} \end{bmatrix} \begin{Bmatrix} C_{mn}^{w} \\ C_{mn}^{\phi_x} \\ C_{mn}^{\phi_y} \end{Bmatrix} = \begin{Bmatrix} 0 \\ 0 \\ 0 \end{Bmatrix} \tag{4.8.33}$$

where

$$A_{11} = K_s Gh \left(\frac{m^2\pi^2}{a^2} + \frac{n^2\pi^2}{b^2}\right) - \sigma_1 h \left(\frac{m^2\pi^2}{a^2}\right) - \sigma_2 h \left(\frac{n^2\pi^2}{b}\right) \tag{4.8.34a}$$

$$A_{12} = K_s Gh \left(\frac{m\pi}{a}\right) \tag{4.8.34b}$$

$$A_{13} = K_s Gh \left(\frac{n\pi}{b}\right) \tag{4.8.34c}$$

$$A_{22} = \frac{\alpha Eh^3}{12}\left(\frac{m^2\pi^2}{a^2}\right) + \frac{Gh^3}{12}\left(\frac{n^2\pi^2}{b^2}\right) + K_s Gh \tag{4.8.34d}$$

$$A_{23} = \left(\frac{\beta Eh^3}{12} + \frac{Gh^3}{12}\right)\left(\frac{mn\pi^2}{ab}\right) \tag{4.8.34e}$$

$$A_{33} = \frac{\gamma Eh^3}{12}\left(\frac{n^2\pi^2}{b^2}\right) + \frac{Gh^3}{12}\left(\frac{m^2\pi^2}{a^2}\right) + K_s Gh \tag{4.8.34f}$$

The critical buckling stress can be determined by setting the determinant of the matrix $[A]$ to zero.

Consider a square plate (i.e., $a = b$) constructed from an aluminum alloy where $E = 10.7$ msi, $\nu = 0.32$, $\sigma_0 = 61.4$ ksi, and the Ramberg–Osgood parameters $c = 20$ and $k = 0.3485$. The plate is subjected to a uniaxial load. The buckling stresses, obtained on the basis of the deformation theory (DT) and the incremental theory (IT), are given in

Table 4.18. The use of the deformation theory leads to a lower buckling stress value when compared to the corresponding value obtained using the incremental theory, since the latter theory gives a stiffer response in the plastic range. Also, it can be seen from Table 4.18 that Bleich's buckling results, known to agree well with experimental test results, are closer to the results of the deformation theory.

**Table 4.18:** Buckling stresses $\sigma_c$ (in ksi) for a simply supported plate under uniaxial load.

| $b/h$ | Incremental Theory (DT) | Deformation Theory (DT) | Bleich's Theory* |
|---|---|---|---|
| 22 | 70.844 | 60.080 | 56.125 |
| 23 | 65.166 | 58.836 | 55.139 |
| 24 | 60.713 | 57.397 | 54.109 |
| 25 | 57.363 | 55.730 | 52.988 |
| 26 | 54.598 | 53.806 | 51.712 |
| 27 | 51.938 | 51.569 | 50.185 |
| 28 | 49.112 | 48.962 | 48.269 |

* Note that Bleich's Theory gives

$$\sigma_c = \frac{\pi^2 E \sqrt{\frac{E_T}{E}}}{12(1-\nu^2)} \left(\frac{h}{b}\right)^2 \left[\frac{\frac{a}{b}}{n[\frac{E_T}{E}]^{\frac{1}{4}}} + \frac{\frac{E_T}{E}}{n[\frac{a}{b}]^{\frac{1}{4}}}\right]^2$$

where $n$ is the number of half-waves in which the plate buckles in the $x$-direction.

As presented in Figs. 4.26 and 4.27, critical buckling stress factors $(\sigma_c h b^2/\pi^2 D)$ are determined for simply supported, square plates with different thickness-to-width ratios $h/b$ and various values of $c$ and $E/\sigma_0$. Note that $D = Eh^3/[12(1-\nu^2)]$ is the plate flexural rigidity. The Poisson ratio $\nu = 0.3$ and the shear correction factor $K_s = 5/6$ are used in all calculations. The plate is subjected to either a uniaxial inplane load or an equibiaxial inplane load. It can be observed that the buckling stress factors obtained by the deformation theory are consistently lower than those obtained by the incremental theory.

Generally, the differences of results of these two theories increase with (1) increasing plate thickness (i.e., $h/b$ values) as evident from Figs. 4.26a and 4.26b, and (2) increasing $E/\sigma_0$ values as can be seen from

Figs. 4.27a and 4.27b. The Ramberg–Osgood hardening index $c$ and the loading configuration (i.e., uniaxial load or equibiaxial loads) also affect the divergence of results from the two theories. It is interesting to note that both theories give somewhat similar results when the plate is thin and equibiaxially loaded and the $c$ value is large (say, 20). Apart from the aforementioned situation, there is a marked difference in buckling stress factors from the two theories, which could be exploited when designing experimental tests to establish which one of the theories gives better estimates of the buckling loads for thick plates.

Figures 4.28a and 4.28b contain plots of variations of the buckling stress factors with respect to the aspect ratio $a/b$ of uniaxially loaded and equibiaxially loaded simply supported plates (of $h/b = 0.025$) for various values of $c$. It is worth noting that the kinks, where the number of half-wave switches, are displaced as a result of transverse shear deformation as well as the inelastic characteristics. In contrast to the uniaxial loaded plate case, there are no kinks in the variations of the buckling stress factors with respect to the aspect ratio, indicating that there is no mode switching.

## Rectangular Plates with Two Opposite Sides Simply Supported

Next, we consider rectangular plates with two opposite edges simply supported (edges $y = 0$ and $y = b$), while the other edges (edge $x = 0$ and edge $x = a$) may take on any combination of free, simply supported and clamped edges. The boundary conditions for the two simply supported parallel edges ($y = 0$ and $y = b$) are

$$w(x,0) = M_{yy}(x,0) = \phi_x(x,0) \tag{4.8.35a}$$
$$w(x,b) = M_{yy}(x,b) = \phi_x(x,b) \tag{4.8.35b}$$

and the boundary conditions for the other two edges ($x = 0$ and $x = a$) are given by (Xiang et al., 1996):

$$\text{Free edge}: \quad M_{xx} = M_{yx} = 0,$$
$$Q_x - \sigma_1 h \frac{\partial w}{\partial x} = 0 \tag{4.8.36}$$
$$\text{Simply supported edge}: \quad w = M_{xx} = \phi_y = 0 \tag{4.8.37}$$
$$\text{Clamped edge}: \quad w = \phi_x = \phi_y = 0 \tag{4.8.38}$$
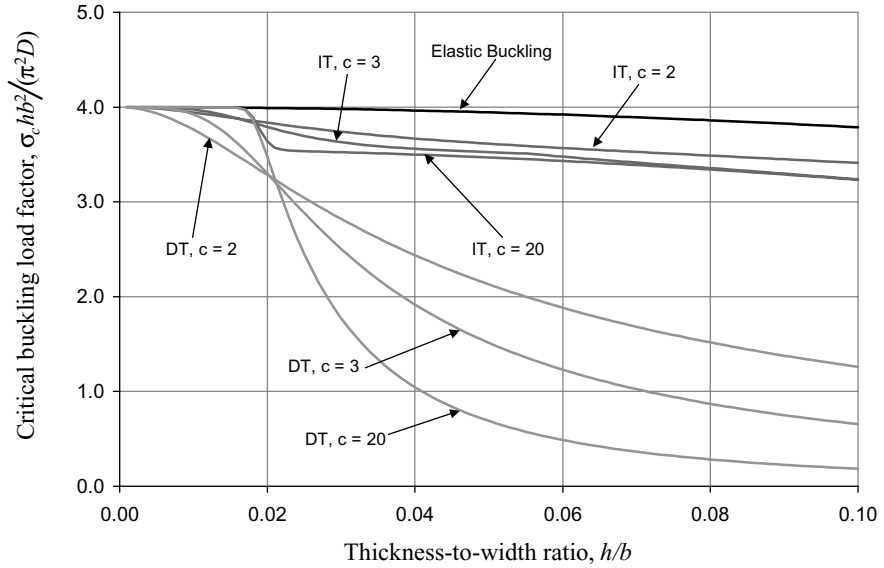
(a)
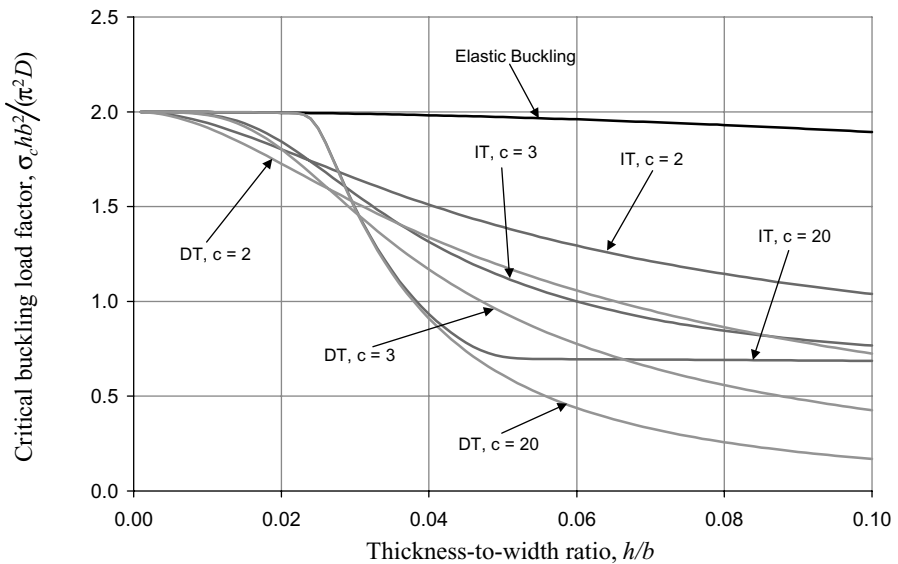


(b)

**Figure 4.26:** Critical buckling stress factors $\sigma_c h b^2/(\pi^2 D)$ versus thickness ratio $h/b$ for simply supported plates subjected to (a) uniaxial, and (b) equibiaxial loads ($E/\sigma_0 = 750$, $a/b = 1$, $\nu = 0.3$, $K_s = 5/6$, $k = 0.25$).
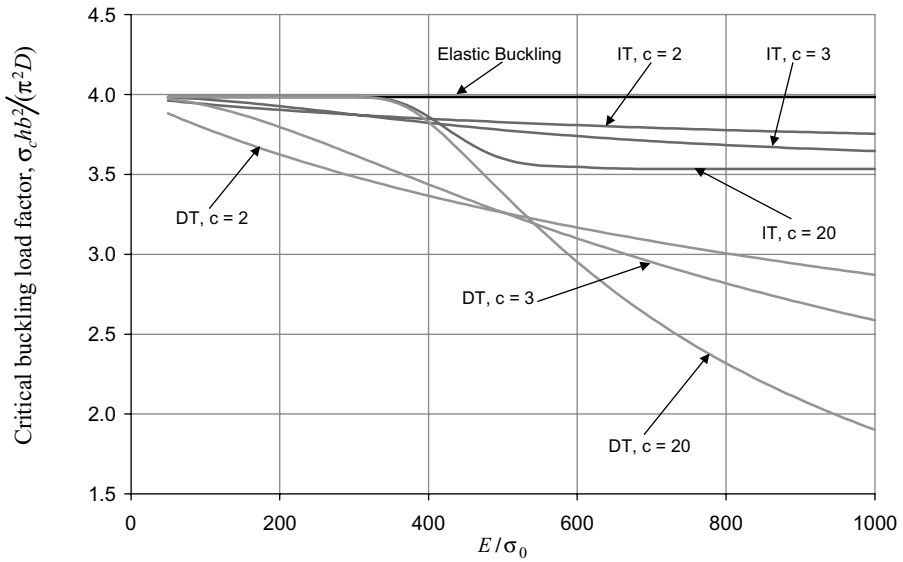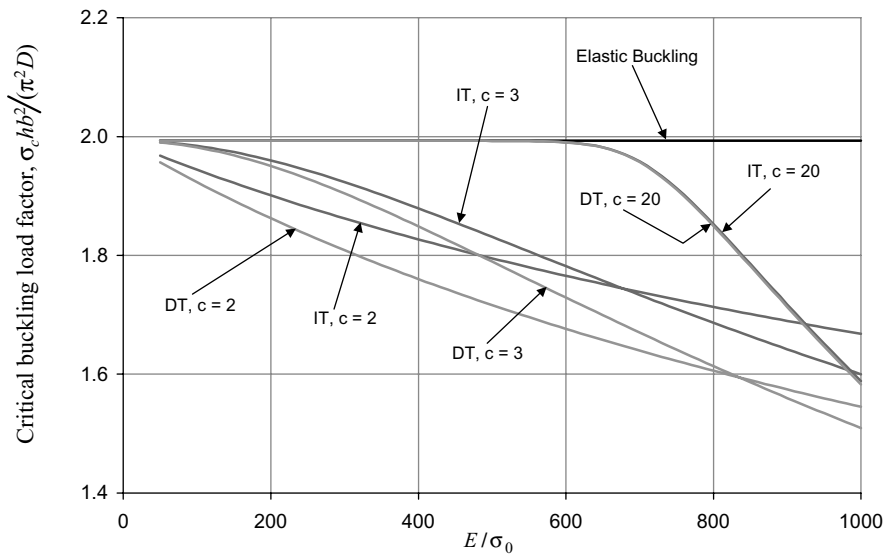
**Figure 4.27:** Critical buckling stress factors $\sigma_c hb^2/(\pi^2 D)$ versus $E/\sigma_0$ for simply supported plates subjected to (a) uniaxial, and (b) equibiaxial loads ($h/b = 0.025$, $a/b = 1$, $\nu = 0.3$, $K_s = 5/6$, $k = 0.25$).

**Figure 4.28:** Critical buckling stress factors $\sigma_c h b^2/(\pi^2 D)$ versus aspect ratio $a/b$ for simply supported plates subjected to (a) uniaxial, and (b) equibiaxial loads ($E/\sigma_0 = 750$, $h/b = 0.025$, $\nu = 0.3$, $K_s = 5/6$, $k = 0.25$).

in which

$$Q_x = K_s Gh \left( \phi_y + \frac{\partial w}{\partial x} \right) \tag{4.8.39a}$$

$$M_{xx} = \frac{Eh^3}{12} \left( \alpha \frac{\partial \phi_x}{\partial x} + \beta \frac{\partial \phi_y}{\partial y} \right) \tag{4.8.39b}$$

$$M_{yy} = \frac{Eh^3}{12} \left( \beta \frac{\partial \phi_x}{\partial x} + \gamma \frac{\partial \phi_y}{\partial y} \right) \tag{4.8.39c}$$

$$M_{xy} = \frac{Gh^3}{12} \left( \frac{\partial \phi_x}{\partial y} + \frac{\partial \phi_y}{\partial x} \right) \tag{4.8.39d}$$

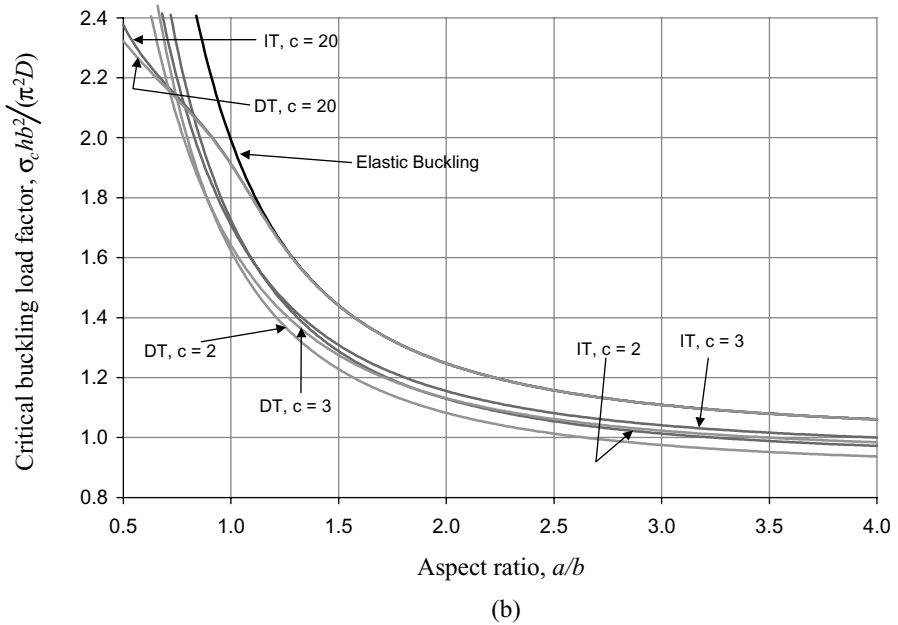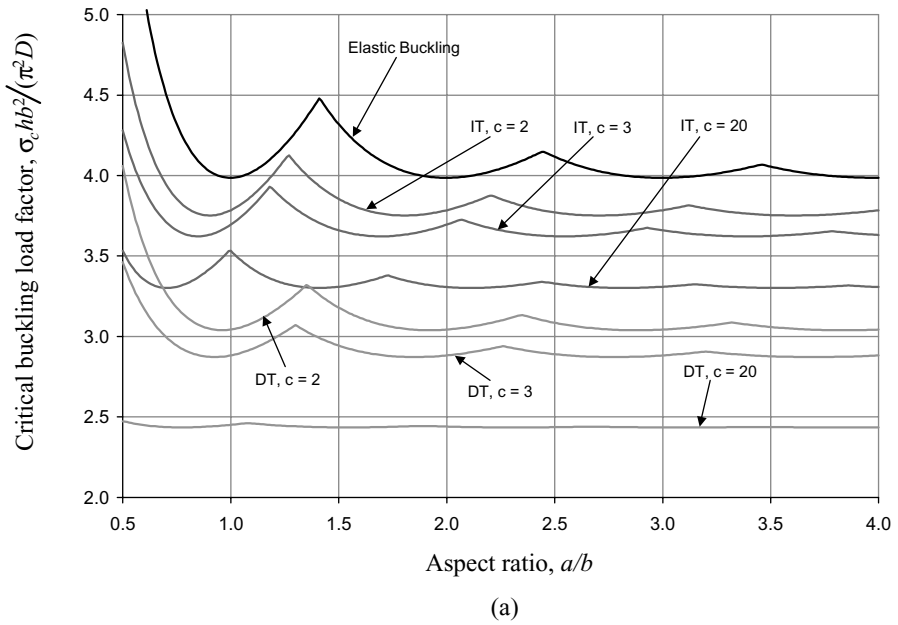For such rectangular plates with two opposite sides simply supported, the Levy type solution procedure may be used to solve the governing differential equations [Eqs. (4.8.28a–c)] for buckling of plates. The velocity fields of the plate may be expressed as (Xiang et al., 1996):

$$\left\{ \begin{array}{c} w(x,y) \\ \phi_x(x,y) \\ \phi_y(x,y) \end{array} \right\} = \left\{ \begin{array}{c} \eta_w(x) \sin \frac{m \pi y}{b} \\ \eta_x(x) \sin \frac{m \pi y}{b} \\ \eta_y(x) \cos \frac{m \pi y}{b} \end{array} \right\} \tag{4.8.40}$$

in which $\eta_w(x)$, $\eta_x(x)$ and $\eta_y(x)$ are unknown functions to be determined, and $m = 1, 2, \cdots, \infty$ is the number of half-waves of the buckling mode shape in the $y$-direction. Equation (4.8.40) satisfies the simply supported boundary conditions on edges $y = 0$ and $y = b$.

By substituting Eq. (4.8.40) into Eq. (4.8.28a–c), the following differential equation system can be derived:

$$\psi' = \mathbf{H} \psi \tag{4.8.41}$$

where $\psi = (\eta_w, \eta_w', \eta_x, \eta_x', \eta_y, \eta_y')$ and $\psi'$ is the first derivative of $\psi$ with respect to $x$, the prime ($'$) denotes the derivative with respect to $x$, and $\mathbf{H}$ is a $6 \times 6$ matrix with the following nonzero elements:

$$H_{12} = H_{34} = H_{56} = 1, \quad H_{21} = \frac{(K_s Gh - \sigma_2 h)(m \pi / b)^2}{K_s Gh - \sigma_1 h}$$

$$H_{24} = \frac{-K_s Gh}{K_s Gh - \sigma_1 h}, \quad H_{25} = \frac{K_s Gh (m \pi / b)}{K_s Gh - \sigma_1 h}, \quad H_{42} = \frac{-K_s Gh}{(\alpha Eh^3 / 12)}$$

$$H_{43} = \frac{-K_s Gh + (Gh^3 / 12)(m \pi / b)^2}{(\alpha Eh^3 / 12)}$$

$$H_{46} = \frac{[(\beta Eh^3 / 12) + (Gh^3 / 12)](m \pi / b)}{(\alpha Eh^3 / 12)}$$

$$H_{61} = \frac{K_s Gh(m\pi/b)}{(Gh^3/12)}, \quad H_{64} = \frac{-[(\beta Eh^3/12) + (Gh^3/12)](m\pi/b)}{(Gh^3/12)}$$

$$H_{65} = \frac{[K_s Gh + (\gamma Eh^3/12)(m\pi/b)^2]}{(Gh^3/12)} \tag{4.8.42}$$

The solution of the differential equation system [Eq. (4.8.41)] can be obtained as:

$$\Psi = e^{\mathbf{H}x}\mathbf{c} \tag{4.8.43}$$

where $\mathbf{c}$ is a constant column vector that can be determined from the boundary conditions of the plate and $e^{\mathbf{H}x}$ is the general matrix solution. The detailed procedure in determining Eq. (4.8.43) may be found in the paper by Xiang et al. (1996).

Applying the boundary conditions on the edges parallel to the $y$-axis, a homogeneous system of equations is obtained:

$$\mathbf{Kc} = \mathbf{0} \tag{4.8.44}$$

The buckling stresses $\sigma_1$ and $\sigma_2$ are determined by setting the determinant of $\mathbf{K}$ to be equal to zero. As the buckling stresses are imbedded in matrix $\mathbf{H}$, it cannot be obtained directly from Eq. (4.8.27). A numerical iteration procedure was used for the calculations (Xiang et al., 1996).

Tables 4.19 to 4.21 present the critical buckling stress factors of square plates under uniaxial and equibiaxial loads. In the calculations, $K_s = 5/6$ and $\nu = 0.3$ were taken. For brevity, we shall use the letters $F$ for free edge, $S$ for simply supported edge and $C$ for clamped edge and a four-letter designation to represent the boundary conditions of the plate. Thus, for example, a CSFS plate will have a clamped edge along $x = 0$, a simply supported edge along $y = 0$, a free edge along $x = a$ and a simply supported edge along $y = b$. It can be observed that for very thick plates ($h/b = 0.1$) and high values of $c$, the critical buckling load factors of the incremental theory do not vary much with respect to the $E/\sigma_0$ ratios. In contrast, the corresponding buckling results from the deformation theory decrease significantly with increasing $E/\sigma_0$ values for very thick plates. The buckling factors are much lower when compared to their thin plate counterparts due to the effect of transverse shear deformation.

In general, the deformation theory gives consistently lower values of critical buckling stress factor when compared to the corresponding results obtained using the incremental theory. The difference between the results of these two theories tends to increase with increasing thickness ratios, $E/\sigma_0$ values and the $c$ values of the Ramberg–Osgood

relation. Generally, plastic buckling stress factors are much reduced from its elastic counterparts, especially when the plate is thick, and the hardening index $c$ has a large value. The critical buckling stress factors obtained using the deformation theory are consistently lower than the corresponding factors of the incremental theory. The divergence of these two results increases with increasing plate thickness, $E/\sigma_0$ and $c$ values. This marked difference in buckling stress factors observed for thick plates could be exploited when designing experimental tests on plates to establish which of the two considered theories of plasticity give better buckling results.

### 4.8.6 Buckling of Simply Supported Polygonal Plates

It can be shown that the governing equation for inelastic buckling of a simply supported polygonal plate can be expressed in terms of the transverse velocity $w$ as (Wang, 2004)

$$\nabla^2 \left( \nabla^2 + \lambda \right) w = 0 \qquad (4.8.45)$$

where the plastic buckling stress factor $\lambda$ is given by

$$\lambda = \frac{\sigma h}{\frac{\alpha E h^3}{12} \left( 1 - \frac{\sigma h}{K_s G h} \right)} \qquad (4.8.46)$$

For a straight, simply supported edge, the boundary conditions along the edge are

$$w = 0, \quad \nabla^2 w = 0 \qquad (4.8.47)$$

The governing plastic buckling equation (4.8.45) and the boundary conditions given by Eq. (4.8.47) are of the same form as those of their corresponding elastic buckling problem of simply supported, thin plates of polygonal shape (Irschik, 1985; Wang, 1995). For the latter problem, the elastic buckling stress factor $\lambda_e$ is given by

$$\lambda_e = \frac{\sigma_e h}{D} \qquad (4.8.48)$$

in which $\sigma_e$ is the critical elastic buckling stress and $D$ the flexural rigidity of the plate. Thus, for the same polygonal plate dimensions, the plastic buckling stress based on the Mindlin plate theory may be related to its elastic buckling stress based on the classical thin plate theory as

$$\lambda = \lambda_e \implies \frac{\sigma h}{\alpha(1 - \nu^2) \left( 1 - \frac{\sigma}{K_s G} \right)} = \sigma_e \qquad (4.8.49)$$

**Table 4.19:** Critical buckling stress factors $\sigma_c h b^2/(\pi^2 D)$ for FSFS square plates ($K_s = 5/6$, $\nu = 0.3$, $k = 0.25$).

| $c$ | $E/\sigma_0$ | $\sigma_c h b^2/(\pi^2 D)$ | | | | | |
|-----|-----|-----|-----|-----|-----|-----|-----|
| | | $h/b = 0.025$ | | $h/b = 0.050$ | | $h/b = 0.075$ | |
| | | IT* | DT* | IT | DT | IT | DT |
| *Plates under uniaxial load in the x-direction* | | | | | | | |
| Elastic | – | 1.999 | 1.999 | 1.946 | 1.946 | 1.888 | 1.888 |
| 2 | 200 | 1.967 | 1.872 | 1.835 | 1.582 | 1.683 | 1.315 |
| | 300 | 1.952 | 1.819 | 1.794 | 1.473 | 1.624 | 1.188 |
| | 500 | 1.925 | 1.729 | 1.729 | 1.316 | 1.542 | 1.024 |
| 3 | 200 | 1.987 | 1.964 | 1.815 | 1.629 | 1.551 | 1.216 |
| | 300 | 1.974 | 1.925 | 1.722 | 1.447 | 1.433 | 1.015 |
| | 500 | 1.937 | 1.826 | 1.577 | 1.188 | 1.306 | 0.783 |
| 5 | 200 | 1.998 | 1.996 | 1.805 | 1.694 | 1.381 | 1.115 |
| | 300 | 1.994 | 1.988 | 1.624 | 1.424 | 1.240 | 0.858 |
| | 500 | 1.965 | 1.926 | 1.392 | 1.060 | 1.133 | 0.599 |
| 10 | 200 | 1.999 | 1.999 | 1.828 | 1.786 | 1.226 | 1.034 |
| | 300 | 1.999 | 1.999 | 1.520 | 1.413 | 1.113 | 0.892 |
| | 500 | 1.994 | 1.992 | 1.242 | 0.961 | 1.104 | 0.484 |
| 20 | 200 | 1.999 | 1.999 | 1.881 | 1.869 | 1.136 | 0.999 |
| | 300 | 1.999 | 1.999 | 1.467 | 1.418 | 1.104 | 0.819 |
| | 500 | 1.999 | 1.999 | 1.198 | 0.916 | 1.104 | 0.473 |
| *Plates under equibiaxial loads* | | | | | | | |
| Elastic | – | 0.9280 | 0.9280 | 0.9207 | 0.9207 | 0.9106 | 0.9106 |
| 2 | 200 | 0.9147 | 0.8992 | 0.8735 | 0.8241 | 0.8195 | 0.7372 |
| | 300 | 0.9083 | 0.8860 | 0.8531 | 0.7882 | 0.7852 | 0.6856 |
| | 500 | 0.8961 | 0.8618 | 0.8173 | 0.7308 | 0.7306 | 0.6119 |
| 3 | 200 | 0.9258 | 0.9241 | 0.8911 | 0.8693 | 0.8033 | 0.7468 |
| | 300 | 0.9232 | 0.9194 | 0.8605 | 0.8227 | 0.7304 | 0.6582 |
| | 500 | 0.9151 | 0.9052 | 0.7910 | 0.7302 | 0.6186 | 0.5346 |
| 5 | 200 | 0.9279 | 0.9279 | 0.9118 | 0.9074 | 0.7964 | 0.7659 |
| | 300 | 0.9278 | 0.9277 | 0.8821 | 0.8670 | 0.6709 | 0.6314 |
| | 500 | 0.9265 | 0.9257 | 0.7701 | 0.7367 | 0.5072 | 0.4618 |
| 10 | 200 | 0.9280 | 0.9280 | 0.9204 | 0.9204 | 0.8129 | 0.8021 |
| | 300 | 0.9280 | 0.9280 | 0.9125 | 0.9105 | 0.6298 | 0.6157 |
| | 500 | 0.9280 | 0.9280 | 0.7703 | 0.7582 | 0.4299 | 0.4114 |
| 20 | 200 | 0.9280 | 0.9280 | 0.9207 | 0.9207 | 0.8461 | 0.8428 |
| | 300 | 0.9280 | 0.9280 | 0.9206 | 0.9207 | 0.6217 | 0.6174 |
| | 500 | 0.9280 | 0.9280 | 0.7914 | 0.7877 | 0.4000 | 0.3930 |

*IT = Incremental theory of plasticity; DT = Deformation theory of plasticity.

**Table 4.20:** Critical buckling stress factors $\sigma_c h b^2/(\pi^2 D)$ for SSFS square plates ($K_s = 5/6$, $\nu = 0.3$, $k = 0.25$).

| | | $\sigma_c h b^2/(\pi^2 D)$ | | | | |
|---|---|---|---|---|---|---|---|
| $c$ | $E/\sigma_0$ | $h/b = 0.025$ | | $h/b = 0.050$ | | $h/b = 0.075$ | |
| | | IT* | DT* | IT | DT | IT | DT |
| *Plates under uniaxial load in the x-direction* | | | | | | | |
| Elastic | – | 2.312 | 2.312 | 2.245 | 2.245 | 2.169 | 2.169 |
| 2 | 200 | 2.232 | 2.132 | 2.013 | 1.758 | 1.797 | 1.436 |
| | 300 | 2.199 | 2.061 | 1.943 | 1.624 | 1.714 | 1.288 |
| | 500 | 2.143 | 1.942 | 1.844 | 1.437 | 1.606 | 1.101 |
| 3 | 200 | 2.278 | 2.250 | 1.965 | 1.773 | 1.610 | 1.283 |
| | 300 | 2.242 | 2.185 | 1.822 | 1.549 | 1.466 | 1.060 |
| | 500 | 2.154 | 2.033 | 1.632 | 1.250 | 1.318 | 0.811 |
| 5 | 200 | 2.307 | 2.305 | 1.926 | 1.809 | 1.402 | 1.143 |
| | 300 | 2.292 | 2.282 | 1.678 | 1.482 | 1.240 | 0.874 |
| | 500 | 2.199 | 2.149 | 1.408 | 1.085 | 1.151 | 0.607 |
| 10 | 200 | 2.311 | 2.311 | 1.926 | 1.880 | 1.228 | 1.043 |
| | 300 | 2.311 | 2.311 | 1.544 | 1.439 | 1.135 | 0.749 |
| | 500 | 2.280 | 2.272 | 1.248 | 0.968 | 1.129 | 0.485 |
| 20 | 200 | 2.311 | 2.311 | 1.973 | 1.959 | 1.150 | 1.002 |
| | 300 | 2.311 | 2.311 | 1.479 | 1.430 | 1.129 | 0.697 |
| | 500 | 2.310 | 2.310 | 1.215 | 0.919 | 1.129 | 0.435 |
| *Plates under equibiaxial loads* | | | | | | | |
| Elastic | – | 1.046 | 1.046 | 1.032 | 1.032 | 1.015 | 1.015 |
| 2 | 200 | 1.034 | 1.010 | 0.991 | 0.916 | 0.936 | 0.811 |
| | 300 | 1.028 | 0.994 | 0.973 | 0.874 | 0.905 | 0.752 |
| | 500 | 1.017 | 0.965 | 0.939 | 0.807 | 0.852 | 0.669 |
| 3 | 200 | 1.044 | 1.041 | 1.004 | 0.967 | 0.911 | 0.818 |
| | 300 | 1.041 | 1.034 | 0.973 | 0.910 | 0.836 | 0.716 |
| | 500 | 1.033 | 1.016 | 1.902 | 0.801 | 0.720 | 0.578 |
| 5 | 200 | 1.046 | 1.046 | 1.022 | 1.013 | 0.886 | 0.831 |
| | 300 | 1.045 | 1.045 | 0.987 | 0.957 | 0.748 | 0.677 |
| | 500 | 1.044 | 1.042 | 0.858 | 0.798 | 0.579 | 0.492 |
| 10 | 200 | 1.046 | 1.046 | 1.032 | 1.032 | 0.877 | 0.855 |
| | 300 | 1.046 | 1.046 | 1.016 | 1.010 | 0.675 | 0.646 |
| | 500 | 1.046 | 1.046 | 0.827 | 0.804 | 0.477 | 0.429 |
| 20 | 200 | 1.046 | 1.046 | 1.032 | 1.032 | 0.892 | 0.885 |
| | 300 | 1.046 | 1.046 | 1.031 | 1.032 | 0.647 | 0.636 |
| | 500 | 1.046 | 1.046 | 0.827 | 0.819 | 0.431 | 0.404 |

*IT = Incremental theory of plasticity; DT = Deformation theory of plasticity.

**Table 4.21:** Critical buckling stress factors $\sigma_c h b^2/(\pi^2 D)$ for CSFS square ($K_s = 5/6$, $\nu = 0.3$, $k = 0.25$).

| | | $\sigma_c h b^2/(\pi^2 D)$ | | | | | |
|---|---|---|---|---|---|---|---|
| | | $h/b = 0.025$ | | $h/b = 0.050$ | | $h/b = 0.075$ | |
| $c$ | $E/\sigma_0$ | IT* | DT* | IT | DT | IT | DT |
| *Plates under uniaxial load in the x-direction* | | | | | | | |
| Elastic | – | 2.336 | 2.336 | 2.268 | 2.268 | 2.189 | 2.189 |
| 2 | 200 | 2.251 | 2.150 | 2.022 | 1.767 | 1.801 | 1.441 |
| | 300 | 2.217 | 2.077 | 1.950 | 1.631 | 1.716 | 1.292 |
| | 500 | 2.157 | 1.955 | 1.848 | 1.442 | 1.607 | 1.103 |
| 3 | 200 | 2.300 | 2.271 | 1.972 | 1.780 | 1.611 | 1.285 |
| | 300 | 2.262 | 2.204 | 1.825 | 1.553 | 1.466 | 1.061 |
| | 500 | 2.168 | 2.046 | 1.632 | 1.252 | 1.319 | 0.812 |
| 5 | 200 | 2.332 | 2.329 | 1.931 | 1.815 | 1.402 | 1.144 |
| | 300 | 2.315 | 2.304 | 1.679 | 1.483 | 1.241 | 0.874 |
| | 500 | 2.215 | 2.163 | 1.408 | 1.085 | 1.153 | 0.607 |
| 10 | 200 | 2.336 | 2.336 | 1.929 | 1.883 | 1.228 | 1.043 |
| | 300 | 2.336 | 2.335 | 1.544 | 1.439 | 1.137 | 0.749 |
| | 500 | 2.300 | 2.292 | 1.250 | 0.968 | 1.131 | 0.485 |
| 20 | 200 | 2.336 | 2.336 | 1.976 | 1.962 | 1.151 | 1.002 |
| | 300 | 2.336 | 2.336 | 1.479 | 1.431 | 1.131 | 0.697 |
| | 500 | 2.355 | 2.335 | 1.216 | 0.919 | 1.131 | 0.435 |
| *Plates under equibiaxial loads* | | | | | | | |
| Elastic | - | 1.130 | 1.130 | 1.112 | 1.112 | 1.090 | 1.090 |
| 2 | 200 | 1.119 | 1.089 | 1.075 | 0.981 | 1.020 | 0.862 |
| | 300 | 1.114 | 1.071 | 1.059 | 0.934 | 0.991 | 0.798 |
| | 500 | 1.104 | 1.038 | 1.028 | 0.860 | 0.943 | 0.707 |
| 3 | 200 | 1.128 | 1.124 | 1.084 | 1.035 | 0.991 | 0.866 |
| | 300 | 1.125 | 1.116 | 1.055 | 0.970 | 0.917 | 0.755 |
| | 500 | 1.118 | 1.094 | 0.985 | 0.849 | 0.800 | 0.607 |
| 5 | 200 | 1.130 | 1.130 | 1.100 | 1.086 | 0.953 | 0.873 |
| | 300 | 1.130 | 1.129 | 1.062 | 1.018 | 0.810 | 0.707 |
| | 500 | 1.128 | 1.125 | 0.925 | 0.838 | 0.638 | 0.511 |
| 10 | 200 | 1.130 | 1.130 | 1.111 | 1.111 | 0.923 | 0.889 |
| | 300 | 1.130 | 1.130 | 1.087 | 1.075 | 0.712 | 0.666 |
| | 500 | 1.130 | 1.130 | 0.870 | 0.833 | 0.523 | 0.441 |
| 20 | 200 | 1.130 | 1.130 | 1.112 | 1.112 | 0.921 | 0.909 |
| | 300 | 1.130 | 1.130 | 1.109 | 1.112 | 0.667 | 0.649 |
| | 500 | 1.130 | 1.130 | 0.851 | 0.839 | 0.477 | 0.411 |

*IT = Incremental theory of plasticity; DT = Deformation theory of plasticity.

Equation (4.8.49) may be used to compute exact plastic buckling loads of simply supported Mindlin plates upon supplying the corresponding exact elastic buckling loads according to the classical thin plate theory.

## REFERENCES

Bartdorf, S. B. (1949), "Theories of plastic buckling," *Journal of the Aeronautical Sciences,* **16**, 405–408.

Bijlaard, P. P. (1949), "Theory and tests on the plastic stability of plates and shells," *Journal of the Aeronautical Sciences*, **9**, 529–541.

Bleich, F. (1952), *Buckling Strength of Metal Structures.* McGraw-Hill, New York.

Braun, M. (1993), *Differential Equations and Their Applications,* 4th ed., Springer, New York.

Brunelle, E. J. (1971), "Buckling of transversely isotropic Mindlin plates," *AIAA Journal*, **9**(6), 1018–1022.

Bulson, P. L. (1970), *The Stability of Flat Plates,* Chatto and Windus, London, United Kingdom.

Chakrabarty, J. (2000), *Applied Plasticity*, Springer-Verlag, New York.

Chou, F. S., Wang, C. M., Cheng, G. D. and Olhoff, N. (1999), "Optimal design of internal ring supports for vibrating circular plates," *Journal of Sound and Vibration*, **219**(3), 525–537.

Durban, D. and Zuckerman, Z. (1999), "Elastoplastic buckling of rectangular plates in biaxial compression/tension," *International Journal of Mechanical Sciences*, **41**, 751–765.

Eisenberger, M. and Alexandrov, A. (2000),"Stability analysis of stepped thickness plate," *Computational Methods for Shell and Spatial Structures,* IASS-IACM 2000, M. Papadrakakis, A. Samartin and E. Onate (Eds.), ISASR-NTUA, Athens, Greece.

El-Ghazaly, H. A. and Sherbourne, A. N. (1986), "Deformation theory for elastic–plastic buckling analysis of plates under non-proportional planar loading," *Computers and Structures*, **22**(2), 131–149.

Gupta, P. R. and Reddy, J. N. (2002), "Buckling and vibration of orthotropic plates with internal line hinge," *International Journal of Structural Stability and Dynamics*, **2**(3), 385–408.

Han, L. S. (1960), "The buckling and deflection of isosceles–triangular plates," *Journal of Applied Mechanics,* **27**, 207–208.

Handelman, G. H. and Prager, W. (1948), "Plastic buckling of rectangular plates under edge thrusts," NACA Tech. Note No. 1530, Washington, DC.

Harik, I. E. and Andrade, M. G. (1989), "Stability of plates with step variation in thickness," *Computers and Structures,* **33**, 257–263.

Hong, G. M., Wang, C. M. and Tan, T. J. (1993), "Analytical buckling solutions for circular Mindlin plates: inclusion of inplane prebuckling deformation," *Archive of Applied Mechanics*, **63**, 534–542.

Illyushin, A. A. (1947), "The elastic plastic stability of plates," NACA Technical Memorandum, 1188, Washington, DC.

Inoue, T. and Kato, B. (1993), "Analysis of plastic buckling of steel plates," *International Journal of Solids and Structures*, **30**(6), 835–856.

Irschik, H. (1985), "Membrane-type eigen motions of Mindlin plates," *Acta Mechanica,* **55**, 1–20.

Kanaka Raju, K. and Venkateswara Rao, G. (1983), "Postbuckling analysis of moderately thick elastic circular plates," *Journal of Applied Mechanics*, **50**, 468–470.

Kaufmann, W. (1936), "Uber unelastisches Knicken rechtiger Platten," *Ing. Archiv.*, **7**(6), 156.

Kerr, A. D. (1962), "On the stability of circular plates," *Journal of Aerospace Science,* **29**(4), 486–487.

Kollbrunner, C. F. (1946), "Das Ausbeulun der auf einseitigen, gleichmassig verteilten Druck beanspruchten Platten im elastichen und plastichen Bereich," Mitteilungen 17, Institut fur Baustatic, Eidgenossische Technische Hoschule, Zurich.

Laura, P. A. A., Gutierrez, R. H., Sanzi, H. C. and Elvira, G. (2000), "Buckling of circular, solid and annular plates with an intermediate circular support," *Ocean Engineering*, **27**, 749–755.

Liew, K.M., Xiang, Y. and Kitipornchai, S. (1996), "Analytical buckling solutions for Mindlin plates involving free edges," *International Journal of Mechanical Sciences*, **38**(10), 1127–1138.

McFarland, D., Smith, B. L. and Bernhart, W. D. (1972), *Analysis of Plates,* Spartan Books, Philadelphia, PA.

Mindlin, R.D. (1951), "Influence of rotatory inertia and shear on flexural motions of isotropic, elastic plates," *Journal of Applied Mechanics*, **18**, 31–38.

Ore, E. and Durban, D. (1989), "Elastoplastic buckling of annular plates in pure shear," *Journal of Applied Mechanics*, **56**, 644–651.

Panc, V. (1975), *Theories of Elastic Plates,* Noordhoff, Leyden, The Netherlands.

Pearson, C. E. (1950), "Bifurcation criteria and plastic buckling of plates and columns," *Journal of the Aeronautical Sciences*, **7**, 417–424.

Reddy, J. N. (1984), *Energy and Variational Methods in Applied Mechanics,* John Wiley, New York.

Reddy, J. N. (1999), *Theory and Analysis of Elastic Plates,* Taylor & Francis, Philadelphia, PA.

Reddy, J. N. (2002), *Energy Principles and Variational Methods in Applied Mechanics,* 2nd ed., John Wiley, New York.

Reddy, J. N. (2004), *Mechanics of Laminated Composite Plates and Shells: Theory and Analysis,* 2nd ed., CRC Press, Boca Raton, FL.

Reismann, H. (1952), "Bending and buckling of an elastically restrained circular plate," *Journal of Applied Mechanics,* **19**, 167–172.

Shrivastava, S. C. (1979), "Inelastic buckling of plates including shear effects," *International Journal of Solids and Structures*, **15**, 567–575.

Stowell, E. Z. (1948), "A unified theory of plastic buckling of columns and plates," Tech. Note, NACA-1556.

Szilard, R. (1974), *Theory and Analysis of Plates. Classical and Numerical Methods,* Prentice-Hall, Englewood Cliffs, NJ.

Thevendran, V. and Wang, C. M., (1996), "Buckling of annular plates elastically restrained against rotation along edges," *Thin-Walled Structures,* **25**(3), 231–246.

Timoshenko, S. P. and Woinowsky-Krieger, S. (1970), *Theory of Plates and Shells,* McGraw–Hill, Singapore.

Timoshenko, S. P. and Gere, J. M. (1961), *Theory of Elastic Stability,* McGraw-Hill, New York.

Tugcu, P. (1991), "Plate buckling in the plastic range," *International Journal of Mechanical Sciences*, **33**(1), 1–11.

Ugural, A. C. (1981), *Stresses in Plates and Shells,* McGraw-Hill, New York.

Wang, C. M. (1995), "Allowance for prebuckling deformations in buckling load relationship between Mindlin and Kirchhoff simply supported plates of general polygonal shape," *Engineering Structures*, **17**(6), 413–418.

Wang, C. M. (2004), "Plastic buckling of simply supported, polygonal Mindlin plates," *Journal of Engineering Mechanics,* **130**(1), 117–122.

Wang, C. M. and Liew, K. M. (1994), "Buckling of triangular plates under uniform compression," *Engineering Structures,* **16**(1), 43–50.

Wang, C. M., Reddy, J. N. and Lee, K. H. (2000), *Shear Deformable Beams and Plates. Relationships with Classical Solutions,* Elsevier, Cambridge, UK.

Wang, C. Y. and Wang, C. M. (2001), "Buckling of circular plates with an internal ring support and elastically restrained edges," *Thin-Walled Structures*, **39**, 821–825.

Wang, C. M., Xiang, Y. and Chakrabarty, J. (2001), "Elastic/plastic buckling of thick plates," *International Journal of Solids and Structures,* **38**, 8617–8640.

Wang, C. M., Chen, Y. and Xiang, Y. (2004), "Stability criteria for rectangular plates subjected to intermediate and end inplane loads," *Thin-Walled Structures*, **42**, 119–136.

Xiang, Y. (2003), "Exact solutions for buckling of multi-span rectangular plates," *Journal of Engineering Mechanics, ASCE,* **129**(2), 181–187.

Xiang, Y. and Reddy, J. N. (2001), "Buckling and vibration of stepped, symmetric cross-ply laminated rectangular plates," *International Journal of Structural Stability and Dynamics*, **1**(3), 385–408.

Xiang, Y., Liew, K. M. and Kitipornchai, S. (1996), "Exact buckling solutions for composite laminates; proper free edge condition under inplane loadings," *Acta Mechanica*, **117**(1–4), 115–128.

Xiang, Y. and Wang, C. M. (2002), "Exact solutions for buckling and vibration of stepped rectangular plates," *Journal of Sound and Vibration,* **250**(3), 503–517.

Xiang, Y., Wang, C. M. and Wang, C. Y. (2001), "Buckling of rectangular plates with internal hinge," *International Journal of Structural Stability and Dynamics,* **1**(2), 169–179.

Xiang, Y., Wang, C. M. and Kitipornchai, S. (1994), "Exact vibration solution for initially stressed Mindlin plates on Pasternak foundation," *International Journal of Mechanical Sciences*, **36**(4), 311–316.

Xiang, Y., Wang, C. M. and Kitipornchai, S. (2003), "Exact buckling solutions for rectangular plates under intermediate and end uniaxial loads," *Journal of Engineering Mechanics,* **129**(7), 835–838.

Yamaki, N. (1958), "Buckling of a thin annular plate under uniform compression," *Journal of Applied Mechanics*, **25**, 267–273.

Ye, J. (1995), "Axisymmetric buckling of homogeneous and laminated circular plates," *Journal Structural Engineering, ASCE*, **121**(8), 1221–1224.

# BUCKLING OF SHELLS

## 5.1 Preliminary Comments

In this chapter, we present the exact elastic buckling solutions of cylindrical shells, spherical shells and conical shells. For the derivation of the governing equations, the reader may refer to the following textbooks which have at least a chapter that is devoted to shell buckling: Timoshenko and Gere, 1961; Brush and Almroth, 1975; Donnell, 1976; Calladine, 1983; Bažant and Cedolin, 1991; and Ugural, 1999.

## 5.2 Axisymmetric Buckling of Circular Cylindrical Shells under Uniform Axial Compression

Consider a circular cylindrical shell of thickness $h$, radius $R$ and subjected to a uniform axial compressive force $N$ (positive for compression). The governing equation of the axisymmetric buckling of such a loaded shell is given by (Lorenz, 1908; Timoshenko, 1910)

$$D\frac{d^4w}{dx^4} + N\frac{d^2w}{dx^2} + \frac{Eh}{R^2}w = 0 \qquad (5.2.1)$$

where $x$ is the axial coordinate, $w$ the radial deflection and $D = Eh^3/[12(1-\nu^2)]$ the bending rigidity. Equation (5.2.1) is similar to the buckling equation of a column/beam with elastic foundation.

For a simply supported cylindrical shell having the shell length $L$ which is a multiple of the half sine waves $m$ in the longitudinal direction, or if the shell is very long and the boundary conditions are not considered, the exact solution to the fourth-order differential equation (5.2.1) takes the form of

$$w = C\sin\frac{m\pi x}{L} \qquad (5.2.2)$$
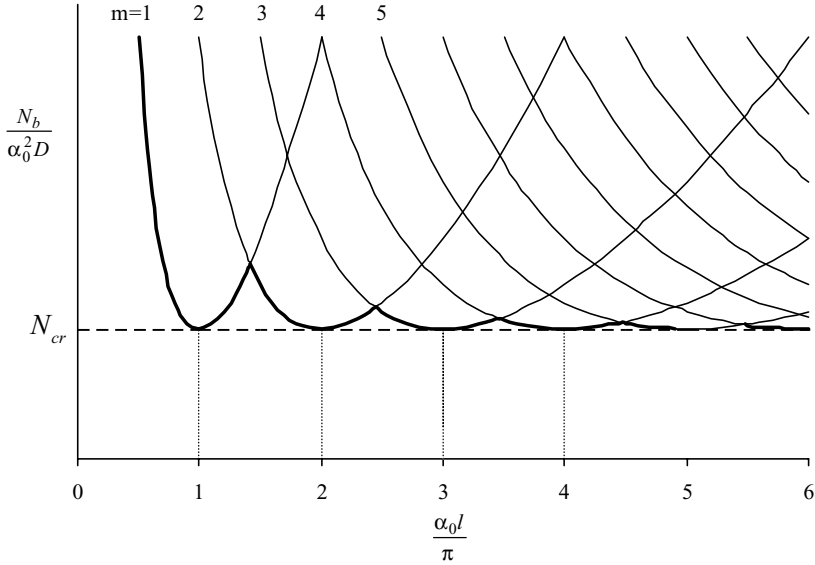
where $C$ is a constant.

**Figure 5.1:** Critical axisymmetric buckling load of cylindrical shell.

The substitution of Eq. (5.2.2) into Eq. (5.2.1) provides the exact buckling load $N_b$

$$N_b = D \left[ \alpha^2 + \frac{Eh}{\alpha^2 R^2 D} \right] \tag{5.2.3}$$

which clearly depends on $\alpha = m\pi/L$. By taking the stationarity condition of Eq. (5.2.3) with respect to $\alpha$ gives

$$\alpha_o = \left[ \frac{Eh}{R^2 D} \right]^{1/4} \tag{5.2.4}$$

and its substitution into Eq. (5.2.3) yields the least positive value of the critical buckling load

$$N_{cr} = \frac{1}{\sqrt{3(1 - \nu^2)}} \left( \frac{Eh^2}{R} \right) \tag{5.2.5}$$

If the length of the shell $L$ is not compatible with the half-wavelength, the critical load and the number of half-waves can be determined from Figure 5.1 which shows the various numbers $m$ of half-waves with respect to $\alpha = m\pi/L$.

It can be seen that the critical axisymmetric buckling load is proportional to $Eh^2/R$ and represents an upper bound on the actual collapse load.

## 5.3 Nonaxisymmetric Buckling of Circular Cylindrical Shells under Uniform Axial Compression

For nonaxisymmetric buckling of cylindrical shells, the governing differential equations are given by (Timoshenko and Gere, 1961; Brush and Almroth, 1975)

$$\frac{\partial^2 u}{\partial x^2} + \frac{1+\nu}{2R}\frac{\partial^2 v}{\partial x\partial\theta} - \frac{\nu}{R}\frac{\partial w}{\partial x} + \frac{1-\nu}{2R^2}\frac{\partial^2 u}{\partial\theta^2} = 0 \qquad (5.3.1)$$

$$\frac{1+\nu}{2R}\frac{\partial^2 u}{\partial x\partial\theta} + \frac{1-\nu}{2}\frac{\partial^2 v}{\partial x^2} + \frac{1}{R^2}\frac{\partial^2 v}{\partial\theta^2} - \frac{1}{R^2}\frac{\partial w}{\partial\theta} - \frac{N(1-\nu^2)}{Eh}\frac{\partial^2 v}{\partial x^2}$$
$$+ \frac{h^2}{12R^2}\left[\frac{1}{R^2}\frac{\partial^2 v}{\partial\theta^2} + \frac{1}{R^2}\frac{\partial^3 w}{\partial\theta^3} + \frac{\partial^3 w}{\partial x^2\partial\theta} + (1-\nu)\frac{\partial^2 v}{\partial x^2}\right] = 0 \qquad (5.3.2)$$

$$\nu\frac{\partial u}{\partial x} + \frac{1}{R}\frac{\partial v}{\partial\theta} - \frac{w}{R} - \frac{h^2}{12R^2}\left[\frac{1}{R}\frac{\partial^3 v}{\partial\theta^3} + (2-\nu)R\frac{\partial^3 v}{\partial x^2\partial\theta} + R^3\frac{\partial^4 w}{\partial x^4}\right.$$
$$\left. + \frac{1}{R}\frac{\partial^4 w}{\partial\theta^4} + 2R\frac{\partial^4 w}{\partial x^2\partial\theta^2}\right] - \frac{NR(1-\nu^2)}{Eh}\frac{\partial^2 w}{\partial x^2} = 0 \qquad (5.3.3)$$

in which $u$, $v$, $w$ are the longitudinal displacement, tangential displacement and radial displacement, respectively.

If the origin of coordinates is located at one end of the cylindrical shell, the general solution of Eqs. (5.3.1) to (5.3.3) can be expressed as

$$u = \frac{C_1}{\nu R}x + C_2 + \sum_{m}^{\infty}\sum_{n}^{\infty} A_{mn}\sin n\theta\cos\frac{m\pi x}{L} \qquad (5.3.4)$$

$$v = \sum_{m}^{\infty}\sum_{n}^{\infty} B_{mn}\cos n\theta\sin\frac{m\pi x}{L} \qquad (5.3.5)$$

$$w = C_1 + \sum_{m}^{\infty}\sum_{n}^{\infty} C_{mn}\sin n\theta\sin\frac{m\pi x}{L} \qquad (5.3.6)$$

where $A_{mn}$, $B_{mn}$, $C_{mn}$ are the unknown buckling amplitudes. Note that for the particular case in which the solution is expressed only in terms of $C_1$ and $C_2$, we have the cylindrical form of equilibrium where the compressed cylindrical shell uniformly expands laterally. For long cylindrical shells, the simply supported shell results from Eqs. (5.3.4) to (5.3.6) can be used irrespective of the type of edge restraints.

Denoting $\beta = m\pi R/L$ and by substituting Eqs. (5.3.4) to (5.3.6) into Eqs. (5.3.1) to (5.3.3), one obtains the following algebraic equations

$$A_{mn}\left(\beta^2 + \frac{1-\nu^2}{2}n^2\right) + B_{mn}\frac{n(1+\nu)\beta}{2} + C_{mn}\nu\beta = 0 \qquad (5.3.7)$$

$$A_{mn}\frac{n(1+\nu)\beta}{2} + B_{mn}\left[(1-\nu)\left(\frac{1}{2}+\frac{h^2}{12R^2}\right)\beta^2 + \left(1+\frac{h^2}{12R^2}\right)n^2\right.$$

$$\left. - \frac{N(1-\nu^2)}{Eh}\beta^2\right] + C_{mn}n\left[1+\frac{h^2}{12R^2}(n^2+\beta^2)\right] = 0 \qquad (5.3.8)$$

$$A_{mn}\nu\beta + B_{mn}n\left\{1+\frac{h^2}{12R^2}\left[n^2+(2-\nu)\right]\beta^2\right\}$$

$$+ C_{mn}\left[1 - \frac{N(1-\nu^2)}{Eh}\beta^2 + \frac{h^2}{12R^2}(n^2+\beta^2)^2\right] = 0 \quad (5.3.9)$$

The exact buckling load of the cylindrical shell is determined by setting the determinant of these three linear equations to zero. Sample critical buckling factors are given in Table 5.1 for simply supported, cylindrical shells under axial compression.

**Table 5.1:** Critical buckling factors $N_c R\sqrt{3(1-\nu^2)}/Eh^2$ for simply supported cylindrical shells under axial compression ($\nu = 0.3$)

| $h/R$ | $L/R$ | $N_c R\sqrt{3(1-\nu^2)}/Eh^2$ |
|-------|-------|-------------------------------|
| 1/100 | 1 | 0.962416 ($m=1, n=7$) |
|       | 5 | 0.904858 ($m=1, n=3$) |
|       | 10 | 0.886141 ($m=3, n=4$) |
| 1/500 | 1 | 0.984486 ($m=1, n=11$) |
|       | 5 | 0.924240 ($m=1, n=5$) |
|       | 10 | 0.924240 ($m=2, n=5$) |

If we neglect the terms containing the squares of $h^2/12a^2$ and $N(1-\nu^2)/Eh$, as they are rather small with respect to unity, the expanded characteristic equation may be expressed as

$$N = \frac{Eh}{1-\nu^2}\frac{\Phi}{\Psi} \qquad (5.3.10)$$

where

$$\Phi = (1-\nu^2)\beta^4 + \frac{h^2}{12R^2}\left[(n^2+\beta^2)^4 - (3-\nu)(2+\nu)n^2\beta^4\right.$$

$$\left. + 2(1-\nu^2)\beta^4 - (7+\nu)n^4\beta^2 + (3+\nu)n^2\beta^2 + n^4 - 2n^6\right] (5.3.11)$$

$$\Psi = \beta^2 \left\{ (n^2 + \beta^2)^2 + \left( n^2 + \frac{2}{1-\nu}\beta^2 \right) \left[ 1 + \frac{h^2}{12R^2}(n^2 + \beta^2)^2 \right] \right.$$

$$\left. - \frac{2\nu^2\beta^2}{1-\nu} + \frac{h^2}{12R^2}\left( n^2 + \frac{2}{1-\nu}\beta^2 \right)\left[ n^2 + (1-\nu)\beta^2 \right] \right\} \quad (5.3.12)$$

The foregoing equation includes the ring and chessboard buckling modes as special cases. For a ring buckling mode, the radial displacements are in the form of waves along the length of the shell with the displacements constant around the perimeter of any transverse section. The chessboard buckling mode takes the form of waves in both the longitudinal and transverse directions, giving a pattern of rectangular depressions and bulges all over the shell.

By observing that the minimum value of $N$ takes place when $\beta^2$ and $n^2$ are large numbers, the expression in Eq. (5.3.10) may be simplified to

$$N = \frac{Eh}{(1-\nu^2)} \left[ \frac{h^2}{12R^2} \frac{(n^2 + \beta^2)^2}{\beta^2} + \frac{(1-\nu^2)\beta^2}{(n^2 + \beta^2)^2} \right] \quad (5.3.13)$$

The buckling mode associated with Eq. (5.3.13) is of the chessboard type. Note that when $n = 0$, the above expression reduces to the critical axisymmetric buckling load of shells given by Eq. (5.2.3).

In order to determine the minimum value of $N$, we let $\xi = (n^2 + \beta^2)^2/\beta^2$ and equation (5.3.13) becomes

$$N = \frac{Eh}{(1-\nu^2)} \left[ \frac{h^2}{12R^2}\xi + \frac{(1-\nu^2)}{\xi} \right] \quad (5.3.14)$$

Taking the stationarity condition of $N$ with respect to $\xi$ furnishes

$$\xi = \sqrt{\frac{12R^2(1-\nu^2)}{h^2}} \quad (5.3.15)$$

and when substituted into Eq. (5.3.14) yields the minimum value of $N$

$$N_{\min} = \frac{1}{\sqrt{3(1-\nu)}} \left( \frac{Eh^2}{R} \right) \quad (5.3.16)$$

Interestingly, this buckling load coincides with Eq. (5.2.5). It is worth noting that the critical buckling load depends on the material properties, thickness and radius and it is independent of the length of the cylindrical shell.

Xiang et al. (2004) obtained exact buckling solutions for axially compressed, cylindrical shells with intermediate ring supports as shown in Fig. 5.2. In solving the buckling problem, they first divided the shell into segments at the locations of the ring supports. The displacement fields for the $i$th segment may be expressed as

$$
\begin{aligned}
u_i(x,\theta) &= U_i(x)\cos n\theta \\
v_i(x,\theta) &= V_i(x)\sin n\theta \\
w_i(x,\theta) &= W_i(x)\cos n\theta
\end{aligned}
\qquad (5.3.17)
$$

where the subscript $i$ $(i = 1, 2, \ldots, m)$ denotes the $i$th segment of the shell, $2n$ is the number of half-waves of the buckling mode in the circumferential direction, and $U_i(x)$, $V_i(x)$ and $W_i(x)$ are unknown functions to be determined. Using the state space technique and the domain decomposition method, a homogenous differential equation system for the $i$th segment can be derived in view of Eqs. (5.3.1) to (5.3.3) and Eqs. (5.3.17a–c) after appropriate algebraic operations:

$$
\mathbf{\Psi}_i' - \mathbf{H}_i \mathbf{\Psi}_i = \mathbf{0} \qquad (5.3.18)
$$

in which

$$
\mathbf{\Psi}_i = \{\, U_i \quad U_i' \quad V_i \quad V_i' \quad W_i \quad W_i' \quad W_i'' \quad W_i''' \,\}^{\mathrm{T}} \qquad (5.3.19)
$$

The prime in Eq. (5.3.19) denotes the derivative with respect to $x$, and $\mathbf{H}_i$ is an $8 \times 8$ matrix with the following nonzero elements:
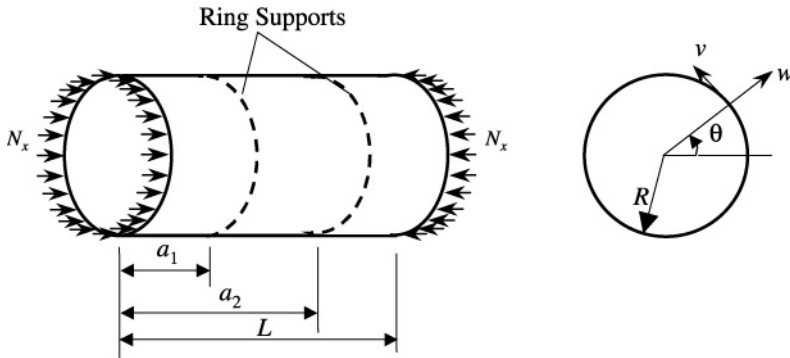


**Figure 5.2:** Geometry and coordinate system of a circular cylindrical shell with intermediate ring supports and subjected to axial compression.

$$(H_i)_{12} = (H_i)_{34} = (H_i)_{56} = (H_i)_{67} = (H_i)_{78} = 1$$

$$(H_i)_{21} = \frac{(1-\nu)n^2}{2R^2}, \quad (H_i)_{24} = -\frac{(1+\nu)n}{2R}$$

$$(H_i)_{26} = -\frac{\nu}{R}, \quad (H_i)_{42} = \frac{1}{\Delta_1}\left[\frac{(1+\nu)n}{2R}\right]$$

$$(H_i)_{43} = \frac{1}{\Delta_1}\left[\frac{(1+k)n^2}{R^2}\right], \quad (H_i)_{45} = \frac{1}{\Delta_1}\left[\frac{(1+kn^2)n}{R^2}\right]$$

$$(H_i)_{47} = \frac{1}{\Delta_1}\left(-kn\right), \quad (H_i)_{82} = -\frac{1}{kR^2}\left[\frac{\nu}{R} - \frac{k(2-\nu)(1+\nu)n^2}{2R\Delta_1}\right]$$

$$(H_i)_{83} = -\frac{1}{kR^2}\left[\frac{n}{R^2} - \frac{k(2-\nu)(1+k)n^3}{R^2\Delta_1} + \frac{kn^3}{R^2}\right]$$

$$(H_i)_{85} = -\frac{1}{kR^2}\left[\frac{1}{R^2} + \frac{kn^4}{R^2} - \frac{k(2-\nu)(1+kn^2)n^2}{R^2\Delta_1}\right]$$

$$(H_i)_{87} = -\frac{1}{kR^2}\left[-2kn^2 + \frac{(2-\nu)k^2n^2}{\Delta_1} + \frac{N_x}{C}\right] \tag{5.3.20}$$

where

$$k = h^2/(12R^2), \quad C = Eh/(1-\nu^2), \quad \Delta_1 = \frac{1-\nu}{2} + k(1-\nu) - \frac{N_x}{C} \tag{5.3.21}$$

The solution for Eq. (5.3.18) can be expressed as

$$\boldsymbol{\Psi}_i = e^{\mathbf{H}_i x}\mathbf{c}_i \tag{5.3.22}$$

where $e^{\mathbf{H}_i x}$ is a general matrix solution of Eq. (5.3.18) and $\mathbf{c}_i$ is an $8 \times 1$ constant column matrix that is to be determined using the boundary conditions and/or interface conditions between the shell segments.

The boundary conditions at the shell ends are given below for various types of support.

*Simply Supported End*

$$w_i = 0, \quad (M_x)_i = 0, \quad (N_x)_i = 0, \quad v_i = 0 \tag{5.3.23}$$

*Free End*

$$(N_x)_i = 0, \quad (N_{x\theta})_i + \frac{(M_{x\theta})_i}{R} = 0, \quad (M_x)_i = 0$$

$$(Q_x)_i + \frac{1}{R}\frac{\partial(M_{x\theta})_i}{\partial\theta} - N_x\frac{\partial w_i}{\partial x} = 0$$

(5.3.24)

*Clamped End*

$$u_i = 0, \quad v_i = 0, \quad w_i = 0, \quad \frac{\partial w_i}{\partial x} = 0 \qquad (5.3.25)$$

where $i$ takes the value 1 or $M$, and the stress resultants are given by

$$N_x = \frac{Eh}{(1-\nu^2)}(\varepsilon_x + \nu\varepsilon_\theta), \quad N_\theta = \frac{Eh}{(1-\nu^2)}(\varepsilon_\theta + \nu\varepsilon_x)$$

$$N_{x\theta} = \frac{Eh}{2(1+\nu)}\varepsilon_{x\theta}, \quad M_x = \frac{Eh^3}{12(1-\nu^2)}(\kappa_x + \nu\kappa_\theta) \qquad (5.3.26)$$

$$M_{x\theta} = M_{\theta x} = \frac{Eh^3}{24(1+\nu)}\tau, \quad Q_x = \frac{\partial M_x}{\partial x} + \frac{1}{R}\frac{\partial M_{\theta x}}{\partial\theta}$$

and the strain, curvature and twist of middle surface terms are related to the displacement fields by

$$\varepsilon_x = \frac{\partial u}{\partial x}, \quad \varepsilon_\theta = \frac{1}{R}\left(\frac{\partial v}{\partial\theta} + w\right), \quad \varepsilon_{x\theta} = \frac{1}{R}\frac{\partial u}{\partial\theta} + \frac{\partial v}{\partial x}$$

$$\kappa_x = -\frac{\partial^2 w}{\partial x^2}, \quad \kappa_\theta = \frac{1}{R^2}\left(\frac{\partial v}{\partial\theta} - \frac{\partial^2 w}{\partial\theta^2}\right), \quad \tau = -\frac{2}{R}\left(\frac{\partial^2 w}{\partial x\partial\theta} - \frac{\partial v}{\partial x}\right)$$

(5.3.27)

Two types of constraints of the intermediate ring supports are considered and they are defined as follows:

**1. Type I Ring Supports:** The displacement $w = 0$ is imposed at the ring supports. Along the interface between the $i$th and $(i+1)$th segments, the following essential and natural continuity conditions must be satisfied:

$$w_i = 0, \quad w_{i+1} = 0, \quad u_i = u_{i+1}, \quad v_i = v_{i+1}, \quad \frac{\partial w_i}{\partial x} = \frac{\partial w_{i+1}}{\partial x}$$

$$(M_x)_i = (M_x)_{i+1}, \quad (N_x)_i = (N_x)_{i+1}, \quad \left(N_{x\theta} + \frac{M_{x\theta}}{R}\right)_i = \left(N_{x\theta} + \frac{M_{x\theta}}{R}\right)_{i+1}$$

(5.3.28)

**2. Type II Ring Supports:** The displacements $u = 0, v = 0$ and $w = 0$ are imposed at the ring supports. Along the interface between the $i$th and $(i+1)$th segments, the following essential and natural continuity conditions must be satisfied:

$$u_i = 0, \quad u_{i+1} = 0, \quad v_i = 0, \quad v_{i+1} = 0, \quad w_i = 0, \quad w_{i+1} = 0$$
$$\frac{\partial w_i}{\partial x} = \frac{\partial w_{i+1}}{\partial x}, \quad (M_x)_i = (M_x)_{i+1} \tag{5.3.29}$$

In view of Eq. (5.3.22), a homogeneous system of equations can be derived by implementing the boundary conditions of the shell [see Eqs. (5.3.23)–(5.3.25)] and the interface conditions between two segments [Eqs. (5.3.28) and (5.3.29)] when assembling the segments to form the whole shell. We have

$$\mathbf{Kc} = \mathbf{0} \tag{5.3.30}$$

where $\mathbf{K}$ is an $8m \times 8m$ matrix and $\mathbf{c}$ is an $8m \times 1$ vector. The buckling load $N_x^0$ is evaluated by setting the determinant of $\mathbf{K}$ in Eq. (5.3.30) to be zero and solving the characteristic equation.

Tables 5.2 and 5.3 present sample exact buckling factors for simply supported and clamped shells with one intermediate ring support. The location of the ring support is at $a/L = 0.1, 0.3$ and $0.5$; the thickness-to-radius ratio $h/R$ is set to be $1/100$ and $1/500$; and the length-to-radius ratio $L/R$ is fixed at 1 and 5, respectively.

**Table 5.2:** Buckling load factors $N_c R\sqrt{3(1-\nu^2)}/(Eh^2)$ for simply supported cylindrical shells with one intermediate ring support (values in brackets are $n$ where $2n$ denotes the number of half-waves of the buckling modes in the circumferential direction).

| Type of Ring Support | $h/R$ | $L/R$ | $a/L = 0.1$ | $a/L = 0.3$ | $a/L = 0.5$ |
|---|---|---|---|---|---|
| Type I | 1/100 | 1 | 0.979227 (7) | 0.986687 (9) | 0.984639 (9) |
| | | 5 | 0.969032 (6) | 0.970115 (6) | 0.955306 (5) |
| | 1/500 | 1 | 0.996949 (20) | 0.995912 (17) | 0.993557 (15) |
| | | 5 | 0.991097 (14) | 0.993269 (13) | 0.960711 (7) |
| Type II | 1/100 | 1 | 0.988980 (9) | 0.991294 (9) | 0.993897 (8) |
| | | 5 | 0.971191 (7) | 0.976794 (8) | 0.985376 (9) |
| | 1/500 | 1 | 0.998834 (17) | 0.997507 (20) | 0.998834 (17) |
| | | 5 | 0.994004 (15) | 0.995092 (17) | 0.998834 (17) |

**Table 5.3:** Buckling load factors $\lambda = N_x^o R\sqrt{3(1-\nu^2)}/(Eh^2)$ for clamped shells with one intermediate ring support (values in brackets are $n$ where $2n$ denotes the number of half-waves of the buckling modes in the circumferential direction).

| Type of Ring Support | $h/R$ | $L/R$ | $a/L = 0.1$ | $a/L = 0.3$ | $a/L = 0.5$ |
|---|---|---|---|---|---|
| Type I | 1/100 | 1 | 1.01149 (9) | 1.00941 (9) | 1.01167 (9) |
| | | 5 | 0.98072 (8) | 0.98072 (8) | 0.98072 (8) |
| | 1/500 | 1 | 0.99833 (20) | 0.99829 (20) | 0.99822 (20) |
| | | 5 | 0.99602 (18) | 0.99602 (18) | 0.99602 (18) |
| Type II | 1/100 | 1 | 1.01729 (9) | 1.02325 (8) | 1.02314 (8) |
| | | 5 | 0.98871 (9) | 0.98422 (9) | 0.98570 (9) |
| | 1/500 | 1 | 0.99868 (20) | 1.00009 (20) | 1.00130 (19) |
| | | 5 | 0.99770 (20) | 0.99820 (20) | 0.99756 (20) |

## 5.4 Buckling of Circular Cylindrical Panels under Uniform Axial Compression

Consider a simply supported, cylindrical panel of length $L$, radius $R$, thickness $h$ and central angle $\phi$. The panel is under a uniform axial compressive force $N$ as shown in Fig. 5.3.
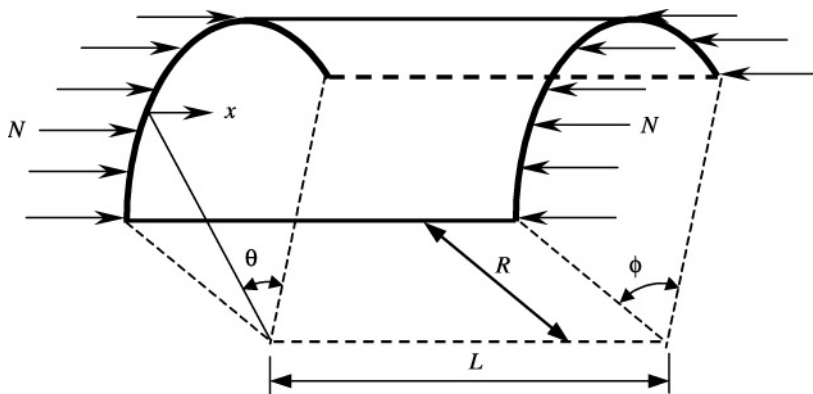


**Figure 5.3:** Cylindrical panel under uniform compression.

The governing buckling equations are the same as those for the circular cylindrical shells [i.e., Eqs. (5.3.1) to (5.3.3)]. The displacement functions are, however, given by

$$u = \sum_{m}^{\infty} \sum_{n}^{\infty} A_{mn} \sin \frac{n\pi\theta}{\phi} \cos \frac{m\pi x}{L} \qquad (5.4.1)$$

$$v = \sum_{m}^{\infty} \sum_{n}^{\infty} B_{mn} \cos \frac{n\pi\theta}{\phi} \sin \frac{m\pi x}{L} \qquad (5.4.2)$$

$$w = \sum_{m}^{\infty} \sum_{n}^{\infty} C_{mn} \sin \frac{n\pi\theta}{\phi} \sin \frac{m\pi x}{L} \qquad (5.4.3)$$

By substituting Eqs. (5.4.1) to (5.4.3) into Eqs. (5.3.1) to (5.3.3), we obtain the same equations as Eqs. (5.3.7) to (5.3.9); the only change is $n$ being replaced by $n\pi/\phi$. So Eq. (5.3.13) becomes

$$N = \frac{Eh}{(1-\nu^2)} \left[ \frac{h^2}{12R^2} \frac{(\frac{n^2\pi^2}{\phi^2} + \beta^2)^2}{\beta^2} + \frac{(1-\nu^2)\beta^2}{(\frac{n^2\pi^2}{\phi^2} + \beta^2)^2} \right] \qquad (5.4.4)$$

Therefore, the buckling load for a cylindrical panel under uniform axial compression is given by

$$N_{\min} = \frac{1}{\sqrt{3(1-\nu^2)}} \left( \frac{Eh^2}{R} \right) \qquad (5.4.5)$$

which is the same as that of its circular cylindrical shell counterpart.

When the angle $\phi$ is very small, the buckling behavior of the cylindrical panel approaches that of a longitudinally compressed rectangular plate. The critical buckling load is furnished by taking $n = 1$, i.e.,

$$N = \frac{Eh}{(1-\nu^2)} \left[ \frac{h^2}{12R^2} \frac{(\frac{\pi^2}{\phi^2} + \beta^2)^2}{\beta^2} + \frac{(1-\nu^2)\beta^2}{(\frac{\pi^2}{\phi^2} + \beta^2)^2} \right] \qquad (5.4.6)$$

## 5.5 Buckling of Circular Cylindrical Shells under Lateral Pressure

For buckling of circular cylindrical shells under uniform lateral pressure $p$, the governing equations are given by (Timoshenko and Gere, 1961)

$$\frac{\partial^2 u}{\partial x^2} + \frac{1+\nu}{2R}\frac{\partial^2 v}{\partial x \partial \theta} - \frac{\nu}{R}\frac{\partial w}{\partial x} + \frac{1-\nu}{2R^2}\frac{\partial^2 u}{\partial \theta^2}$$
$$+\frac{p(1-\nu^2)}{Eh}\left(\frac{\partial^2 v}{\partial x \partial \theta} - \frac{\partial w}{\partial x}\right) = 0 \qquad (5.5.1)$$

$$\frac{1+\nu}{2R}\frac{\partial^2 u}{\partial x \partial \theta} + \frac{1-\nu}{2}\frac{\partial^2 v}{\partial x^2} + \frac{1}{R^2}\frac{\partial^2 v}{\partial \theta^2} - \frac{1}{R^2}\frac{\partial w}{\partial \theta}$$
$$+\frac{h^2}{12R^2}\left[\frac{1}{R^2}\frac{\partial^2 v}{\partial \theta^2} + \frac{1}{R^2}\frac{\partial^3 w}{\partial \theta^3} + \frac{\partial^3 w}{\partial x^2 \partial \theta} + (1-\nu)\frac{\partial^2 v}{\partial x^2}\right] = 0 \qquad (5.5.2)$$

$$-\frac{h^2}{12R^2}\left[\frac{1}{R}\frac{\partial^3 v}{\partial \theta^3} + (2-\nu)R\frac{\partial^3 v}{\partial x^2 \partial \theta} + R^3\frac{\partial^4 w}{\partial x^4} + \frac{1}{R}\frac{\partial^4 w}{\partial \theta^4} + 2R\frac{\partial^4 w}{\partial x^2 \partial \theta^2}\right]$$
$$+\nu\frac{\partial u}{\partial x} + \frac{1}{R}\frac{\partial v}{\partial \theta} - \frac{w}{R} - \frac{p(1-\nu^2)}{Eh}\left(w + \frac{\partial^2 w}{\partial \theta^2}\right) = 0 \qquad (5.5.3)$$

For simply supported cylindrical shells in which the boundary conditions at the ends are $w = 0$ and $\partial^2 w/\partial x^2 = 0$, the displacement functions take on the following expressions

$$u = C_1 \sin n\theta \, \sin \frac{\pi x}{L} \qquad (5.5.4)$$

$$v = C_2 \cos n\theta \, \cos \frac{\pi x}{L} \qquad (5.5.5)$$

$$w = C_3 \sin n\theta \, \cos \frac{\pi x}{L} \qquad (5.5.6)$$

Note that the shell buckles with a half-wave of a sine curve while the circumference is divided into $2n$ half-waves.

By substituting Eqs. (5.5.4) to (5.5.6) into Eqs. (5.5.1) to (5.5.3) and using the notation that $\lambda = \pi R/L$, one obtains

$$-C_1\left(\lambda^2 + \frac{1-\nu^2}{2}n^2\right) + C_2 n\lambda\left[\frac{(1+\nu)}{2} + \frac{pR(1-\nu^2)}{Eh}\right]$$
$$+C_3\lambda\left[\nu + \frac{pR(1-\nu^2)}{Eh}\right] = 0 \quad (5.5.7)$$

$$C_1\frac{(1+\nu)}{2}n\lambda - C_2\left[\frac{1-\nu}{2}\lambda^2 + n^2 + \frac{h^2}{12R^2}\{n^2 + (1-\nu)\lambda^2\}\right]$$
$$-C_3 n\left[1 + \frac{h^2}{12R^2}(n^2 + \lambda^2)\right] = 0 \qquad (5.5.8)$$

$$C_1 \nu \lambda - C_2 n \left\{ 1 + \frac{h^2}{12R^2} \left[ n^2 + (2 - \nu) \right] \lambda^2 \right\}$$

$$- C_3 \left[ 1 + \frac{h^2}{12R^2} (n^2 + \lambda^2)^2 + \frac{pR(1 - \nu^2)}{Eh} (1 - n^2) \right] = 0 \qquad (5.5.9)$$

By setting the determinant of the above equations to zero, we obtain the following characteristic equation

$$\frac{pR(1 - \nu^2)}{Eh} \left\{ (1 - n^2)(n^2 + \lambda^2)^2 - \nu \lambda^4 - \frac{pR(1 + \nu)^2}{Eh}(1 - n^2)n^2 \lambda^2 \right.$$

$$+ \frac{h^2}{12R^2} \Omega \right\} + (1 - \nu^2) \lambda^4 + \frac{h^2}{12R^2} \left\{ \Theta + \frac{h^2}{12R^2} \lambda^4 (n^2 + \lambda^2) \right.$$

$$\times \left. \left[ (1 - \nu)n^2 + 2\lambda^2 \right] \right\} = 0 \qquad (5.5.10)$$

where

$$\Omega = (1 - n^2) \left( n^2 + \frac{2\lambda^2}{1 - \nu} \right) [n^2 + (1 - \nu)\lambda^2] + \frac{1 + 3\nu}{1 - \nu} n^4 \lambda^2$$

$$+ \frac{2 + 3\nu - \nu^2}{1 - \nu} n^2 \lambda^4 - \frac{2\nu n^2 \lambda^2}{1 - \nu} - 2\nu \lambda^4 - \frac{1 + \nu}{1 - \nu} n^2 \lambda^2 (n^2 + \lambda^2)^2 \quad (5.5.11)$$

$$\Theta = (n^2 + \lambda^2)^4 - 2n^2 \left( n^2 + \frac{3 - \nu}{2} \lambda^2 \right) [n^2 + (2 + \nu)\lambda^2]$$

$$+ [n^2 + (1 - \nu)\lambda^2][n^2 + 2(1 + \nu)\lambda^2] \qquad (5.5.12)$$

By neglecting small terms, Eq. (5.5.10) may be simplified to

$$p = \frac{Eh}{R(1 - \nu^2)} \left\{ \frac{1 - \nu^2}{(n^2 - 1)(1 + \frac{n^2}{\lambda^2})} + \frac{h^2}{12R^2} \left( n^2 - 1 + \frac{2n^2 - 1 - \nu}{1 + \frac{n^2}{\lambda^2}} \right) \right\}$$
$$(5.5.13)$$

In view of Eq. (5.5.13), the elastic critical pressure of a *very long* cylindrical shell (i.e., $\lambda \gg n$), with free ends, is given by (with $n = 2$)

$$p_{cr} = \frac{1}{4(1 - \nu^2)} \frac{Eh^3}{R^3} \qquad (5.5.14)$$

For *short* cylindrical shells with ends held in the circular direction but otherwise unconstrained, the critical buckling pressure is given by

$$p_{cr} = 0.807 \left[ \frac{1}{(1 - \nu^2)^3} \left( \frac{L}{R} \right)^2 \right]^{1/4} \frac{Eh^2}{RL} \qquad (5.5.15)$$

For closed-ended cylindrical shells subjected to both axial and lateral pressure, the critical axisymmetric buckling pressure is given by

$$p_{cr} = \frac{2}{\sqrt{3(1-\nu^2)}} \frac{Eh^2}{R^2} \tag{5.5.16}$$

## 5.6 Buckling of Spherical Shells under Hydrostatic Pressure

Consider a complete spherical shell of radius $R$, thickness $h$ and subjected to an external hydrostatic pressure $p$. The shell's buckled surface is symmetrical with respect to a diameter of the sphere. In view of this symmetry, the governing equations for the elastic buckling of such loaded spherical shells are given by (Timoshenko and Gere, 1961)

$$\left(1 + \frac{h^2}{12R^2}\right)\left(\frac{d^2u}{d\theta^2} + \cot\theta\frac{du}{d\theta} - (\nu + \cot^2\theta)u\right) - (1+\nu)\frac{dw}{d\theta}$$

$$+ \frac{h^2}{12R^2}\left[\frac{d^3w}{d\theta^3} + \cot\theta\frac{d^2w}{d\theta^2} - (\nu + \cot^2\theta)\frac{dw}{d\theta}\right]$$

$$- \frac{pR(1-\nu^2)}{2Eh}\left(u + \frac{dw}{d\theta}\right) = 0 \tag{5.6.1}$$

$$(1+\nu)\left(\frac{du}{d\theta} + u\cot\theta - 2w\right) + \frac{h^2}{12R^2}\left[-\frac{d^3u}{d\theta^3} - 2\cot\theta\left(\frac{d^2u}{d\theta^2} + \frac{d^3w}{d\theta^3}\right)\right.$$

$$+ (1+\nu+\cot^2\theta)\left(\frac{du}{d\theta} + \frac{d^2w}{d\theta^2}\right) - \cot\theta(2-\nu+\cot^2\theta)\left(u + \frac{dw}{d\theta}\right)$$

$$\left. - \frac{d^4w}{d\theta^4}\right] - \frac{pR(1-\nu^2)}{2Eh}\left(-u\cot\theta - \frac{du}{d\theta} + 4w + \cot\theta\frac{dw}{d\theta} + \frac{d^2w}{d\theta^2}\right) = 0 \tag{5.6.2}$$

Let us introduce an auxiliary variable $\psi$ where $u = d\psi/d\theta$ and also the Legendre functions for the two variables, i.e.,

$$\psi = \sum_{n=0}^{\infty} A_n P_n \tag{5.6.3}$$

$$w = \sum_{n=0}^{\infty} B_n P_n \tag{5.6.4}$$

where $P_n$ is the Legendre function of order $n$.

By substituting Eqs. (5.6.3) and (5.6.4) into Eqs. (5.6.1) and (5.6.2), one obtains the following two homogeneous equations

$$A_n \left[ n(1+n) - 2 + (1+\nu) + \frac{pR(1-\nu^2)}{2Eh} \right]$$
$$+ B_n \left\{ \frac{h^2}{12R^2} [n(1+n) - 2] + (1+\nu) + \frac{pR(1-\nu^2)}{2Eh} \right\} = 0 \tag{5.6.5}$$

$$A_n \left\{ \frac{h^2}{12R^2} [n(1+n) - 2]^2 + n(1+n) \left[ (1+\nu) + \frac{pR(1-\nu^2)}{2Eh} \right] \right\}$$
$$+ B_n \left\{ \frac{h^2}{12R^2} [n(1+n) - 2][n(1+n) + 1 + \nu] + 2(1+\nu) \right.$$
$$\left. - \frac{pR(1-\nu^2)}{2Eh} n(1+n) \right\} = 0 \tag{5.6.6}$$

By setting the determinant of these two equations to zero, the buckling pressure may be expressed as

$$p = \frac{2Eh}{R(1-\nu^2)} \left( \frac{(1-\nu^2) + \frac{h^2}{12R^2} \{\xi(2+\xi) + (1+\nu)^2\}}{\xi + 1 + 3\nu} \right) \tag{5.6.7}$$

where $\xi = n(1+n) - 2$.

In order to determine the critical buckling pressure which is the smallest positive value of $p$, we take the stationarity condition of $p$ with respect to $\xi$

$$\frac{dp}{d\xi} = 0 \tag{5.6.8}$$

By neglecting the small terms, Eq. (5.6.8) gives

$$\xi^2 + 2(1+3\nu)\xi - \frac{12R^2}{h^2}(1-\nu^2) = 0$$
$$\Rightarrow \xi = -(1+3\nu) + \sqrt{\frac{12R^2}{h^2}(1-\nu^2)} \tag{5.6.9}$$

The substitution of Eq. (5.6.9) into Eq. (5.6.7) yields the critical buckling pressure $p_{cr}$ of a spherical shell

$$p_{cr} = \frac{2Eh}{R(1-\nu^2)} \left( \sqrt{\frac{(1-\nu^2)}{3}} \frac{h}{R} - \frac{\nu h^2}{2R^2} \right) \tag{5.6.10}$$

If the second term in the bracket is neglected, the buckling pressure expression simplifies to

$$p_{cr} = \frac{2}{\sqrt{3(1-\nu^2)}} \left( \frac{Eh^2}{R^2} \right) \qquad (5.6.11)$$

## 5.7 Buckling of Truncated Conical Shells under Axial Vertex Load

Consider a long truncated conical shell with constant thickness $h$, semivertex angle $\phi$, modulus of elasticity $E$, Poisson's ratio $\nu$ and subjected to an axial vertex load $P$ as shown in Fig. 5.4. The governing equations for the axisymmetric buckling of such a loaded shell are given by (Seide, 1956).

$$s\frac{d^2u}{ds^2} + \frac{du}{ds} - \frac{u}{s} + \left( \frac{w}{s} - \nu\frac{dw}{ds} \right) \cot \phi = 0 \qquad (5.7.1)$$

and

$$s\frac{d^4}{ds^4}\left( s\frac{dw}{ds} \right) + \frac{12P(1-\nu^2)}{\pi Eh^3 \sin 2\phi}\left[ \frac{d^2}{ds^2}\left( s\frac{dw}{ds} \right) - \frac{1}{s}\frac{d}{ds}\left( s\frac{dw}{ds} \right) \right]$$

$$+ \frac{12\nu \cot^2 \phi}{h^2}\left[ \frac{d}{ds}\left( s\frac{dw}{ds} \right) - \frac{w}{s} \right]$$

$$- \frac{12\cot^2 \phi}{h^2}\left\{ \frac{d}{ds}\left[ s\left( s\frac{d^2u}{ds^2} + \frac{du}{ds} - \frac{u}{s} \right) \right] + \nu\left( s\frac{d^2u}{ds^2} + \frac{du}{ds} - \frac{u}{s} \right) \right\} = 0$$

$$(5.7.2)$$

where $u$ is the displacement in the direction of cone generator, $w$ is the displacement normal to the middle surface of the cone due to buckling and $s$ the distance from the vertex.

By denoting $\Phi = s(dw/ds)$ and substituting Eq. (5.7.1) into Eq. (5.7.2), one obtains

$$s^2\frac{d^4\Phi}{ds^4} + \frac{P}{D\pi \sin 2\phi}\left( s\frac{d^2\Phi}{ds^2} - \frac{d\Phi}{ds} \right) + \frac{12(1-\nu^2)\cot^2 \phi}{h^2}\Phi = 0 \quad (5.7.3)$$

where $D = Eh^3/[12(1-\nu^2)]$. By differentiating once, Eq. (5.7.3) may be expressed as

$$\left( s\frac{d^2}{ds^2} + \frac{P}{2\pi D \sin 2\phi} \right)\left( s\frac{d^2\Phi'}{ds^2} - \frac{P}{2\pi D \sin 2\phi}\Phi' \right)$$

$$- \left( \frac{P}{2\pi D \sin 2\phi} \right)^2 \left[ 1 - \left( \frac{2Eh^2\pi \cos^2 \phi}{P\sqrt{3(1-\nu^2)}} \right)^2 \right]\Phi' = 0 \quad (5.7.4)$$

where $\Phi' = d\Phi/ds = d(sdw/ds)/ds$. The solution of Eq. (5.7.4) is given by

$$\Phi' = \frac{d\Phi}{ds} = \frac{d}{ds}\left(s\frac{dw}{ds}\right)$$
$$= -b_1\left\{C_1[2\sqrt{b_1s}]J_1[2\sqrt{b_1s}] + C_2[2\sqrt{b_1s}]Y_1[2\sqrt{b_1s}]\right\}$$
$$- b_2\left\{C_3[2\sqrt{b_2s}]J_1[2\sqrt{b_2s}] + C_4[2\sqrt{b_2s}]Y_1[2\sqrt{b_2s}]\right\} \quad (5.7.5)$$

where $J_p$ and $Y_p$ are Bessel functions of the first and second kinds, respectively, and

$$b_{1,2} = \frac{P}{2\pi D \sin 2\phi}\left\{1 \pm \sqrt{1 - \left(\frac{2Eh^2\pi}{P\sqrt{3(1-\nu^2)}}\cos^2\phi\right)^2}\right\} \quad (5.7.6)$$

The integration of Eq. (5.7.5) yields the general solution for $w$, i.e.,

$$w = C_1\left\{2J_0[2\sqrt{b_1s}] + [2\sqrt{b_1s}]J_1[2\sqrt{b_1s}]\right\}$$
$$+ C_2\left\{2Y_0[2\sqrt{b_1s}] + [2\sqrt{b_1s}]Y_1[2\sqrt{b_1s}]\right\}$$
$$+ C_3\left\{2J_0[2\sqrt{b_2s}] + [2\sqrt{b_2s}]J_1[2\sqrt{b_2s}]\right\}$$
$$+ C_4\left\{2Y_0[2\sqrt{b_2s}] + [2\sqrt{b_2s}]Y_1[2\sqrt{b_2s}]\right\} + C_5 \quad (5.7.7)$$
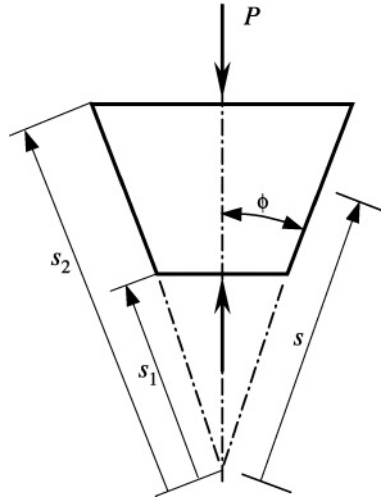


**Figure 5.4:** Truncated conical shell under axial vertex load.

The solution of Eq. (5.7.1) that can be written as

$$\frac{d}{ds}\left[s^3 \frac{d}{ds}\left(\frac{u}{s}\right)\right] = \left(\nu s \frac{dw}{ds} - w\right) \cot\phi \qquad (5.7.8)$$

furnishes the corresponding expression for the displacement $u$

$$
u = 2\cot\phi\left[C_1\left\{2\frac{J_1[2\sqrt{b_1 s}]}{2\sqrt{b_1 s}} + \nu J_1[2\sqrt{b_1 s}]\right\}\right.
$$

$$
+ C_2\left\{2\frac{Y_1[2\sqrt{b_1 s}]}{2\sqrt{b_1 s}} + \nu Y_2[2\sqrt{b_1 s}]\right\}
$$

$$
+ C_3\left\{2\frac{J_1[2\sqrt{b_2 s}]}{2\sqrt{b_2 s}} + \nu J_2[2\sqrt{b_2 s}]\right\}
$$

$$
\left. + C_4\left\{2\frac{Y_1[2\sqrt{b_2 s}]}{2\sqrt{b_2 s}} + \nu Y_2[2\sqrt{b_2 s}]\right\}\right] + C_5 \cot\phi \quad (5.7.9)
$$

Note that although there are five unknown constants of integration, only four boundary conditions are needed to determine the buckling load since the constant $C_5$ in both $u$ and $w$ corresponds to a rigid body movement in the direction of the cone axis.

For simply supported edges and rigid rings, the boundary conditions at the edges (i.e., at $s = s_1$ and $s = s_2$) are

$$\frac{d^2 w}{ds^2} + \frac{\nu}{s}\frac{dw}{ds} = 0 \qquad \text{and} \qquad u\sin\phi - w\cos\phi = 0 \qquad (5.7.10\text{a, b})$$

The substitution of Eqs. (5.7.7) and (5.7.9) into the boundary conditions (5.7.10a, b) and setting the determinant of the matrix to be zero yields the stability criterion

$$\frac{P\sqrt{3(1-\nu^2)}}{2Eh^2\pi\cos^2\phi} = \frac{1}{2}\left[\frac{X_n^2}{\frac{8s_1}{h}\sqrt{3(1-\nu^2)}\cot\phi} + \frac{\frac{8s_1}{h}\sqrt{3(1-\nu^2)}\cot\phi}{X_n^2}\right]$$

$$(5.7.11)$$

where $n = 1, 2, 3, \ldots$ and $X_n^2 = 4\frac{b_{1,2}s_1^3}{s_2}$.

For large values of the parameter $\Psi = \frac{8s_1}{h}\sqrt{3(1-\nu^2)}\cot\phi$, the minimization of Eq. (5.7.11) with respect to $\Psi/X_n^2$ yields the critical buckling load

$$P_{cr} = \frac{2\pi Eh^2\cos^2\phi}{\sqrt{3(1-\nu^2)}} \qquad (5.7.12)$$

# REFERENCES

Bažant, Z. P. and Cedolin, L. (1991), *Stability of Structures*, Oxford University Press, New York.

Brush, D. O. and Almroth, B. O. (1975), *Buckling of Bars, Plates and Shells*, McGraw-Hill, New York.

Calladine, C. R. (1983), *Theory of Shell Structures*, Cambridge University Press, London, UK.

Donnell, L. H. (1976), *Beams, Plates and Shells*, McGraw-Hill, New York.

Lorenz, R. (1908), "Achsensymmetrishce Verzerrungen in dünnwandigen Hohlzylindern," *Zeitschrift des Vereines Deutscher Ingenieure*, **52**(43), 1706–1713.

Seide, P. (1956), "Axisymmetrical buckling of circular cones under axial compression," *Journal of Applied Mechanics*, **23**, 625–628.

Timoshenko, S. P. (1910), "Einige Stabilittsprobleme der Elastizitätstheorie," *ZAMP*, **58**(4), 337–385.

Timoshenko, S. P. and Gere, J. M. (1961), *Theory of Elastic Stability*, McGraw-Hill, New York.

Ugural, A. C. (1999), *Stresses in Plates and Shells*, 2nd ed., McGraw-Hill, New York.

Xiang, Y., Wang, C. M., Lim, C. W. and Kitipornchai, S. (2004), "Buckling of intermediate ring supported cylindrical shells under axial compression," in review.